THE ROLE OF MAP KINASE PHOSPHATASE-2 (MKP-2) IN CARDIAC FUNCTION

A thesis presented by

AHMED LAWAN

For the degree of Doctor of Philosophy

of

UNIVERSITY OF STRATHCLYDE

October 2010

Strathclyde Institute of Pharmacy and Biomedical Sciences (SIPBS),

Glasgow, UK

COPYRIGHT STATEMENT

ABSTRACT

Mitogen-activated protein kinase phosphatase-2 (MKP-2) is a type I dual specific phosphatase that functions to regulate the activity of the ERK and JNK. The MAPKs are a large class of enzymes involved in mediating a number of physiological and pathological changes in the heart. This project utilized a novel MKP-2 knockout mouse and investigated the effects of MKP-2 deletion on MAPK-mediated signalling and cellular proliferation and correlated these findings with effects on cardiac phenotype and function.

Experiments in MEFs demonstrated that in response to serum, MKP-2 induction was dependent on prior ERK activation in wild type MEFs but not JNK or p38 MAPK. It was established that cell growth was substantially reduced in MKP-$2^{-/-}$ MEFs which was linked with significant increase in cell doubling time. Over-expression of Adv.MKP-2 reversed the deficit in cell growth. Analysis of the cell cycle showed that these cells were delayed in G_2/M phase which was associated with enhanced accumulation of cyclin B1 and increased phosphorylation of cdc-2 kinase. MEFs derived from MKP-$2^{-/-}$ mice displayed increased apoptosis in response to anisomycin which correlated with enhanced caspase-3 cleavage and phosphorylation of γH2AX. In addition, over-expression of Adv.MKP-2 reversed the enhanced apoptosis in MKP-$2^{-/-}$ MEFs which correlated with specific inhibition of JNK signalling.

Similar to the findings in MEFs, CF exhibited decreased cellular proliferation. However, assessment of these mice using echocardioraphy *in vivo* revealed that the LVESD, LVEDD were increased in the KO mice compared with the wild type littermates. In contrast, FS was decreased in the KO compared with the wild type. Analysis of the MTAB heart homogenates demonstrated that MKP-2 expression was decreased in MTAB in comparison to sham operated animals. In contrast, ERK phosphorylation was transiently increased in MTAB compared with sham operated animals.

This current study has established that MKP-2 plays an important role in cell proliferation and survival, regulating both cell cycle progression and apoptosis. It also suggests that MKP-2 can influence growth characteristics of cardiac fibroblasts and this has the potential to regulate heart size and possibly myocyte function.

ACKNOWLEDGEMENT

As always, I thank Allah (SWT) so much for blessing me with abililty to realise my dreams. Firstly, I would like to express my sincere and profound gratitude to my major supervisor Prof. R. Plevin for his guidance and support throughout the course of my PhD. Thank you for spending significant amount of time discussing and providing feedback for my thesis which has really improved my writing skill. Secondly, I would like to express my gratitude to my second supervisor Dr. S. Currie for being into the project from the beginning to the end, i am grateful for your support and encouragement during my PhD.

I wish to extend my thanks to lab members, both past and present for their help and support. These include Mary, Katy, Margaret, Fadia, Gary, Yuen, Shalu, Carly, Juliane and Rebecca and my friends Sameer and Muhannad. My special thanks go to Dr. Laurence Cadalbert whom I have learnt a lot. I am also grateful to Dr. Mashael Almutairi who has treated me like her own brother. I would like to extend my thanks to members of CV lab in particular Prof. Kathy Kane and Diana. My special thanks to also Tamara and Laura for proofreading my thesis. The assistance of all the technical and post-doctoral staff and PhD students in SIPBS is appreciated. I would like to thank Dr Craig Roberts and Dr Trevor Bushell for their support.

I would like to thank Kano State Government of Nigeria and University of Strathclyde for funding my PhD programme.

I wish to extend my gratitude to all members of my family in particular my elder brother Mahmoud for his support throughout the duration of my PhD. I also thank Dr. Haruna Salihi for his support.

The last but not the list I thank my friend Farida for her support and encouragement.

ABBREVIATIONS

°C: degrees centigrade

7–AAD: 7-Amino-Actinomycin

Ab: antibody

Abs: absorbance

ADP: Adenosine monophosphate

Amp: ampicillin

AngII: Angiotensin II

ANP: Atrial natriuretic peptide

APS: ammonium per sulfate

ATP: adenosine triphosphate

ATP: Adenosine triphosphate

bp: base pairs

BrdU: bromo-deoxy uridine

BSA: bovine serum albumin

CaMKII: Calcium/calmodulin-dependent protein kinase II

cAMP: cyclic adenosine monophosphate

cDNA: complementary deoxyribonucleic acid

CFP: cyan fluorescent protein

CFs: Cardiac fibroblasts

CI-MKP-2: Catalytically inactive MAP kinase phosphatase-2

Co-IP: co-immunoprecipitation

Cx: Connexin

DAPI: 4', 6-Diamidino-2-phenylindole

DMEM: dulbeccós modified Eagle's medium

DMSO: dimethyl sulphoxide

DNA: Deoxy ribonucleic acid

dNTP: deoxynucleotide triphosphate

DTT: Dithiothreitol

DUSPs: Dual specificity phosphatases

E.coli: Escherichia coli

EC: Excitation-contraction coupling

ECM: Extracellular matrix

EDTA: ethylene diamine tetra acetic acid

EGF: Epidermal growth factor

ELISA: enzyme linked immunosorbant assay

ERK: Extracellular signal-regulated kinase

FACS: fluorescence activated cell sorter

FBS: fetal bovine serum

FCS: Fetal calf serum

FGF: Fibroblast growth factor

GFP: green fluorescent protein

gm: grams

GnRH: Gonadotropin-releasing hormone

GPCRs: G-protein-coupled receptors

GTP: guanosine triphosphate

hr(s) hour(s)

HRP: horse radish peroxide

IEG: Immediate early gene

IL: Interleukin

IP: immunoprecipitation

JNK: c-jun N-terminal kinase

kb: kilo bases

kDa: kilodalton

M: molar

MAPK: Mitogen activated protein kinase

MEF2: Myocyte enhancer factor 2

MEFs: Mouse embryonic fibroblasts

MEK: Mitogen activated protein kinase kinase

MEKK: Mitogen activated protein kinase kinase kinase

mg: milligrams

min: minute (s)

MKB: MAPK binding domain

MKPs: Mitogen activated protein kinase phosphatases

ml: milliliter

MLC-2a: Myosin Light chain

mM: millimolar

MMP: Matrix metalloproteinases

mRNA: Messenger ribonucleic acid

MTAB: Minimally invasive transverse aortic Banding

NES: Nuclear export signal

ng: nanograms

NGF: Nerve growth factor

NLS: Nuclear localization signal

nm: nanometer

O.D: optical density

ORF: open reading frame

PAGE: polyacrylamide gel electrophoresis

PBS: phosphate buffered saline

PCR: polymerase chain reaction

PE: Phycoerthrin

Pen/strep: penicillin / streptomycin

PFA: paraformaldehyde

PFU: Plaque-forming unit

PKA: Protein kinasse A

PKC: Protein kinase C

PLB: Phospholamban

pM: pico molar

PMA: Phorbol 12-myristate 13-acetate

PMSF: phenylmethylsulfonyl fluoride

PTP: Protein tyrosine phosphates

PVDF: polyvinylidene fluoride

RNA: Ribonucleic acid

rpm: revolutions per minute

RT: room temperature

RTKs: Receptor tyrosine kinses

SDS-PAGE: SDS-polyacrylamide gel electrophoresis

SDS: Sodum dodecyl sulphate

SERCA: Sarcoplasmic reticulum calcium ATPase

siRNA: small interfering ribo nucleic acid

SR: Sarcoplasmic reticulum

TAE: tris/Acetate/EDTA-buffer

TEMED: N, N, N′, N′-Tetramethylethylenediamide

TGFR: Transforming growth factor β receptor

TN-C: Troponin-C

TTP : Thymidine triphosphate

v: volt

WB: western blotting

YFP: yellow fluorescent protein

β-MHC: Beta myosin heavy chain

µg: micrograms

µl: micro litre

µM: micro molar

CONTENTS **PAGE**

LIST OF FIGURES

Chapter 1

Chapter 3

CHAPTER 1

INTRODUCTION

Chapter 1: Introduction

1.1 Physiological structure of the heart

The heart is the central pump that drives the blood through the blood vessels. The heart of a normal adult male has a size of a clenched fist and weighs about 300 g (Abu-Sita *et al*., 2003). It lies in the chest cavity with all its chambers at approximately the same horizontal level. It is surrounded by a serous sac; the pericardium, which allows cardiac mobility without friction with the surrounding structures. The heart consists of two sheets of cardiac muscles. One sheet comprised of the two atria and the interatrial septum. The other makes up the ventricles and the interventricular septum. The wall of the left ventricle is much thicker (15 mm) than the wall of the right ventricle (5 mm), yet the capacities and outputs of both ventricles are equal. The thickness of the ventricular wall reflects the pressure load on the left ventricle (the aortic pressure) which is much higher than the pressure load on the right ventricle (the pulmonary arterial pressure). The wall of the atria and ventricles are surrounded by layers of tightly bound cardiac muscle cells known as cardiac myocytes or cardiomyocytes (Abu-Sita *et al*., 2003; Boron and Boulpaep, 2005).

The contraction and relaxation of these cardiac muscle chambers are responsible for the mechanical events of the cardiac cycle, which regulates the function of the heart (Vander *et al*., 2004). This cycle is divided into 2 phases named in response to events occurring in the ventricles, called systole (period of contraction) and diastole (period of relaxation). The initial trigger of an action potential (AP) and the resulting membrane depolarization commences in the sinoatrial node in the right atrium and propagates throughout the atria. It then enters via the atrioventricular node (AV-node) and spreads throughout the ventricles. This wave of depolarization results in the contraction of the ventricles thus pushing blood out of the chambers into the

circulation systems. The set of events that occur between depolarization of the AV-node to the trigger of ventricular contraction is known as systole. During the systolic cycle, a separate set of events known as excitation-contraction coupling (EC-coupling) occur. This is the process that controls cardiac calcium (Ca^{2+}) cycling within each cardiac myocyte (Bers and Guo, 2005). Following systole, the heart enters into the second phase called diastole where the ventricular muscles relax. This is vital to permit blood to fill the chambers before the trigger of another AP. This orderly rhythm of the heart continues throughout its lifespan (Vander *et al*., 2004; Boron and Boulpaep, 2005). Abnormalities in the regulation of these events in the heart could lead to remodeling and cardiac pathology.

In the mammalian heart normal cardiac function is controlled by active interactions of the two major cell types, cardiac myocytes and cardiac fibroblasts (CF), which together comprise about 90% of the cells in the myocardium (Baudino *et al*., 2006). CF, which constitute about 60–70% of the cells in the human heart, serve as the main source of the extracellular matrix (ECM) that regulates the structure of the heart and hence mechanical, biochemical and electrical signalling in the heart (Kizana *et al.,* 2006). Cardiac myocytes, although fewer in number, make up the bulk volume of the normal cardiac muscle and are contractile cells that provide mechanical force, transmission of which is one of the principal functions of the ECM (Hinz *et al*., 2007). Collagen is the major stress-bearing constituent within the ECM and forms a three-dimensional structure around bundles of myocytes to generate a stress-tolerant network that transmits the mechanical force provided by myocytes resulting in contraction. Hence the significance of CF extends far beyond being simple regulators of ECM production as was previously assumed (Porter and Turner, 2009).

1.1.1 The physiological role of cardiac fibroblasts in the heart

As outlined above, in the heart, the major cellular composition includes cardiac fibroblasts, myocytes, endothelial cells, and vascular smooth muscle cells, with the majority of cells comprising fibroblasts and myocytes (Baudino *et al*., 2006; Camelliti *et al*., 2005; Harvey and Rosenthal, 1999). Initially, CFs were mainly considered as cells that secrete ECM. In spite of this, accumulating evidence now shows that CF are not only a significant participant in the response to cardiac pathophysiology, but are critical contributors in normal cardiac physiology (Figure 1.1). Interest in cardiac fibroblasts has developed with the acknowledgment that cardiac fibrosis is a well-known contributor to different forms of cardiac disease. (Brilla *et al*., 1992; Weber and Brilla, 1992; Weber *et al*., 1992; Weber *et al*., 1989; Weber *et al*., 1991). This was originally demonstrated through the discovery of angiotensin receptors on the surface of cardiac fibroblasts, linking the renin–angiotensin–aldosterone system directly with pathological myocardial and matrix extracellular remodeling. (Crabos *et al*., 1994; Villarreal *et al*., 1993). Apart from serving as the main source of extracellular matrix, CF also secrete proteases that control and arrange matrix (Gaudesius *et al*., 2003). Recent studies have revealed paracrine and also direct cell-to-cell communication between CF and cardiac myocytes through gap junctions (Camelliti *et al*., 2004). The direct connections between cardiac myocytes and CF occur through gap junctional connexins namely Cx40, Cx43, and Cx45 to function in electrical conduction in the heart (Camelliti *et al*., 2004; Gaudesius *et al*., 2003; Manabe *et al*., 2002).

A distinctive effect of embryonic cardiac fibroblasts on developing myocytes has been established. Embryonic CF exists in the developing compact myocardium and increase in number over the course of development. They express many constituents of the extracellular matrix, including fibronectin, collagens, periostin, hyaluronan, and proteoglycan link protein 1 (Ieda et. al.,

2009; Porter and Turner, 2009). Embryonic myocytes grown on culture plates supplemented with fibronectin, collagen type III, periostin, or laminin show an increase in cell growth, involving β-1-integrin signalling and heparin-binding epidermal growth factor–like growth factor (HB-EGF) with activation of ERK and p38 MAPK signalling (see section 1.2). These and other studies demonstrate the importance of ECM derived from CF (Stewart *et. al*., 2006). Furthermore, when embryonic mouse cardiac myocytes are co-cultured with adult CF, a hypertrophic rather than a proliferative phenotype is observed, with increased cell size and sarcomeric organization (Ieda *et. al*., 2009). This shows that paracrine factors resulting from CF may affect the phenotype of cardiac myocytes during development in a way separate from effects in the adult (Ieda et. al., 2009).

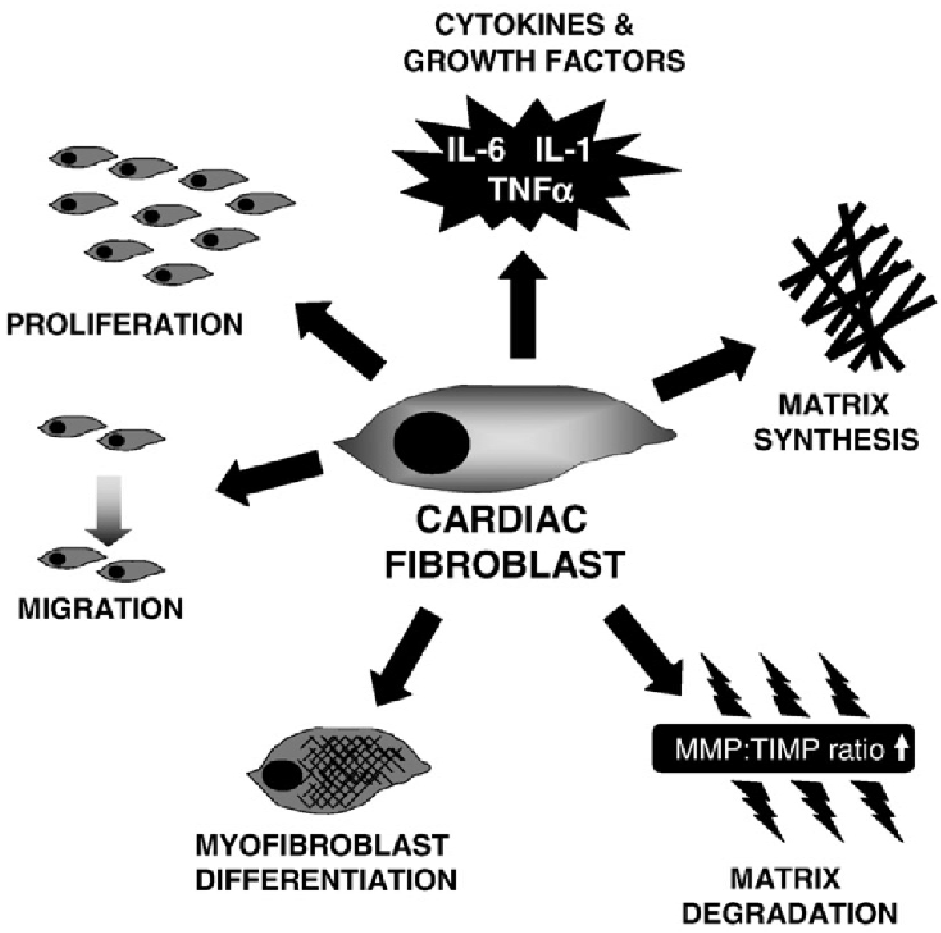

Figure 1.1. Modulation of cardiac fibroblast function associated with myocardial remodeling. The CF responds to environmental stimuli in multiple ways, including transformation to a myofibroblast phenotype, proliferation, migration, secretion of cytokines and growth factors, and altering extracellular matrix turnover through changes in matrix protein synthesis and matrix degradation (increase in MMP:TIMP ratio). While these changes in fibroblast function are an important adaptive response to altered environment that can aid myocardial recovery, they can become maladaptive leading to pathological remodeling, fibrosis and heart failure. (Adapted from Porter and Turner, 2009).

1.1.1.1 Cardiac Fibroblast-Myocyte Interaction *in vitro*

The capacity of CF and myocytes to form homogeneous and heterogeneous gap junctions *in vitro* has been investigated in a number of direct electrophysiological studies. For instance, it has been shown that freshly isolated and cultured cardiomyocytes and CF readily form functional gap junctions, with single channel conductances (at room temperature) of 22 pS between CF, 43 pS between myocytes, and 29 pS between CF and myocytes (Rook *et al*., 1989; Rook *et al*., 1992). In the last decade the concept of CF as conductors of electrical excitation from the single cell level to longer distances has been investigated in more detail using a combination of functional and structural studies. Some of these studies demonstrated that CF were able to synchronize the electrical activity of cultured neonatal rat myocytes across gaps up to 300 μm in length. Using immunocytochemistry has established the presence of Cx43 and Cx45 at points of heterogeneous and homogeneous cell contact in neonatal cardiomyocytes and CF co-cultured in monolayers (Gaudesius *et al*., 2003; Oyamada *et al*., 1994). These data confirm that CF and myocytes are able to develop electrically conducting gap junctional channels, and that CF actively affect the electrophysiology of myocytes, *in vitro.*
myocytes began contracting within 24 h at clonal or mass densities with 5% of cells expressing vimentin.

Recently, the effect of medium containing factors derived from CF on the activities of isolated neonatal ventricular myocytes was investigated. In myocytes that are expressed in co-cultures of CF, myocytes contraction was observed within 24 h at mass densities where only 5% of cells expressing vimentin in the culture. Immunocytochemical analysis showed progressive expression of α-smooth muscle actin in myocytes after 24 h in all conditions. However, only myocytes in CF-conditioned medium stopped contracting by 72 h (LaFramboise *et al*., 2007). The results established that CF could induce changes in myocyte phenotype distinct from the dedifferentiation phenotype

observed *in vitro*. These changes included modification of myocyte structural and functional features including hypertrophy, intracellular expression of vimentin, and reduction of chronotropic contractile activity. These results confirmed that under the control of CF-conditioned medium, myocytes exhibited obvious hypertrophy, reduced contractile ability, and phenotype plasticity different from the dedifferentiation trend observed under *in vitro* conditions. This implies that CF could affect the function of myocytes and ultimately heart function. It would also be interesting to see whether the same process is seen in the adult CF.

1.1.1.2 Cardiac Fibroblast-Myocyte Interaction *in vivo*

The first evidence for electrical coupling between CF-myocyte *in vivo* was demonstrated by early electrophysiological studies, conducted using double-barreled microelectrodes inserted into subendocardial layers of spontaneously beating rat right atria. These studies demonstrated changes in the CF membrane potential were similar to the action potential in adjacent myocytes (Kohl *et al*., 1994). However, some studies used a combination of immunohistochemical and dye transfer coupling techniques, and established the presence of functional homogeneous and heterogeneous gap junctions at many sites in the rabbit sinoatrial node (Camelliti *et al*., 2004). In the heart, Cx40, which is mostly expressed by non-myocytes, was found at sites of contact between CF while Cx45, which is linked with both myocytes and CF, was involved in CF, myocytes and CF-myocyte coupling. The functional significance of homogeneous and heterogeneous cell coupling in the rabbit sinoatrial node was confirmed by dye transfer studies using Lucifer yellow (a gap-junction-permeable fluorescent probe), which showed that CF form a wide coupled network of cells able to form conductive bridges between myocytes that are themselves not in direct contact (Camelliti *et al*., 2005).

While the above study established CF-myocyte interaction in the sinoatrial node, similar heterogeneous coupling may also occur in ventricular tissue.

Goldsmith *et al*., 2004 demonstrated that ventricular myocytes and fibroblasts express both Cx43 and Cx45 in 4-day neonatal rat hearts with Cx43 contained at points of homogeneous and heterogeneous contacts, and Cx45 mostly restricted to CF and sometimes between the two cell types. The theory that CF may be a regular and important partner to myocyte coupling throughout the whole heart was further supported by preliminary immunohistochemical experiments showing potential heterogeneous cell interaction in rabbit and sheep ventricular tissue through Cx43 (Camelliti *et al*., 2004). More research is required to quantify such communication in the ventricle and other cardiac regions, and also the physiological output.

Findings by researchers indicate that integrins within cell–matrix adhesions can act as 'strain gauges', triggering MAPK and NF-kB pathways in response to changes in mechanical stress (Gaudesius *et al*., 2003; Stewart *et al*., 2006) (see section 1.4.1). As a consequence of mechanical stress a huge number of intracellular signalling pathways can be elicited in fibroblasts and other adherent cells in response to various mechanical stimuli. These changes in fibroblasts leads to increased ECM production.

1.2 Cardiac hypertrophy and heart failure

Remodeling is generally defined as changes in the geometry of the myocardium and is a vital process that allows the heart to adapt to changes in mechanical, chemical and electrical signals (Diwan and Dorn II, 2007). It is a multifaceted process involving all of the components of the heart, cellular and acellular. Remodeling is a normal process associated with heart growth, particularly during the maturation of the heart from the neonatal period to adulthood. When the heart undergoes hypertrophy or dilation, remodeling must again occur (Kenchaiah and Pfeffer, 2004). If the modulating signals become pathological, then the process of remodeling becomes damaging to cardiac function (Manabe, 2002). Characteristically myocardial remodeling

involves changes in the amount and organization of ECM components (Arnaout *et al*., 2007). A number of disease conditions of the heart are linked with structural and functional remodeling which include CFs proliferation and infiltration and growth of fibrous tissue, including collagen deposition (Frey *et al*., 2004). As a result, the pathological heart is frequently rich in CFs, which contribute to changing both structural and functional features of the diseased heart (Fredj *et al*., 2005). As described above CFs that interact with other fibroblasts and or to cardiomyocytes, may play a significant function in the electrical, mechanical, and biochemical performance of the diseased myocardium as well as in the structural and functional remodeling.

1.2.1 Cellular changes during cardiac hypertrophy

Cardiac fibroblasts (CF) constitute about two-thirds of the heart by cell number and about one-sixth by cell mass (Kamkin *et al*., 2003). CF have a number of properties with the potential to be pharmacologically regulated to beneficially alter the progress of cardiac disease including cell growth and division, production and remodeling of extracellular matrix, generation of secreted or diffusable local signalling molecules, and mobility (Heineke and Molkentin, 2006). Changes in myocardial structure and function in response to injury, collectively referred to as myocardial remodeling (Swynghedauw, 1999), may initially augment cardiac performance, but over the longer period may progress to a maladaptive response and heart failure. In terms of the cardiac myocyte, these alterations include myocyte hypertrophy; disarray of myocyte organization; and increased wall thickness, which in a majority of cases is followed by wall thinning and chamber dilation, with accompanying myocyte apoptosis or necrosis (Benerjee *et al*., 2006). Concomitant changes in cardiac fibroblasts include increased fibroblast proliferation as well as accelerated and aberrant remodeling of extracellular matrix and net accumulation of ECM, resulting in cardiac fibrosis (Lijnen and Petrov, 2003; Diez *et al*. 2001). This fibrosis may be reparative, replacing areas of myocyte

loss with structural scar, or reactive, involving diffuse increases in ECM deposition at sites unrelated to focal injury (Bellini and Mattoli, 2007). Differences in the characteristics of fibrosis are observed depending on the heart disease etiology. Fibrosis has important functional consequences for the heart. Firstly, increased ECM content results in exaggerated mechanical stiffness and contributes to diastolic dysfunction. Progressive increases in fibrosis can cause systolic dysfunction and left ventricular hypertrophy (LVH). Secondly, increased collagen content disrupts electrotonic connectivity between cardiac myocytes and provides an electrical substrate for reentrant arrhythmogenesis. Thirdly, perivascular fibrosis surrounding intracoronary arterioles impairs myocyte oxygen availability, reduces coronary reserve, and aggravates myocyte ischemia (Lijnen and Petrov, 2003). Within this framework, heart failure is characterized by substantial heterogeneity of disease severity and progression even in cases of comparable heart failure etiologies, apparently reflecting polygenic and environmental influences in the disease phenotypes of individual patients (Hilfiker-Kleiner *et al*., 2006).

1.2.2 Animal Models of Cardiac hypertrophy and Heart failure

Research using animal models normally aims to mirror a response in humans. These models are usually highly specific to a particular study. It is usually very difficult to obtain human tissue for experimental protocols. The use of human subjects is difficult because these studies would involve studying humans for a long period or in some cases throughout their lifetimes, which is impractical, or performing invasive procedures which are unethical (Shephard and Semsarian, 2009). For instance, mice are widely used because they are small, abundant and their genome is very similar to that of humans, which implies that most human genes have their exact homolog in mice. Transgenic animals are proving more vital in the discovery and development of new treatments and cures for many serious diseases. Therefore, animal models closely mimicking the characteristics and development of human

ventricular hypertrophy and heart failure are very important. Some of these models include pressure overload such as transverse aortic constriction, suprarenal aortic constriction, volume overload. (Jaarsma *et al*., 2005).

1.2.2.1 Pressure Overload

Models involving an abnormal pressure load have been most useful in the study of the pathogenesis of hypertrophy, subcellular failure, and vascular changes (Barbosa *et al*., 2005). Hypertrophy is associated with an increased risk for the development of heart failure. Induction of hypertension and ventricular hypertrophy should be considered when the evaluation of new treatment of heart failure is tested in an animal model. In order to create cardiac hypertrophy in animals, surgical procedures were developed that mimic coarctation of the aorta that result in pressure overload (Rockman *et al*., 1994; Dorn *et al*., 1994). The generation of these animal models of pressure overload, joint with the ability to genetically manipulate mice, has resulted in a number of important findings that have implications towards the clinical management of patients.

1.2.2.1.1 Aortic Banding

Pressure overload in response to aortic constriction is one of the most potent stimuli for hypertrophy. One of the most commonly used surgical intervention for pressure overload induced hypertrophy is coarctation of the ascending aorta i.e. aortic banding (Kerkela and Force, 2006). Transverse aortic constriction (TAC) in the mouse is commonly used as a surgical model of cardiac hypertrophy and subsequent failure. This system has been very well characterized and proven to be highly reproducible with a low mortality rate of 10-20% or less in experienced hands. Aortic banding is an excellent model system to evaluate the process of development of left ventricular hypertrophy in response to hemodynamic stress. Furthermore, after several months, a subset of animals progresses into heart failure (Zu, 2006).

1.2.2.1.1.1 Minimally invasive aortic banding in mice (MTAB)

Rockman and colleagues (1994), developed a model of transverse aortic constriction in the mouse. The use of this model has provided significant insight into the cellular and molecular pathways responsible for the development of left ventricular hypertrophy (LVH). While transverse aortic constriction in mice is now done routinely by a number of groups, the technical difficulty of the surgical procedure has limited the availability of this model. Development of minimally invasive model (Hu *et al*, 2003) has proved a significant advance on previous transverse aortic constriction (TAC) models. Previously, published methods for the creation of TAC in mice require microsurgical skills and the ability to provide mechanical ventilation when the thorax is entered. The requirement for tracheal intubation and low-volume, high-rate mechanical ventilation mandates additional time and expense associated with these procedures. Moreover, inflammatory reactions within the chest may cause difficulties of the analyses of cardiac function and pathology. The minimally invasive transverse aortic banding (MTAB) procedure in mice prevents the need for providing mechanical ventilation because the pleural space is not entered. The procedure can be performed rapidly and with low mortality. This approach produces consistent and sustained increases in LV pressure of 40–60 mmHg and approximately 50% cardiac hypertrophy over a period of 2-4 weeks (Hu *et al*., 2003).

1.2.3 Heart Failure

The incidence of heart failure mortality and morbidity is on the rise world wide (Bursi *et al*., 2006). Despite significant improvements in the medical therapy of congestive heart failure, the mortality rate is in excess of 50% after 5 years (Owan *et al*., 2006). Surgical treatment, including heart transplantation, cardiac bioassist techniques, and left ventricular assist devices, is used to interrupt the progression toward death. Research associated with heart failure has focused on identification, quantification, and

characterization of the injured tissue, evaluation of different therapeutic modalities, and understanding the mechanism of heart failure (Little *et al*., 2009; Kjaer, 2000). A requirement of all studies on heart failure is an adequate and appropriate model of heart failure. The ideal model should be able to reproduce each of the aspects of the progression of naturally occurring congestive heart failure. However, none of the models available is able to entirely reproduce congestive heart failure. Some models reproduce neuroendocrine changes (acute models) whereas others better reproduce the remodeling that occurs during chronic heart failure (chronic models). Therefore, the correct model should be used to evaluate specific aspects of the treatment of heart failure. Each model has inherent limitations including a lack of stability, a lack of predicability of damage, and a lack of adjustability (Goldberg, 2010; Monnet and Chachques, 2005). Much is being learned from large animals such as dog and pig, although small animal models (rat and hamster) have many favourable features, and as genetic methods and miniaturized physiologic techniques mature, the mouse is beginning to provide gene-based models of cardiac failure aimed at better understanding of molecular mechanisms (Hongo *et al*., 1997).

1.2.3.1 Animal models of heart failure

There are numerous animal models of heart failure including those occurring naturally and experimentally induced in normal animals. These models look like, at least in part, heart failure in humans, examples include dilated cardiomyopathy, myocardial ischemia and infarction which utilizes different species of animals such as large-breed dogs, Syrian hamsters etc (Skavdahl *et al*., 2005; Mann *et al*., 2005). Some of the models are being used increasingly while others are underused because of many reasons which include size of the animal, extent of investigation, predictable disease progression, and cost of the procedure (Monnet and Chachques, 2005).

1.3 Cardiac Fibroblast-Myocyte Interaction in pathological heart

A number of disease conditions of the heart are linked with structural and functional remodeling which include CF proliferation and infiltration and growth of fibrous tissue, including collagen deposition (Bronzwaer and Paulus, 2005). The pathological heart is frequently rich in CF, which contribute to changing both structural and functional features of the diseased heart (Flack *et al*., 2006). As described in section 1.1.1.1, CF that interact with other fibroblasts and/or cardiomyocytes, may play a significant function in the electrical, mechanical, and biochemical performance of the diseased myocardium and structural and functional remodeling. Matsushita and Takamatsu, in 1997, reported broad changes in distribution of gap junction and cell coupling in a model of sheep coronary occlusion infarct (from 12 h to 4 weeks after infarction). In this study they found that Cx43 displayed a more punctate discrete configuration along the surface of structurally compromised myocytes that interact with CF in the infarct border zone, in contrast to the normal localization of Cx43 in the intercalated disks between myocytes. This shows that remodeling after myocardial infarction could affect Cx43 structure and possibly function.

Differences were observed in the connexin distribution in this model compared with other reports in human and rat scar tissue models (Smith *et al*., 1991). Based on connexin patterns, two spatially and temporally separate CF phenotypes were recognized. These were Cx45 expressing CF which become visible in the damaged tissue within a few hours after infarction and reach their peak concentration after 1 week and Cx43 expressing CF, which become visible at a later stage with their concentration continues to increase until at least 4 weeks after infarction (Camelliti *et al*., 2004). These CF expressing Cx43 and Cx45 were found in close contact to myocytes at the infarct border zone. It will be important to assess the physiological

significance of this finding and its role in the remodeling process after infarction.

Recently, the role of the transcription factor–encoding gene Krüppel-like factor 5 (Klf5), which is mainly expressed in CF in the adaptive response of the heart to pressure overlaod was examined (Takeda *et al*., 2010). The authors used cardiac myocyte specific Klf5 deletion mouse and CF specific deletion of Klf5 mouse. This study demonstrated the potential importance of CF in hypertrophy that Klf5 in fibroblasts is important for the response to pressure overload. It also showed that CF play an essential role in the myocardial adaptive response to pressure overload, and this function could be partially regulated by Klf5.

Taken together these studies have shown that apart from the importance of physical connections between CF and myocyte, CF responds to a wide range of humoral and mechanical inputs via cell surface receptors (Gaudesius *et al*., 2003). These environmental stimuli are incorporated through receptor-mediated signalling pathways like the mitogen activated protein kinase (MAPK) leading to activation of nuclear transcription factors and altered gene expression (Kyriakis and Avruch, 2001). This is also evident by the ability of these cells to react to both inflammatory and fibrogenic growth factors with different phenotype, and to secrete extra autocrine and paracrine mediators that amplify signals from the initial stimuli (Stewart *et. al*., 2006). On the other hand, in cardiac hypertrophy, CF perform crucial roles in remodeling characterized by myocyte death or hypertrophy, migration and proliferation of fibroblasts and changes in the synthesis and deposition of ECM (Flack *et al*., 2006). While such events serve primarily as an adaptive response that may boost cardiac function, in the long term this develops to maladaptation and eventually heart failure. This means that the change of ECM and the CF contained within are essential not only to normal cardiac function but also in pathological conditions.

1.4 Mitogen activated protein kinase (MAPKs) signalling pathways and their functions

Phosphorylation and dephosphorylation of proteins are widely known as vital mechanism for controlling cellular function by a diversity of physiological stimuli (Dhanasekaren and Johnson, 2007). Protein phosphorylation acts as an essential mechanism in regulating many cellular functions thereby controlling the function of many organs. For example in the heart it acts by modulating specific levels of autonomic control on cardiac force/length relationships, Ca^{2+} handling regulation, contraction and transcription (Rapundalo, 1998). A major pathway involving the phosphorylation and activation of kinases is the mitogen activated protein kinase pathway (Kyriakis and Avruch, 2001). This pathway is known to play a central role in a vast array of physiological and pathological processes including growth, differentiation, apoptosis.

Between the late 1980s and early 1990s the sequences of the first mammalian MAP kinases ERK1, ERK2 and ERK3, were identified, demonstrating that these enzymes were members of a newly identified protein kinase family (Boulton *et al*., 1990; Boulton *et al*., 1991). Mitogen activated protein kinases comprise a conserved family of enzymes that regulate a large number of physiological functions in the cells which include embryogenesis, proliferation, differentiation, development, immune function, stress responses and apoptosis (for review see Kyriakis and Avruch, 2001). Mammalian MAPKs consist of 3 major groups which are classified based on sequence similarity, differential activation by agonists and substrate specificity, these include extracellular signal-regulated kinases (ERK1/2), c-Jun N terminal kinases (JNK1/2/3), and p38 MAPK. (See figure 1.2) MAPKs are activated (in many cells) by a wide range of stimuli such as serum, growth factors for example, PDGF and EGF, environmental stresses such as osmotic shock, UV light and cytokines such as TNF alpha (Torii *et al*., 2004).

These and other stimuli act through different receptor families that are coupled to MAPK pathways and include; G-protein-coupled receptors (GPCRs), receptor tyrosine kinses (RTKs), transforming growth factor β receptor (TGFR), cytokine receptors, or via protein kinase C (PKC) isoforms, calcium, or stress stimuli (Schramek, 2002). Activation of MAPKs occur through the phosphorylation upon the threonine and tyrosine residues within a conserved signature sequence TxY by a MAPK kinase (MKK or MEK) which is in turn phosphorylated and activated by a MAPK kinase kinase (MKKK or MEKK), (See Figure 1.2). These kinases are in turn regulated by a series of protein molecules which link the MAPK pathway to the receptor involved. Once activated JNKs, ERKs and p38 MAPK each phosphorylate a wide range of cytosolic and nuclear substrates, which includes numerous transcription factors (eg c-jun. c-fos, elk-1) resulting in the reprogramming of cellular gene expression (Turjanski *et al*., 2007; Molkentin and Dorn, 2001). The constituent kinases of the MAPK cascade may interact sequentially, but can also be organised into signalling complexes through interaction with specific scaffold proteins.

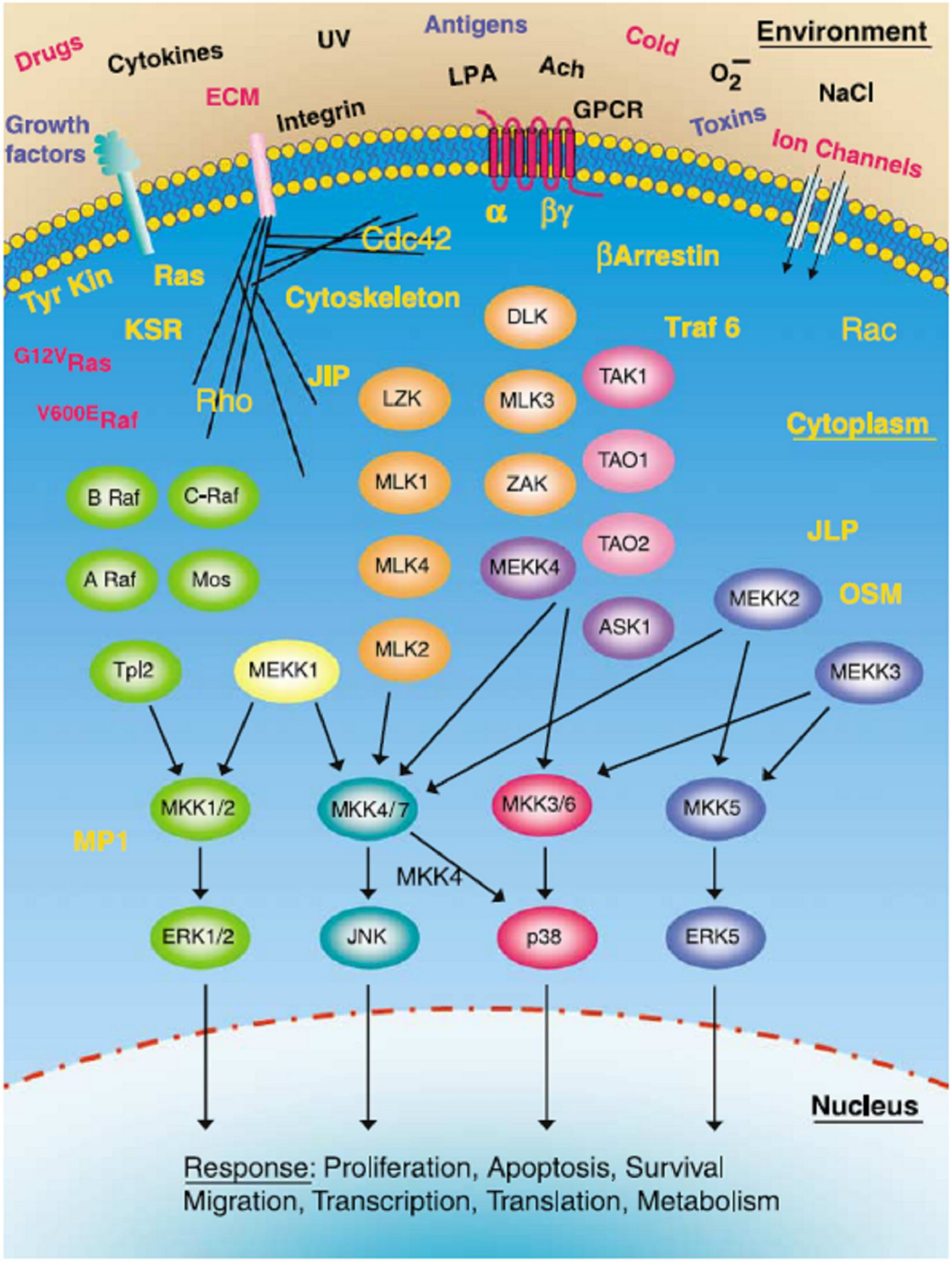

Figure 1.2: Integration of the MAPK pathway in the cellular response to environmental stimuli (Adapted from Dhanasekaran and Johnson, 2007).

Interactions among components of the MAPK signalling pathways occur in many ways to generate responses and moderate cellular outputs. Substantial data demonstrates that MAP kinases have both distinct and overlapping substrate specificities (Lewis *et al*., 1998; Waskiewicz *et al*., 1997). For example, it was reported that in PC12 cells, epidermal growth factor (EGF) transiently stimulates ERK1/2 leading to cellular proliferation. However, in contrast, nerve growth factor (NGF) stimulation leads to the sustained activation of ERK1/2 and subsequently leads to neuronal differentiation (Kao *et al*., in 2001). This is linked to nuclear translocation of ERK. As mentioned earlier, studies using knockout mice have been valuable in revealing vital information regarding the physiological functions of many signalling pathways. The resulting activities of the substrates reflect the combination of kinase mediated and overall output of the pathway. The MAPK signalling pathways also form complexes that aid their activation and influence their localization, specificity, and substrates (Choi *et al*., 1994; Marcus *et al*., 1994; Yasuda *et al*., 1999). Possible scaffold proteins and adaptor or linker molecules have been found for some of the kinase modules which facilitate activation. However, the regulation of complex formation by these intermediates also provides another site for cross talk between MAPK signalling pathways.

1.4.1 Extracellular Signal-Regulated Kinase (ERK) Pathway

As outlined above the most well known and best-characterized members of the MAPK family, the ERKs consist of at least six isoform family members (ERK1–5 and ERK7/8). The most studied among these are ERK1/2 and ERK-5. ERK1 and ERK2 are activated by a pair of closely related MEKs, MEK1 and MEK2. Both of these MEKs have been shown to fully activate ERK1/2 *in vitro* (Zheng and Guan, 1993; Goldsmith and Cobb, 1996). ERK1/2 were the first members to be characterized and ERK1 (p44 MAPK) and ERK2 (p42 MAPK) share 83% identity and are regulated by similar factors and conditions (Ray and Sturgill, 1988; Bogoyevitch and Court, 2004). Both ERK1/2 are found in the human, mouse, rat and zebrafish genomes (Jonhson *et al*., 2005; Saba-El-

Leil *et al*., 2003). The signalling events activating ERK1/2 are usually initiated at the plasma membrane principally via receptor tyrosine kinases, GPCRs and channels, in part, through the Raf-MEK1/2-ERK cascade (Schramek, 2002). The physiological responses regulated depends on cell surface receptor density, the amount of ligand, the duration of signalling and the cell type under consideration and the subcellular distribution of ERK itself (McKay and Morrison, 2007).

1.4.1.1 ERK pathway in the heart

Early studies on ERK have demonstrated that it has numerous functions. In the immune system it has been shown that, in ERK1 KO mice, thymocyte maturation beyond the CD4+CD8+ stage was reduced by half, with a similar reduction in the thymocyte subpopulation expressing high levels of T cell receptor (Page's *et al*., 1999). Apart from its function in immunity system development, ERK has been implicated in neuronal synaptic plasticity and necessary for several forms of learning. In mice deficient of ERK1, an improvement of striatum-dependent long-term memory has been reported, which correlates with a facilitation of long-term potentiation in the nucleus accumbens (Mazzucchelli *et al*., 2002). Some studies have also implicated the role of ERK pathway in adipocyte differentiation and regulation of adiposity and high-fat diet induced obesity (Saba-El-Leil *et al*., 2003; Bost *et al*., 2005)

Most of the early studies on the role of ERK in the heart were mainly conducted in ischemia models (Mizukami and Yoshida, 1997). The ERK cascade has been shown to be activated during ischemia in the rat and pig *in vivo* models, in neonatal rat cardiac myocytes (Barancik *et al*., 1997; Yue *et al*., 2000; Yoshida *et al*., 2001), and in human hearts (Talmor *et al*, 2000). Some studies demonstrated that ERK activation was observed during ischemia and reperfusion in human, bovine, rat and guinea pig heart (Knight and Buxton, 1996; Takeishi *et al*., 2001). Other studies reveal that the activation of ERKs plays a vital role in prevention of myocardial necrosis and cell death (Fryer *et*

al., 1995; Ping *et al*., 1999). It has also been demonstrated that inhibition of the ERK cascade during sustained ischemia or ischemia/reperfusion considerably increased the size of myocardial infarction in pig myocardium, excessive reperfusion injury in isolated rat hearts and enhanced ischemia/reperfusion-induced cell death in neonatal myocytes has also been reported (Strohm *et al*., 2000; Yue *et al*., 2000).

Both ERK1 and ERK2 have been identified in neonatal and adult ventricular myocytes. Endothelin-1 (ET-1), phenylephrine, angiotensin II (Ang II) and isoprenaline all activate the MAPK signalling cascade in cardiac ventricular myocytes (Clerk *et al*., 2001). Although it appears that each of these agonists attain ERK activation by different pathways (Lazou *et al*., 1994; Bogoyevitch *et al*., 1994; Clerk *et al*., 1994; Sodoshima *et al*., 1995). Similarly, MAPK activity has also been investigated in rat cardiac fibroblasts (Bogoyevitch *et al*., 1994). Stimulation of cardiac fibroblasts with angiotensin II or platelet-derived growth factor (PDGF) leads to activation of ERK and proliferation of these fibroblasts (Booz *et al*., 1994; Bogoyevitch *et al*., 1994). Whilst these and other studies clearly demonstrate that ERK has a potential role in cardiac pathophysiology, more recent studies have used genetic manipulation of ERK to drive better quality information regarding the role of ERK in the heart (Purcell *et al*., 2007).

1.4.1.1.1 Over-expression/Transgenic studies

Over-expression studies using mutated components of the ERK pathway including constitutively active or dominant negative mutants have been used to explain the role of this cascade in the heart (Raman *et al*., 2007). It has been reported that cardiac expression of a constitutively active Ras-mutant (H-v12-Ras), induced substantial left ventricular hypertrophy, decreased contractility, diastolic dysfunction linked with interstitial fibrosis, induction of the fetal-gene program and sudden death (Mitchell *et al*., 2006; Zheng *et al*., 2004). Also, stable activation of MEK1 by over-expression of a MEK1-mutant, MEK1

^{S217E,S221E}, which activated Raf-1 phosphorylation, caused left ventricular hypertrophy (Bueno *et al*., 2000). The induction of cardiac hypertrophy in these mice was independent of transgene expression levels and hearts showed improved systolic but decreased diastolic function and increased expression of hypertrophic markers (such as ANF, BNP, α- skeletal actin and β-MHC) (Mitchell *et al*., 2006). Both studies demonstrated an increase in hypertrophy in these mice although Ras activation causes marked effects compared with MEK1 activation.

Studies using dominant negative mutants have been used to investigate the physiological function of ERK1/2. Mice with cardiac specific over-expression of a dominant-negative Raf mutant (Raf-1^{K375H}) had no obvious phenotype, but exhibited little hypertrophy and hypertrophic gene expression (e.g. ANF, β-MHC) in response to cardiac pressure overload (transverse aortic constriction (TAC)) (Harris *et al*., 2004; Muslin *et al*., 2008; Wang *et al*., 2007). In spite of this, cardiac myocyte apoptosis and animal mortality were considerably enhanced subsequent to TAC. The activity of ERK1/2 was decreased in these mice, signifying that Raf-1 signalling is essential for the induction of cardiac hypertrophy and for myocyte survival in response to pressure overload.

In general, over-expression studies showed that the activation of ERK, in heart after pressure overload adds to the development of pathological cardiac hypertrophy.

1.4.1.1.2 Gain or loss of function studies

It was obvious that studies *in vitro* alone would not give substantial information on the physiological role of the Raf/MEK/ERK1/2 pathway and hence it is necessary to employ *in vivo* gain or loss of function studies in mouse mutants in order to identify specific role of this pathway in the heart. Studies in heart specific Raf-1 KO mice demonstrated normal weight and cardiac myocyte size, systolic dysfunction and dilatation and an increase in number of apoptotic cells (Giroux *et al.,* 1999; Hindley and Kolch, 2002; Mikula *et al*., 2001; Yamaguchi *et al*., 2004). However, ERK1/2 signalling was not affected in these hearts, possibly because the absence of Raf-1/ERK function was compensated by other proteins, such as other Raf-isoforms.

Similarly, Purcell *et al*., in 2007, reported that when ERK1 ($ERK1^{-/-}$) KO mouse and heterozygous ERK2 ($ERK2^{+/-}$) where exposed to pressure overload and to exercise, these mice exhibited a normal hypertrophic response. In another study to inhibit the activity of ERK a model was developed in which MKP-3 was inducibly expressed in cardiac tissue (Luttrell and Luttrell, 2003; Owens and Keyse, 2007; Purcell *et al*., 2007). ERK1/2 activation was induced in response to pressure overload and phenylephrine infusion, over-expression of MKP-3 totally abolished ERK phosphorylation, whereas ERK5, JNK and p38 MAPK were not affected. Furthermore, the extent of left ventricular hypertrophy following exposure to TAC, neuroendocrine agonist infusion and exercise was basically the same in both $ERK1^{-/-}$ and $ERK2^{+/-}$ compared to non-transgenic mice. However, fibrosis and apoptosis were enhanced in MKP-3 transgenic hearts in response to TAC. As described above there are quite a number of studies that demonstrated the role of MEK and ERK1/2 in the induction of cardiac hypertrophy, however, this latter mouse model supported the theory that cardiac hypertrophy can progress independently of ERK1/2 and also suggests that ERK1/2 plays a protective function under stress conditions.

These data demonstrate that in terms of normal ERK1/2 activity in the heart, Raf-1 may encourage myocyte survival via a MEK/ERK independent mechanism.

1.4.1.1.3 Pharmacological inhibition studies

Whilst over-expression and gene deletion studies in mice generate important information an additional approach involves the use of kinase inhibitors. Two such pharmacological inhibitors, U0126 and PD98059, have been used *in vitro* and *in vivo* to inhibit specifically MEK function (Munzel *et al*., 2005). It was reported that neither dominant-negative ERK1 and 2 nor PD98059 were sufficient to block isoprenaline induced ANF promoter activity in cultured myocytes, suggesting that ERKs are not important for ANF gene expression (Post *et al*, 1996). In another study to examine the role of ERK in response to hypertrophic agonists ET-1 and PE in rat cardiac myocytes, administration of U0126 inhibited increase in cell size, sarcomeric reorganization and ANF production induced by the these agonists (Yue *et al*., 2000). However, in a recent study to establish the significance of ERK1/2 in the early cardiac myocyte transcriptomic response to endothelin-1, the authors used RNA expression analysis using microarrays and qPCR. Cardiac myocytes were exposed to ET-1 for 1 h with or without PD184352 (to inhibit ERK1/2). ERK1/2 signalling positively regulated about 65% of the early gene expression response to ET-1 with a small (about 2%) negative effect (Marshall *et al*., 2010). It was reported that PD98059 did not inhibit the activation of MAPKK and MAP kinase homologues in response to osmotic shock and IL-1 stimulated kinase pathways in PC12 cells *in vitro* (Alessi *et al*., 1995).

These data suggests that ERK1/2 could play an important role in regulating the early stages of myocyte hypertrophy.

1.4.2 Big mitogen-activated protein kinase-1 (BMK-1/ERK5)

In addition to the classical ERK1/2 is ERK5, also known as big MAP kinase 1 (BMK1), found in human, mouse, rat, frog and zebrafish (Nishimoto *et al*., 2005). Activation of ERK5 is mediated by MEK5. The ERK5 pathway is activated by oxidative stress, hyper-osmolarity and growth factors (Hayashi et al, 2004). ERK5 has a single carboxy-terminal domain, which interacts with the transcription factor myocyte enhancer factor 2 (MEF2). The functional role of ERK5 has been extensively characterized (see review by Wang and Tournier, 2006) and a number of studies have indicated its importance in cardiac function. In particular, the targeted deletion of the ERK5 and MEK5 genes in mice has provided genetic evidence for an important role of the ERK5 signalling pathway during heart development (Wang, and Tournier, 2006). However, mice die around embryonic day 10 (E10) due to cardiovascular defects that include disorganisation of the trabeculae and underdevelopment of the myocardium. The normal development of mice lacking ERK5 in cardiomyocytes confirms that the abnormal development of the heart displayed by the ERK5 KO embryo is a result of abnormal vasculogenesis and angiogenesis (Hayashi and Lee, 2004; Yan *et al*, 2003). Therefore, the role of ERK5 in adult cells *in vivo* remains unclear.

1.4.3 C-Jun NH_2-terminal kinase (JNK)

As outlined in section 1.4 an additional MAPK family also consists of the JNK family which are activated by stress, cytokines, and growth factors. These stimuli activate the signalling cascade comprising of MAPKKK-MKK4/7-JNK (Bogoyevitch and Kobe, 2006; Raman *et al*., 2007; Roberts and Der, 2007). More specifically, JNK-related MAPKKKs are composed of MEKK1, MEKK4, dual leucine zipper-bearing kinase, MLK1–4, leucine zipper-bearing kinase, TAK-1, ASK1, and zipper sterile-α-motif kinase and in turn, these signal via MKK4 and MKK7, activating the JNKs (Raman *et al*., 2007; Roberts and Der, 2007). The JNK family consists of three isoforms, JNK1, JNK2, and JNK3,

which are divided into splice variants. The 4 splice variants of JNK1 are given as follows: 1 and 1 splice forms (p46) and 2 and 2- splice forms (p54) (Bogoyevitch and Kobe, 2006). The 1 and 1 splice forms (p46) differ from each other by alternative exon usage, leading to replacement between kinase domains IX and X, which decide substrate specificity. The same exon usage distinguishes the difference between the 2 and 2 splice forms. The p46 vary from the p54 splice forms by the C-terminal region that is on the other hand spliced. The functional significance related with the longer C-terminal region found in p54 and lacking in p46 remains uncertain (Tsuiki *et al*., 2003). JNK2 also has splice variants (1, 2, 1, and 2) and molecular masses similar to that of JNK1, whereas JNK3 has only the 1 (p46) and 2 (p54) splice forms (Waetzig and Herdegen, 2005). Based on the available literature very few studies compare the effects of all 10 splice variants in a single biological system. Both JNK1 and JNK2 are widely expressed, whilst JNK3 is restricted to the brain, heart and testis. As with ERK, JNK has a number of key substrates which mediate the action of the kinase. These include transcription factors such as c-jun, JDP2, ELK-1, p53 etc. In addition a number of cytosolic substrates have been identified including Bcl2, Bim, Bax, akt etc. (Gupta *et al*., 1996; Yang *et al*., 1998; Tsuiki *et al*., 2003).

1.4.3.1 JNK pathway in the heart

Similar to ERK, early studies on JNK indicated that it has many functions (Tournier *et al*., 2000). In the innate immune response, it has been shown that in fibroblasts, the deficiency of JNK2 resulted in severe reduction of multiple cytokines production including type I interferon and IL-6 (Chu *et al*., 1999). In adaptive immune response, the study of JNK1 and JNK2 KO mice discovered the critical roles of JNK in CD4+ T cell proliferation and effector T cell function (Dong *et al*., 2001; Dong *et al*., 2002). Th cells from the JNK1 KO mice displayed greatly reduced JNK activity after activation. These mice exhibited an exaggerated Th2 response which led to greatly exacerbated disease with failure to heal skin lesions upon Leishmania infection (Constant *et al*., 2000).

The role for JNK1 in mediating insulin resistance in Type 2 diabetes has been indicated (Hirosumi *et al*., 2002). However, the study of JNK2 KO mice has involved this isoform in the development of non-obese Type 1 diabetes, via the JNK2 dependent effects on cytokine production (Jaeschke *et al*., 2005). In the same way, the loss of JNK1 or JNK2 expression influenced different features of arthritis, with loss of JNK2 displaying enhanced arthritic scores (Han *et al*., 2002). There is clear indication that JNK1 and JNK2 are involved in apoptotic signalling and most of these studies used to UV irradiation, DNA-alkylating agent methyl methanesulfate and translation inhibitor anisomycin to induce apoptosis (For review See Bogoyevitch *et al*., 2004; Tournier *et al*., 2000).

In the heart, JNK signalling pathway shows a different pattern of activation compared to ERK and p38 MAPK (Kuida K, Boucher DM. (2004). Some studies demonstrated that JNK pathway is moderately or not activated during ischemia. In spite of this, a stronger activation of JNKs was observed during reperfusion following a transient ischemic stimulus (Bogoyevitch *et al*., 1996; Knight and Buxton, 1996). The exact role of JNK in the pathophysiology of ischemic injury remains unclear.

1.4.3.1.1 Over-expression/Transgenic studies

While activation of the ras-Raf-MKK-ERK cascade in the heart promotes cardiac hypertrophy, studies have suggested that components of the JNK pathway do not. Transgenic mice were generated with cardiac specific over-expression of a constitutively activated form of MKK7, called MKK7D (Petrich *et al*., 2004). These mice exhibited increased activation of both JNK1 and JNK2 in cardiac tissue, without activation of ERK1/2 or p38α and died at around 7 weeks of age with signs of congestive heart failure including edematous lungs and ascites. Although there was biatrial enlargement in transgenic MKK7D mice, there was no left ventricular hypertrophy and cardiomyocyte cell size was not increased. However, ANF and α-skeletal actin

mRNA levels were increased in MKK7D cardiac tissue. Diastolic left ventricular filling was impaired in MKK7D transgenic mice. Interestingly, MKK7D mice also exhibited reduced connexin 43 protein levels and gap junction formation between cardiomyocytes in ventricular sections (Petrich *et al*., 2004).

In related work, transgenic mice with cardiac specific over-expression of an MKK7-JNK1 fusion protein were generated and found to have normal ventricular weight at baseline, but resistance to cardiac hypertrophy induced by over-expression of calcineurin A (Liang *et al*., 2003). The ability of JNK1 activation to antagonize calcineurin A-induced cardiac hypertrophy may be explained by the ability of JNK1 to phosphorylate members of the nuclear factor of activated T cell transcription factor family (NFATs), thereby preventing their nuclear translocation. Indeed, over-expression of JNK1 and MKK7 in cultured cardiomyocytes blocked calcineurin A-induced nuclear translocation of an NFATc3-green fluorescent protein fusion protein (Liang *et al*., 2003).
Overall over-expression studies suggest that JNK activation leads to reduced gap junction formation and promotes cardiac hypertrophy.

1.4.3.1.2 Gain or loss of function studies

A similar series of knockout studies and gain of function approaches have also been used to assess the role of JNK in the heart (Liang *et al*., 2003). Mice either homozygous or heterozygous for JNK isoforms ($JNK1^{-/-}$, $JNK2^{-/-}$, $JNK1^{+/-}$), or with cardiac-specific over-expression of dominant negative forms of JNK1 and JNK2 (MHC-DN-JNK1/2) were subjected to pressure overload by TAC. While $JNK1^{-/-}$ and $JNK2^{-/-}$ mice developed cardiac hypertrophy to a similar extent as wild type mice, $JNK1^{+/-}$ mouse and MHC-DN-JNK1/2 transgenic mice developed an exaggerated form of cardiac hypertrophy in response to TAC. In addition, 7 month-old $JNK1^{+/-}$ mouse and MHC-DN-JNK1/2 transgenic mice developed spontaneous cardiac

hypertrophy with cardiac myocyte enlargement in the absence of pressure overload (Liang *et al*., 2003). As highlighted above, MHC-DN-JNK1/2 also exhibited increased cardiac NFAT activity measured by use of an NFAT binding element-luciferase reporter construct.

Recently Tachibana *et al*., 2007, has also used knockout model to investigate the role of JNK1, JNK2 and JNK3 in response to pressure overload. These mice were subjected to TAC for 7 days and the results showed that although all the mice developed significant hypertrophy, no difference was observed between the KOs and the wild type counterparts. Tachibana and co workers also used echocardigraphy to examine the cardiac function in response to TAC, both JNK2 and JNK3 KO mice showed no difference in heart function compared with the wild type. On the contrary cardiac function was significantly decreased in JNK1 KO after 3 and 7 days of pressure overload, with intact left ventricular end-diastolic dimension (LVEDD) and considerable increase in left ventricular end-systolic dimension (LVESD), causing a decline in fractional shortening compared with the wild type littermates. JNK1 KO mice showed an irregular reaction to TAC revealed by reduced fractional shortening 12 weeks after the surgery which ultimately returned to normal.

Taken together these data demonstrate that JNK performs a protective function to keep left ventricular systolic function in the early phase following pressure overload.

1.4.3.1.3 Pharmacological inhibition studies

Recently, JNK specific inhibitors namely CEP-1347 and SP600125 have been developed and used extensively (Barr *et al*., 2002). One study demonstrated that, without trophic effect, the death of cultured rat embryonic neurons was accompanied by 4-fold increases in JNK activity. CEP-1347 both rescued the neurons and inhibited JNK activation. This was the first demonstration that

this molecule improves motorneuron survival and that concurrently inhibits the JNK1 signalling cascade (Maroney *et al*., 1998). Another study demonstrated in a hamster model of dilated cardiomyopathy that chronic treatment with SP600125 improved cardiac myocyte apoptosis and deteriorated pathology. To date, neither this nor other JNK targeted inhibitors have been used in other hypertrophy or other heart failure models *in vivo*. (Bogoyevitch *et al*., 2004). Similarly, the apoptosis of cardiac myocytes using a rat cardiac I/R animal model was inhibited by a JNK inhibitor (Ferrandi *et al*., 2004). In summary, more studies *in vivo* are required in order to ascertain the exact functional significance of pharmacological inhibition of JNK.

1.4.4 p38 MAPK

Another member of the MAPK pathway activated by stress, cytokines, growth factors and other agents such as AMPK (Du *et al*. 2005) is p38 MAPK. This signalling module consists of MAPKKK- MKK3/4/6-p38MAPK (Roberts and Der, 2007; Han and Sun, 2007). The MAPKKKs are composed of MLK2 and MLK3, dual leucine zipper-bearing kinases, ASK1, MAP three kinase-1, and TAK-1. These kinases, in turn, activate MKK3/4/6, which phosphorylate p38 MAPK (Brancho *et al*., 2003; Han and Sun, 2007; Raman *et al*., 2007; Roberts and Der, 2007). The p38 MAPK family, which is also part of the stress activated MAPK is comprised of four isoforms (α, β , γ , and δ). Expression patterns differ depending on the isoform, p38 α and β MAPKs, which are the most extensively studied of family members, are widely expressed (Cuenda and Rousseau, 2007; Mayor *et al*., 2007). In contrast, p38 γ MAPK is expressed mainly in skeletal muscle, whereas p38 δ MAPK is expressed in small intestine, pancreas, testis, and kidney. In addition, the level of expression of these isoforms as well as their upstream activators, MKK3 and MKK6, differ across cell types (Adams *et al*., 2000). Also numerous transcription factors have been demonstrated to be phosphorylated and activated by p38 MAPK. These transcription factors include activating transcription factor-2 (ATF-2), ATF-1, SRF accessory protein 1 (Sap1), CHOP (growth arrest and DNA

damage inducible gene 153, or GADD153), p53, C/EBP, myocyte enhance factor 2C (MEF2C), and MEF2A (Raingeaud *et al*., 1996; Tan *et al*., 1996).

Numerous studies using expression of dominant negative mutants, isoform specific knockout mice and pharmacological inhibitors in particular SB203580 have identified a number of important functions in pathophysiology. The p38α knockout mice are lethal due to defects in placental angiogenesis (Mudgett *et al*., 2000; Adams *et al*., 2000). Mice deficient of p38β, p38γ or p38δ survive normally and do not show any apparent phenotypes. Also the p38γ or p38δ double knockout mice were viable and fertile and had no obvious health problems. Although some studies have suggested the role for p38 MAPKs in inflammatory responses, these knockout mice do not show pathological changes, which suggests an indistinct physiological functions for p38β, p38γ and p38δ (Kuida and Boucher, 2004; Beardmore *et al*., 2005; Sabio *et al*., 2005).

1.4.4.1 p38 MAPK pathway in the heart

Similar to ERK and JNK, p38 MAPK was first known for its role in inflammation in regulating the biosynthesis of pro-inflammatory cytokines, namely IL-1 and TNFα, in endotoxin-stimulated monocytes (Lee *et al*., 1994). The role of p38 MAPKs in cellular differentiation has been established (Roux and Blenis, 2004). Furthermore, its role in the differentiation of skeletal muscle and stem cells, suggests that this pathway could be an important regulator of both tissue regeneration or cell renewal processes elicited in response to tissue lost or damage. The role of p38 MAPK in cell migration has been demonstrated (Rousseau *et al*., 1997). The role of p38 MAPK in Alzheimer's disease has been investigated. Aberrantly activated p38 MAPK have been reported to be associated with cells that contain filamentous Tau in some neurodegenerative diseases. Based on this finding it was suggested that this pathway may contribute to the hyperphosphorylation of Tau protein (Zhu *et al*., 2001).

Similar to the ERK cascade the role of p38 MAPK in myocardial responses to ischemic injury has been extensively investigated, but most of these studies are controversial. Inrespective of the species or model these studies have demonstrated that activation of p38 MAPK occurs either during ischemia only, or continue throughout reperfusion, and others reported a negative role of p38 MAPK during ischemia/reperfusion injury. It has been reported that inhibition of p38 MAPK activation obstructed the growth of infarcts, increased cell survival, reduced myocardial cell death and enhanced postischemic recovery of cardiac function (Ma *et al*., 1999; Schneider *et al*., 2001). On the contrary, others established that the inhibition of p38 MAPK during lethal ischemia did not affect the degree of ischemia/reperfusion-induced injury or even increased it which suggests that p38 MAPK activation may play a protective role during ischemia (Mocanu *et al*., 2000; Nakano *et al*., 2000).

1.4.4.1.1 Over-expression/Transgenic studies

Activation of the p38 MAPK pathway in cardiac tissue does not encourage cardiac hypertrophy as demonstrated by transgenic mice with cardiac specific over-expression of activated mutant forms of MKK3 (MKK3bE) and MKK6 (MKK6bE) (Liao *et al*., 2001). Both MKK3bE and MKK6bE transgenic mice exhibited increased p38 MAPK kinase activity in cardiac tissue but died between 5 and 7 weeks of age with signs of congestive heart failure. Neither MKK3bE nor MKK6bE transgenic mice develop left ventricular hypertrophy or cardiac myocyte enlargement, though they both develop biatrial growth. Substantial interstitial cardiac fibrosis was observed in both types of transgenic mice, and ANF, β-myosin heavy chain, and α-skeletal actin mRNA levels were increased. Left ventricular systolic function was depressed in MKK3bE mice with decreased left ventricular wall thickness, but systolic function was not reduced in MKK6bE mice. Both types of transgenic mice demonstrated increased diastolic chamber stiffness (Liao *et al*., 2001).

To further investigate the role of p38 MAPK in cardiac hypertrophy, transgenic mice with cardiac specific over-expression of a dominant negative form of p38α or p38β were examined (Zhang *et al*., 2003; Wang *et al*., 1998). Both DN-p38α and DN-p38β transgenic mice exhibited cardiac hypertrophy to a comparable degree as nontransgenic mice, though there was a tendency towards greater hypertrophy in DN-p38β mice. In addition, the authors reported that both DN-p38α and DN-p38β transgenic mice showed reduced interstitial fibrosis following TAC when compared to nontransgenic mice. In contrast, Braz *et al*., 2003 showed that transgenic mice over-expressing cardiac specific DN-p38α, DN-MKK3, or DN-MKK6 all exhibited significant cardiac hypertrophy in response to pressure overload induced by TAC with increased myocyte size. Moreover, the entire 3 types of transgenic mice demonstrated spontaneous cardiac hypertrophy in the absence of pressure overload.

Altogether, over-expression and transgenic studies demonstrated that p38 MAPK activation promotes cardiac fibrosis and hypertrophy.

1.4.4.1.2 Gain or loss of function studies

In order to investigate the role of p38α *in vivo*, Nishida *et al*., in 2004 created mice with floxed p38α alleles and crossbred them with mice expressing the Cre recombinase under the control of the α-myosin heavy-chain promoter to generate cardiac myocyte specific p38α KO mice. Administration of pressure overload by TAC, resulted in cardiac hypertrophy in p38α KO mice which was similar but somewhat greater in degree than control mice. Also, cardiac myocyte apoptosis and fibrosis was significantly increased following TAC in p38α KO mice. In this study, low-level and/or transient p38α activation was found to have a vital anti-apoptotic function in myocytes, however high-level and/ or prolonged p38α activation promoted apoptosis.

1.4.4.1.3 Pharmacological inhibition studies

As mentioned earlier besides its role in gene regulation, p38 MAPK is implicated in the control of myocyte contractility and cell death. This is being best elucidated using the p38 MAPK inhibitor SB203580. Activation of p38 MAPK leads to decreased contractility with no effect on intracellular calcium cycling (Liao *et al*. 2002). Further investigation revealed that the negative inotropic effect of p38 MAPK activity seems to be an epigenomic occurrence because it is both rapid and reversible and also the alteration of sarcomere proteins observed in p38 MAPK activated heart is related with decreased force generation in isolated myofilaments (Vahebi *et al*., 2007).

The role of p38 MAPK in cardiac protection or as proapoptotic in the heart is contentious. Some studies have demonstrated that inhibiting p38 MAPK activity in cultured myocytes or whole heart decreased apoptotic cell death under stress stimulation such as pressure overload or ischemia-reperfusion (Kerkela *et al*., 2006; Baines and Molkentin, 2005). So inhibition of p38 MAPK is constantly seen to enhance cardiac function and diminish remodeling in the heart following ischemia-reperfusion injury or infarction (Li *et al*., 2004; Kaiser *et al*., 2004; Ren *et al*., 2005). In spite of this, Kaiser *et al*., 2005 also demonstrated that such useful effect was not observed in pig, signifying species specificity. In contrast, specific activation of p38 MAPK in the heart is not adequate to induce myocyte apoptosis (Petrich and Wang, 2004). Also cardiac specific inactivation of p38 MAPK leads to decreased apoptosis in response to pressure overload (Nishida *et al*., 2004). In addition, Martindale *et al*., 2005 showed that activation of p38 MAPK in the heart led to small heat shock protein phosphorylation linked with better protection against ischemia-reperfusion injury.

In recent times, some studies have suggested a novel and fascinating role for p38 MAPK in regulating proliferation in terminally differentiated cardiac

myocytes (Engel *et al*., 2005). Initially, Engel *et al*., 2005, assessed proliferation of neonatal cardiac myocytes by stimulation with FGF1 in the presence of p38 MAPK inhibitor (SB203580) *in vitro* and found that proliferation of myocytes were increased as shown by the BrdU and H3P analysis. The authors further assessed proliferation *in vivo* using a conditional KO mice in which p38 MAPK activity was disrupted specifically in myocytes. BrdU incorporation in neonatal myocytes increased by about 17.2% compared with wild type mice. Also H3 phosphorylation was increased by about 92.3% indicating that reduced p38 MAPK protein resulted in increased mitosis in myocytes *in vivo*.

They assessed whether p38 MAPK inhibition promotes growth factor mediated DNA synthesis in adult cardiac myocytes, using similar proliferation assays in ventricular myocytes from 12 week old rats with an extra cardiac myocyte specific marker (transcription factor Nkx2.5). The isolated cells were stimulated every 3 days with growth factors in the presence or absence of SB203580 for 12 days and assayed for BrdU. FGF1 alone and FGF1 + IL-1 induced BrdU incorporation in more than 2% of adult myocytes. Inhibition of p38 MAPK doubled the effect of growth factors. The authors also investigated whether adult myocytes can undergo cytokinesis by assaying aurora B. The results demonstrated that inhibition of p38 MAPK increased cytokinesis 3.8 fold, with the highest effect observed with p38 MAPK inhibition and FGF1. Altogether, these data demonstrated that combining p38 MAPK inhibition and stimulation with fibroblast growth factors causes an increased in cardiac myocyte proliferation *in vitro* and *in vivo* and that p38 MAPK plays a very important role in this phenomenon. These data also reveal that p38 MAPK inhibition promotes growth factor induced DNA synthesis in adult myocytes and that adult ventricular myocytes can divide.

Altogether these data demonstrated that in the heart, p38 MAPK function could be both protective and damaging to myocyte survival in response to stress. And it also suggests that in treating heart diseases p38 MAPK inhibition has more potential.

Though considerable advance is being made in elucidating the role of MAPK signalling in the heart, the functional roles for MAPK in cardiac regulation have still not been fully considered. The use of genetic and molecular tools has provided more information that individual MAPK members have essential but different functions in cardiac regulation and disease progression (Kontaridis *et al*., 2008). But, the present understanding of MAPK signalling in the heart is still not enough to show mechanistically how targeting MAPKs can be used as a valid therapeutic approach for cardiac disease (Mayor *et al*., 2007). MAPK cascades modulate the hypertrophic response of the heart to pressure overload (Braz *et al*., 2003). Activation of the ERK cascade promotes the growth of individual myocytes, while activation of the JNK and p38 MAPK aggravates the growth of individual myocytes. In addition, activation of ERK promotes myocyte survival after pressure overload, while activation of p38α MAPK promotes cardiac myocyte contractile dysfunction and fibrosis (Engel *et al*., 2005). Most of these studies use pressure overload to induce pathological hypertrophy, the issue of the role of ERK pathway in physiological hypertrophy for example induced by competitive sports like swimming are not considered.

An improved understanding of the role of MAPK pathways and targeting MAPK pathways as a potential therapy to prevent the development of cardiac hypertrophy and its progression to heart failure demand major progress in several areas (Mayor *et al*., 2007). The need to have full understanding of the interaction of various MAPKs in the heart under basal and different stress conditions is evident. It is important to understand the primary and secondary effects of MAPK activation particularly as regards their

dephosphorylation by phosphatases that regulate their function. These will provide mechanistic links between the molecular network and physiological / pathological outcome and will help to identify potential signal pathways and nodules critical to the different aspects of cardiac pathogenesis (Baines and Molkentin, 2005).

The vast majority of the studies outlined above relate MAPK functions to cardiovascular disease *in vivo* through regulation of MAPK function within the myocyte, there are very few studies which link the disease to CF. Much of the data on the role of CF as well as myocytes has been obtained from neonatal rat as a convenient model, however caution should be exercised in extrapolating results from these developmentally immature cells to those of the adult CF (Baudino *et al*., 2006). Although most of these findings demonstrate that CFs are critical in the neonatal heart, little is known about their development and their roles in the adult heart. It is only now that the independent contribution of CF in cardiac function and pathophysiology is being valued. In CF, it has been shown that the activation of ERK could be achieved by various stimuli such as growth factors, Ang II, mechanical force which regulate proliferation, collagen deposition and differentiation of these cells (Du *et al*., 2004; Wang *et al*., 2003; Zou *et al*., 1998).

In spite of these distinctive features of the physiological role of CF in myocardial remodeling, comprehensive knowledge of these cells is not fully investigated. So studies that would further elucidate the molecular role of these cells in cardiac function and disease will be of immense importance towards efforts to establish novel therapies that specifically target the CF in the heart.

1.5 Regulation of MAPK Signalling Pathways by Protein Phosphatases

Protein phosphatases are enzymes that remove inorganic phosphate from proteins (Keyse, 2000). Phosphatases are enzymes that can hydrolyse the phosphoester bonds on protein, lipid or small-molecule substrates (Theodosiou and Ashworth, 2002). MAPKs are inactivated totally by dephosphorylation of either the tyrosine or threonine residues, or both (Canagarajah *et al*., 1997). Many phosphatases are devoted to dephosphorylating one or both of the phosphosites in the active site of MAPKs to control the strength and extent of MAPK activity in various cell types. Under physiological conditions, dephosphorylation and subsequent inactivation of MAPKs occurs with kinetics that vary from minutes to several hours depending on the cell type and activating stimulus (Camps *et al*., 2000).

1.5.1 The Protein Tyrosine Phosphatase Family (PTPs)

The family of cysteine-dependent protein tyrosine phosphatases (PTPs) comprises 106 genes in humans and shares a canonical C(X)5R motif in their active sites (Tonks, 2005). PTPs can be divided into two general categories. The first group is the tyrosine-specific PTPs that dephosphorylate protein substrates on tyrosine (Theodosiou and Ashworth, 2002). Tyrosine-specific PTPs consists of receptor-like PTPs and non-transmembrane PTPs. The second group is the DSPs (dual-specificity phosphatases) that dephosphorylate protein substrates on tyrosine, serine and threonine residues, and lipid substrates (Alonso *et al*., 2004; Tiganis and Bennett, 2007). This led to the elucidation of the molecular mechanisms of action for the PTPs. Using a combination of biochemical and genetic techniques many substrates that these enzymes dephosphorylate were identified (see Andersen, *et al*., 2004). A subfamily of the DSPs called the mitogen-activated protein kinase phosphatases (MKPs) has been found to dephosphorylate MAPKs on both tyrosine and threonine residues within the activation motif of

the kinase. These MKPs display different specificities towards the members of MAPKs and so function as essential negative regulators of MAPK-mediated signalling in wide range of biological processes (for review see Keyse, 2000).

1.5.2 MAP Kinase Phosphatases structure

All the DUSPs share strong amino-acid sequence identity over their catalytic domains (37- 50%), with members of certain groups sharing up to 75% identity for example MKP-3 with MKP-X (Keyse and Emslie, 1992).. The catalytic domain comprise of a highly conserved consensus sequence **D**X_{26} (V/L)X(V/I)H**C**XAG(I/V)-S**R**SXT(I/V)XXAY(L/I)M, in the single letter amino-acid code where X is any amino acid. The 3 amino acids shown in bold have been demonstrated to be totally necessary for catalysis. The cysteine is necessary for the nucleophilic attack of the phosphorus of the substrate and the formation of the thiol-phosphate intermediate (Denu and Dixon, 1998). In mammalian cells, the MKPs comprise a family of 10 dual-specificity (Thr/Tyr) MAPK phosphatases. They are able to dephosphorylate MAPKs and as such regulate their functions. MKPs are composed of two domains, the MAPK-binding (MKB) domain in the N-terminal half and the dual-specificity phosphatase domain in the C-terminal half. The C-terminal DSP domain is homologous to the prototypic dual specificity protein phosphatase VH-1 of vaccine virus, and the N-terminal MKB domain, which is homologous to the rhodanese family of sulphotransferases, contains two regions of sequence homology with the catalytic domain of the cdc25 phosphatase (Keyse and Ginsburg, 1993). The DSP domain of all MKPs share strong homology with each other. Because the DSP domain alone does not show exact selectivity towards members of MAPKs (Muda *et al*. 1998; Tanoue *et al*. 2000), the N-terminal MKB domain plays a major role in regulating their enzymatic specificity through docking interaction with MAPKs (see figure 1.3). The MKB domain contains a cluster of positively charged amino acids, which play a role in determining binding specificity of MKPs towards MAPKs (Tanoue *et*

al. 2001; Tanoue *et al*. 2002). In addition a cluster of hydrophobic amino acids and another cluster of positively charged amino acids are required for the specific interaction of MKPs with MAPKs (Tanoue *et al*. 2002). It has been demonstrated that several MKPs are catalytically activated by substrate binding to its MKB domain (Camps *et al*. 2000; Chen *et al*. 2001; Zhang *et al*. 2005). Binding of phosphorylated MAPK to the MKB domain alters the structure of the DUSP domain. This conformational change, and in combination with the interaction of the catalytic domain with MAPK, greatly increases the catalytic activity of MKPs (Farooq *et al*. 2001; Farooq and Zhou, 2004).

1.5.3 Catalytic mechanism of redox regulation of PTPs and DUSPs

Protein tyrosine phosphatases and DUSPs share comparable active site structural design and catalytic mechanism, characterized by the conserved HCX5R(S/T) pattern (Zhang *et al*., 1994; Denu and Dixon, 1995). The exclusive nature of the microenvironment within the HCX5R(S/T) motif reduces the pKa value of the active site cysteine, enhancing both nucleophilicity and oxidation vulnerability (Grzyska *et al*. 2004; Denu and Tanner, 1998). Endogenous or stimulated generation of reactive oxygen species can result in oxidative second messenger signalling responses capable of temporary and reversible post-translational inactivation of both PTPs and DUSPs via oxidation of the catalytic cysteine (Meng *et al*., 2002; Lou *et al*., 2008). This oxidative susceptibility and modification differs among PTPs and DUSPs, a likely result of slight variations in active site conformations or mediated through distinctive regulatory domains (Groen *et al*., 2005; Ross *et al*., 2007; Weibrecht *et al*., 2007). Supporting data suggests that redox mediated oxidation of PTPs is an active modification that can differentially control PTPs (Meng *et al*., 2002; Fox *et al*., 2007). Sulfenic acid, cyclic sulfenamide and disulfide bond formation have all been revealed to facilitate stable, reversible active site modifications among various PTPs and DUSPs (Denu and Tanner,

1998; Tonks, 2005; Chiarugi *et al*. 2001). Also, some data suggests that oxidation mainly targets the active site cysteine, while other cysteinyl residues remain in the reduced state (Lou *et al*., 2008, Chiarugi *et al*., 2001).

1.5.4 Regulation of MKPs (DUSPs) Expression and Activity by MAPKs

The expression, activity and function of the MAP kinase phosphatases (MKPs) are subject to various levels of regulation. First of all is the strong, transcriptional activation of MKPs in response to a variety of stimuli either through immediate early gene (IEG) activation in the case of MKP-1 and MKP-2, or by other transcription factors such as those for MKP-3 and MKP-2, mediated through activity of the MAPKs themselves (for review see Keyse, 2008). For example, MAPK-dependent activation of E-box and AP2 transcription factors leads to DUSP transcription. Secondly, protein stability and catalytic activity of DUSPs is highly regulated through binding to MAPK substrates in both negative and positive ways. The binding of ERK to DUSPs can increase protein stablility to provide feedback to MAPK activity for example as in the case for MKP-7 (Camps *et al*., 1998). Occasionally however, as is the case for MKP-1, MAPK binding can decrease protein stability and encourage MKP-1 proteolysis via the ubiquitin ligase SCFkp2, thereby sustaining MAPK activity (Lin and Yang *et al*., 2006). Thirdly, reactive oxygen species (ROS) that regulate some immune responses and activate the upstream kinase MAP3K5 (also known as ASK1) directly inactivate the catalytic site within DUSPs by oxidation at the conserved cysteine 257 (Tonks, 2005). The induction of MKP expression and regulation of activity is essential to control the magnitude and kinetics of MAPK activity and is essential for the induction of IEGs and formation of transcription factor complexes over time.

1.5.5 Classification of DUSPs

MKPs are extremely specific for MAP kinases but vary in the substrate specificity among the MAP kinase family members. In addition there are variations in their tissue distribution, subcellular localization and inducibility by extracellular stimuli. Based on the sequence similarity, protein structure, substrate specificity and subcellular localization, the MKP family can be divided into three groups namely; Type I, Type II and Type III (Farooq and Zhou, 2004; Theodosiou and Ashworth, 2002) (see table 1.1) .Type I MKPs include MKP-1, MKP-2, PAC1 and hVH3. This group of MKPs localize in the nuclear compartment and are induced by many stimuli that activate MAPKs. Based on this, it has been proposed that these MKPs play a vital role in the feedback control of MAPK signalling in the nucleus. MKPs in this group consist of 300-400 amino acid residues, and contain a nuclear localization signal (NLS) sequence in their N-terminus (Wu *et al*., 2005). Type II MKPs include MKP-3, MKP-X and MKP-4. This category of MKPs have a nuclear export signal (NES) and they are localized in the cytoplasm. Type III consists of MKP-5, MKP-7, and M3/6. Even though they are too large to enter the nucleus by passive diffusion, they shuttle between the cytoplasm and nucleus, (See figure 1.3). They selectively dephosphorylate JNK and p38 but not ERK1/2. They have an extended region either in the N-terminus (MKP-5) or in the C-terminus (MKP-7 and M3/6) in addition to the MKB and DUSP domains. The function of this region of MKP-5 is not clear (Matsuguchi *et al*., 2001). Although biochemical and structural properties of MKPs have been studied extensively over the past decade, the physiological function of MKPs, including substrate specificity *in vivo*, has not been fully defined (see Table 1.1).

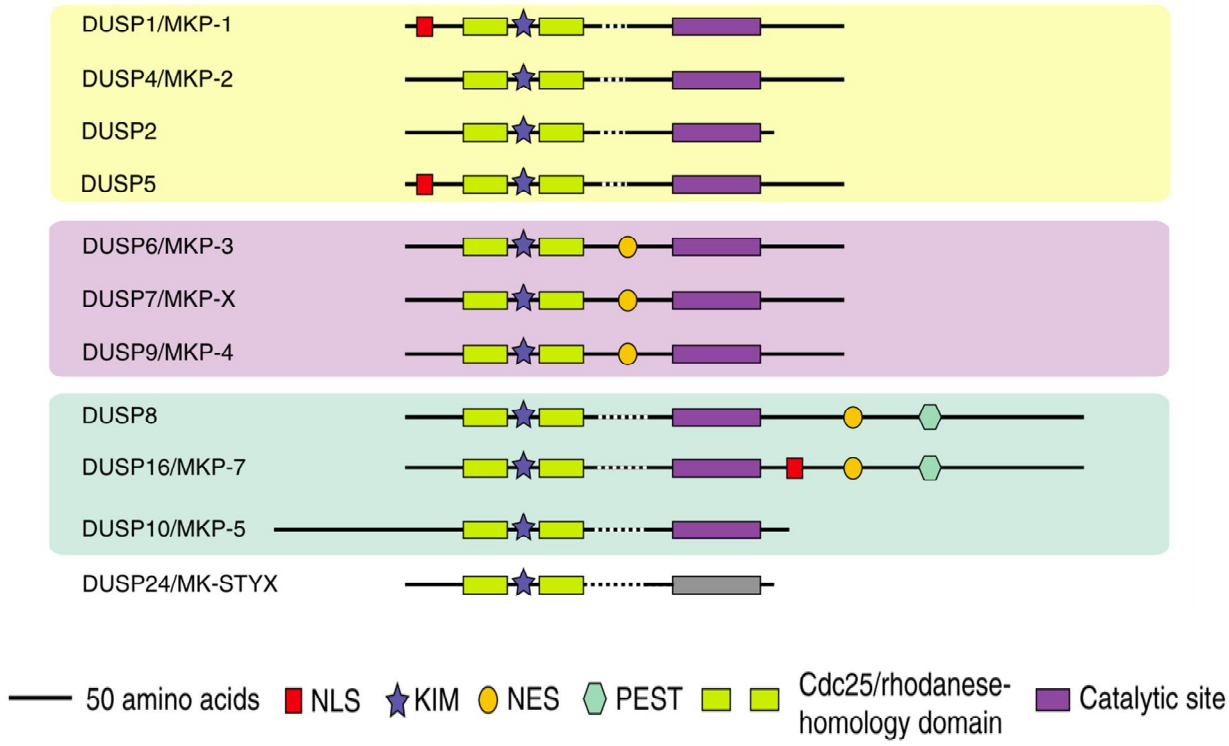

Figure 1.3: The family of dual-specificity phosphatases (DUSPs)

Shown here are those representing the MAP kinase phosphatases (MKPs). MKPs that are shown in gray shuttle between the nucleus and cytoplasm. MK-STYK is presumed to be catalytically inactive, containing a substitution for the essential cysteine residue. (Adapted from Dickinson and Keyse, 2006).

1.5.6 Physiological Functions of MPKs

1.5.6.1 MKP-1 (DUSP 1)

MKP-1, the prototype member of MKP family was identified as an immediate-early response gene (Keyse and Emslie, 1992). The cDNA for this gene was initially cloned because of its inducibility by serum and peroxide-induced stress in human fibroblasts, and was established to be similar to Vaccinia virus H1 phosphatase (Lau and Nathans, 1985). MKP-1 was found to be expressed in wide variety of tissues and cells with the exception of the testes. Highest levels were observed in the heart, lungs and liver (Charles *et al*., 1992; Noguchi *et al*, 1993). Using immunofluorescent microscopy and subcellular fractionation studies, MKP-1 was found to be located in the nucleus. Both *in vitro* and *in vivo* studies have demonstrated that MKP-1 preferentially dephosphorylates activated p38 MAPK and JNK over ERK (Wu and Bennett, 2005) (see Table 1.1).

The function of MKP-1 has been extensively studied using primarily KO mice models (Wu *et al*., 2006). Quite a number of studies have reported the role of MKP-1 in many pathological conditions, including cancer, immune dysregulation, diabetes and obesity (Wu and Bennett, 2005; Roth *et al*., 2009)). The MKP-1 gene is over-expressed in nonsmall cell lung and oral cancer, hepato-carcinoma, and gastric carcinomas , and may inhibit cell death in rat mesangial cells. In another study it has been shown that MKP-1 is downregulated in prostate cancer (Vicent *et al*., 2004; Yokoyama *et al*., 1997; Li *et al*., 2004; Bang *et al*., 1998; Guo *et al*., 1998; Tsujita *et al*., 2005; Rauhala *et al*., 2005).

In the immune system, KO models were used to investigate MKP-1. MKP-1 deficiency in mice leads to a markedly high vulnerability to endotoxic shock (a murine model of sepsis) and autoimmune arthritis, highlighting an important role for MKP-1 in controlling innate immunity (Chi *et al*., 2006;

Hammer *et al*., 2006; Salojin *et al*., 2006; Zhao *et al*., 2006). In addition MKP-1 has been reported to have a role in cardiovascular function. One study examined the role of MKP-1 KO animals in energy metabolism, and it reported that MKP-1 deficient mice are also resistant to diet-induced obesity (Wu *et. al*., 2006). Some studies have also suggested that MKP-1 protect cells against oxidative stress and heat shock (Liu *et. al*., 2005; Zhou *et al.,* 2006).

1.5.6.1.1 MKP-1 in heart pathology

Early studies have examined the effect of constitutive expression of MKP-1 on gene expression following stimulation with hypertrophic agonists in neonatal rat ventricular myocytes (Fuller *et al*., 1997). These cells were transfected with luciferase reporter genes linked to ANF, ventricular myosin light chain 2, β-myosin heavy chain, skeletal muscle α-actin and c-fos-SRE. Stimulation with phenylephrine, PMA and endothelin 1 induced the expression of these genes by about 2.5–20 fold. However, MKP-1 reversed these effects by about 60–85%, although it has less effect on the morphology of myocyte following agonist induced cardiac hypertrophy. These data suggests that MKP-1 could mediate transcriptional responses in myocytes most likely through the regulation of some members of the MAPKs (Fuller *et al*., 1997). It has been demonstrated that stimulation of cardiac myocytes with retinoic acid enhanced the expression level of MKP-1 and MKP-2 which was associated with deactivation of MAPKs (Palm-leis *et al*., 2004). Furthermore, over-expression of wild type MKP-1 attenuated JNK and p38 MAPK phosphorylation in myocytes. This suggested that these MKPs were involved in the inhibitory effect of retinoic acid on MAPKs.

The fact that the MAPKs have the potential to play important roles in cardiac pathophysiology suggests that the MKPs may also be involved. Linking the effects of MKP-1 in animal systems to heart disease in humans has proved difficult and few studies have examined this area. Dong *et al*., 2006 examined

the expression of MKP- 1 and ERK from normal subjects and end-stage HF patients using immunohistochemistry. Both MKP-1 and ERK were expressed in nuclear and perinuclear regions of cardiac myocytes. In patients with HF, ERK phosphorylation score and positive staining area were considerably increased in the following regions of the heart; right atrium (RA), left atrium (LA), right ventricle (RV), and left ventricle (LV) compared with control subject RA, LA, and RV. On the contrary, MKP-1 expression score and positive staining areas were substantially decreased in HF patients RA, LA, RV, and LV myocardium compared with control group. Furthermore, assessment of the myocyte diameter revealed a significant increase in HF myocardium compared with normal subjects. These data demonstrated that activation of ERK and inhibition of MKP-1 may play an important part in pathophysiology of cardiac hypertrophy and congestive heart failure

In a similar study the pathophysiogical role of MKP-1 and MKP-2 including the MAPKs were examined. Communal *et al*., 2002, compared the protein levels of MKP-1 and MKP-2 and ERK, JNK and p38 MAPK in the heart of patients with end-stage heart failure (5 to 7 patients) and normal subjects (5 to 7 subjects). Expression of MKP-2 was considerably increased in failing hearts, while expression of MKP-1 was increased in 5 of 7 failing hearts. The protein levels for JNK1/2 and p38 MAPK were basically the same in failing hearts as normal hearts, but the activities of these proteins were decreased. There was about 3 fold increase in the protein level for ERK1/2 in failing hearts compared with control subjects, but the activity of ERK1/2 was not altered.

Whilst this study has shown that JNK1/2 and p38 MAPK activities are reduced in failing human heart and could be correlated with increased expression of MKP-1 and MKP-2 no course and relation has been established. This remains a limitation with these types of human studies. These studies demonstrated the idea that more studies are needed to define the precise roles of MKP-1 in cardiac pathophysiology.

Gene / MKP	**Trivial names**	**Molecular mass (kDa)**	**Chromosomal localization**	**Subcellular localization**	**Substrate specificity**	**Physiological function(s)/phenotype**
DUSP1 / MKP-1	CL100, erp, 3CH134, hVH1	39.30	5q34	Nuclear	JNK=p38>ERK	Negative regulator of immune function, protects mice from lethal endotoxic shock. Plays a key role in metabolic homeostasis & mediates resistance to cellular stress in fibroblasts. (Wu and Bennett, 2005; Zhao *et al*., 2006; Chi *et al*., 2006).
DUSP4 / MKP-2	Typ1, Sty8, hVH2	42.95	8p12-p11	Nuclear	JNK=ERK>p38	KO mice displayed decreased TNFα, IL-1β, IL-6, IL-10 in response to endotoxin (Cornell *et al*., 2010).
DUSP2 / None	PAC-1	34.40	2q11	Nuclear	ERK=p38>JNK	Positive regulator of inflammatory responses, KO mice are resistant to immune inflammation (Jeffrey *et al*., 2006).
DUSP5 / None	hVH3, B23	42.05	10q25	Nuclear	ERK	Unknown
DUSP6 / MKP-3	Pyst1, rVH6	43.32	12q22-q23	Cytoplasmic	ERK>JNK=p38	Negative regulator of ERK2 downstream of FGFR signalling (Dickinson *et al*., 2002a). KO mice showed enhanced myocyte growth affecting disease susceptibility (Maillet *et al*., 2008).
DUSP7 / MKP-X	Pyst2, B59	40.55	3p21	Cytoplasmic	ERK>JNK=p38	Unknown
DUSP9 / MKP-4	Pyst3	41.87	Xq28	Cytoplasmic	ERK>p38>JNK	Vital for placental & labyrinth formation (Christie *et al*., 2005).
DUSP8 / None	M3/6, hVH5, HB5	65.84	11p15.15	Cytoplasmic / nuclear	JNK=p38>ERK	Unknown
DUSP10 / MKP-5	None	52.64	1q41	Cytoplasmic / nuclear	p38=JNK>ERK	Functions in innate & adaptive immunity (Zhang *et al*., 2004).
DUSP16 / MKP-7	None	73.10	12p12	Cytoplasmic / nuclear	JNK=p38>	Unknown

Table 1.1. Nomenclature, properties and physiological functions of MKPs

(adapted and modified from Keyse, 2008).

1.5.6.2 MKP-2 (DUSP 4)

MKP-2, was originally isolated from PC12 cells (Misra-Press *et al*., 1995). The gene was found to encode a protein of 394 amino acids with a predicted molecular mass of 43 kDa, with sequence homology with MKP-1 (about 60%). MKP-2 mRNA was detected in many tissues including the brain, spleen, and testes with the highest expression in heart and lung with lesser expression in skeletal muscle and kidney (Misra-Press *et al*., 1995). MKP-2 expression was not detected in the liver. Interestingly, MKP-2 and MKP-1 were found to have opposite expression patterns in testes and liver which suggested that these two proteins had different physiological functions. MKP-2 was induced by serum, growth factors, phorbol esters, gonadotropin-releasing hormone (GnRH), retinoic acid and the oncogene v-jun (Guan and Butch, 1995; Misra-Press *et al*., 1995; Brondello, 1997; Zhang *et al*., 2001; Fu *et al*., 2000; Torres *et al*., 2003; Palm-Leis *et al*., 2004). Studies indicated that MKP-2 and MKP-1 were similar in structure and splicing pattern. Both genes have four exons and three introns with similar exon lengths in rat and human (Noguchi *et al*., 1993). These findings suggested that MKP-1 and MKP-2 genes have a common origin. On the other hand important structural differences between the genes were found. The 30 UTR of the rat MKP-2 gene was markedly longer than that of the human and mouse MKP-1 genes.

Similar to MKP-1, fluorescent microscopy confirmed that MKP-2 was located to the nucleus due to the presence of two nuclear location sequences (Sloss *et al*., 2005). Initial studies demonstrated that MKP-2 specifically dephosphorylated ERK1/2 and JNK *in vitro*, and interaction of MKP-2 with ERK1/2 and JNK enhanced its catalytic activity (Chu *et al*., 1996; Chen *et al*., 2001). However, the substrate specificity of MKP-2 *in vivo* is still unclear. It has been reported that MKP-2 dephosphorylates JNK, but not ERK1/2 in UV-C or cisplatin treated cells (Cadalbert *et al*., 2005). In these cells, while JNK

translocates to the nucleus, ERK1/2 remains in the cytoplasm. Consequently, MKP-2 may dephosphorylate nuclear JNK, but not cytoplasmic ERK1/2.

A few studies have demonstrated that MKP-2 and its regulation perform essential regulatory roles in numerous physiological and pathological conditions, including cellular senescence, stress-induced cell death and cancer. However, nothing is known of its role in cardiac pathphysiology. Activation of the ERK1/2 pathway induces MKP-2 expression. Furthermore, cellular senescence increases MKP-2 protein by blocking its degradation (Torres *et al*., 2003). Similarly, it was reported that knock-down of MKP-2 expression, through transduction of MKP-2 sequence-specific short hairpin RNA, or expression of the phosphatase resistant ERK2 (D319N) mutant, abrogates the effects of increased endogenous MKP2 levels and senescence is delayed (Tresini *et al*., 2007)

It has been reported that MKP-2 is up-regulated in malignant breast cancers and malignant hepatomas (Wang *et al*., 2003; Yokoyama *et al*., 1997) Over-expressed MKP-2 has been revealed to dephosphorylate constitutively active ERK, thus compensating for K-ras activation in multiple pancreatic tumor cell lines bearing an activated K-ras (Yokoyama *et al*., 1997). Besides its role in cancer, MKP-2 is stabilized in senescent fibroblasts indicating a valuable role in cellular senescence (Torres *et al*., 2003). Also MKP-2 is able to prevent stress-induced pro-apoptotic signalling through the JNK pathway suggesting a mechanistic rationale for the up-regulation of MKP-2 in malignant cancers (Cadalbert *et al*., 2005). Accumulating evidence shows the occurrence of various splice variants among some members of the MKP family. Recently, Cadalbert *et al*, 2010 reported the presence of a novel splice variant of MKP-2 which is not capable of binding to ERK and may be important in the dysfunction of MAPK signalling in some disease conditions, especially in breast and prostate cancers. As a result, cellular signalling pathways relating MKP-2 may be essential in a range of pathological conditions.

1.5.6.3 MKP-3 (DUSP 6)

MKP-3 was cloned from superior cervical ganglion cDNA library (Muda *et al*., 1996). MKP-3 cDNA was isolated as a DUSP that was robustly induced in NGF-1-induced PC12 cells, and its over-expression reduces ERK-2 phosphorylation. MKP-3 links with its main substrate ERK-2 via its N-terminal domain as well as with protein kinase CK2a (Groom *et al*., 1996; Liu *et al*., 2006; Tarrega *et al*., 2005; Zhou *et al*., 2001; Castelli *et al*., 2004). MKP-3 is primarily cytoplasmic by nature of a leucine-rich nuclear export signal in its linker domain. MKP-3 transcription is induced by fibroblast growth factor receptor (FGFR) activation. MKP-3 mRNA was detected at elevated levels in lungs and at lower levels in heart, brain, spleen, liver, and kidney. MKP-3 mRNA was not detected in skeletal muscle and testis (Muda *et al*., 1996). This pattern of expression overlaps with other MKPs in some tissues, like MKP-1 and MKP-2 while in some tissues like the liver there are obvious differences. MKP-3 forms an expression pattern along the chick limb bud to modulate FGF-8 responses (Smith *et al*., 2006; Vieira and Martinez, 2005). In zebrafish, MKP-3 regulation of the MAPK signalling downstream of the FGFR is important for axial polarity during development and is also involved in Drosophila development. It has been revealed that mice lacking MKP-3 have excess perinatal mortality and developmental defects with skeletal dwarfism, coronal craniosynostosis and deafness due to otic ossicle malformation and all these defects were probably related with enhanced FGFR signalling (Tsang *et al*., 2005; Li *et al*., 2007).

In certain pathological conditions such as cancer, MKP-3 may play a role as tumuor suppressor whose inactivation is often linked with pancreatic and other cancers mediated by promoter hypermethylation or chromosomal loss (Furukawa *et al*., 2006; Furukawa and Horii, 2004). It was also reported that over-expression of MKP-3 decreases tumor growth (Marchetti *et al*., 2004).

1.5.6.3.1 Function of MKP-3 in the heart

Early studies examined the transcriptional regulation of GLUT1 expression. Cardiac myocytes were transfected with luciferase reporter constructs under the control of the GLUT1 promoter. In response to phenylephrine, GLUT1 promoter transcription was induced and this was reversed by cotransfection of MKP-1 and MKP-3 in these cells (Montessuit and Thorburn, 1999).

As mentioned above MKP-3 is one of the DUSP that is expressed in the heart. The function of MKP-3 in the heart has been investigated by generation of MKP-3 KO mice, Maillet *et al*., in 2008 reported that MKP-3 KO mice showed no apparent phenotypic defects, they bred normally, had body weights similar to wild type littermates, and also had increased basal ERK signalling compared with wild type mice. But MKP-3 KO mice at 1 and 2 months of age showed considerably larger hearts normalized to body weight (HW/BW), and at 1 year of age also showed a significantly larger increase in heart weight. This increase in heart weight was not pathological, because cardiac function assessed by echocardiography in 1 year old MKP-3 KO mice was similar to wild type mice (FS = 28.6% in MKP-3 KO compared with 28.2% in wild type). Histological examination of myocyte surface areas showed no difference at 1 and 2 months old between MKP-3 KO and wild type hearts, suggesting that the increase in heart weight size was due to greater cellularity. In order to support the above findings the authors further investigated the hearts from 3 day old MKP-3 KO neonates by immunohistochemistry which showed a 30% increase in phos-pho-histone H3 labeling compared with wild type hearts, but myocyte surface areas were similar. They also observed a 30% increase in BrdUrd incorporation into the hearts of 13.5 day old MKP-3 KO embryos compared with wild type embryos. On the other hand, no alteration was observed in the proportion of mono and bi-nucleated myocytes isolated from 2 months old hearts. These results has demonstrated that differences in DNA synthesis is possibly created by cell

number differences, and that deletion of MKP-3 had a developmental effect that rendered the heart with greater proliferation rates and more myocytes, (similar phenotype was observed in MEFs derived from MKP-3 KO embryos).

1.5.6.3.2 Role of MKP-3 in cardiac hypertrophy

Following the observation that there is increase in myocyte number associated with MKP-3 deletion as described above, Maillet *et al*., 2008 further investigated the adult heart using a disease model. When 2 month old MKP-3 KO and wild type mice were initially subjected to agonist stimulation with angiotensin II and Phenylephrine administration over 2 weeks, it produced a comparable cardiac hypertrophic response in both groups. In the same way, administration of isoprenaline for 2 weeks produced a substantial hypertrophic response and relative percent increase from baseline in both MKP-3 KO and wild type mice, although the hearts from MKP-3 KO were considerably larger after isoprenaline infusion than wild type controls. On the other hand, when 8 weeks of pressure overload by TAC was used, both MKP-3 KO and wild type mice resulted in a similar pattern of hypertrophic response. The transaortic pressure gradients across the constriction were basically the same in the 2 groups (80 mmHg in MKP-3 KO and 68.5 mmHg in wild type mice). The authors further examined myocyte cross-sectional surface areas from histological sections that showed less cellular hypertrophy in MKP-3 KO compared with wild type mice. Taken together, these results have demonstrated that increased ERK1/2 basal signalling linked with the MKP-3 gene deletion decreased the growth of individual myocytes during long term pressure overload in the adult heart. Also, despite the fact the MKP-3 KO hearts are larger, no difference was observed between the 2 groups when exposed to TAC. And this means that adult MKP-3 KO mice are partly protected from agonists that induce cardiac hypertrophy.

1.5.6.4 MKP-X (Pyst2)

In addition to MKP-3 and 4 members of type 2 family, MKP-X was identified as overlapping clones containing the Pyst1 and Pyst2 genes using high stringency screening of the human genomic library with the full length Pyst1 cDNA and partial Pyst2 cDNA (Groom *et al*., 1996). The organisation of the two genes is extremely conserved, with exon 1 encoding the amino termini of the two proteins and ending within the second of two short regions of homology between all mammalian dual-specificity MAP kinase phosphatases and the cdc25 proteins (Keyse and Ginsburg, 1993). The Phosphatase active site is found within exon 3 in both Pyst1 and Pyst2. Sequence comparison of the two genes reveals that all splice junctions conform to the donor and acceptor sequence consensus (Breathnach and Chambon, 1981) and that the intron/exon boundaries of the two genes are identical (see Keyse, 2000).

MKP-X mRNA is found in a variety of human tissues including muscle, brain heart and liver (Groom *et al*., 1996). MKP-X which is mainly a cytosolic protein is also widely detected in numerous human cell lines including human skin fibroblasts (FEK4), HeLa cells, and ovarian (1847) Green *et al*., 1984), bladder (EJ138) (O'Toole *et al*., 1983) and breast cancer (MCF-7) (Soule *et al*., 1973) derived cell lines. MKP-X specifically dephosphorylates ERK2 both *in vitro* and *in vivo*.

1.5.6.5 MKP-5 (DUSP10)

One of the members of type 3 family is MKP-5 which was cloned to p38 MAPK in a yeast two-hybrid experiment. *In vitro* substrates are p38 MAPK and JNK, but not ERK (Tanoue *et al*., 1999). MKP-5 consists of an N-terminal MAPK binding domain (150 amino acid) that binds to p38 MAPK and is essential for p38 MAPK dephosphorylation, and two CDC25-like domains (Tao and Tong, 2007). The MKP-5 gene is well conserved among mammals and its expression was found in the heart, lung, liver, skeletal muscle and

kidney but was not detected in the brain, spleen or testis (Tanoue *et al*., 1999). Similar to some DUSPs its expression is extremely controlled and it is induced by TNF-α, anisomycin and osmotic stress, but not by UV irradiation or phorbol ester (Jeong *et al*., 2006; Masuda *et al*., 2000).

Recent studies have demonstrated that calcitriol, vitamin D, curcumin, resveratrol and gingerol also increase MKP-5 expression, ensuing in inactivation of p38 MAPK (Stephens *et al*., 2005; Krishnan *et al*., 2007; Nonn *et al*., 2006; Nonn *et al*., 2007). This kind of action make it clear the chemopreventive activity of these agents in prostate cancer, but how MKP-5 transcription is controlled by these agents remains unknown. Similarly, MKP-5 was also identified as a tumor-suppressor gene whose promoter is hypermethylated and whose expression is reduced in mantle cell lymphoma (Kawamata *et al*., 2005). A recent study identified a leukemia patient whose lymphoma contained a chromosomal deletion that resulted in the predicted expression of a fusion protein of MKP-5 and MEL1/PRDM16 (Noguchi *et al*., 2007). It is currently unclear whether unchecked cell proliferation in this case was linked to lack of normal MKP-5 expression, like in mantle cell lymphoma, or to loss of normal MEL1 expression, whose deletion was observed in other lymphomas, or has a different cause.

Taken together the role of MAPK signalling in regulating heart function and also in pathology have been documented in the literature although variable, hyperactivation of the ERK pathway can result to hypertrophic cardiomyopathy and at the same time inhibition of the pathway can predispose the cardiac myocytes to stress induced apoptosis (Schramek, 2002; Harris *et al*., 2004). JNK pathway is involved in many signalling mechanisms in the heart, therefore the role of different JNK isoforms and splice variants need to be established (Tachibana *et al*., 2007). Also the specific outcome of activating each isoform is not clearly understood especially under stress

conditions in the heart. Activation of p38 MAPK can lead to survival or induce apoptosis in cardiomyoctes particularly if the heart is stressed (Nishida *et al*., in 2004). It is important to understand the mechanism how p38 MAPK elicits these different functions. Calcium signalling is very important in regulating the heart function, studies are needed to specifically identify the exact role of MAPK pathway in this regard both under normal and pathological conditions (Bers and Guo, 2005).

The significance of selecting appropriate models is crucial in interpreting the value of experimental data. While many factors have been identified that regulate CF growth and migration (Chiqueta *et al*., 2003; Baines and Molkentin, 2005), less is known about the signalling mechanisms involved in these processes. Most of the studies described in chapter 1 utilized over-expression, gain or loss of function and pharmacological inhibition approaches, and were mainly conducted in neonatal myocytes *in vitro* with very few studies on adult CF, and it is obvious that these cells are very essential in the structure and function of the heart (Stewart *et al*., 2006).

Regarding the role of MAPK in the heart, there is still more need to be done in order to fully characterize and elucidate their exact function especially considering their regulation by MKPs. There is a paucity of information on the role of MKPs (both *in vitro* and *in vivo*) and particularly, MKP-2 in cardiac function and hypertrophy (Dong *et al*., 2006; Wu and Bennett, 2005). Hence the generation of MKP-2 KO mice would be potentially valuable in investigating its physiological role in the heart. Although the knockout models have many advantages in elucidating the physiological function of a particular protein, the targeted gene disruption and transgenic techniques also have their own limitations (Cefalu, 2006). Basically by over- or under-expressing a particular gene will affect the expression of some others as a compensatory mechanism, for example, Tamemoto *et al*., 1994, reported that completely knocking-out the insulin receptor substrate 1 gene produces small

in the way of effect given the essential role that this protein has in intracellular signalling, but redundancy within the insulin signalling cascade prevail over the genetic manipulation. Homozygote knockouts of the insulin receptor substrate 2 gene, do develop diabetes by 10 days of age, linked with insulin resistance in the liver and reduced pancreatic β-cell mass (Withers *et al*., 1998).

Another issue with standard gene disruption procedures is the fact that homozygote knockouts are sometimes lethal in utero so making it demanding for adults to be studied (Hayashi and Lee, 2004). Also some genes have fairly different functions during embryogenesis in comparison to adult life and the knockout model cannot be scheduled to occur during specific periods of the animal's life (Cefalu, 2006). The deletion of the gene could produce animals with altered gene expression in many tissues, not necessarily just those that are physiologically relevant. This limitation could be controlled by generating animals in which the gene being studied is only knocked out in specific tissues (Kontaridis *et al*., 2008). This has led to many research groups currently generating tissue specific knockout.

Given that cardiac remodeling is a complex process, using only one type of preparation would not be ideal to investigate these mechanisms properly because data need to be interpretaed from various aspects of heart function. Therefore this study will involve the use of a wide range of preparations both *in vitro* (cell and tissue preparations), *in vivo*, and heart homogenate. An understanding of these mechanisms are essential to the development of rational pharmacological approaches to prevent and potentially reverse the pathological changes associated with cardiac hypertrophy.

1.5.6.6 Aims and Objectives

Given the lack of information on MKP-2 and adult cardiac preparations and the obvious physiological advantage of using these preparations, the following aims will be addressed.

1. Initially characterize the cellular functions of MKP-2 and MAPK mediated signalling in primary cells (mouse embryonic fibroblasts MEFs), isolated from novel DUSP-4 deletion mouse by:
   i. characterization of MKP-2 induction
   ii. correlating loss of DUSP-4 with changes in MAPK signalling
   iii. correlating these effects with cellular proliferation and cell survival.

2. To examine whether MKP-2 contributes to cardiac phenotype and function by characterizing MKP-2 signalling in adult CF by:

i. Examining responses to a variety of agonists.

ii. Establishing proliferation response of CF's isolated from MKP-2 $^{-/-}$ and MKP-2 $^{+/+}$ hearts.

3. Assessing cardiac function in MKP-2 $^{-/-}$ and MKP-2 $^{+/+}$ mice *in vivo* using echocardiography.

4. Establishing MKP-2/MAPK protein expression in mouse model (MTAB) of cardiac hypertrophy.

CHAPTER 2

MATERIALS AND METHODS

Chapter 2: Materials and Methods

2.1 General Reagents

All materials and reagents used were of the highest commercial grade available, and were obtained from the following companies.

Amersham International Plc, Aylsbury, Buckinghamshire, UK.

ECL detection reagents

Bio-Rad Laboratories, Hertfordshire, UK.

Pre-stained SDS-PAGE molecular weight markers.

Boehringer Mannheim, East Sussex, UK.

Bovine Serum Albumin (BSA; Fraction V), Dithiothreitol (DTT).

Corning Costar, Buckinghamshire, UK

All tissue culture plastics including graduated pipettes, flasks and plates.

Gibco Life Technologies Ltd, Renfrewshire, UK.

Tissue culture growth media, DulBeccos Modified Eagle Medium (DMEM), antibiotics (Penicillin / Streptomycin), Fetal Calf Sersum (FCS), L-Glutamate.

Sigma Aldrich, Chemical Company Ltd, Dorset, UK.

Sodium Dodecyl Sulphate (SDS), Tween-20, Sodium Chloride, Glycine, Lithium Chloride, Acrylamide, bis-Acrylamide, Tris, Sigmacote, TEMED, Kodak X-Omat Film, HCl, picro-sirus red.

Whatmann, Kent, UK.

Nitrocellulose Membranes, 3MM blotting paper.

BD Biosciences, Oxford, UK.

PE Annexin V Apoptosis Detection Kit

Pierce Biotechnology, USA.

Coomassie Plus Reagent and the albumin standards (2mg / ml)

2.2 Antibodies

Amersham International Plc, Alyesbury, Buckinghamshire, UK.

Horseradish peroxidase (HRP)-conjugated sheep anti-mouse IgG.

Biosource EU, Belgium, Europe

Rabbit polyclonal anti-phospho p38 IgG.

Santa Cruz Biotechnology Inc, CA, USA.

Mouse monoclonal anti-phospho ERK

Rabbit polyclonal MPK-2

Rabbit polyclonal anti-p38

Anti- ERK-1

Mouse monoclonal anti Cyclin B1

Jackson Immunoresearch Laboratories Inc, PA, USA.

HRP-conjugated goat anti-rabbit IgG

Cell Signalling Technology, UK.

Phospho-cdc-2

Caspase-3

Rabbit polyclonal anti-JNK

Millipore, USA.

Anti-phospho-H2A.X

2.3 Enzymes

Worthington Biochemical Corporation, USA.

Collagenase, Type 2

Sigma Aldrich, Chemical Company Ltd, Dorset, UK.

Protease, Type XIV

2.4 Generation of MKP-2 deficient mice

The deletion of the MKP-2 (DUSP-4) gene was performed by Genoway, Lyon, France using standard procedures. Briefly, the short arm and the long arm flanking both side of the cluster of exon 2-4 of the mouse MKP-2 gene was obtained by PCR using the following primers for the small homology arm: 5'-GTGCCTGGTTCTGTGTGTGTCTGTTCTCC-3' for the forward primer and 5'-TCTTACAGCCCTCTTTCCTCACGGTCG-3' for the reverse primer producing a PCR fragment of 3009 bp. For the long homology arm: 5'-CTTTAGGAGCGACGGCCAGGAACACAGG-3'for the forward primer and 5'-ACCCTGCCACACAGGTTGGAGCAAGG-3' for the reverse primer producing a PCR fragment of 6336 bp. Selected clones obtained from these PCR amplifications were sequenced to minimise the number of point mutation carried through. Both arms were introduced into a pBS vector in either side of the neomycin cassette. The final vector was transfected into 129Sv mouse embryonic stem cells (ES). Only the clones that had homologous recombination events were selected for first by PCR and then using Southern blotting for the short and the long arm on the construct. The screening for the short arm was further used to screen the animal carrying the construct. Four different ES clones were injected into C56Bl/6 blastocystes and reintroduced into OF1 pseudo-pregnant females. Fourteen different male chimeras were obtained and crossed with C57Bl/6 female to obtain the F1 generation. The F1 generation was screened for germ line transmission of the mutation. Three males and 2 females from the F1 generation were heterozygotes for the mutation and were subsequently used for breeding purposes.

2.4.1 Southern blotting

The genomic DNA was obtained by the digestion of tail tip in the presence of proteinase K (100 mg/ml) in lysis buffer (100 mM Tris-HCl pH 8.5, 5 mM EDTA pH 8.0, 0.2% SDS, 200 mM NaCl) overnight at 55ºC. The lysate protein content was cleaned twice using phenol/Chloform/isoamylic acid. The DNA was precipitated from the aqueous phase using isopropanol. The DNA was pelleted, washed in 70% Ethanol and dried before being resuspended in 30 ml bidistillated water. Of this 10 ml was digested with HpaI restriction enzyme overnight. The DNA fragments were separated on a 0.8% agarose gel. The gel was pretreated in sodium hydroxide denaturing solution for 20 min and neutralised in neutralising solution. The gel was transferred using the capillary method onto positively charged nylon membrane (Amersham) overnight. The blot was crosslink using UV crosslinker 1500 J/m^2 and hybridised with a random primer radiolabelled probe K (prime-gene labelling system, promega, UK). The hybridisation was performed overnight at 64ºC. The blot was washed twice in 2XSSC at 65ºC and exposed under autoradiography film (Omax film, Kodak, Sigma-Aldrich, UK) for 2 to 3 days.

2.5 DNA Preparation for Mouse Genotyping

2.5.1 DNA extraction

A small section of mouse tail (about 4 mm) was removed using a sterile pair of scissors and placed in eppendorf tubes containing 0.5 ml of lysis buffer. The samples were incubated at 65° C overnight on a shaker. Samples were spun at 15120 g for 20 minutes to remove the insoluble material. The supernatant were transferred into new eppendorf tubes containing 1/10 vol. NaAc pH 5.5; 3 M, then ½ vol. isopropanol was added and tubes were inverted several times. Samples were spun for 2 minutes at 13000 rpm, the supernatant was discarded before addition of 0.5 ml of ice cold 70% ethanol. Samples were spun once more and the supernatant discarded. The samples were air dried for 30 minutes at room temperature. Then 100 µl of autoclave

water was added and heated for 30 minutes at 65° C. Samples were stored at -20° C (1 μl per PCR reaction for genotyping was used).

2.5.2 Polymerase chain reaction (PCR) amplification

The extracted DNA was used directly for PCR using MKP-2 primers P7-P8 (WT) and PE1-PF2 (KO). The PCR amplfications were in a volume of 50 μl containing 49 μl of PCR master mix performed with Taq DNA polymerase (Promega USA).

MKP-2 primers: WT forward primer; 5′-CTTCAGACTGTCCCAATCAC-3' and WT reverse primer 5'-GACTCTGGATTTGGGGTCC-3′ KO forward primer; 5′- TGACTAGGGGAGGAGTAGAAGGTGGC- 3′ and KO reverse primer 5′- ATAGTGACGCAATGGCATCTCCAGG- 3′. PCR conditions for MKP-2: denaturation 95° C 2 min; 35 cycles and each cycle have denaturation 95° C 30 s, annealing 58° C 30 s, extension 2° C 5 min and final extension 72° C 5 min. The PCR products were separated by agarose gel electrophoresis.

2.5.3 DNA detection

The amplified PCR products were separated and detected by using agarose gel (1%) electrophoresis. One gram of agarose and the electrophoresis buffer 1X TAE (consisting of Tris 40 mM, EDTA 1 mM and acetic acid 1.1%) were mixed and heated for 3-4 min in a standard microwave until the agarose was dissolved. The resulting solution was transferred into the gel cast to allow for solidification, this was then transferred to the electrophoresis chamber containing 1X TAE buffer. Gels were run at 90-120 volts for 45-90 min. Ethidium bromide was directly added to the agarose gel solution. For sample loading 10 μl was used. Bands were visualized under UV-light (nm) on an image station (Genesnap from Syngene).

2.6 Cell Culture

All cell culture work was conducted in a class II cell culture hood, following strict aseptic conditions. Unless otherwise stated all cells were grown in 10 cm dishes or 25 cm^2 tissue culture flasks.

2.6.1 Isolation of Mouse Embryonic Fibroblast (MEFs)

Mouse embryonic fibroblast isolation procedure and other procedures complied with the United Kingdom Animals (Scientific Procudures) Act 1986. Ple1MKP-2 $^{-/-}$ or $^{+/+}$ mice were crossed and the females were checked for vaginal plug the following morning. Pregnant females were sacrificed at 13.5 dpc and embryos were removed from placenta under sterile conditions. The embryos were decapitated and heart and liver were removed. The remaining tissue was incubated in the presence of trypsin/EDTA under shear stress for 30min. Dissociated cells were plated in 10 cm dishes in Dulbecco's modified Eagle's medium (DMEM; Invitrogen) containing 10% fetal calf serum (FCS), L-glutamine, Penicillin and Streptomycin. Isolated cells were left over night to recover from digestion at 37°C, 5% CO_2. The following day the medium was changed to remove the trypsin and the cells were allowed to recover a further 2 days. The cells were split onto 6-well plates to 100% confluency and serum starved overnight prior to experiment. All experiments were performed within three passages.

2.6.2 Isolation of Cardiac Fibroblast (CFs)

CFs were prepared from the ventricles of adult mice (8-10 weeks old) from C57Bl/6 MKP-$2^{+/+}$ and MKP-$2^{-/-}$ (weighing between 20-30 g). Mice were anaesthetized with i.p. injection of 50 mg/kg body weight pentobarbital sodium BP and 100 IU/kg heparin. Terminal anaesthesia was comfirmed before any procedure was performed by testing the pedal reflex. The heart was rapidly removed and washed in Krebs-Heinseleit (Krebs) solution (120.9 mM NaCl, 20 mM Hepes, 2.3 mM KCl, 0.52 mM NaH_2PO_4, 3.5 mM $MgCl_2.6H_20$, 20 mM taurine, 11.4 mM creatine, 11 mM glucose anhydrous, pH

7.4). The ventricles were minced, pooled, and digested with collagenase type 2 and protease XIV (0.8 and 0.03 mg/ml) (Meszaros *et al*., 2000). Cardiac myocytes were pelleted by centrifugation at 72 g for 3 min, and supernatant containing the fibroblasts was removed. The CFs were then pelleted at 805 g for 10 min and resuspended in DMEM supplemented with penicillin, streptomycin, and 20% FCS. After a 4 h period of attachment to T-25 tissue culture plates, cells that were weakly attached or unattached (myocytes, endothelial cells, smooth muscle cells, and red blood cells) were rinsed free and discarded. After 4–5 days, subconfluent cultures were passaged by trypsinization and replated into 12 well plates. Passage 1 cells were used in all experiments. In all experiments, DMEM containing 20% FCS was washed out, and the cells were equilibrated in serum-free DMEM overnight before agonist stimulation.

2.7 Characterization of Cardiac Fibroblasts by immunofluorescence

CFs and smooth muscle cells were grown on plain cover slips and fixed by aspirating the culture medium and applying 4% paraformaldehyde for 10 min. This was followed by a 10 min exposure to cold methanol. The slides were then washed with PBS (x3 washes) and exposed to 0.01% triton-x for 10min. Non specific binding was blocked using 1% BSA in PBS for 1 h at room temperature and then primary antibody α-smooth muscle actin was added without washing at concentrations of 1:100, 1:250, 1:500 & 1: 1000 made in PBS containing 1% BSA and the cells were incubated overnight at 4°C. The α-smooth muscle actin primary antibody was raised in rabbit. The secondary antibody anti rabbit was applied at a dilution of 1:200 in sterile PBS and followed by incubation at room temperature for 1 hour. After washing, cover slips were mounted using Vectashield® mounting medium containing DAPI (Vecta laboratory) and stored in the dark at 4°C until they were viewed and photographed. The DAPI in the mounting medium stained the cells' nucleus blue. Pictures were taken using Nikon Eclipes™ E600 Oil Immersion

microscope connected to a photometrics (CoolSnap™ Fx) digital camera managed by MetaMorph™ software (Universal Imaging Corporation, West Chester, PA).

2.8 Proliferation by [^{3}H] Thymidine incorporation assay

DNA synthesis was used as a measure of mouse embryonic fibroblast (MEFs) or cardiac fibroblasts (CFs) proliferation. MEFs or CFs were plated on 24-well tissue culture plates and grown to approximately 70% confluency at 37°C and made quiescent with serum free media for 24h. The quiescent cells were stimulated with graded FCS concentration (0, 0.5, 1, 2.5, 5 and 10%) or 20% FCS for 24 h. Cells were treated in triplicate for a period of 24h, with [^{3}H]-thymidine (0.1 μCi/well) being added to the media during the final 5-6 h of the 24 h stimulation to allow the estimation of DNA synthesis via incorporation of [^{3}H] Thymidine into the newly formed DNA. At 24 h the media containing the label was removed and the cells washed twice with 1ml PBS. This was followed by 4-6 x 1 ml washes with 10% trichloroacetic acid (TCA) at intervals of 15 min. The remaining cell contents were dissolved in 250 μl 0.1% NaOH/Sodium lauryl sulphate solution. The contents of each well were then transferred to scintillation vials containing 2 ml of Emulsifier-safe™ scintillation fluid (PerkinElmer, Boston, USA). Vials were vortexed thoroughly before radioactive counts were measured by scintillation counter (Packard 1500 TRI-CARB®). Counts were measured in DPMs (disintegrations per minute).

2.9 Proliferation by Cell Counting by haematoxylin staining

Confluent MEFs or CFs were detached with trypsin-EDTA, seeded on coverslips into 24-well plates (5,000 cells/well) in 20% FCS-DMEM, and allowed to attach for 24 h. Cells were starved in serum free media for 24 h and then stimulated for either 24, 48, 72 h (each point performed in triplicate) with 10% FCS. Cultures were washed twice with cold PBS and then fixed in 70%

methanol for 30 min at room temperature. Fixed cells were then washed (2x5 min) with cold PBS, and stained with 1 ml Haematoxylin for 20 min at room temperature. Excess Haematoxylin was removed by rinsing with distilled water until coverslips become transparent. A drop of mounting medium (mowial) was added on to the each coverslip. The average number of cells per time point was determined by counting and averaging the number of cells in 10 random fields per coverslip using MF-830 Microforge Microscope connected to Motic Images Plus 2.0 software.

2.10 Assessment of MEFs doubling time

Confluent MEFs were trypsinized and seeded in 6-well plates at 2 x 10^4 cells per well. Cell doubling time protocol was an adaptation of culture of animal cells technique described previously (Freshney, 1994). Cells were incubated for 24 h at 37°C, 5% CO_2. After 24 h cells in 2 wells were trypsinized and counted with haemocytometer (mean ± SD of the density was calculated). The procedure was repeated after 48 h and 72 h. Results were plotted graphically as cells / well vs time the mean doubling time was calculated from the graph for at least two densities (i.e 3 x 10^4 – 6 x10^4; 5 x 10^4 – 1 x10^5), and the doubling time in days was estimated from these experimentss.

2.11 G1/S Cell Synchronization Using Double Thymidine Block

Mouse embryonic fibroblasts were grown in 3.5 cm dishes in DMEM Invitrogen, containing 10% FCS, L-glutamine, Penicillin and Streptomycin to about 40% confluency. Thymidine triphosphate (TTP) that had been resuspended in PBS was added to achieve a final concentration of 2 mM in the media. The cells were incubated at 37º C for strictly 19 h. After the incubation, media was removed and cells were washed 3x with PBS or media. Fresh media was then added without TTP and incubated for 9 hrs at 37º C. TTP (2 mM final conc) was re-added to the media and incubated for another 16 h. Cells were washed with PBS or media 3x and fresh media was added. At

this stage the cells are now in G1 and will be 'released' to progress through the cell cycle over the next 15 h. The cells should be uniform for about 1-2 cell divisions and then regain their asynchronous state. Cells were harvested at different time points and the cell-cycle profile was analysed by western blotting.

2.12. Minimally Invasive Transverse Aortic Banding (MTAB)

Adult male C57BL/6 mice weighing between 20-30 g were used for these experiments. Surgical protocol was an adaptation of an MTAB technique described previously (Hu et al., 2003). Briefly, animals were anaesthetised in a Perspex chamber with 3% Isoflurane (Concord Pharmaceuticals Ltd.) in the presence of 100% Oxygen at a flow rate of 2 l/min. Animals were given 60 μg/kg Buprenorphine intramuscularly and body temperature was maintained within physiological limits (37.0°C ± 0.5°C) using a homeothermic blanket (Harvard, U.K.) or heat lamp. Then a small horizontal skin incision ~0.5 - 1.0 cm in length was made at the level of the suprasternal notch. Following ligation of the arch of aorta, the skin was sutured and the mice were left to recover until fully awake. Sham-operated animals went through the same procedure except the aortic arch was not tied. Straight away after surgery 0.5 ml saline and another dose of Buprenorphine was given subcutaneously. Animals were housed in heated cages for 24 h following surgery and were left for 2 or 4 weeks to allow cardiac remodeling to occur.

2. 13 Adult Mouse Transthoracic Echocardiography

Adult MKP-$2^{+/+}$ and MKP-$2^{-/-}$ mice weighing between 20-30 g were used for these experiments. Mice were anaesthetised in a Perspex chamber with 3% Isoflurane (Concord Pharmaceuticals Ltd.) in the presence of 100% Oxygen at a flow rate of 2 l/min. After 2 to 3 minutes mice were placed supine (or in the left lateral decubitus position) on a face- mask and were maintained with 1.5 - 2% Isoflurane in the presence of 0.5 - 1L/min oxygen (to maintain light

anesthesia and spontanenous breath). Body temperature was maintained within physiological limits (37.0° C ± 0.5° C) using a homeothermic blanket (Harvard, U.K.) or heat lamp. A topical depilatory cream (Veet, Reckitt Benckiser, U.K.) was used to remove fur from the upper chest area of the mice. Transthoracic echocardiography was performed using a HDI 3000 ultrasound machine (U.K.) with a 13MHz transducer and ultrasound transmission gel. After a two-dimensional (2D) image was obtained in the parasternal long axis view at the level close to papillary muscles, the probe was angled 90° with respect to this axis to achieve the parasternal short axis view. A 2D guided M-mode trace crossing the anterior and posterior wall of the left ventricle was recorded. Caution was given not to apply excessive pressure over the chest, which could cause bradycardia and deformation of the heart. The following parameters were measured digitally on the M-mode tracings and averaged from three cardiac cycles: anterior and posterior wall thickness, left ventricular dimensions in systole and diastole and these measurements were used to calculate fractional shortening as shown by the following equation:

Fractional shortening (FS) was calculated using left ventricle dimensions in end of systole and diastole (LVES and LVED, respectively) according to the formula:

$$FS = [(LVED - LVES) / LVED] \times 100 (\%).$$

The duration of the procedure was 20 min. Mice were recovered by removing anaesthesia and allowing them to breathe oxygen before putting them under a heat lamp to maintain body temperature. Time to loss and restoration of the righting reflex were also determined. Isoflurane produced high initial heart rates (HR), (450 beats / min) and the most stable percent fractional shortening (%FS) and end-diastolic dimension (EDD) (Roth *et al*., 2002).

2.14 Preparation of heart homogenate

Whole heart homogenates were prepared from sham and MTAB operated mice and were used for the quantitative experiments. Mice were anaesthetized with i.p. injection of 50 mg/kg body weight pentobarbital sodium BP and 100 IU/kg heparin and the heart quickly excised and washed with ice-cold Krebs solution to clear the heart chambers of blood. All following steps were then carried out on ice. Both left ventricles were excised, weighed and homogenized in 5 volumes of homogenization buffer (20 mM tris-base buffer, pH 7.4, 10 μl/ml protease inhibitor cocktail, 1 mM DTT) using an ultraturax (Labortechnik). The tissue samples were then assayed for total protein content (as described in section 2.15) and stored at -80° C until use.

2.15 Protein Assay

Total protein content of heart tissue preparations was evaluated using Coomassie Plus Protein Reagent with BSA to create a standard curve with concentrations ranging from 0.1 to 1.0 mg/ml. Samples were prepared at appropriate dilutions, which should fall within the linear range of the protein BSA standard curve. A total volume of 10 μl of each albumin standard curve and tissue sample was loaded into 96-well plate in triplicate with one row of distilled water as a blank background. The plate was read using a microplate reader (Model 680, BioRad) at 595 nm absorbance. Standards were plotted using a sigmoidal fit and only samples with absorbance readings falling in the linear area of the curve were quantified.

2.16 Western Blotting

2.16.1 Preparation of samples for SDS-PAGE

Cells were plated onto appropriate tissue culture plastic dishes, quiesced and stimulated with the selective agonists for the required time periods after which the cells were placed on ice to stop the agonist reaction. Cells were

then washed twice with 1ml of ice cold PBS after which 200 μl of SDS-PAGE sample buffer (63mM Tris-HCL, pH 6.8, 2mM $Na_4P_2O_7$, 5mM EDTA, 10% (v/v) glycerol, 2% (w/v) SDS, 50 mM DTT, 0.007% (w/v) bromophenol blue) was added. Cells were then scraped, resulting in shearing of chromosomal DNA by passing through a 21 gauge needle repeatedly. Samples were then transferred into a pierced 1.5 Eppendorf tubes, after which they were boiled for 5 minutes, to achieve protein denaturation. Samples were then stored at -20^{o}C until required for SDS-PAGE

2.16.2 SDS-Polyacrylamide Gel Electrophoresis (SDS-PAGE)

Resolving gels were prepared containing appropriate amounts (7.5% (w/v), 9% (w/v), 10% (w/v), 11% (w/v) of acrylamide: N'-methylenebis-acrylamide (30:0.8), 0.375M Tris pH 8.8, 0.1% (w/v) SDS and 0.05% (w/v) ammonium persulfate (APS) . Polymerisation was initiated by the addition of 0.05% (v/v) N,N,N,N', N'-tetramethylethylenediamine (TEMED). The solution was then mixed thoroughly and poured between 2 assembled glass plates, allowing enough space at the top for stacking gel after which they were overlaid with 150 ml of 0.1% (w/v) SDS. Once polymerised, the 0.1% SDS was poured off and the gel surface rinsed with distilled water to remove excess polyacrylamide, then the stacking gel containing 10% (v/v) acrylamide. N,N'-methylenebisacrylamide (30:0.8), in 125 mM Tris, pH 6.8, 0.1% (w/v), SDS, 0.05% APS and 0.05% (v/v) TEMED was poured on top of the resolving gel, and an appropriate Teflon spacer comb inserted into the stacking gel. The stacking gel was allowed to polymerize for about 15 minutes before the removal of the comb and the gels were then assembled in a Bio-Rad Mini-PROTEAN II ™ electrophoresis tank. Both the inner and the outer reservoirs were filled with electrophoresis running buffer (24.8 mM Tris, 191.8 mM glycine, 0.1% SDS (w/v). Standardized protein samples were loaded into the wells of the stacking gel using a Hamilton micro-syringe and run concurrently with a pre-stained SDS protein marker of known molecular weight. An electrical current of 130V was passed between the electrodes from

a Hoeffer P250/2.5 amp DC power supply until the loading dye bands had passed out of the resolving gel.

2.16.3 Electrophoretic Transfer of Proteins to Nitrocellulose Membrane

Proteins resolved by SDS-PAGE were then transferred to nitrocellulose membrane by means of electrophoretic transfer (Towbin *et al*., 1992). The gel was placed against a nitrocellulose sheet and assembled in a transfer cassette, where it was sandwiched between 3MM paper and 2 sponge pads. The cassette was then immersed in blotting buffer (25 mM Tris, 19 mM Glycine, 20% (v/v) Methanol) in a Bio-Rad Mini Trans-Blot ™ tank where a constant current of 250 mA was applied for 1 hour 50 minutes. The tank was cooled during this transfer by inclusion of an ice reservoir. The presence of SDS in the resolving gel would confer a negative charge on the proteins so the cassette was orientated with nitrocellulose towards the anode.

ANTIBODY	COMPANY	CATALOGUE	DILUTION	SECONDARY
Total ERK	Santa Cruz	sc-94	1:7500	HRP α-Rabbit
Total p38	Santa Cruz	sc-728	1:7500	HRP α-Rabbit
Total JNK	Santa Cruz	sc-571	1:7500	HRP α-Rabbit
GAPDH	Abcam	ab8245-100	1:7500	HRP α-Mouse
MKP-2	Santa Cruz	sc-1200	1:5000	HRP α-Rabbit
Cyclin B1	Santa Cruz	sc-245 (GNS1)	1:1000	HRP α-Mouse
Caspase-3	Cell signalling	9661S	1:1000	HRP α-Rabbit
Caspase-9	Cell signalling	9502	1:1000	HRP α-Rabbit
H2AX	Millipore	07-164	1:1000	HRP α-Rabbit
Phospho ERK	Santa Cruz	Sc81492	1:7500	HRP α-Mouse
Phospho JNK	Cell signalling	9251S	1:5000	HRP α-Rabbit
Phospho p38	Biosource	368500	1:7500	HRP α-Rabbit
Phospho cdc2	Cell Signalling	9111S	1:1000	HRP α-Rabbit

Table 2.1: Antibodies Used in Study

2.16.4 Immunological Detection of Proteins

Following the protein transfer to nitrocellulose membrane, the membrane was removed after which it was saturated by incubating the membrane in a solution of 2% (w/v) BSA in NaTT buffer (150 mM NaCl, 20 mM Tris, 0.2% (v/v) Tween 20, pH 7.4), for 2 hours. The 2% BSA blocking buffer was then removed and replaced with 0.2% (w/v) BSA in NaTT buffer, and incubated overnight at room temperature on a platform shaker, with an appropriate

amount of primary antibody added, which is specific to the protein of interest.

The incubated blots were washed for 90 minutes, at intervals of 15 minutes with NaTT buffer on a platform shaker, after which a secondary horseradish peroxidase conjugated IgG antibody which was specifically directed against the primary antibody was added in NaTT buffer containing 0.2% BSA (see table 2.1). The nitrocellulose membrane was then incubated with the secondary antibody at room temperature on the platform shaker for a period of 2 hours. The blots were once again washed at room temperature for 90 minutes, at intervals of 15 minutes with NaTT buffer. Then the Nitocellulose membranes were exposed to enhanced chemiluminescence (ECL) reagent for about 2 minutes and blotted onto paper towel to remove any excess liquid. The blots were then mounted onto an exposure cassette and covered with cling film. Blots were exposed to Kodak X-OMAT LS film for 1-5 minutes under darkroom conditions and developed using a Kodak M35-M X-OMAT processor.

2.16.5 Stripping for reblotting

Antibodies were removed from nitrocellulose by incubation for 1 h at 50-55° C in a stripping buffer containing Tris-HCl 62.5 mM, SDS 2% and β-mercaptoethanol 0.8% pH 6.7. The membranes were washed for 45 min at 15 min interval with NaTT buffer and incubated with new antibodies as described in section 2.16.4.

2.16.6 Scanning densitometry

All data obtained through immunoblotting were scanned on GS-800 Calibrated Densitometer (BIO-RAD). All quantified values were normalized against control values.

2.17 Cell Cycle Analysis

Cell cycle profiles were analysed by staining intracellular DNA with propidium iodide. MEFs were grown to confluency in 6-well plate and serum starved for 24 h, and then released into growth media for another 24 h. MEFs were trypsinized and washed with PBS and prepared at $1x10^6$ in eppendorf tubes. Cells were fixed in ice-cold 70% ethanol (dropwise while vortexing to ensure proper fixation of cells and prevent clumping) at 4° C overnight. Cells were washed with PBS and centrifuged at 358 g for 10 min, then RNase A (50ug/ml) was added and incubated at 37° C for 1 h to ensure only DNA staining. Samples were stained with propidium iodide (PI) at 50 ug/ml. The cell cycle parameters from 10,000 gated events were read in the FACS scan flow cytometer using FACS Diva software (FACS scan, Becton Dickinson, Oxford, UK). The data was analysed using FACS Diva software (Becton Dickinson, Oxford, UK).

2.18 MKP-2 Adenovirus infection of MEFs

Initially the appropriate volume of adenovirus to apply to cells in order to give an appropriate multiplicity of infection (MOI) was determined. For this purpose MKP-$2^{-/-}$ MEFs were infected with increasing concentration of Adv. MKP-2 at 100, 200, 300 and 500 pfu and MKP-2 expression assessed by western blotting. Cells were seeded onto coverslips in 24-well plates and grown to approximately 50% confluency and the cell number was determined using a haemocytometer. MKP-2 adenovirus (300 pfu/cell) were added to the cells and incubated for 24 h in serum free media. After 24 h cells were released into normal growth media for additional 24 h. Cells were then serum starved for 24 h before stimulation with 10% FCS for 24, 48, 72 h. At the end of the stimulation cells were processed for proliferation assay as described in section 2.8.

2.19 Apoptosis assay by flow cytometry

MEFs were grown on 6-well plates and were infected for 40 h then stimulated with anisomycin or UVC for a further 12 h or 24 h respectively prior to analysis. Supernatant was collected and cells were trypsinised and then pelleted at 201 g for 5 min. The pellet was then resuspended in 500 μl of 1x annexin binding buffer (10 mM Hepes/NaOH, pH 7.4, 140 mM NaCl and 2.5 mM $CaCl_2$). Phycoerthyrin-Annexin V and 7-AAD were added to the cells according to the manufacturer's instructions and the samples were read in the FACS scan flow cytometer using FACS Diva software (FACS scan, Becton Dickinson, Oxford, UK). The data was analysed using FACS Diva (Becton Dickinson, Oxford, UK) and RCS Express (De Novo Software, Canada) software. A total of 10,000 events were measured per sample. Gating was determined using Phycoerthrin (PE)-Annexin V FL-2 and 7-Amino-Actinomycin (7–AAD) FL-3 standards attached to beads (Becton Dickinson, Oxford, UK) and preliminary experiments were conducted using paraformaldehyde and serum deprivation to define apoptotic and necrotic populations as outlined by the manufacturer's instructions.

2.20 Data Analysis

All data are presented as mean±s.e.m. Protein levels were compared using student's unpaired two-tailed *t* test (Graphpad Prism 5) comparison of physiologic parameters were made using one- and two-way analysis of variance (ANOVA). Post hoc tests were conducted using Dunnett's test and Bonferroni's multiple comparison tests. A value of $P<0.05$ was considered statistically significant.

CHAPTER 3

CHARACTERIZATION OF CELLULAR FUNCTIONS OF MKP-2 AND MAPK MEDIATED SIGNALLING IN PRIMARY MOUSE EMBRYONIC FIBROBLAST (MEF)

CHAPTER 3: Characterization of cellular functions of MKP-2 and MAPK mediated Signalling in Primary Mouse Embryonic Fibroblast (MEF)

3.1 Introduction

MAPKs are recognized as key proteins in the regulation of diverse physiological functions within the cell including proliferation, differentiation, gene expression and apoptosis. They are normally activated by dual phosphorylation at the unique activation motif Thr-X-Tyr in order to perform their function (Kyriakis and Avruch, 2001). The regulation of the activity of these kinases is dedicated to another important group of proteins, the dual specificity phosphatases (DUSPs), which normally dephosphorylate the MAPKs leading to their inactivation. For one of these DUSPs, MKP-2, there is relatively little information regarding its regulation and function particularly using knockout mice. Utilizing a novel DUSP-4 or MKP-2 deletion mouse developed in the laboratory, the aim of the experiments in this chapter were firstly to describe the characterization of MKP-2 induction, secondly to correlate loss of DUSP-4 with changes in MAPK signalling and thirdly to correlate these effects with cellular proliferation and cell survival. The data presented in this chapter are from primary mouse embryonic fibroblasts (MEFs). Preparations of MEFs have the advantage that molecular biological techniques and protocols can easily be performed, allowing a definitive understanding of potential signal transduction pathways. They are a widely used cell model to characterize systems when knockout animals are generated and will thus provide a frame work for the subsequent analysis of fibroblasts derived from adult hearts.

3.2 RESULTS

3.2.1 MKP-2 knockout generation and Southern blot mouse screening

The deletion of the DUSP-4 gene was performed by Genoway, Lyon, France under instruction by Dr. Laurence Cadalbert (The Beatson Institute for Cancer Research, Switchback Road, Bearsden Glasgow G61 1BD) who devised the deletion strategy. This involved deleting exon 2-4 and replacing the selected region with a Neomycin resistant cassette from the mouse MKP-2/DUSP4 gene (gene sequence available from Ensemble database: ENSMUSG000000120875). Therefore most of the reading frame (starting in exon-1) and also the 3'UTR region of the MKP-2 mRNA (present in exon-4) was deleted (see figure 3.1 A). Details of the construct can be found in section (2.4). The selection for animals carrying the mutation was performed by southern blotting which could distinguish the wild type allele (9.9kb) and the mutant allele (8.3kb) after hybridisation using radiolabelled probe K (figure 3.1 B). Routinely mice were genotyped by PCR of tail tip DNA and backcrosses of 3-5 were used (see figure 3.2). Young adult male MKP-2 KO and wild type mice are shown in figure 3.3 and demonstrated no apparent phenotypic defects, bred normally and had normal body weights similar to wild type littermates. Knockout animals are fertile and displayed no behavioural, developmental or growth abnormalities.

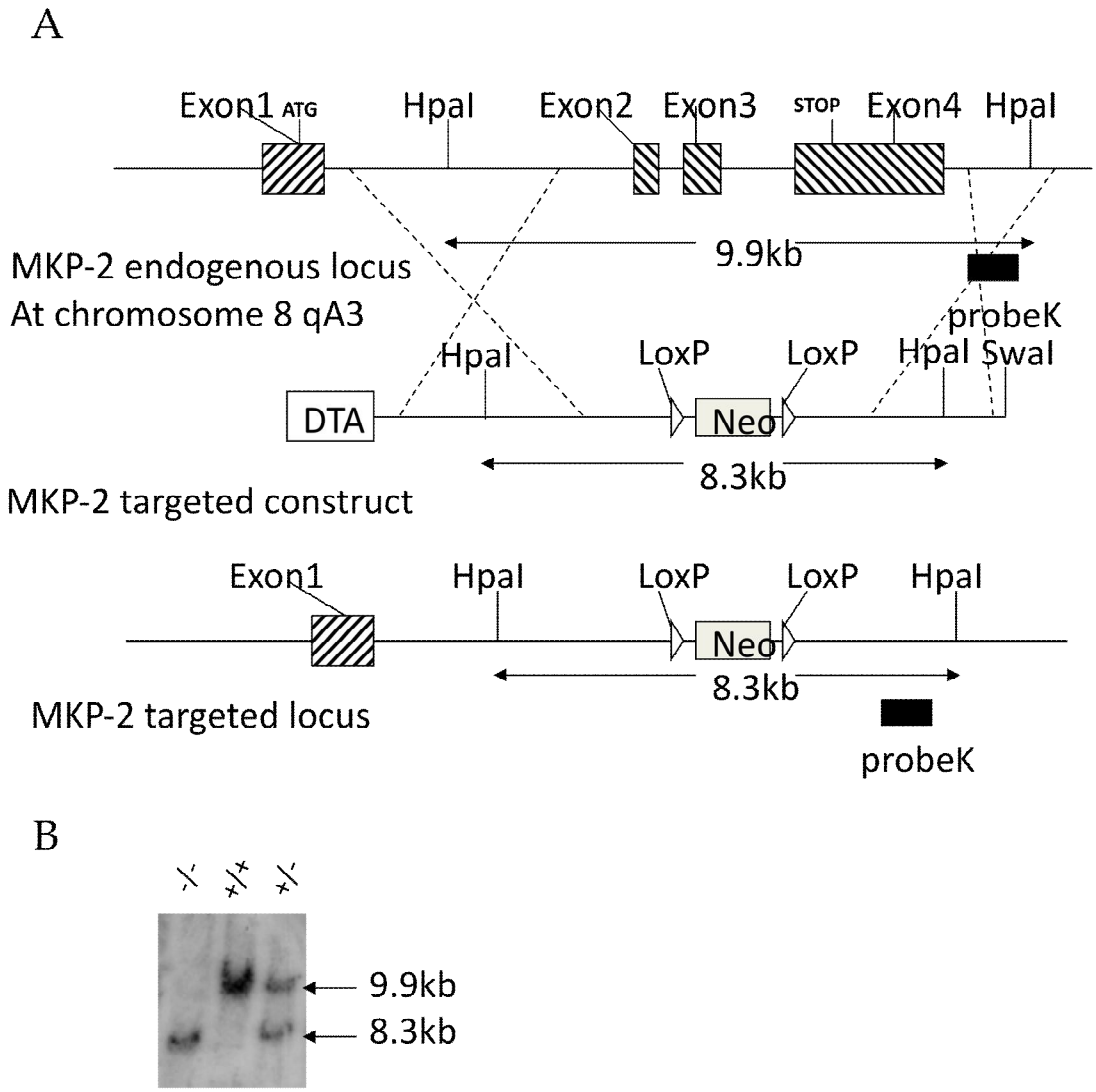

Figure 3.1: Generation of mice lacking DUSP4/MKP-2 gene by targeted homologous recombination: Schematic showing the DUSP4/MKP-2 gene locus, the targeted construct and the resulting targeted allele. Recombination events are indicated by dashed lines and show the replacement of a 8.3kb SwaI DUSP4/MKP-2 genomic fragment containing exon 2-4 by the PGK-Neo cassette. SwaI and HpaI described the restriction sites for the respective enzymes. The pGK-Neo cassette is flanked by LoxP sites. DTA represents the negative selection cassette. Top right panel showed an example of the 3' southern blot analysis of mouse tail tip genomic DNA following digestion with HpaI using an external Probe K as indicated in panel. The autoradiography revealed the 9.9kb (wild type) and 8.3kb (targeted) fragments representing the two different alleles discriminating wild type, heterozygote or homozygote mutant animals.

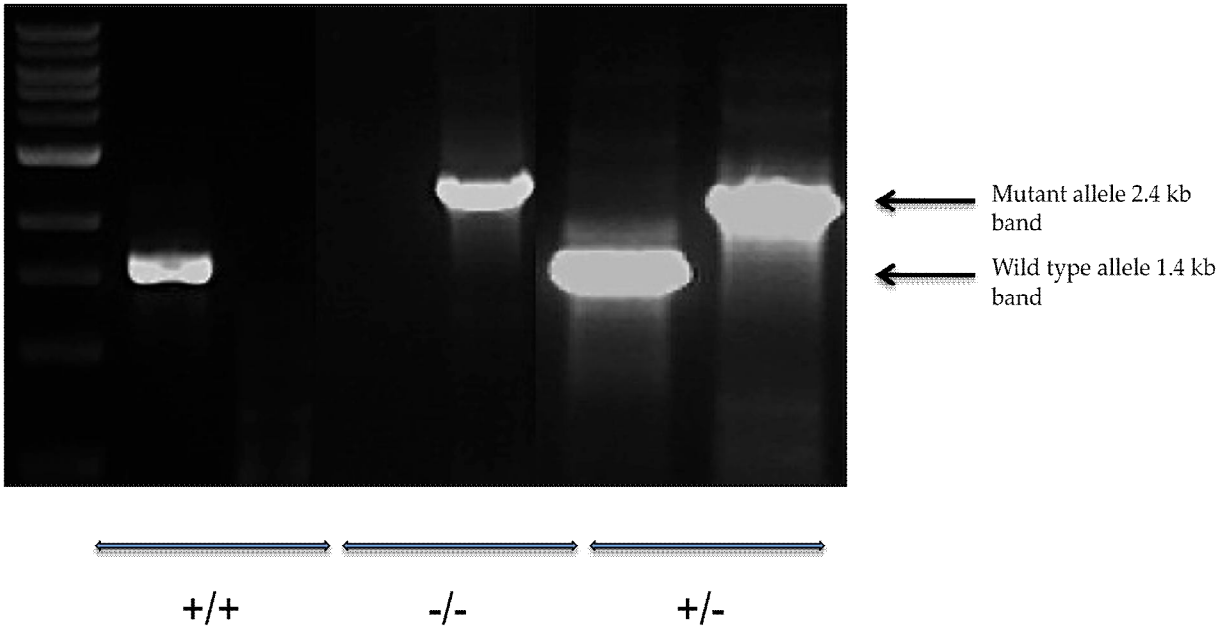

Figure 3.2: MKP-2 mice genotyping by PCR of tail tip DNA

The PCR screening for MKP-2 mice genotype. The arrows illustrate the mutated allele 2.4 kb and wild type allele 1.4 kb localization. Digestion products were analysed on 1% agarose gel.

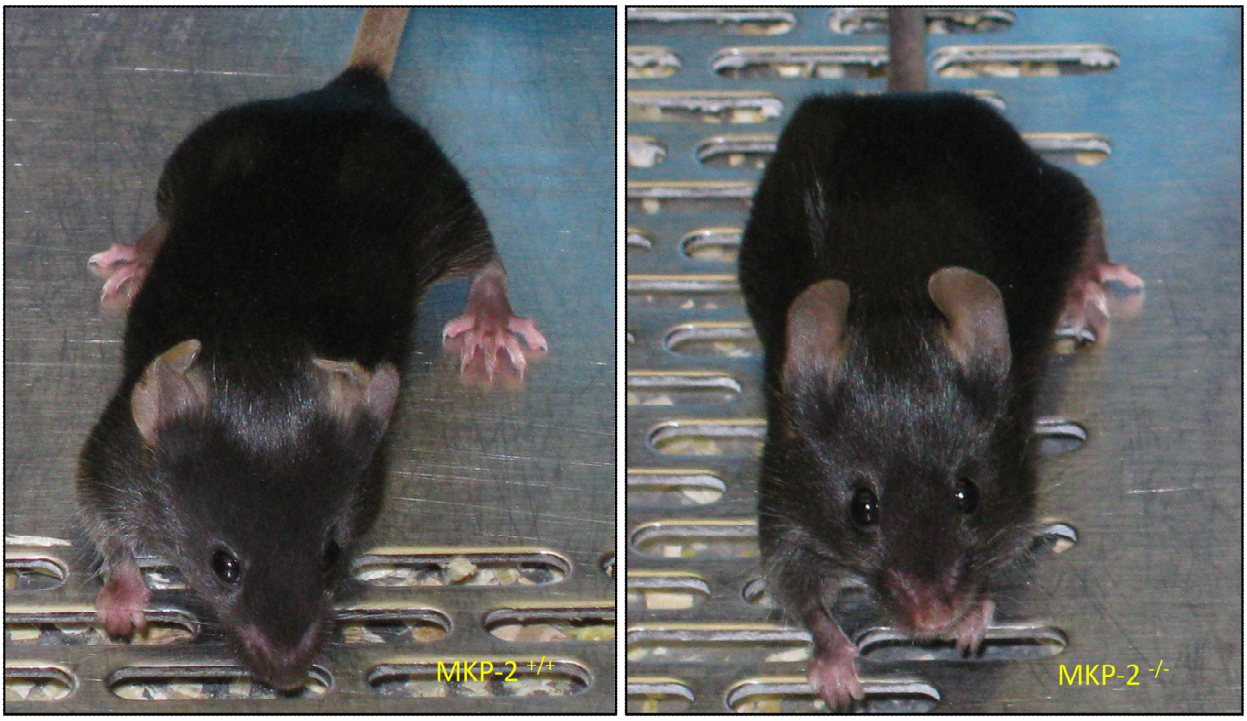

Figure 3.3: Young adult males MKP-2 KO (right) and WT (left). Knockout mice had normal weight, fertile and displayed no behavioural, developmental or growth abnormalities.

3.2.2 Induction of MKP-2

3.2.2.1 Induction of MKP-2 in response to Serum

Initially the kinetics of MKP-2 induction in response to FCS was examined over short (0-120 min) and long time courses (0-24 h). MEFs were grown to confluency in 6-well plates and were serum starved for 24 h before incubation with 10% FCS. Whole cell lysates were analysed by western blotting for MKP-2 expression. The data presented in figure 3.4 shows that after a delay, MKP-2 protein was induced after 120 min in MKP-$2^{+/+}$ MEFs. However, no induction was observed in MKP-$2^{-/-}$ MEFs (panels A & B). In MKP-$2^{+/+}$ MEFs (panel C & D), MKP-2 protein expression was induced after 2 h, peaked at 4 h at approximately 3.5 fold increase of basal values, and was sustained for up to 8 h before returning to basal levels after 24 h. However, no induction was observed in MEFs derived from MKP-$2^{-/-}$ mice. Total p38 MAPK levels were unchanged, indicating equal protein loading. This confirmed the complete absence of MKP-2 protein in MKP-$2^{-/-}$ MEFs and also established that serum is capable of activating endogenous MKP-2 expression in MKP-$2^{+/+}$ MEFs.

Having established the kinetics of MKP-2 induction, a concentration response curve to serum was established. Cells were serum starved for 24 h and incubated with increasing concentration of FCS (0.5, 1, 2, 5 and 10%) for 120 min (see figure 3.5 panels A & B). The results demonstrate that FCS induced a concentration dependent increase in MKP-2 protein expression with the induction beginning at 1% FCS with maximal induction attained with 10% FCS (fold stim. at 120 min in wild type = 1.91 ± 0.10, n=3). However, no expression was observed in MEFs derived from MKP-$2^{-/-}$ mice. This again confirmed the complete absence of MKP-2 protein in MKP-$2^{-/-}$ MEFs. Therefore, since FCS exerts its maximal effect at the concentration of 10%, this concentration was used in the remaining experiments.

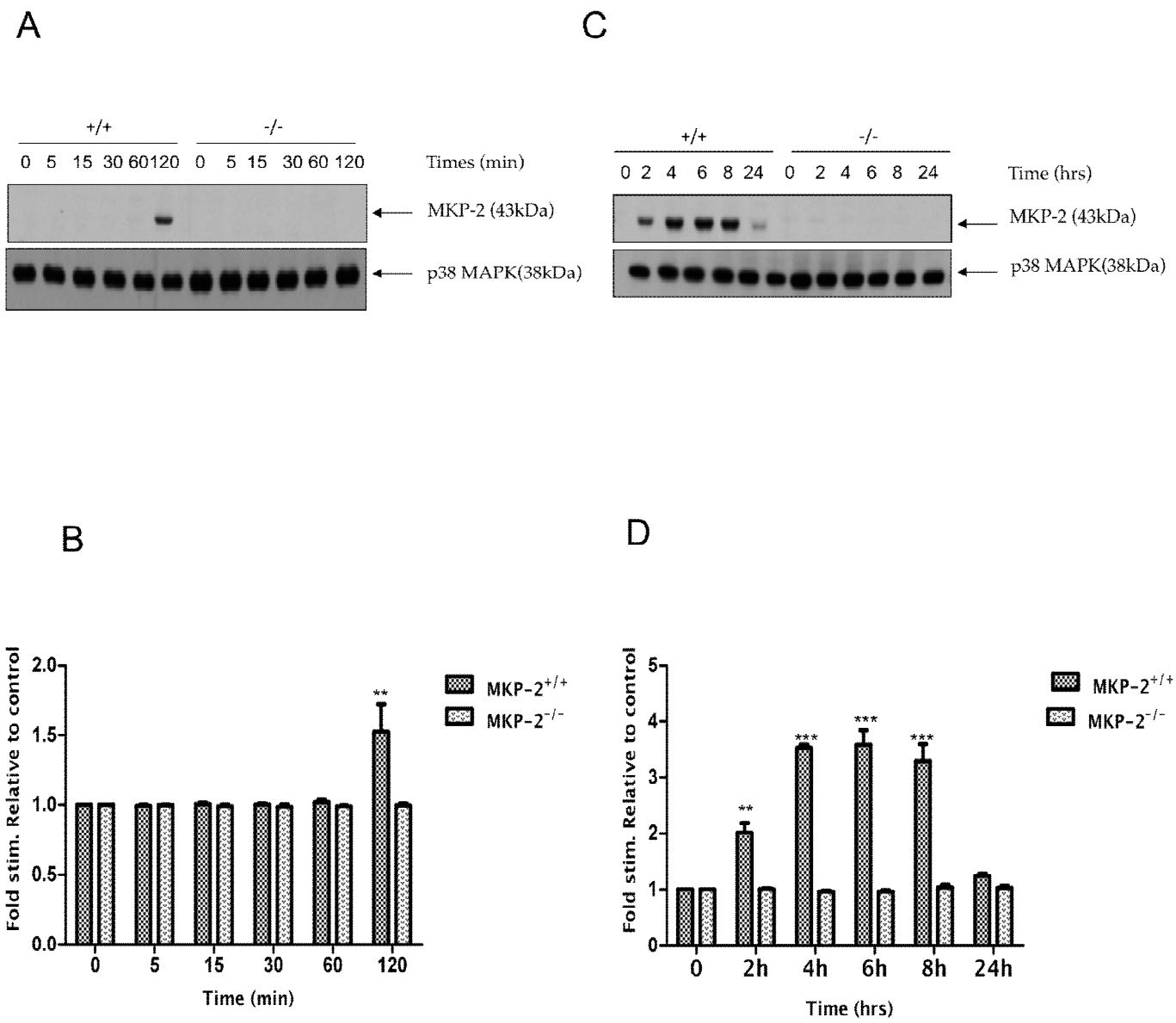

Figure 3.4: Induction of MKP-2 in MEFs in response to 10% FCS. Confluent MEFs were quiesced for 24 h in serum free media. The cells were incubated with 10% FCS for 0-120 min and 0-24 h. Whole cell extracts were resolved by SDS-PAGE and examined by Western blotting for induction of MKP-2 as outlined in section 2.16. Relative induction of MKP-2 is outlined in panel A & C and panel B & D illustrates quantification by densitometry. Data expressed as mean±s.e.m. Statistical analysis was by one-way ANOVA, post hoc test by Dunnett's test, **p<0.05, ***p<0.001 in comparison with control group. Each blot is representative of 3 individual experiments.

A

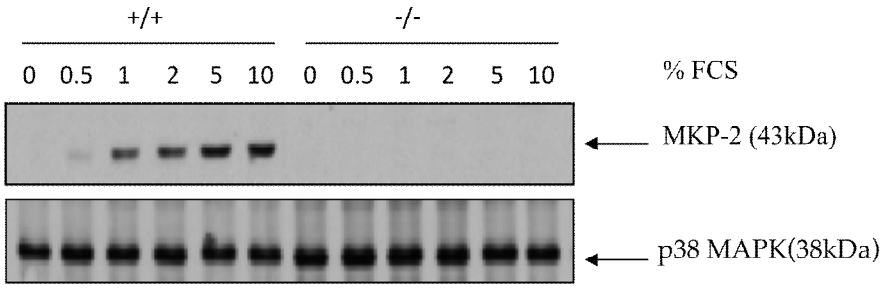

B

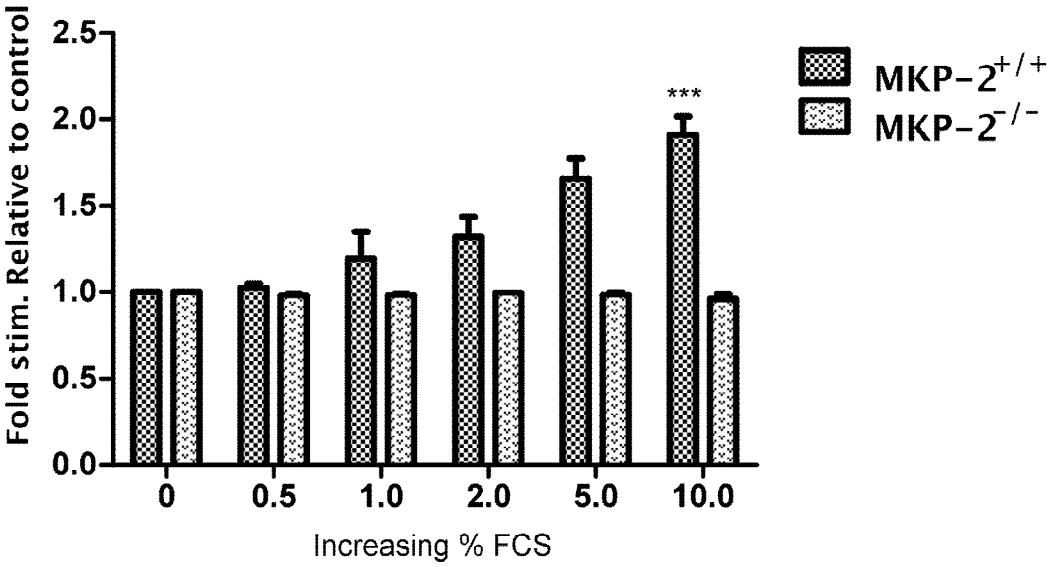

Figure 3.5: Induction of MKP-2 in MEFs in response to increasing FCS concentration.

Confluent MEFs were quiesced for 24 h in serum free media. The cells were incubated with increasing concentration of FCS for 2 h. Whole cell extracts were resolved by SDS-PAGE and examined by Western blotting for induction of MKP-2 as outlined in section 2.16. Relative induction of MKP-2 is outlined in panel A and panel B illustrates quantification by densitometry. Data expressed as mean±s.e.m. Statistical analysis was by one-way ANOVA, post hoc test by Dunnett's test, ***$p<0.001$ in comparison with control group. Each blot is representative of 3 individual experiments.

3.2.2.2 Induction of MKP-2 in response to PMA

Similar to the experiment with serum, PMA (100 nM) was used to assess the induction of MKP-2 in MEFs. The results presented in figure 3.6 demonstrated that similar to serum, PMA caused the induction of MKP-2 protein in wild type MEFs after a delay of at least 60 min with induction only starting to be seen at the 120 min time point (panels A & B). In panels C & D, MKP-$2^{+/+}$ MEFs responded to PMA stimulation with a strong induction of MKP-2 which peaked at 4 h (approximately a 3-4 fold increase in expression compared with control) and was still detectable up to 8 h. Levels decline to near basal values by 24 h. However, no expression was observed in MEFs derived from MKP-$2^{-/-}$ MEFs. This result established that PMA, like serum, activates endogenous MKP-2 expression in wild type MEFs.

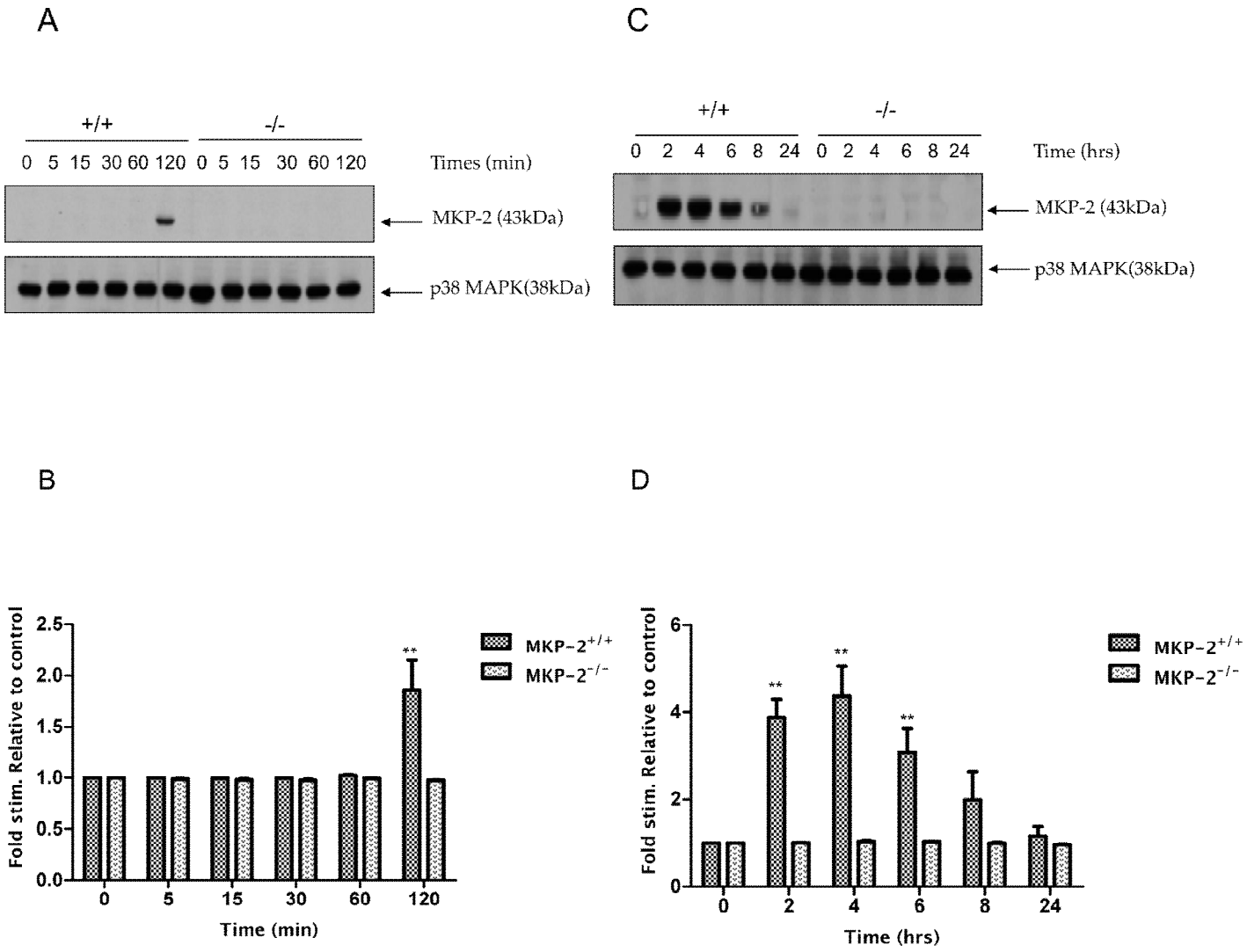

Figure 3.6: Induction of MKP-2 in MEFs in response to PMA.

Confluent MEFs were quiesced for 24 h in serum free media. The cells were stimulated with PMA (100nM) for 0-120 min. Whole cell extracts were resolved by SDS-PAGE and examined by Western blotting for induction of MKP-2 as outlined in section 2.16. Relative induction of MKP-2 is outlined in panel A & C and panel B & D illustrates quantification by densitometry. Data expressed as mean±s.e.m. Statistical analysis was by one-way ANOVA, post hoc test by Dunnett's test, *p<0.05, **p<0.01 in comparison with control group. Each blot is representative of 3 individual experiments.

3.2.2.3 Induction of MKP-2 in response to PDGF

Similar to the experiment with serum and PMA, the growth factor PDGF (10 ng/ml) was used to assess the induction of MKP-2 in MEFs. The results presented in figure 3.7 showed that there was a marked increase in the amount of MKP-2 protein following PDGF treatment after only 120 min, a similar in delay in induction was observed (panels A & C). Assessing induction in MKP-$2^{+/+}$ MEFs over a longer time course, as with serum and PMA (see figures 3.4 and 3.6 respectively), PDGF also caused a time dependent increase in MKP-2 protein expression beginning after 2 h (panels B & D) peaking at 4 h, at approximately 2 fold of basal values and being sustained up to 8 h. Levels again return to basal values by 24 h in MKP-$2^{+/+}$ MEFs. However, no expression was observed in MEFs derived from MKP-$2^{-/-}$ MEFs. These results also confirmed that PDGF, like serum and PMA, activate endogenous MKP-2 expression in wild type MEFs.

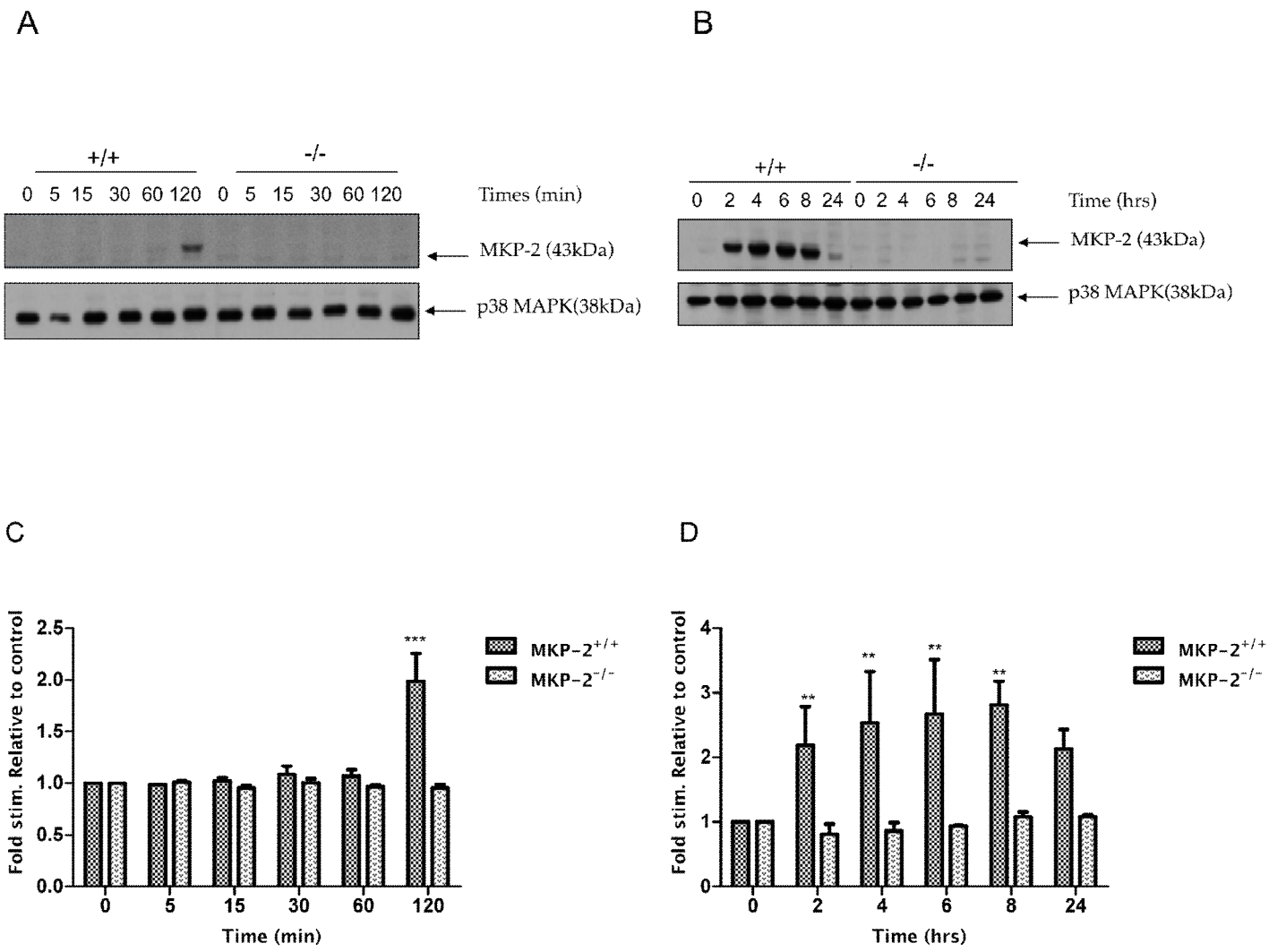

Figure 3.7: Induction of MKP-2 in MEFs in response to PDGF.

Confluent MEFs were quiesced for 24 h in serum free media. The cells were stimulated with PDGF (10 ng/ml) for 0-120 min. Whole cell extracts were resolved by SDS-PAGE and examined by Western blotting for induction of MKP-2 as outlined in section 2.16. Relative induction of MKP-2 is outlined in panel A & C and panel B & D illustrates quantification by densitometry. Data expressed as mean±s.e.m. Statistical analysis was by one-way ANOVA, post hoc test by Dunnett's test, *p<0.05, **p<0.01, ***p<0.001 in comparison with control group. Each blot is representative of 3 individual experiments.

3.2.2.4 MKP-2 induction depends on prior ERK activation

Studies have indicated that MAPKs in particular ERK play a role in the induction of MKPs as part of a negative feedback interaction which could potentially affect the dephosphorylation capacity of this phosphatase towards these kinases. Wild type MEFs were pre-incubated with MEK inhibitor, U0126 (10 μM), JNK inhibitor, SP600125 (10 μM) or p38 MAPK inhibitor, SB203580 (10 μM) for 1 h prior to being stimulated with 10% FCS for the times indicated. This concentration of the inhibitors was used based on previous studies in other cell types (Martial *et al*., 2008; Kucharska *et al*, 2009). Whole cell lysates were analysed by western blotting for MKP-2 expression in the presence or absence of these inhibitors. Figure 3.8 shows a representative Western blot demonstrating that pre-treatment of wild type MEFs with the selective ERK inhibitor U0126 caused a significant inhibition of MKP-2 induction (panels A & B). Inhibition was more effective at later times of induction (10% FCS fold activation, at 240 min: without U0126 = 3.29 ± 0.47, with U0126 = 1.84 ± 0.02, $p<0.01$). In contrast, inhibition of JNK signalling using SP600125 had no significant inhibitory effect on MKP-2 induction, nor did pre-treatment with the p38 MAPK inhibitor SB203580 (panels A, C & D). This confirmed that activation of the ERK pathway promotes the induction of MKP-2 in wild type MEFs derived from the mice (Chen *et al*., 2001). It also suggested that MKP-2 induction is not mediated by either JNK or p38 MAPK.

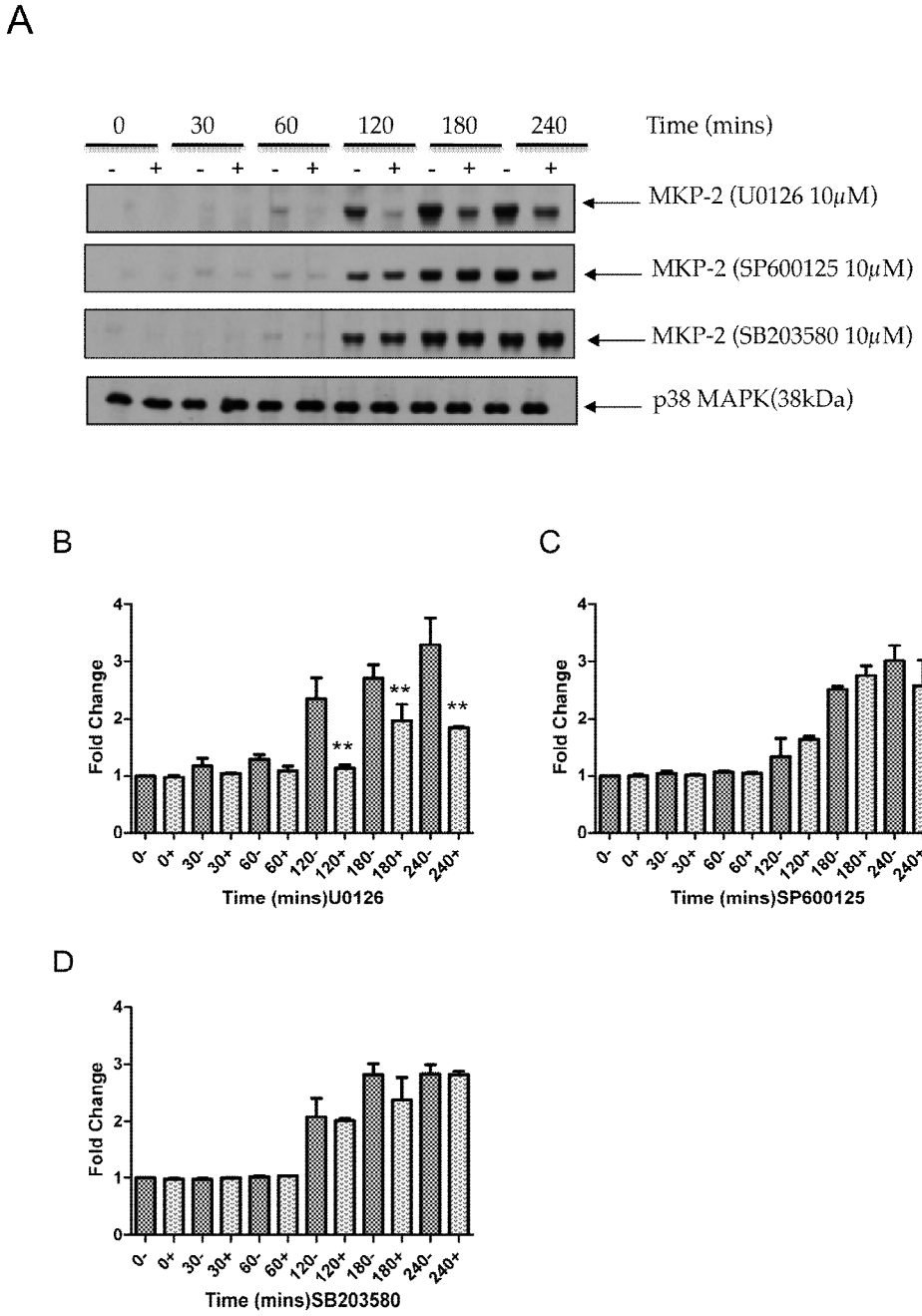

Figure 3.8: Expression of MKP-2 is dependent on prior ERK activation in MEFs

MEFs were grown to confluency on a 6-well plate and quiesced for 48 h in serum free media. Cells were pre-incubated with U0126 (10 μM), SP600125 (10 μM) or SB203580 (10 μM) for 1h prior to being stimulated with 10% FCS for the times indicated. Whole cell extracts were resolved by SDS-PAGE and examined by Western blotting for induction of MKP-2, as described in section 2.16. Relative activation of MKP-2 is outlined in panel A, while panels B-D illustrates the quantification by densitometry. Data expressed as mean±s.e.m. Statistical analysis was by one-way ANOVA, with **p<0.01 considered significant. Each blot is representative of 3 separate experiments.

3.2.3 Regulation of MAPK signalling by MKP-2

3.2.2.4 Effect of MKP-2 deletion on basal ERK and JNK phosphorylation

Given that MKP-2 is a negative regulator of ERK and JNK signalling, initial experiments were conducted to investigate whether the deletion of this protein had any effect on the basal phophorylation levels of ERK and JNK. MEFs were grown to confluency in 6-well plates and serum starved for 48 h. Whole cell lysates were analysed by western blotting for phosphorylation of ERK and JNK in multiple samples. The data presented in figure 3.9 (panels A, B & C) shows a representative Western blot demonstrating that deletion of MKP-2 protein has not altered the basal protein expression of ERK and JNK. Total ERK and JNK levels were unchanged in all conditions, indicating equal protein loading.

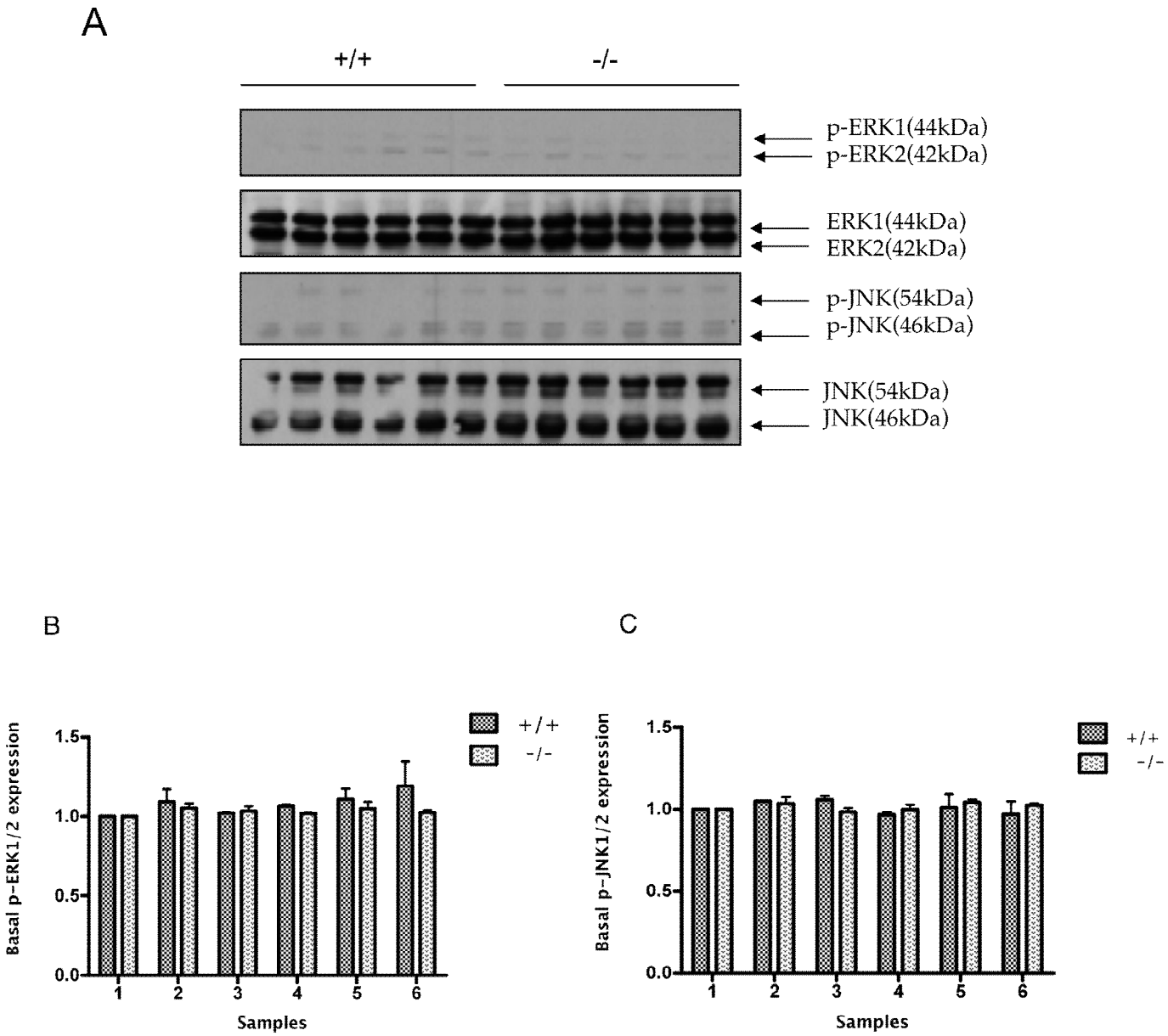

Figure 3.9: Basal protein expression of ERK and JNK in MKP-2$^{+/+}$ and MKP-2$^{-/-}$ MEFs.

MEFs were grown to confluency and quiesced for 48 h in serum free media. Whole cell extracts were resolved by SDS-PAGE and examined by Western blotting for ERK and JNK phosphorylation as described in section 2.16. Relative phosphorylation of ERK and JNK is outlined in panel A while panels B & C illustrate quantification by densitometry, expressed as mean±s.e.m. Statistical analysis was by one-way ANOVA. Each blot is indicative of 3 separate experiments.

3.2.3.1 Serum induced phosphorylation of MAPKs

3.2.3.1.1 Phosphorylation of ERK stimulated by 10% FCS in MKP-2$^{+/+}$ and MKP-2$^{-/-}$ MEFs

From previous experiments it has been demonstrated that serum, PDGF and PMA stimulates MKP-2 protein expression, therefore in order to examine whether the deletion of MKP-2 has altered the phosphorylation kinetics of MAPK signalling these agonists were used. The phosphorylation level of MAPKs was measured by Western blotting with antibodies that specifically recognize both phospho-Tyr and phospho-Thr residues that are regarded to be necessary and sufficient for the activation of MAPKs. Both ERK and JNK phosphorylation was examined over early and prolonged time courses (figures 3.10 and 11). Initially, FCS caused a rapid increase in ERK phosphorylation which peaked at 5 min and was sustained up to 120 min. However, there was no significant difference between MKP-2$^{+/+}$ and MKP-2$^{-/-}$ MEFs in either magnitude or kinetics of phosphorylation (panel A). FCS also promoted a sustained increase in ERK phosphorylation (Figure 3.11) however, the loss of MKP-2 again did not alter the level of stimulation between the two cell types (10% FCS stim. at 2 h: MKP-2$^{+/+}$ = 2.25 ± 0.69, MKP-2$^{-/-}$ = 1.58 ± 0.01). This result suggested that serum was capable of inducing similar phosphorylation of ERK in both MKP-2$^{+/+}$ and MKP-2$^{-/-}$ MEFs.

3.2.3.1.2 Phosphorylation of JNK stimulated by 10% FCS in MKP-2$^{+/+}$ and MKP-2$^{-/-}$ MEFs

The effect of MKP-2 deletion on JNK phosphorylation was also examined over both short and long time courses (figure 3.10 and 11). However, FCS caused a small and minor increase in JNK phosphorylation over both time spans although was not significantly different from controls. Futhermore, there was no significant difference in the level of phosphorylation in MKP-2$^{-/-}$ MEFs relative to MKP-2$^{+/+}$ MEFs (see figure 3.11).

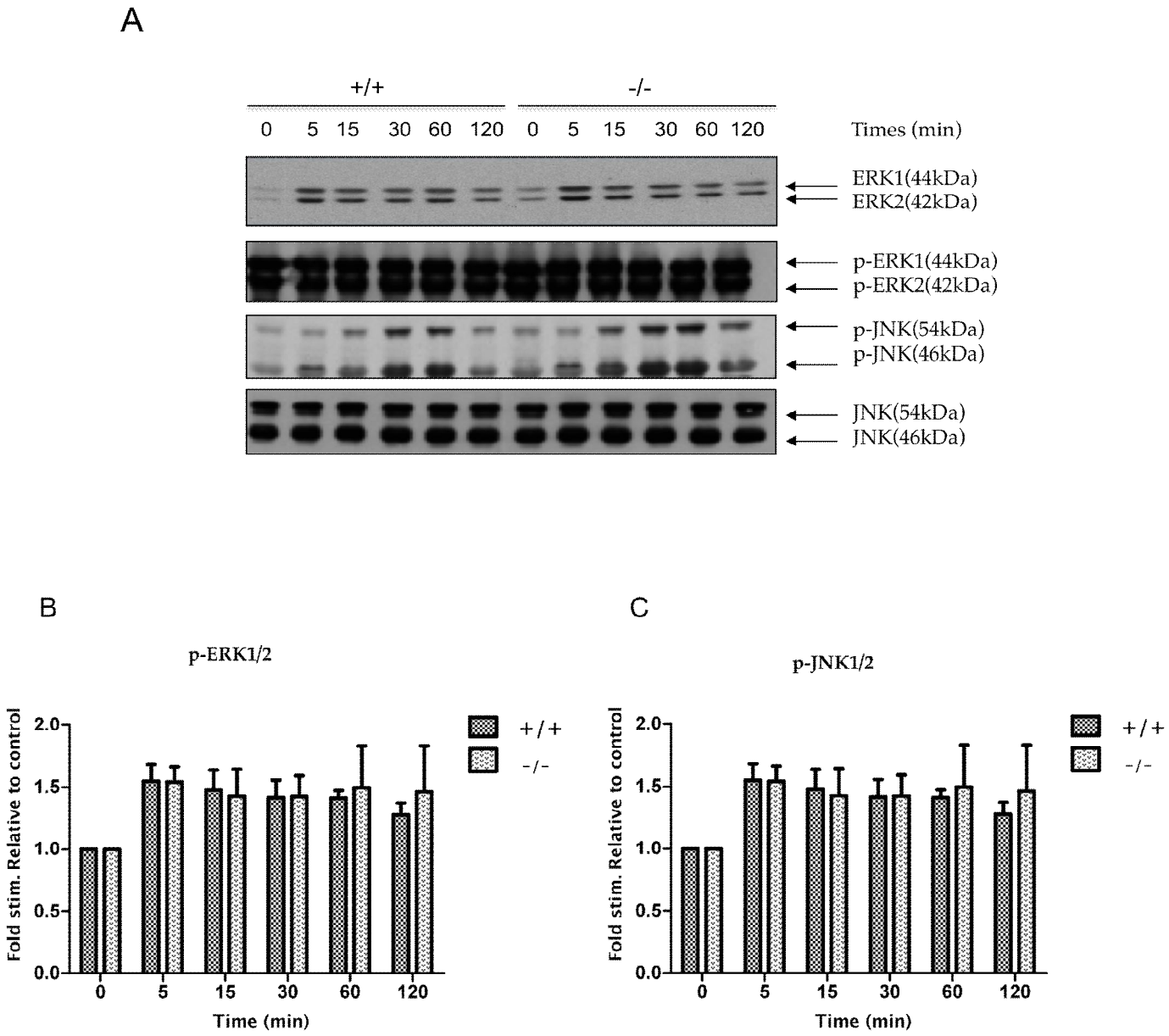

Figure 3.10: Phosphorylation of ERK and JNK by 10% FCS in MKP-2$^{+/+}$ and MKP-2$^{-/-}$ MEFs.

MEFs were grown to confluency and quiesced for 24 h in serum free media. The cells were stimulated with 10% FCS for 0-120 min. Whole cell extracts were resolved by SDS-PAGE and examined by Western blotting for ERK and JNK phosphorylation as described in section 2.16. Relative phosphorylation of ERK and JNK is outlined in panel A while panels B & C illustrate quantification by densitometry, expressed as mean±s.e.m. Statistical analysis was by one-way ANOVA. Each blot is indicative of 3 separate experiments.

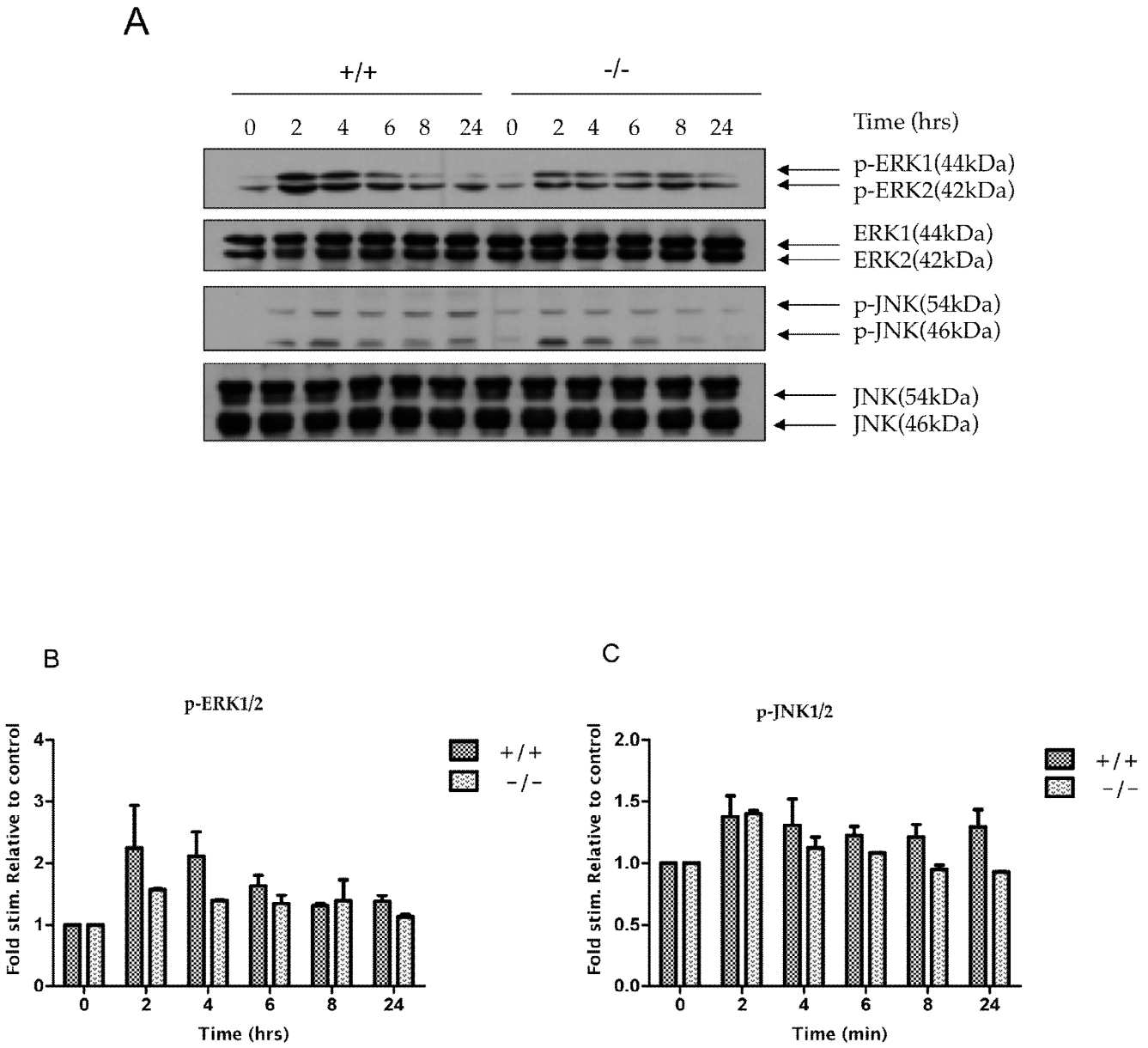

Figure 3.11: Phosphorylation of ERK and JNK by 10% FCS in MKP-2$^{+/+}$ and MKP-2$^{-/-}$ MEFs

MEFs were grown to confluency and quiesced for 24 h in serum free media. The cells were stimulated with 10% FCS for 0-24 h Whole cell extracts were resolved by SDS-PAGE and examined by Western blotting for ERK and JNK phosphorylation as described in section 2.16. Relative phosphorylation of ERK and JNK is outlined in panel A while panels B & C illustrate quantification by densitometry. Data expressed as mean±s.e.m. Statistical analysis was by one-way ANOVA. Each blot is indicative of 3 separate experiments.

3.2.3.2 PMA induced phosphorylation of MAPKs

3.2.3.2.1 Phosphorylation of ERK and JNK stimulated by PMA in MKP-$2^{+/+}$ and MKP-$2^{-/-}$ MEFs

Similar to the experiment with serum, PMA was used to examine the phosphorylation of ERK and JNK in wild type and MKP-$2^{-/-}$ MEFs (figure 3.12 and 13). PMA caused ERK phosphorylation within 5 min, levels then peaked at 30 min (100 nM PMA fold stim., MKP-$2^{+/+}$ = 1.45 ± 0.60, MKP-$2^{-/-}$ = 1.67 ± 0.16) and remained high up to 120 min. Nevertheless, in the absence of MKP-2, ERK phosphorylation was not significantly altered (100 nM PMA, MKP-$2^{+/+}$ = 2.05 ± 0.33, MKP-$2^{-/-}$ = 2.2 ± 0.51). A similar lack of difference was observed over the later time course of PMA stimulation. Furthermore, as with serum stimulation, PMA generated a relatively weak increase in JNK over both short and long time courses which was not significantly affected by the loss of MKP-2.

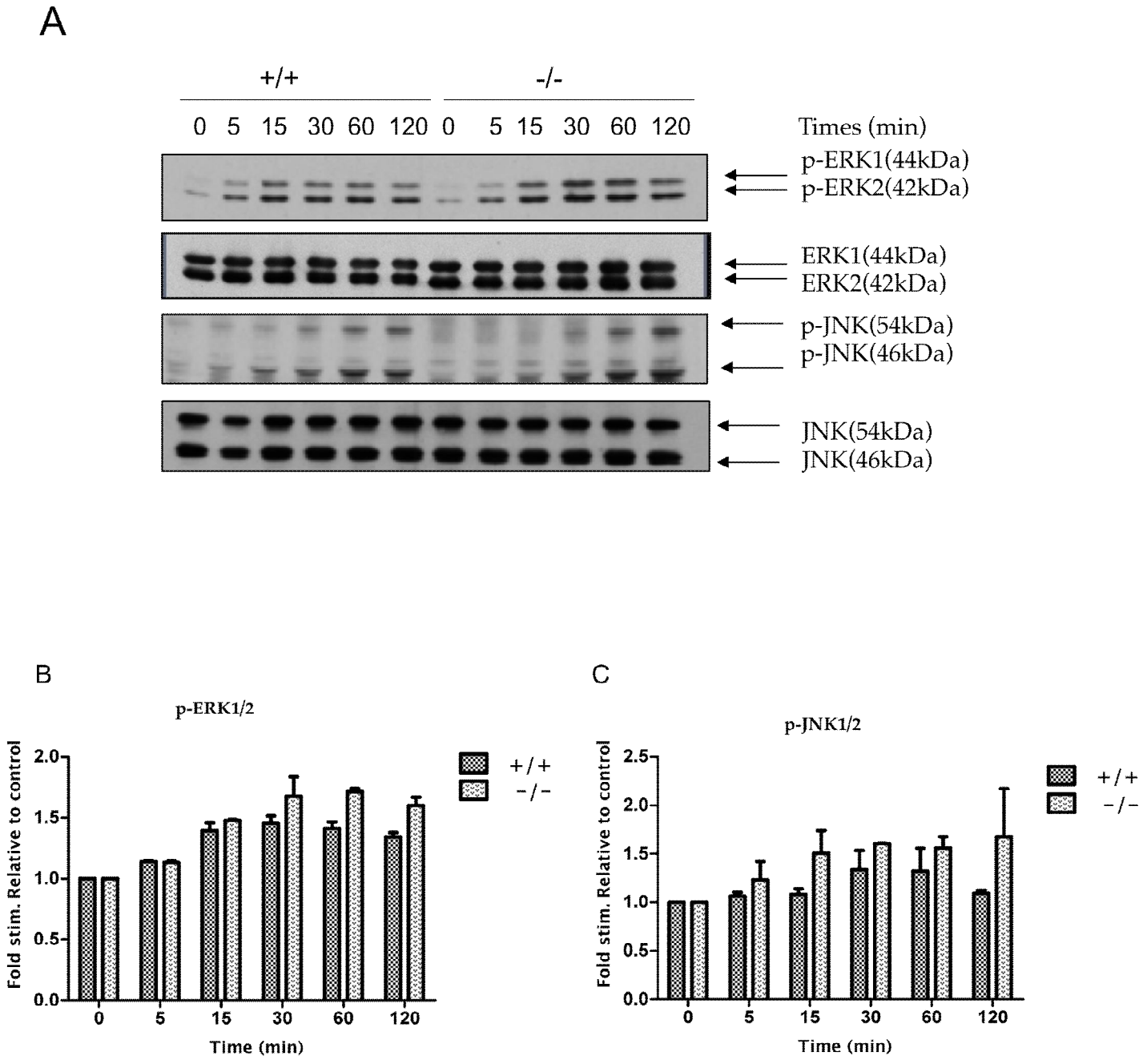

Figure 3.12: Phosphorylation of ERK and JNK by PMA in MKP-2$^{+/+}$ and MKP-2$^{-/-}$ MEFs

MEFs were grown to confluency and quiesced for 24 h in serum free media. The cells were incubated with PMA 100 nM for 0-120 min. Whole cell extracts were resolved by SDS-PAGE and examined by Western blotting for ERK and JNK phosphorylation as described in section 2.16. Relative phosphorylation of ERK and JNK is outlined in panel A while panels B & C illustrate quantification by densitometry. Data expressed as mean±s.e.m. Statistical analysis was by one-way ANOVA. Each blot is indicative of 3 separate experiments.

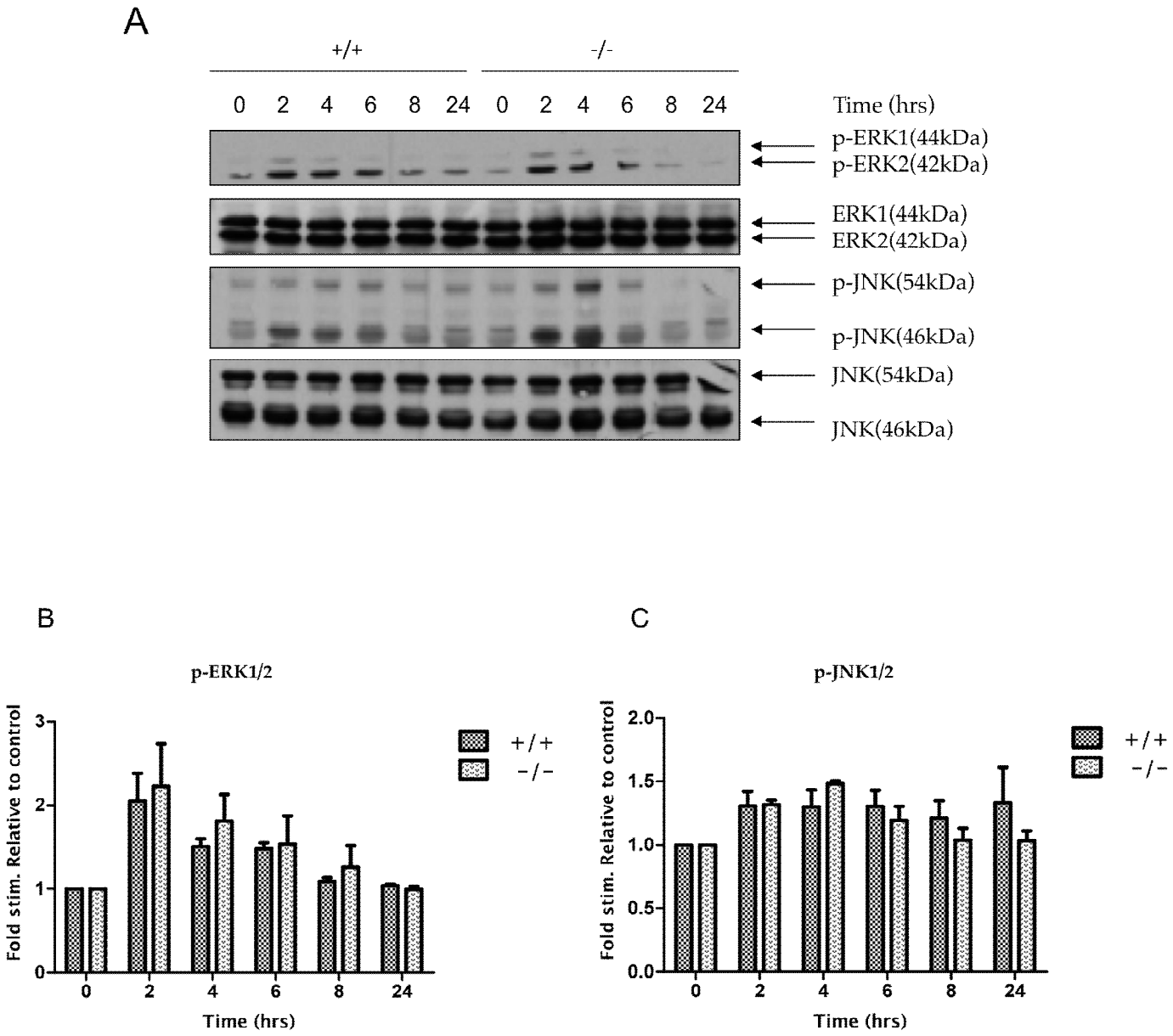

Figure 3.13: Phosphorylation of ERK and JNK by PMA in MKP-2$^{+/+}$ and MKP-2$^{-/-}$ MEFs

MEFs were grown to confluency and quiesced for 24 h in serum free media. The cells were stimulated with PMA 100 nM for 0-24 h. Whole cell extracts were resolved by SDS-PAGE and examined by Western blotting for ERK and JNK phosphorylation as described in section 2.16. Relative phosphorylation of ERK and JNK is outlined in panel A while panels B & C illustrate quantification by densitometry, expressed as mean±s.e.m. Statistical analysis was by one-way ANOVA. Each blot is indicative of 3 separate experiments.

3.2.3.3 PDGF induced phosphorylation of MAPKs

3.2.3.3.1 Phosphorylation of ERK stimulated by PDGF in MKP-$2^{+/+}$ and MKP-$2^{-/-}$ MEFs

An additional comparison utilized the growth factor PDGF. This growth factor induced a rapid phosphorylation of ERK within 5 min which peaked after 30 min and was still detected up to 120 min after stimulation (see figure 3.14 panels A & C). However, no significant difference was observed between MKP-$2^{+/+}$ and MKP-$2^{-/-}$ MEFs over the early time course (10 ng PDGF fold stim. MKP-$2^{+/+}$ = 1.43 ± 0.22, MKP-$2^{-/-}$ = 1.24 ± 0.16). In contrast, sustained ERK phosphorylation was found to be significantly higher in MKP-$2^{-/-}$ MEFs compared with MKP-$2^{+/+}$ MEFs over the longer time course (10 ng PDGF fold stim. at 2 h: MKP-$2^{+/+}$ = 1.68 ± 0.42, MKP-$2^{-/-}$ = 2.45 ± 0.24, $p<0.05$) (see figure 3.14 panels B & D). The results suggested that loss of MKP-2 could enhance PDGF induced ERK phosphorylation at later time points.

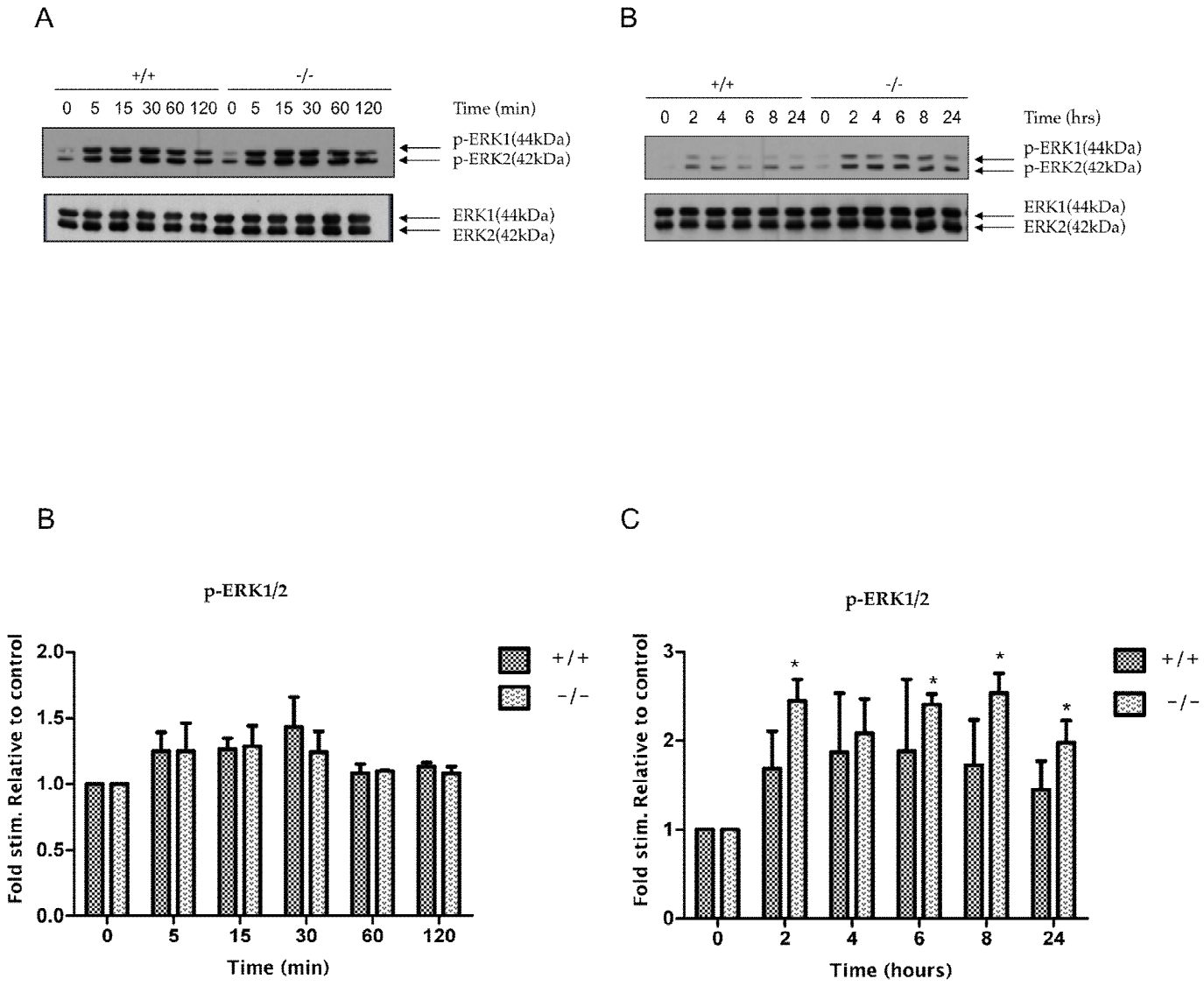

Figure 3.14: Phosphorylation of ERK by PDGF in MKP-2$^{+/+}$ and MKP-2$^{-/-}$ MEFs.

MEFs were grown to confluency and quiesced for 24 h in serum free media. The cells were stimulated with PDGF 10 ng/ml for 0-120 min. Whole cell extracts were resolved by SDS-PAGE and examined by Western blotting for ERK phosphorylation as described in section 2.16. Relative phosphorylation of ERK is outlined in panels A & B while panels C & D illustrate quantification by densitometry. Data expressed as mean±s.e.m. Statistical analysis was by one-way ANOVA. Post hoc test by Bonferroni's multiple comparison tests *$p<0.05$. Each blot is indicative of 3 separate experiments.

3.2.3.4 Enhanced anisomycin-induced phosphorylation of JNK and p38 MAPK in MKP-2$^{-/-}$ MEFs

The effect of MKP-2 deletion on JNK and p38 MAPK phosphorylation was then examined. Two agents were selected that are known to give strong stress induced signalling, anisomycin (5 μM) (figure 3.15) and UVC (30 j/m^2) (figure 3.16). Anisomycin induced specific phosphorylation of both JNK and p38 MAPK (panel A). JNK phosphorylation increased rapidly reaching a peak by 30 min and decreasing slowly over the remainder of the 6 h time course. Loss of MKP-2 resulted in a small but statistically significant enhancement of JNK phosphorylation (fold stim. at 60 min: MKP-2$^{+/+}$ = 2.22 ± 0.28, MKP-2$^{-/-}$ = 3.05 ± 0.26, $p<0.05$). Phosphorylation of p38 MAPK by anisomycin was also increased by 30 min, but was more sustained compared to JNK. Surprisingly, p38 MAPK phosphorylation was again significantly higher in MKP-2$^{-/-}$ when compared to MKP-2$^{+/+}$ MEFs at the 60 min time point (fold stim. at 60 min: MKP-2$^{+/+}$ = 1.73 ± 0.39, MKP-2$^{-/-}$ = 2.85 ± 0.36, $p<0.05$). These data demonstrated that anisomycin induced JNK and p38 MAPK activation was enhanced in MKP-2 deficient fibroblasts as compared with wild type. This demonstrated that MKP-2 is an important regulator of JNK signalling.

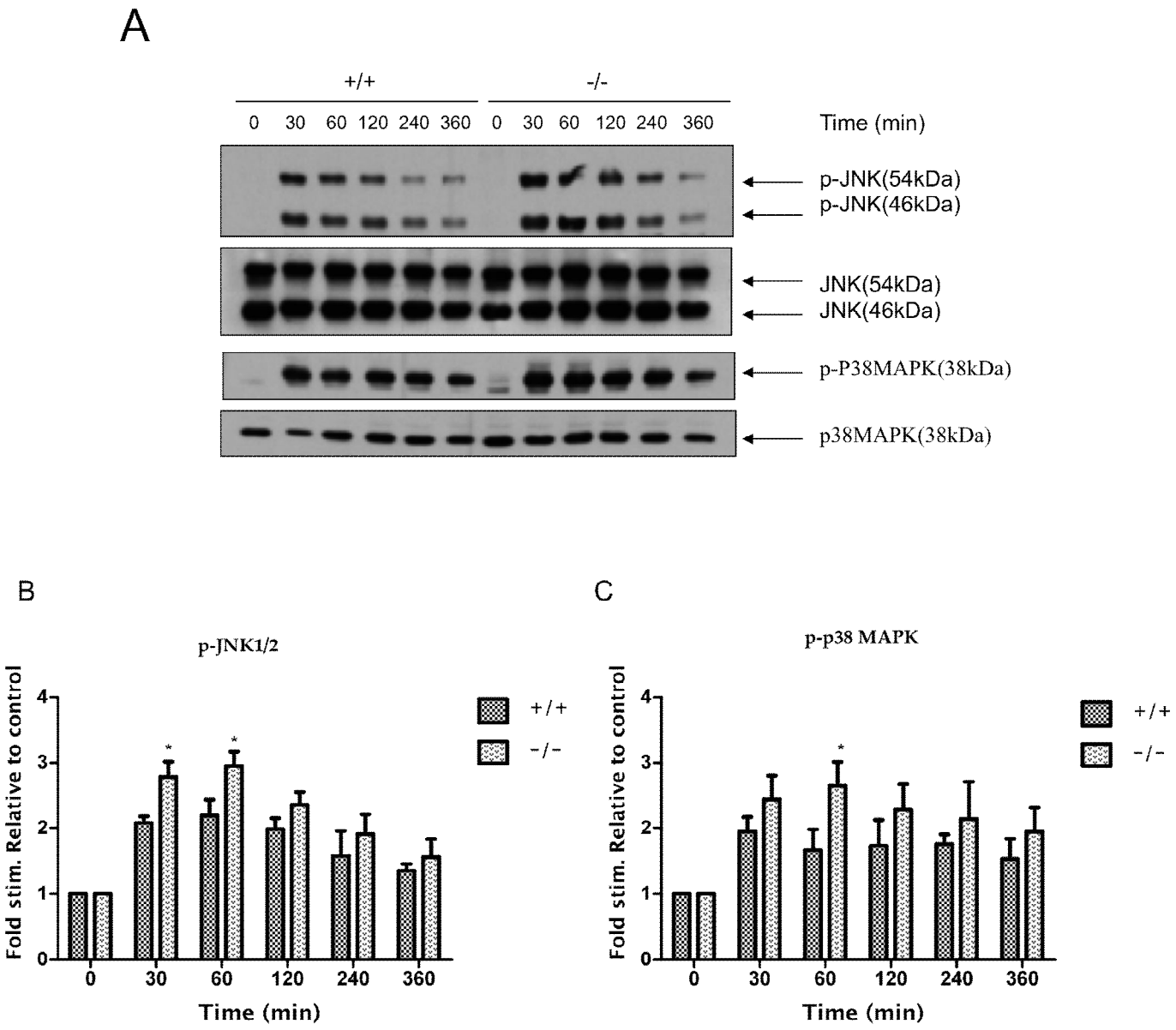

Figure 3.15: Enhanced phosphorylation of JNK and p38 MAPK by anisomycin in MKP-2 deficient MEFs.

MEFs were grown to confluency and quiesced for 24 h in serum free media. The cells were incubated with anisomycin 5 μM for 0-360 min. Whole cell extracts were resolved by SDS-PAGE and examined by Western blotting for JNK and p3 MAPK phosphorylation as described in section 2.16. Relative phosphorylation of JNK and p38 MAPK is outlined in panel A while panels B & C illustrate quantification by densitometry, expressed as mean±s.e.m. Statistical analysis was by one-way ANOVA. Post hoc tests by Bonferroni's multiple comparison tests *p<0.05. Each blot is indicative of 3 separate experiments.

3.2.3.4 Effect of UVC on phosphorylation of JNK and p38 MAPK in MKP-$2^{+/+}$ and MKP-$2^{-/-}$ MEFs.

Given the positive results with anisomycin, the effect of MKP-2 loss upon UVC induced JNK and p38 MAPK signalling was assessed. UVC (30 j/m^2) induced specific phosphorylation of both JNK and p38 MAPK (figure 3.16 panel A). Both JNK and p38 MAPK phosphorylation were increased rapidly reaching a peak by 30 min and decreasing slowly over the remainder of the 6 h time course However, UVC caused a small and minor increase in JNK and p38 MAPK phosphorylation over both time frames which was not significantly different from controls. In addition, there was no difference in the level of phosphorylation in MKP-$2^{-/-}$ MEFs in comparison to MKP-$2^{+/+}$ MEFs (panels B & C). These results demonstrated that UVC induced JNK and p38 MAPK activation in MEFs, but only minor differences were observed between MKP-$2^{-/-}$ and the wild type cells.

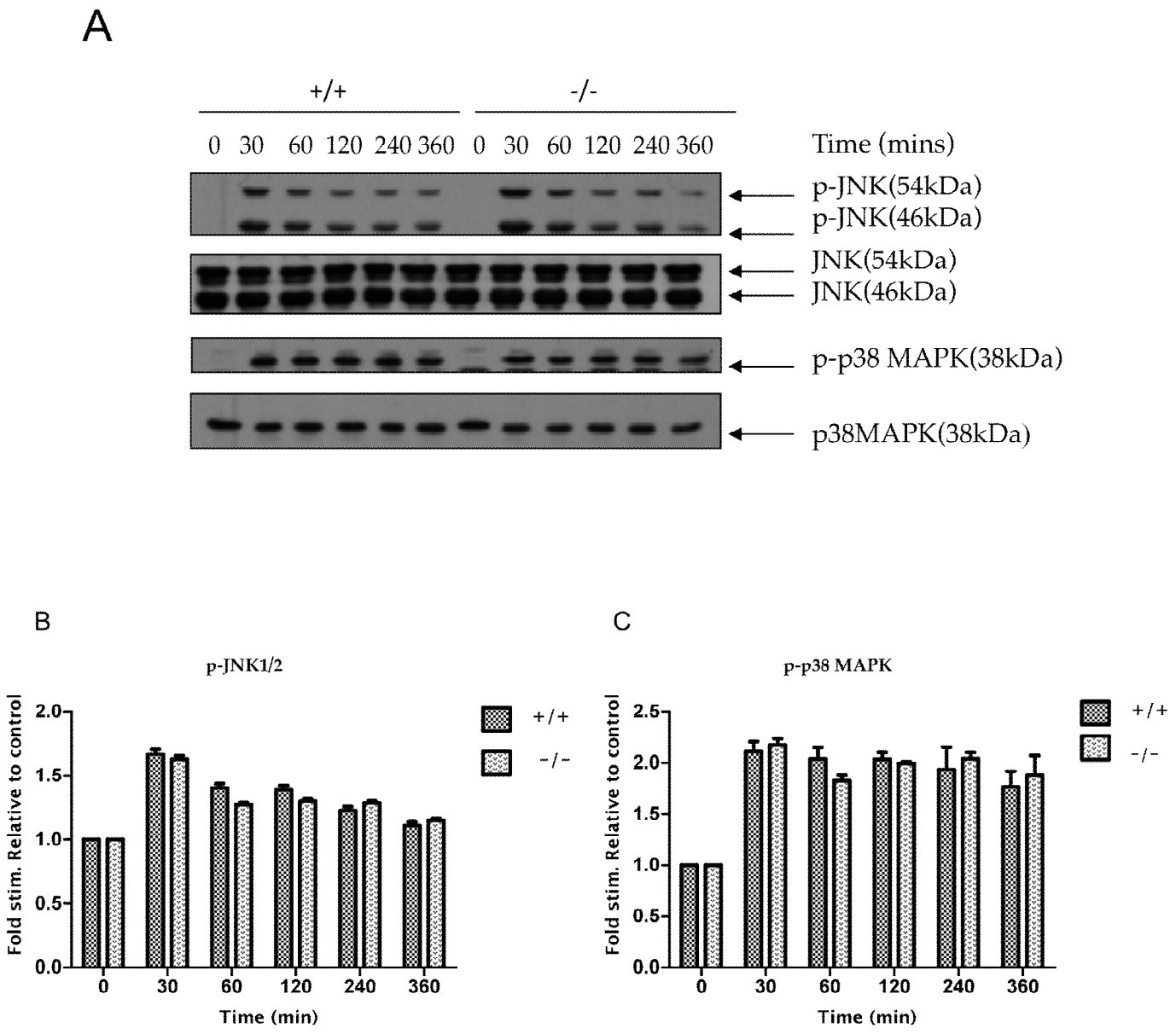

Figure 3.16: Effect of UVC on phosphorylation of JNK and p38 MAPK in MKP-2$^{+/+}$ and MKP-2$^{-/-}$ MEFs.

MEFs were grown to confluency and quiesced for 24 h in serum free media. The cells were incubated with UVC (30 j/m^2) for 0-360 min. Whole cell extracts were resolved by SDS-PAGE and examined by Western blotting for JNK and p3 MAPK phosphorylation as described in section 2.16. Relative phosphorylation of JNK and p38 MAPK is outlined in panel A while panels B & C illustrate quantification by densitometry, expressed as mean±s.e.m. Each blot is indicative of 3 separate experiments. Statistical analysis was by one-way ANOVA.

3.2.4 MKP-2 deficiency leads to alteration of MEF proliferation

3.2.4.1 MKP-2 deletion leads to decrease in MEF proliferation: [^{3}H]-thymidine incorporation assay

Having established the effect of loss of MKP-2 upon MAPK phosphorylation, this was correlated with a number of parameters linked to the regulation of cellular proliferation. Initially, [^{3}H]-thymidine incorporation was examined to allow the estimation of DNA synthesis in MEFs (see section 2.8). The data presented in figure 3.17 demonstrated that in MKP-2$^{+/+}$ fibroblasts, serum gave a concentration dependent increase in [^{3}H]-thymidine incorporation which was maximal between 5 and 10% FCS. In MEFs lacking MKP-2 there was a substantial reduction in DNA synthesis compared with wild type, particularly at the 10% FCS concentration (fold stim. DPM; MKP-2$^{+/+}$ = 716.34 ± 104.3, MKP-2$^{-/-}$ = 237.22 ± 26.9, $p<0.01$). FCS gave about 3 fold increase in cell growth in MKP-2$^{+/+}$ compared with MKP-2$^{-/-}$ MEFs. This suggested that the deletion of MKP-2 protein has significantly inhibited proliferation in these cells signifying that MKP-2 could play a very important role in this process.

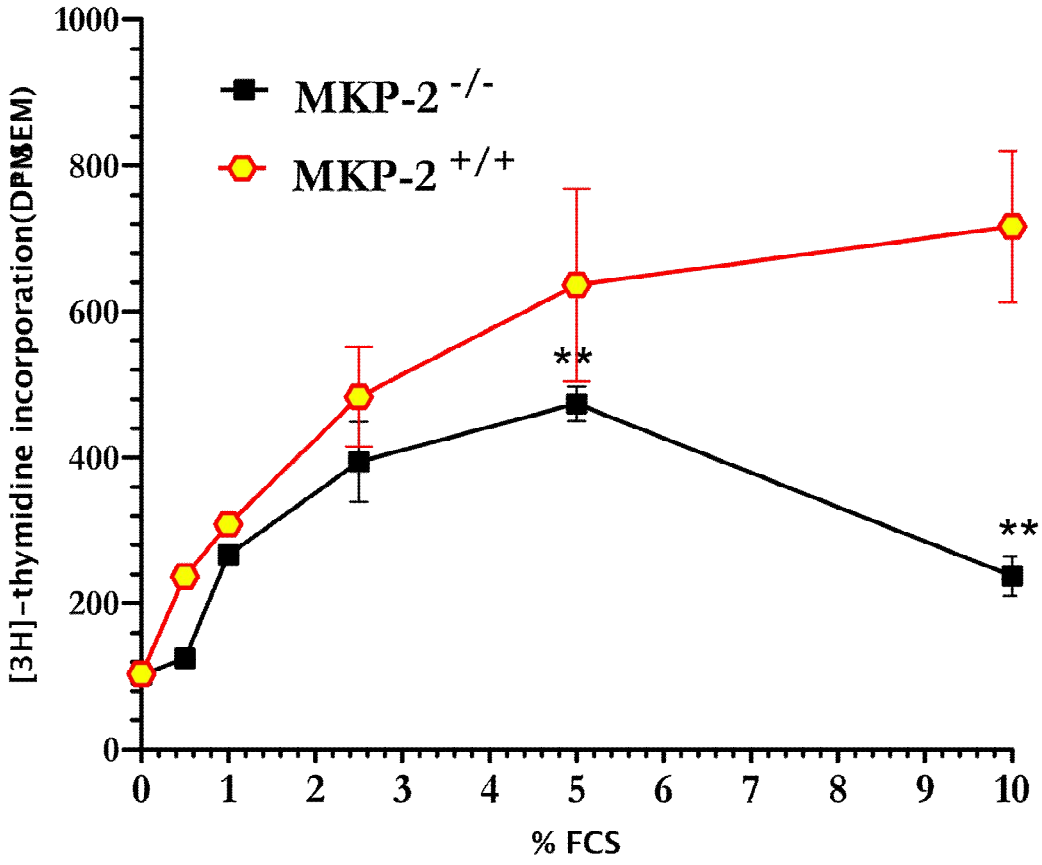

Figure 3.17: MKP-2 deficiency leads to alteration of MEF proliferation. Equal number of MEFs were plated on 24-well tissue culture plates and grown to approximately 60% confluency at 37° C and were serum starved for 24 h. The quiesced cells were stimulated with increasing FCS concentration for 24 h. DNA synthesis was measured using [^{3}H]-thymidine incorporation assay. Counts were measured in DPMs (disintegrations per minute) and cell proliferation was analysed using two-way ANOVA. Each point represents the mean±s.e.m. Post hoc test was by Bonferroni's multiple comparison tests, statistical significant is shown in relation to MKP-2$^{-/-}$, **P<0.01. Control values; DPM; MKP-2$^{+/+}$ = 103.36 ± 8.03, MKP-2$^{-/-}$ = 101.86 ± 2.71. Experiment done in triplicate in cells isolated from separate animals (n=3).

3.2.4.2 MKP-2 deletion leads to decrease in MEF proliferation: Cell counting by Haematoxylin staining

The experiments assessing [^{3}H]-thymidine incorporation, are only an indirect measurement of proliferation and therefore cell counting using haematoxylin staining was used to directly measure cell number (see section 2.9). In MKP-$2^{+/+}$ MEFs, over a 72 h period, serum caused an approximately 3 fold increase in cell number which was apparent as early as 24 h (see figure 3.18). In contrast proliferation in MKP-$2^{-/-}$ MEFs was significantly impaired relative to wild type. No increase in cell number was observed in these cultures until at least 48 h, and by 72 h the difference in growth rate was approximately 50% (cell number per field; MKP-$2^{+/+}$ = 32.03 ± 1.9x10^5, MKP-$2^{-/-}$ = 23.97 ± 0.6x10^5, $P<0.001$). The proliferation assay by cell counting provided additional evidence that absence of MKP-2 has significantly reduced the growth of these cells. These results have established that MKP-2 is essential for fibroblast growth.

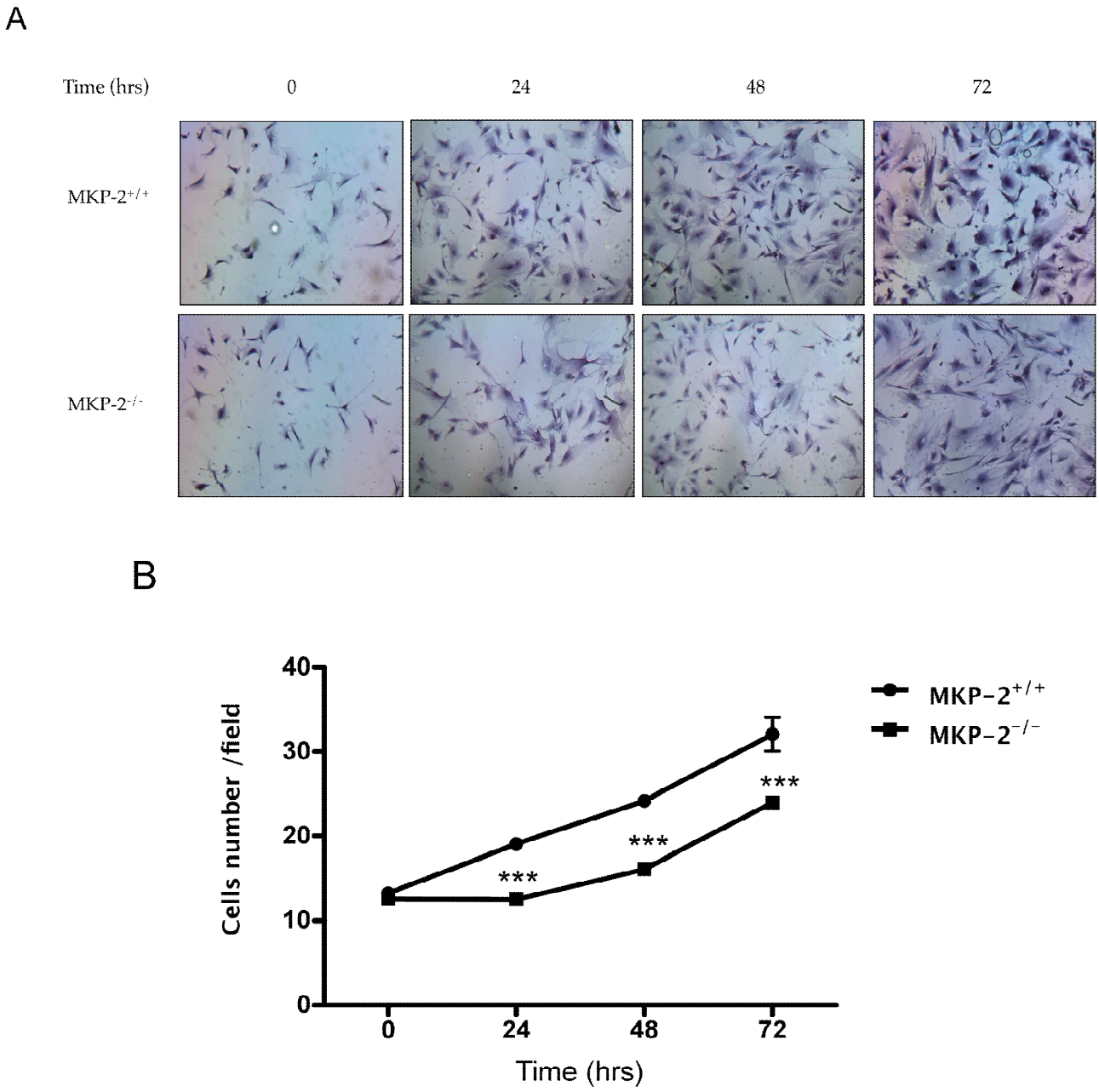

Figure 3.18: MKP-2 deficiency leads to decreased MEFs proliferation

MEFs were serum starved for 24 h in serum free media and then stimulated for either 24, 48, 72 h with 10% FCS. Cultures were washed with PBS, and analysed using haematoxylin (panel A). The number of cells was determined from 10 random fields per each coverslip (panel B) (see section 2.9). Quantified data was analysed using two way ANOVA. Post hoc test was by Bonferroni's multiple comparison tests, Statistical significant is shown in relation to MKP-$2^{-/-}$, ***P<0.001. Control values, (0 h) MKP-$2^{+/+}$ = 13.23 ± 0.32, MKP-$2^{-/-}$ = 12.57 ± 0.32). Each value represents the mean±s.e.m. performed in triplicate from 3 separate experiments (n=3).

3.2.5 MKP-2 deficiency leads to increased doubling times in MEFs

Given the prominent growth deficit observed in MKP-$2^{-/-}$ MEFs these cells were examined in greater detail by assessing the cell doubling times. Cell doubling time protocol was an adaptation of culture of animal cells technique described previously (Freshney, 1994), (see section 2.10). The data presented in figure 3.19 demonstrated that the shortest cell doubling times were found in fibroblasts from MKP-$2^{+/+}$ in comparison with cells from MKP-$2^{-/-}$ (doubling time in days; MKP-$2^{+/+}$ = 3.67 ± 1.25, MKP-$2^{-/-}$ = 8.00 ± 1.77, $p<0.01$). Fibroblasts derived from MKP-$2^{-/-}$ mice had markedly longer cell doubling time approximately 2 fold increase in cell doubling times compared with the wild type. However, considering the early time points, there was not much difference in activity was detected between both cell types. These results establish that MKP-$2^{-/-}$ MEFs are phenotypically different from wild type and these cells are likely to react differently in response to growth, nutritional, or stress stimuli *in vitro.* A lengthy cell doubling time indicates a decrease in cell division rate and is thought to imply a low proliferative ability (Baserga, 1985). These findings have confirmed the previous data from the proliferation experiments.

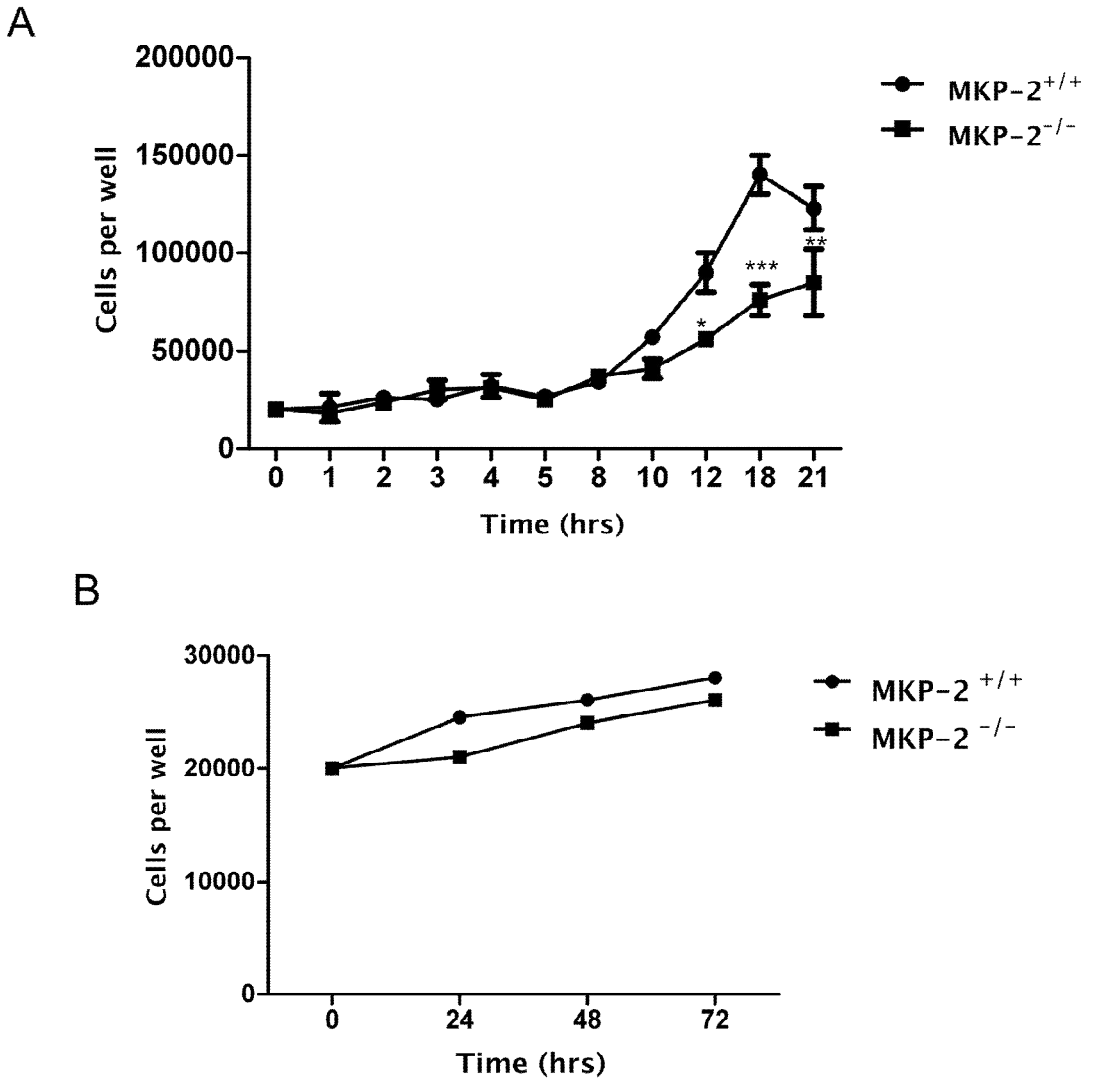

Figure 3.19: MKP-2 deficiency leads to increased doubling times in MEFs

MEFs were seeded in 6-well plates at 2 x10^4 cells per well. After 24 h cells were trypsinized and counted with a haemocytometer over a period of 72 h, panels A & B. Mean±s.e.m of cells per well were plotted graphically and the cell doubling times were calculated for at least two densities (3 x 10^4 – 6 x 10^4) from the graph. Quantified data was analysed using two way ANOVA. Post hoc test was by Bonferroni's multiple comparison tests. Statistical significant is shown in relation to MKP-$2^{-/-}$, *P<0.05, **P<0.01, ***P<0.001. Each point represents the mean±s.e.m. Experiment done in cells isolated from separate animals (n=3).

3.2.6 Over-expression of Adenoviral MKP-2 reversed the decreased proliferation rates in MKP-2$^{-/-}$ MEFs

Having established from previous experiments that MKP-2 deletion significantly inhibited proliferation in MKP-2 deficient MEFs, a gain of function study was conducted to determine whether over-expression of Adv. MKP-2 could reverse this deficit in cell growth. For this purpose MKP-2 $^{-/-}$ MEFs were infected with increasing concentration of Adv. MKP-2 (100-500 pfu) and assessed for MKP-2 expression by Western blotting (see figure 3.20, panel A). Maximum expression was achieved between 300 and 500 pfu. Based on this result the cells derived from MKP-2$^{-/-}$ were infected with Adv. MKP-2 at 300 pfu and cellular proliferation assessed by cell haematoxylin staining. As expected cellular proliferation was reduced in the absence of MKP-2 at all time points assessed. Whilst infection with lacZ control virus had a little effect, cellular proliferation was significantly enhanced following Adv. MKP-2 over-expression in MKP-2$^{-/-}$ MEFs (cells per field, at 72 h, = MKP-2$^{-/-}$ = 27.47 ± 0.4x10^5 MKP-2$^{-/-}$ + Adv. MKP-2 = 56.57 ± 3.8x10^5, $P<0.001$). In fact, addition of Adv. MKP-2 stimulated an increase in cell number which was much greater than that obtained in MEFs derived from wild type mice. These results demonstrated that Adv. MKP-2 over-expression successfully reversed the proliferative deficiency of these cells (see figure 3.20 panels B & C) and confirmed that MKP-2 loss is responsible for the decrease in cell growth observed in these cells. It also suggests that MKP-2 plays a significant role in proliferation in these cells.

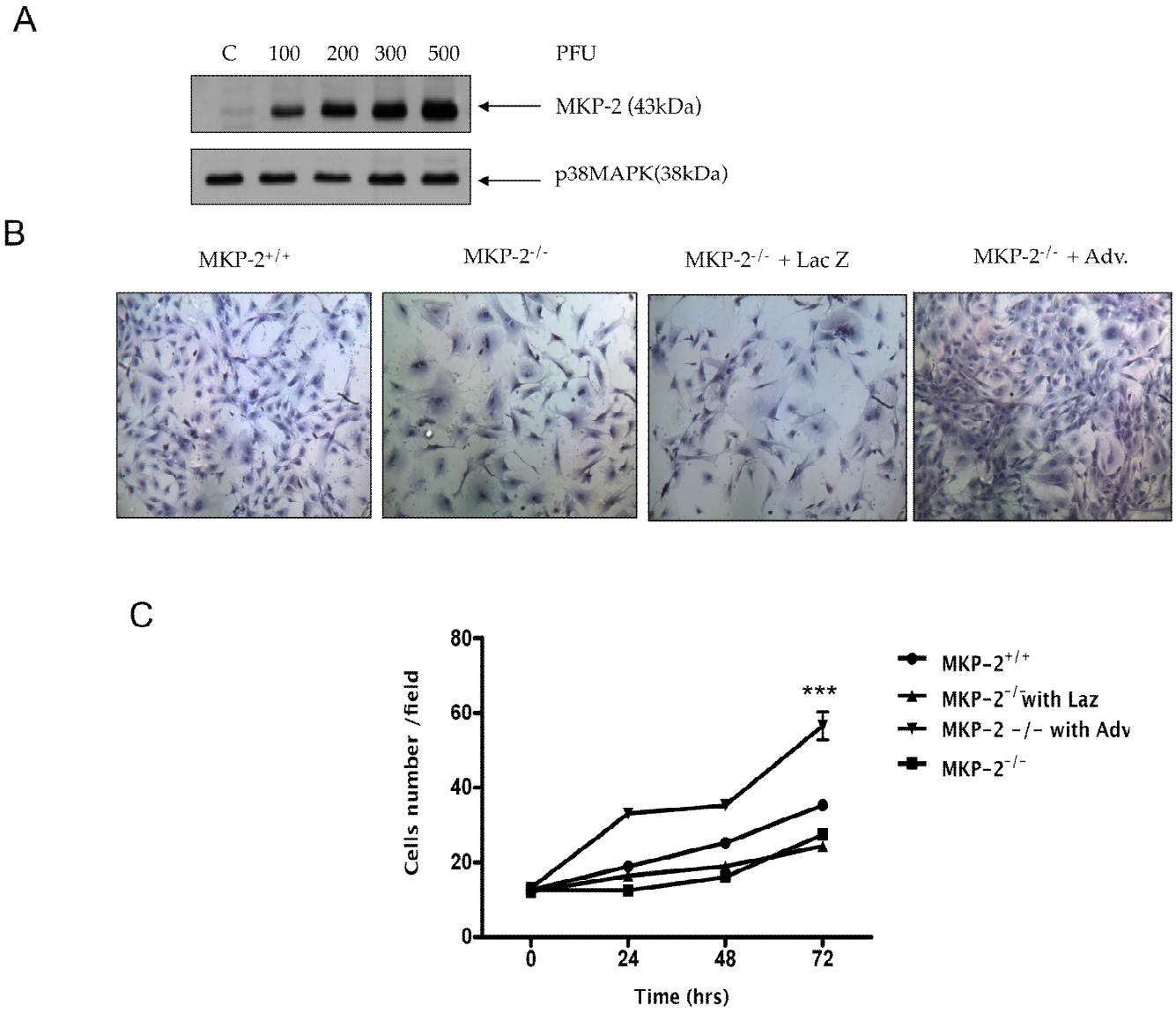

Figure 3.20: MKP-2 is required for MEF proliferation

Confluent MEFs in 10 cm dishes were detached with trypsin-EDTA, seeded onto coverslip in 24-well plates (5,000 cells/well) in 10% FCS-DMEM, and allowed to attach for 24 h. Cells infected with 300 pfu Adv. MKP-2 were serum starved for 24 h in serum free media and then stimulated for either 24, 48, 72 h with 10% FCS. Panel A denotes MKP-2 expression in response to increasing pfu of Adv. MKP-2 for 40 h. Cultures were washed with PBS, and stained with haematoxylin as shown in panel B (picture of CFs taken by Motic Images Plus 2.0 software). The number of cells was determined from 10 random fields per each coverslip, panel C (see section 2.9). Cell proliferation was analysed using two way ANOVA. Post hoc test was by Bonferroni's multiple comparison tests, statistical significant is shown in relation to MKP-$2^{-/-}$, ***P<0.001. Control values, (0 h) MKP-$2^{+/+}$ = 12.63 ± 0.43, MKP-$2^{-/-}$ = 12.57 ± 0.32). Each point represents the mean±s.e.m. from experiments performed in triplicate using cells isolated from separate animals (n=3).

3.2.7 Delayed G_2/M phase transition in MKP-$2^{-/-}$ fibroblasts

Following the observation that the deletion of MKP-2 significantly inhibited MEF proliferation and over-expression of Adv. MKP-2 rescued these effects, further experiments were conducted to elucidate the differences in growth characteristics by investigating cell cycle parameters. DNA analysis using propidium iodide staining was used to assess each phase of the cell cycle. The results presented in figure 3.21 (panels A) demonstrated that MEFs from both MKP-$2^{+/+}$ and MKP-$2^{-/-}$ progress through G1 and S phases of the cell cycle almost at the same rate. Interestingly however it also showed an increase in the DNA content of cells derived from MKP-$2^{-/-}$ in G_2/M phase (23.1%) in comparison with cells from MKP-$2^{+/+}$ (14.2%). These data suggested that MKP-2 deletion has caused the inhibition of the normal progression of these cells through the cell cycle.

Further analysis of the cell cycle was carried out by synchronization of MEFs using thymidine block. Cells were processed as described in section 2.11 and analysed by flow cytometry. The results showed that all cells were essentially blocked in G1 (99.2%) in MKP-$2^{+/+}$ MEFs with no escape into S or G_2/M phase and negligible content in G0. In contrast, although the majority of the cells derived from MKP-$2^{-/-}$ were also blocked in G1 (89.8%), 10.2% percent of cells were found in sub G1 (G0) which suggested that these cells were undergoing apoptosis (see figure 3.21, panel B). This finding demonstrated that the deletion of MKP-2 could be responsible for induction of DNA damage in these cells preventing them from going through the cell cycle efficiently.

In order to correlate these changes in cell cycle parameters with cell cycle regulated proteins at specific phases of the cycle, cyclin B1 expression and cdc-2 phosphorylation were examined. These proteins are well recognized indicators of G_2/M phase transition (Veronique and Medema, 2001) (figure 3.21, panel C). Stimulation of quiescent MKP-$2^{+/+}$ MEFs with serum induced

an increase in cyclin B1 which was apparent by 12 h and increased further up to 24 h. This expression correlated with an increase in cdc-2 phosphorylation an event recognized to be dependent on prior cyclin B1 expression. In MKP-2$^{-/-}$ MEFs both cyclin B1 expression (figure 3.21, panel D) and cdc-2 phosphorylation (figure 3.21, panel E) were enhanced. This data was surprising as G_2 / M phase cycle arrest is usually associated with a loss in both parameters. However, this confirms the effect of MKP-2 is linked to the cell cycle.

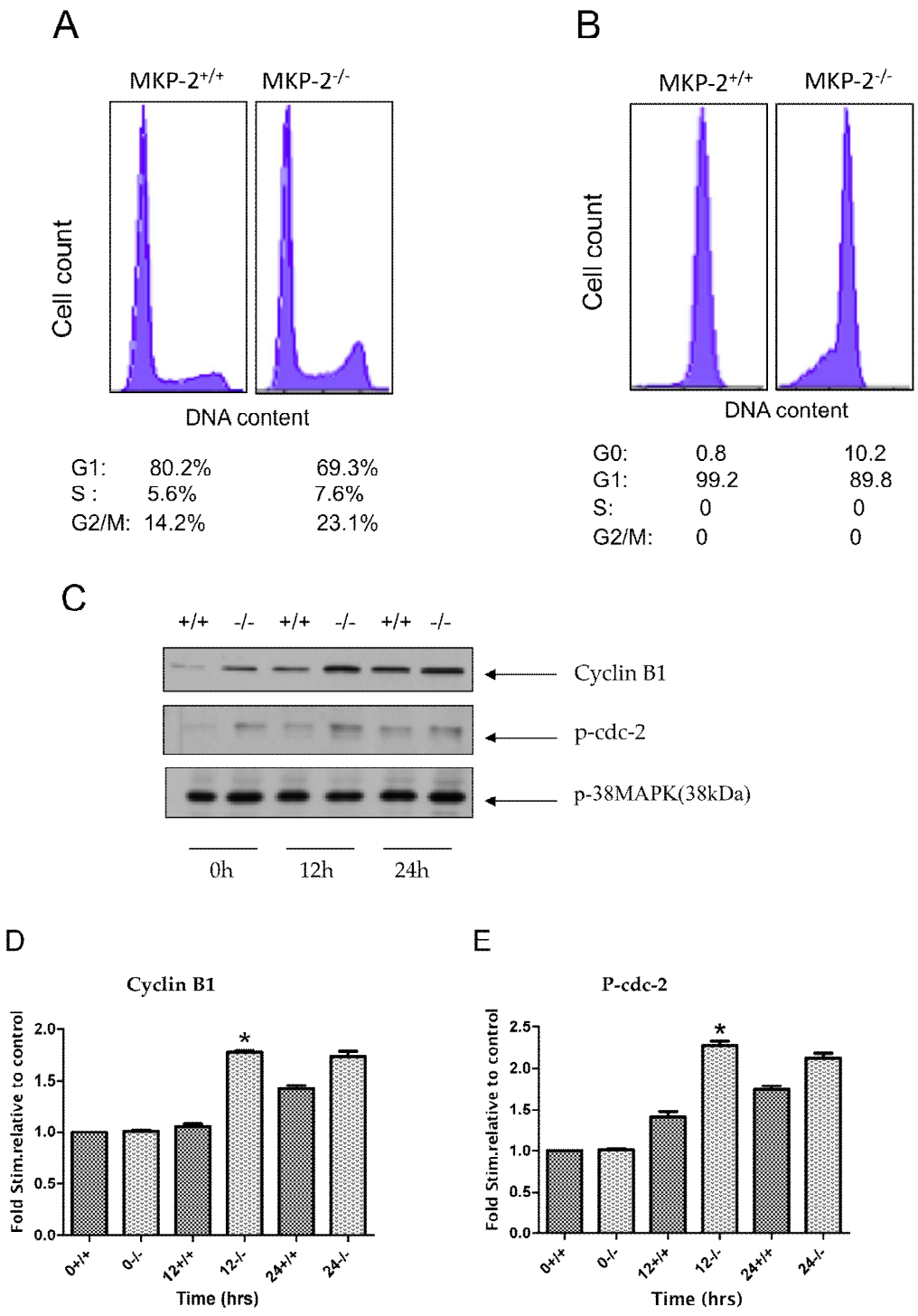

Figure 3.21: Delayed G_2/M phase transition in MKP-2 deficient fibroblasts.

Subconfluent quiescent fibroblasts were stimulated with FCS for 24 hr and assessed by flow cytometry using propidium iodide staining (Panel A). In panel B cells were blocked with thymidine as outlined in section 2.11 and stained for propidium iodide. Relative phosphorylation of cyclin B1 and cdc-2 is outlined in panel C while panels D & E by densitometry, expressed as mean±s.e.m. Statistical analysis was by one-way ANOVA. Post hoc test by Bonferroni's multiple comparison tests, *$p<0.05$ was considered significant in relation to MKP-$2^{-/-}$. Each blot is indicative of 3 separate experiments.

3.2.8 Enhanced anisomycin-induced cleavage of caspase-3 and phosphorylation of γH2AX in MKP-2 deficient MEFs.

The previous analysis of cell cycle progression in double thymidine block cells indicated a potential for enhanced apoptosis in MKP-$2^{-/-}$ MEFs. This was initially assessed by examining biochemical parameters linked to apoptosis such as the phosphorylation of γH2AX and the proteolytic cleavage of caspase-3 in response to anisomycin (Figure 3.22). In MKP-$2^{+/+}$ MEFs anisomycin caused significant phosphorylation of γH2AX which was apparent at both 4 and 6 h of stimulation (panels A & C). In MKP-$2^{-/-}$ MEFs phosphorylation of γH2AX was enhanced at the 4 h time point but not at 6 h (fold stim. at 4 h MKP-$2^{+/+}$ = 1.59 ± 0.21, MKP-$2^{-/-}$ = 2.03 ± 0.12, $p<0.05$). Similarly, in MKP-$2^{-/-}$ MEFs caspase-3 cleavage was also enhanced but to a far greater extent and was significant at both time points (fold stim. at 4 h: MKP-$2^{+/+}$ = 1.74 ± 0.01, MKP-$2^{-/-}$ = 2.97 ± 0.41, $p<0.01$) (panels B & D). These data correlated with the finding that JNK activity was enhanced in MKP-2 deficient fibroblasts and also supported the earlier finding from the cell cycle experiment that MKP-2 deficient MEFs were found to be more in G0 phase of the cell cycle (see section 3.2.7) which signified that MKP-2 deletion is responsible for the enhanced susceptibility to apoptosis seen in the MKP-$2^{-/-}$ fibroblasts. These data suggested that MKP-2 could be an important regulator of cell survival.

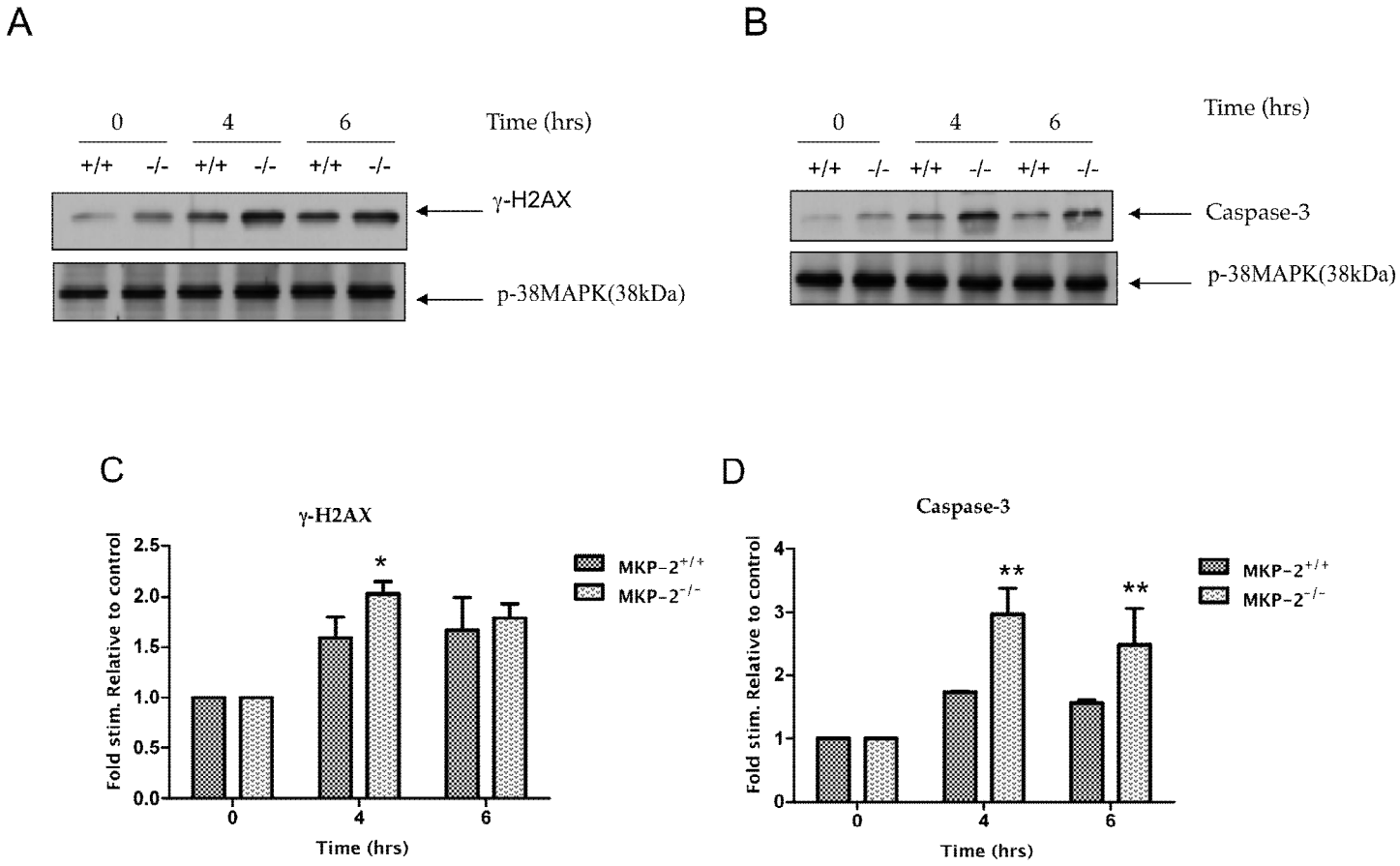

Figure 3.22: Enhanced anisomycin-induced phosphorylation of caspase-3 and γH2AX in MKP-2 deficient MEFs.

MEFs were grown to confluency and quiesced for 24 h in serum free media. The cells were stimulated with anisomycin 5 μm for 0-6 h. Whole cell extracts were resolved by SDS-PAGE and examined by Western blotting for caspase-3 and γH2AX phosphorylation as described in section 2.16. Relative phosphorylation of caspase-3 and γH2AX is outlined in panel A & B and panel C & D illustrates quantification by densitometry, expressed as mean±s.e.m. statistical analysis was by two way ANOVA. Post hoc test was by Bonferroni's multiple comparison tests, statistical significant is shown in relation to MKP-2$^{-/-}$, *P<0.05, **P<0.01. Each blot is indicative of 3 separate experiments.

3.2.9 Over-expression of Adv. MKP-2 reverses anisomycin-induced JNK, caspase-3 and γH2AX phosphoryaltion in MKP-2$^{-/-}$ MEFs.

Having established from previous experiments that MKP-2 deletion significantly enhanced cell death in MKP-2 deficient MEFs, a gain of function experiment was conducted to determine whether over-expression of Adv. MKP-2 could reverse this process. Initially the specificity of Adv. MKP-2 was examined by assessing phosphorylation of the three main MAPKs ERK, JNK and p38 MAPK (figure 3.23). The data presented in panels A and D, showed a representative western blot demonstrating strong and equivalent MKP-2 expression in both MKP-2$^{+/+}$ and MKP-2$^{-/-}$ MEFs. However, as demonstrated in panels B, E, H and I, MKP-2 over-expression inhibited anisomycin-induced JNK phosphorylation in both cultures but neither ERK nor p38 MAPK was affected. This suggested that the effect of MKP-2 is selective for JNK signalling. When caspase-3 cleavage and γH2AX phosphorylation was assessed (panels C, F and G), it was found that Adv. MKP-2 was much more effective in reversing the action of anisomycin in MKP-2$^{-/-}$ MEFs.

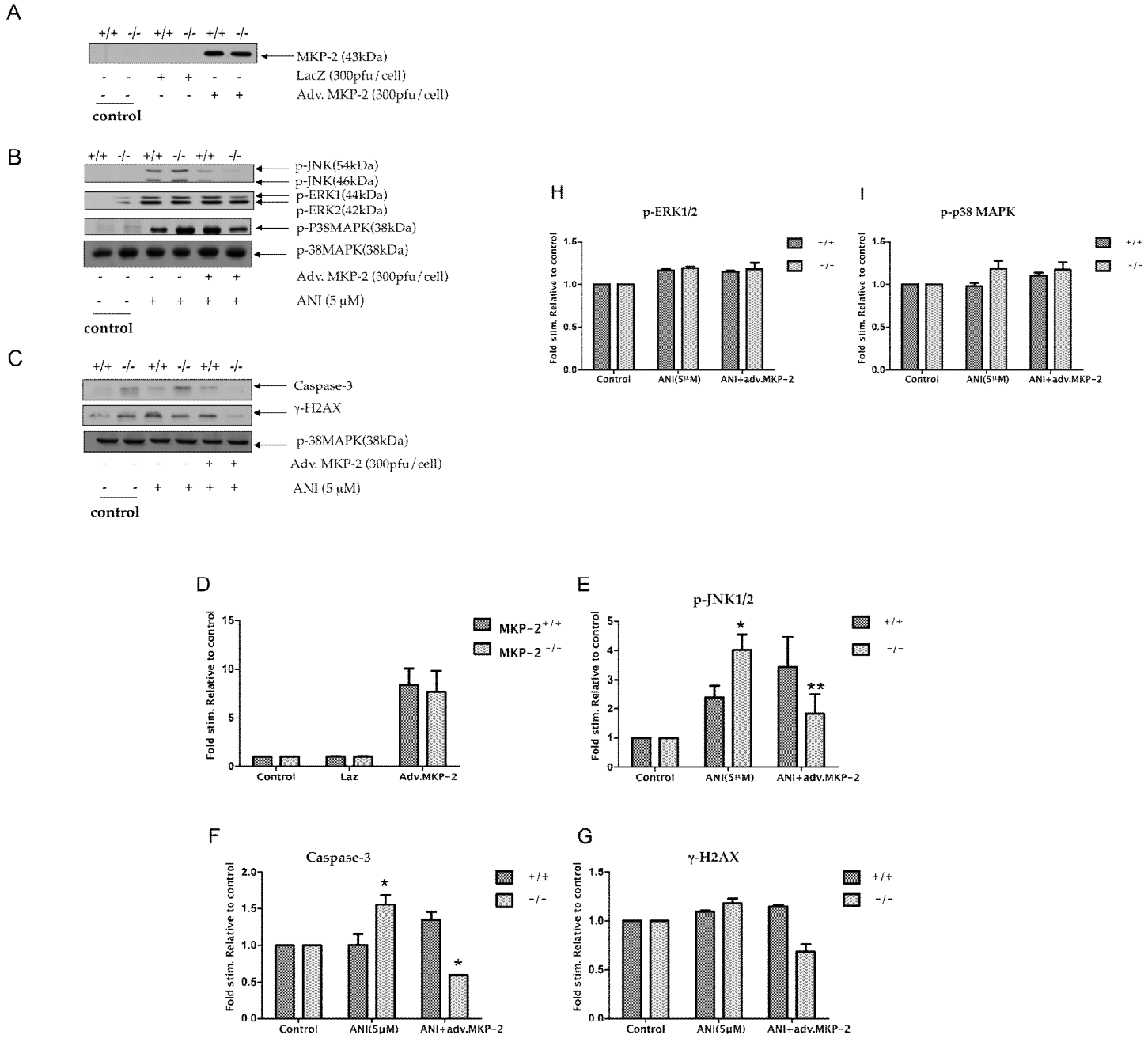

Figure 3.23: Over-expression of Adv. MKP-2 anisomycin-induced JNK, caspase-3 and γH2AX phosphoryalation in MKP-2$^{-/-}$ MEFs.

MEFs were grown to about 50% confluency on 6-well plates and were infected with Adv. MKP-2 (300 pfu) for 48 hr then stimulated with anisomycin for 4 h. Whole cell extracts were resolved by SDS-PAGE and examined by Western blotting for MKP-2 expression, JNK, ERK, caspase-3 and γH2AX phosphorylation as described in section 2.16. Relative expression of MKP-2 is outline in panels A & D, while relative phosphorylation of JNK, ERK, caspase-3 and γH2AX is outlined in panels E – I illustrate quantification by densitometry. Data expressed as mean±s.e.m. statistical analysis was by two way ANOVA. Post hoc test was by Bonferroni's multiple comparison tests, *p<0.05, **p<0.01. Each blot is representative of 3 separate experiments

3.2.10 MKP-2 deletion increased rates of apoptosis in MEFs

To further investigate the effect of MKP-2 deletion on apoptosis, flow cytometry was carried out using Annexin V and 7 ADD (see section 2.19). In both MKP-$2^{+/+}$ and MKP-$2^{-/-}$ MEFs resting levels of apoptosis was similar at approximately 20% (figure 3.24). Anisomycin stimulation increased apoptosis in MKP-$2^{+/+}$ MEFs to approximately 35% by 12 h. However apoptosis was significantly enhanced in MKP-2 deficient fibroblasts compared with the wild type giving values of approximately 50% (% cell death at 12 h; MKP-$2^{+/+}$ = 37.55 ± 0.75, MKP-$2^{-/-}$ = 50.40 ± 1.69, $p<0.05$). These data suggested that MEFs derived from MKP-2 deficient mice were more susceptible to undergo anisomycin mediated apoptosis compared with their wild type counterparts.

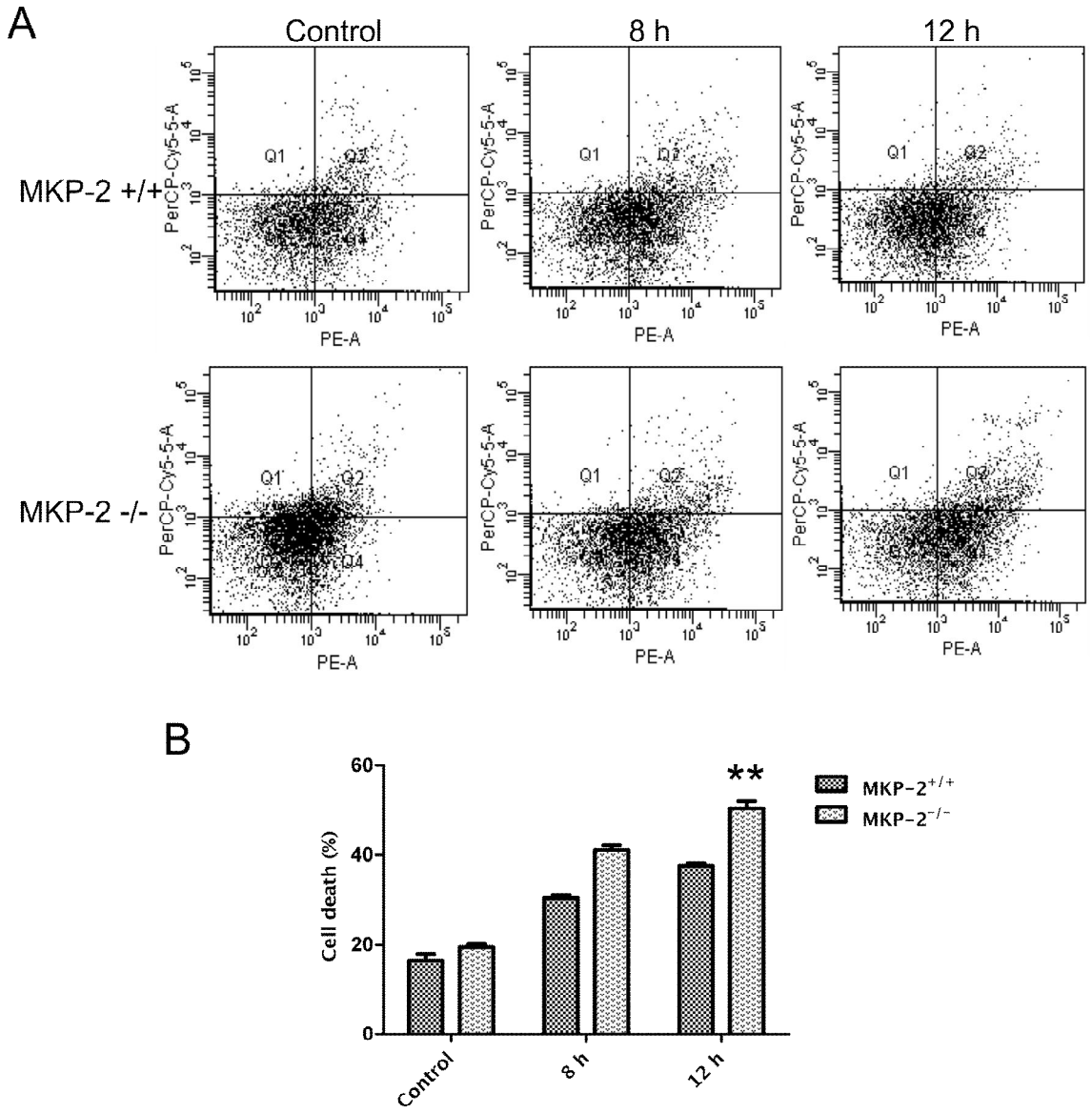

Figure 3.24: Increased rates of apoptosis in MKP-2 deficient MEFs.

MEFs were grown to confluency and quiesced for 24 h in serum free media and were stimulated with anisomycin (2.5 μM) over a period of 12 h (panel A). Samples were assessed for Annexin V and 7-AAD staining and analysed by flow cytometry as outlined in section 2.19. Statistical analysis was by two way ANOVA. Post hoc test was by Bonferroni's multiple comparison tests, **p<0.01, statistical significant is shown in relation to MKP-2$^{-/-}$, each value represents the mean ± s.e.m. of at least 3 separate experiments.

3.2.11 Over-expression of Adenoviral MKP-2 reversed the enhanced anisomycin-mediated apoptosis in MKP-2$^{-/-}$ MEFs

Having established from previous experiments that MKP-2 deletion significantly enhanced cell death in MKP-2 deficient MEFs, a gain of function experiment was conducted to determine whether over-expression of Adv. MKP-2 could reverse this process. MEFs were grown to about 50% confluency on 6-well plates and infected with Adv. MKP-2 (300 pfu) for 48 hr before serum starvation for 24 h. Cells were then further stimulated with anisomycin (2.5 μM) for 12 h prior to analysis by Annexin V and 7-AAD staining (see section 2.19). The data presented in figure 3.25 demonstrates that MKP-2 deletion enhanced anisomycin induced cell death as expected by approximately 10%. Over-expression of Adv. MKP-2 significantly reversed anisomycin-mediated apoptosis in MKP-2 deficient MEFs by almost as much as 90% (2.5 μM anisomycin + Adv. MKP-2 % cell death, MKP-2$^{+/+}$ = 42.00 ± 0.50, MKP-2$^{-/-}$ = 19.65 ± 1.35, $p<0.05$). In contrast Adv. MKP-2 was largely ineffective in reversing increased apoptosis in MKP-2$^{+/+}$ MEFs. Nevertheless these data have established that Adv. MKP-2 can reverse MKP-2 deficiency with respect to apoptosis.

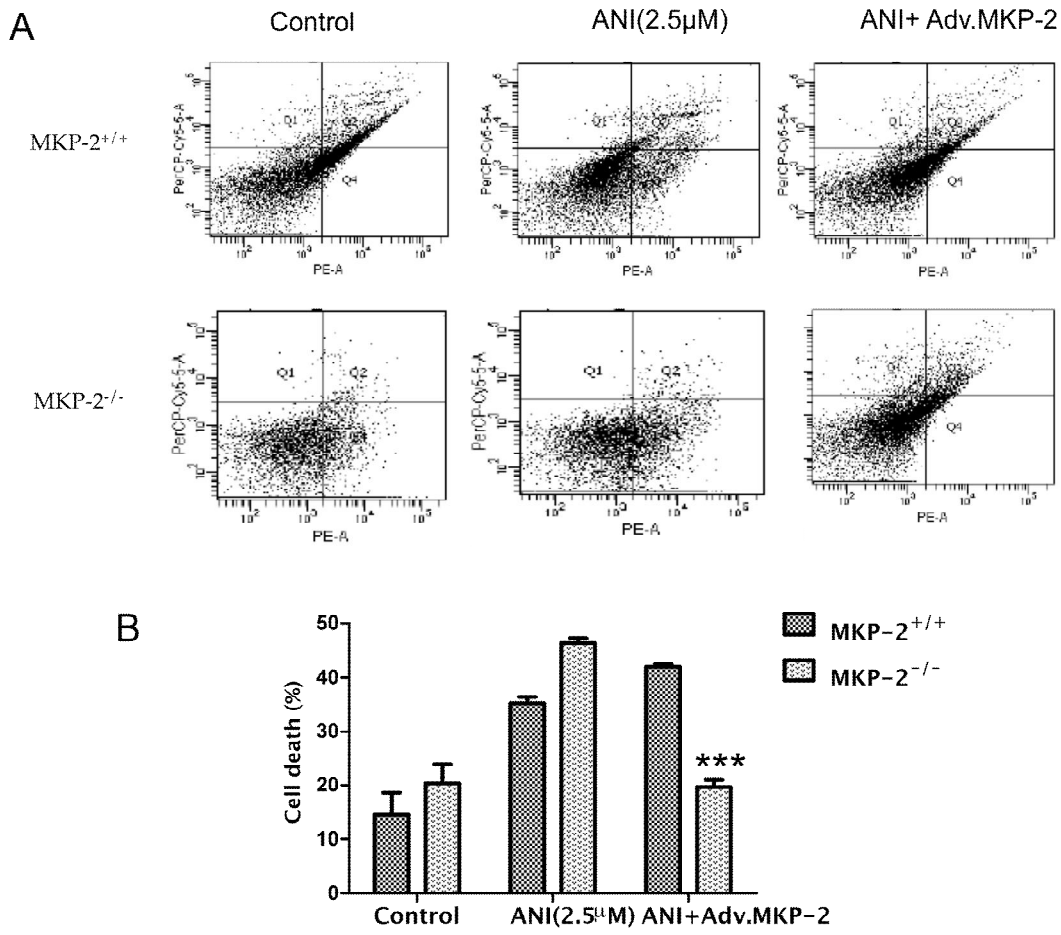

Figure 3.25: Over-expression of Adv. MKP-2 reversed enhanced anisomycin-mediated apoptosis in MKP-2 deficient MEFs.

MEFs were grown to about 50% confluency on 6-well plates and were infected with Adv. MKP-2 (300 pfu) for 48 h prior to stimulation with anisomycin (2.5 μM) for 12 h (panel A). Samples were assessed for Annexin V and 7-AAD staining and analysed by flow cytometry as outlined in section 2.19. Statistical analysis was by two way ANOVA. Post hoc test was by Bonferroni's multiple comparison tests, ***p<0.001, statistical significant is shown in relation to MKP-2$^{-/-}$. Each value represents the mean ± s.e.m. of at least 3 separate experiments.

3.2.12 MKP-2 deletion increased rates of apoptosis in MEFs in response to UVC

Similar to the experiment with anisomycin UVC was used to examine apoptosis by Annexin V and 7-AAD staining (see section 2.19). In both MKP-$2^{+/+}$ and MKP-$2^{-/-}$ MEFs resting levels of apoptosis was similar at approximately 15% (figure 3.26). UVC stimulation increased apoptosis in MKP-$2^{+/+}$ MEFs to approximately 30% after 24 h, however apoptosis was significantly enhanced in MKP-2 deficient fibroblasts compared with the wild type giving values of approximately 40% (% cell death with UVC 30j/m^2; MKP-$2^{+/+}$ = 32.20 ± 0.20, MKP-$2^{-/-}$ = 40.10 ± 0.10, $p<0.05$). These data suggested that MEFs derived from MKP-2 deficient mice were more susceptible to undergo UVC mediated apoptosis compared with their wild type counterparts.

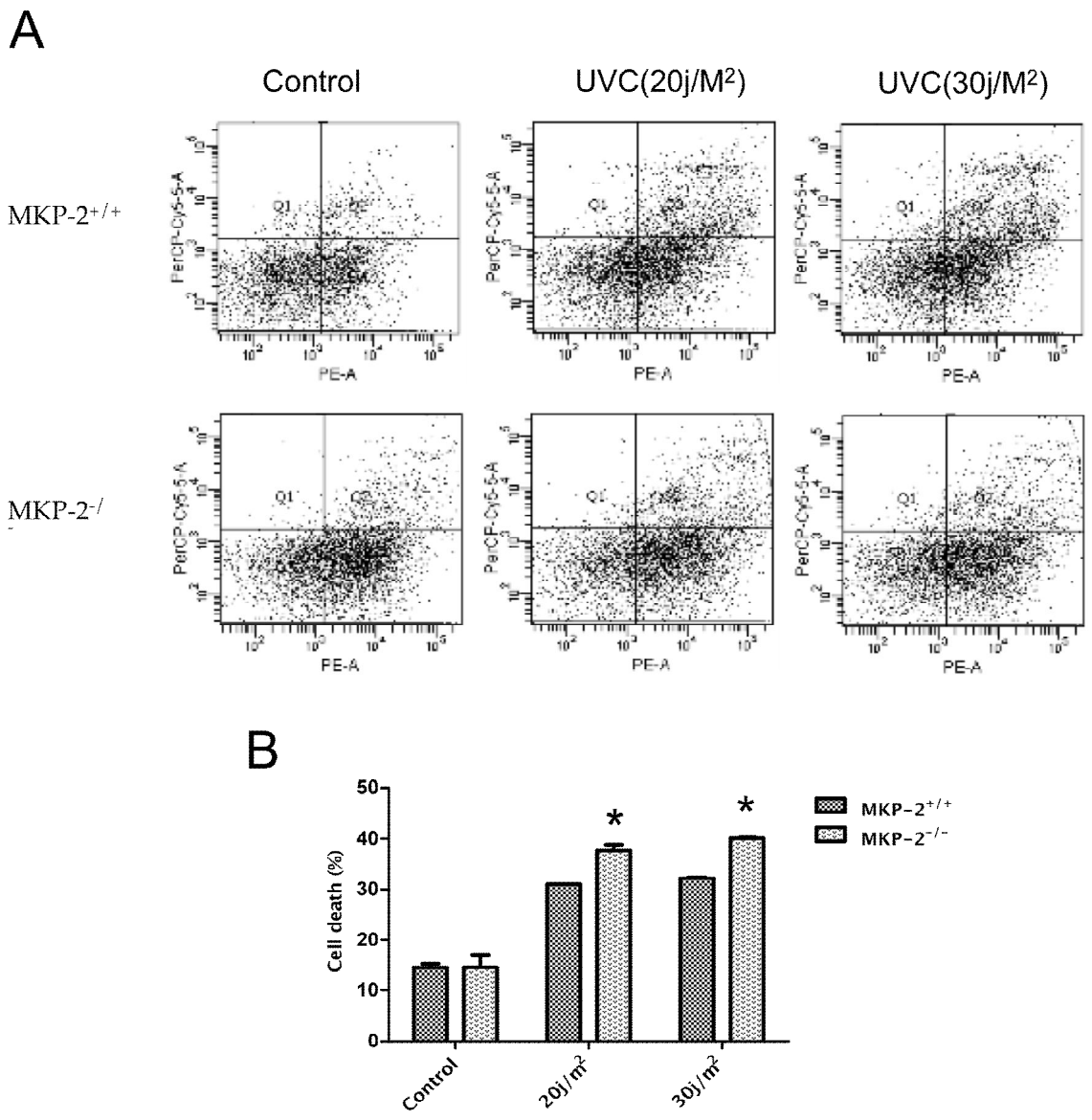

Figure 3.26: Increased rates of apoptosis in MKP-2 deficient MEFs in response to UVC

MEFs were grown to confluency and quiesced for 24 h in serum free media and were stimulated with UVC (20 & 30 j/m^2) for 24 h (panels A & B). Samples were assessed for Annexin V and 7-AAD staining and analysed by flow cytometry as outlined in section 2.19. Statistical analysis was by two way ANOVA. Post hoc test was by Bonferroni's multiple comparison tests, *P<0.05, statistical significant is shown in relation to MKP-2$^{-/-}$, each value represents the mean ± s.e.m. of at least 3 separate experiments.

3.2.13 Over-expression of Adv-MKP-2 reversed enhanced UVC-mediated apoptosis in MKP-2$^{-/-}$ MEFs

Having established from previous experiments that MKP-2 deletion significantly enhanced cell death in MKP-2 deficient MEFs, a gain of function experiment was conducted to determine whether over-expression of Adv. MKP-2 could reverse this process. MEFs were grown to about 50% confluency on 6-well plates and infected with Adv. MKP-2 (300 pfu) for 24 h before serum starvation for 24 h. Cells were then further stimulated with with UVC (30 j/m^2) for 24 h prior to analysis by Annexin V and 7-AAD staining (see section 2.19). The data presented in figure 3.27 demonstrated that MKP-2 deletion enhanced anisomycin induced cell death as expected by approximately 10%. Over-expression of Adv. MKP-2 significantly reversed anisomycin-mediated apoptosis in MKP-2 deficient MEFs by almost as much as 50% (UVC (30 j/m^2) + Adv. MKP-2 % cell death, MKP-2$^{+/+}$ = 24.00 ± 0.60, MKP-2$^{-/-}$ = 15.95 ± 1.12, $p<0.05$). In contrast Adv. MKP-2 was largely ineffective in reversing increased apoptosis in MKP-2$^{+/+}$ MEFs. However these data have confirmed that Adv. MKP-2 can reverse MKP-2 deficiency with respect to apoptosis.

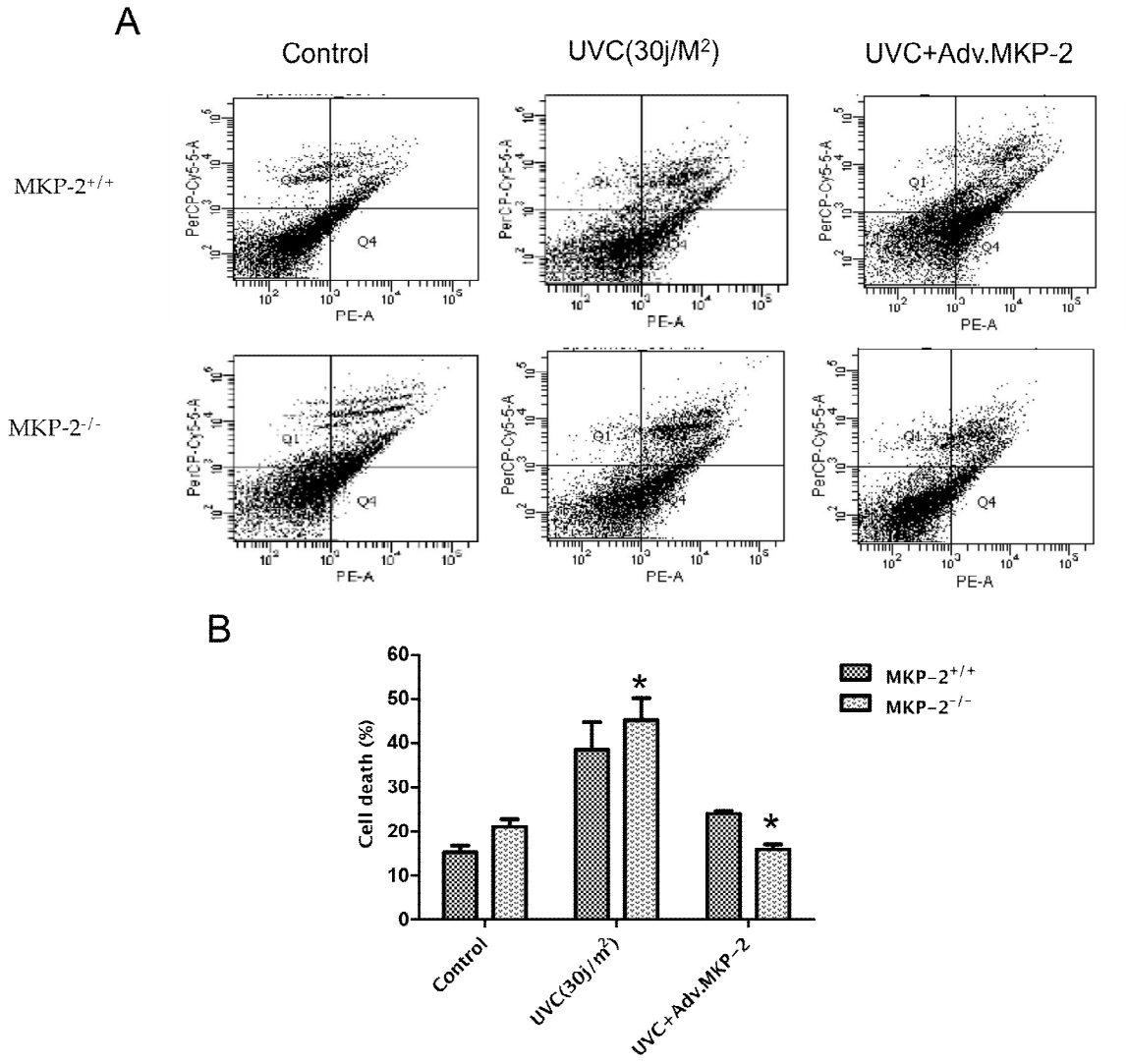

Figure 3.27: Over-expression of Adv. MKP-2 reversed enhanced UVC-mediated apoptosis in MKP-2 deficient MEFs.

MEFs were grown to about 50% confluency on 6-well plates and were infected with Adv. MKP-2 (300 pfu) for 48 h prior to stimulation with anisomycin (30 j/m^2) for 24 h (panels A & B). Samples were assessed for Annexin V and 7-AAD staining and analysed by flow cytometry as outlined in section 2.19. Statistical analysis was by two way ANOVA. Post hoc test was by Bonferroni's multiple comparison tests, *P<0.05, statistical significant is shown in relation to MKP-2$^{-/-}$ compared to wild type, each value represents the mean ± s.e.m. of atleast 3 separate experiments.

3.2.14 DISCUSSION

MAP kinase phosphatase-2 (MKP-2) is a type 1 dual specificity phosphatase (DUSP) that regulates the activities of the MAPKs, ERK and JNK *in vitro* (Dickinson and Keyse, 2006; Guan and Butch, 1995; Misra-Press *et al*. 1995; Owens and Keyse, 2007). However, the cellular functions of this particular family member are not well described. This chapter utilized a novel MAP kinase phosphatase-2 knockout (MKP-2 KO) mouse and assessed the consequences of deletion at the level of both MAPK regulation and in relation to proliferation. MKP-2 is a widely expressed MKP which shows significant sequence identity to MKP-1 and PAC1. Therefore, it may be expected that MKP-2 have overlapping functions particularly with MKP-1. In fact MKP-2 may be functionally redundant. Indeed, the MKP-2 knockout mouse generated did not display an obvious phenotype, they were of normal weight, fertile and displayed no developmental, growth or behavioural abnormalities (figure 3.3). This is consistent with mice lacking MKP-1, which show no phenotypic abnormalities and cells generated from these mice demonstrate no sign of irregular regulation of ERK signalling (Dorfman *et al*., 1996).

The induction of MKP-2 was attained using established agonists that induce this class of protein: serum, PDGF and PMA (Guan and Butch, 1995; Cadalbert *et al*., 2005; Sloss *et al*., 2005; Zhang *et al*., 2001). The induction of MKP-2 was observed 2 h after serum stimulation in wild type MEFs (figure 3.4). This in contrast to MKP-1 induction which is normally detected as early as 30 min to 1 h after treatment with serum (Brondello *et al*., 1997; Wang *et al*., 2008; Wu and Bennett, 2005), suggesting that the mechanisms of induction of these phosphatases may not be the same. MKP-1 is an early gene product induced by growth factors. In serum stimulated fibroblasts the kinetics of p-ERK2 dephosphorylation coincides with the induction of MKP-1 (Alessi *et al*., 1993; Sun *et al*., 1993). In contrast, there is relatively little information regarding MKP-2 expression however, induction of MKP-2 protein in both αT3-1 and rat pituitary cells following treatment with the Gonadotropin-

releasing hormone (GnRH) agonist, buserelin, has been reported. Induction of MKP-2 protein expression was observed 1-2 h in both cell types, which suggests that this may reflect the physiological actions activated by GnRH in fully differentiated primary gonadotrophs, and the activation of ERK is necessary for this induction by GnRH (Zhang *et al*., 2001).

In this current study induction of MKP-2 expression was exclusively controlled by ERK signalling but not by JNK or p38 MAPK, indicating that activation of ERK pathway is sufficient to promote the expression of MKP-2 (figure 3.8). The involvement of Ras/MAPK pathway in the induction of MKP-2 has been demonstrated in CCL39 Chinese hamster lung fibroblasts where constitutive activation of ERK in response to v-ras corresponded with sustained expression of MKP-2 (Brondello *et al*., 1997; Yip-Schneider *et al*., 2001). This further supports earlier studies implicating MKP-2 as part of a negative feedback loop for down regulating ERK phosphorylation and hence mitogenic signalling (Guan and Butch, 1995). MAPKs also regulate the stability of DUSP at the protein level by binding to MAPK substrates (Camps, *et al*. 1998). For example, DUSP5 expression has also been found to be reduced by incubation with the MEK inhibitor U0126, post protein induction (Kucharska *et al*., 2009), suggesting a requirement for ERK activity. Deletion of the KIM domain abolished the ability of ERK to prevent de-stabilization however, the mechanism involved remains uncertain. The stability of MKP-7 is also increased by ERK phosphorylation at ser-446 (Katagiri *et al*., 2005). Sometimes however, as is the case for MKP-1, MAPK binding can decrease protein stability and promote MKP-1 proteolysis through the ubiquitin ligase SCF^{Skp2}, thereby sustaining MAPK activity (Lin and Yang *et al*., 2006). Similarly, treatment with U0126 also decreased MKP-3 mRNA and protein expression (Zeliadt *et al*., 2008). Thus a general pattern has emerged suggesting that ERK binding to MKPs is essential for full protein expression. To date there is no information indicating whether MKP-2 undergoes a

similar stabilization however, a variant of MKP-2 lacking the ERK binding is more prone to proteolytic degradation (Cadalbert *et al*., 2010).

Initial experiments have demonstrated that deletion of MKP-2 did not alter baseline ERK and JNK activity in cultured MEFs (figure 3.9). This is in contrast to similar studies in MKP-3 KO fibroblasts which reported higher basal ERK phosphorylation (Maillet *et al*. 2008), thus suggesting that certain MKPs may function to regulate the baseline tone of some of the MAPKs. The quiescing conditions (48 h) used in these experiments were based on the work of Maillet *et al*. 2008. It was found that ERK phosphorylation was increased in response to PDGF in MKP-$2^{-/-}$ MEFs over a time course that was similar to that of MKP-2 induction. However, this enhancement was not consistent for all agents that were able to activate ERK, (for example serum and PMA) (figures 3.10 & 3.12) and it is likely that the magnitude of activation obscured the potential regulatory effects of MKP-2 deletion. In addition, it is possible that both agonist and cell specific differences can occur since a report by Al-Mutairi *et al*., 2010 observed that in macrophages, ERK signalling was not enhanced subsequent to MKP-2 deletion. There is some controversy about the substrate specificity of MKP-2, over-expression in cell lines or the use of MKP-2 adenovirus demonstrating selective inhibition of JNK (Al-Mutairi *et al*., 2010). It has been shown that TNFα and sorbitol-stimulated JNK activities, which exhibited diverse activation profiles, were not altered by MKP-2 over-expression. However, in response to H_2O_2, JNK activity was considerably reduced in cells overexpressing WT-MKP-2 and delayed in cells expressing CI-MKP-2 (Robinson *et al*., 2001).

Cellular stresses such as anisomycin, UVC and osmotic shock have been shown to activate JNK and p38 MAPK pathways (Cadalbert *et al*., 2005; Kyriaskis and Avruch, 2001; Shin *et al*., 2006) and therefore were used to determine the effects of MKP-2 deletion. The results were largely disappointing as JNK phosphorylation in response to anisomycin was only

marginally, although significantly, increased in MKP-2$^{-/-}$ MEFs. In addition the response to UVC was not affected although this again could be due to the high intensity of the stimulus involved (figures 3.15 & 3.16). A similar minor increase in JNK signalling was reported in MEFs derived from MKP-1 KO mice (Dorfman *et al*., 1996; Wu and Bennett, 2005) suggesting a level of redundancy involving possible compensation by other MKPs. Again a recent study has demonstrated enhancement of JNK signalling in macrophages from MKP-2 KO mice (Al-Mutairi *et al*., 2010), suggesting cell type and agonist specificity. It should also be noted that for several MKPs, selectivity profiles *in vitro* do not reflect specificity in cells from KO mice. For example, with regards to PAC-1, despite it being specific for ERK and p38 MAPK *in vitro* (although with less efficiency compared to other MKPs such as MKP-2) in KO cells ERK phosphorylation was actually decreased in mast cells and macrophages (Jeffrey *et al*., 2006). Thus, the majority of early studies that utilized biochemical assays *in vitro* to describe MAPK substrate specificity for MKPs should be viewed with caution and more studies *in vivo* are needed to specifically establish the targets of MKPs under physiological conditions.

An important and novel finding in this study was the observation that the loss of MKP-2 protein caused alteration in the proliferation of MEFs. MEFs derived from MKP-2$^{-/-}$ exhibited significantly reduced cell growth compared with MKP-2$^{+/+}$ counterparts (figure 3.17 & 3.18). It has been demonstrated that in response to serum, MEFs derived from MKP-1 KO mice displayed equal levels of ERK activity and cell proliferation with that of MKP-1$^{+/-}$ MEFs (Dorfman *et al*., 1996). The authors concluded that MKP-1 plays a redundant function in the control of ERK activity and cell proliferation. However, the finding in this present study is similar to more recent data which showed that deletion of MKP-1 inhibited the proliferation of fibroblasts (Wu and Bennett, 2005). Another report also demonstrated that MKP-1 over-expression in vascular smooth muscle cells (VSMC) led to an inhibition of DNA synthesis thereby inhibiting VSMC proliferation (Li *et al*., 1999). Similarly, it was

reported that MKP-1 KO $CD4^+$ T cells displayed impaired growth rates in comparison to their wild type counterparts (Zhang *et al*., 2009). Furthermore, stimulation of CD4 T cells derived from MKP-5 KO with plate-bound anti-CD3 demonstrated decreased cell growth which suggested that MKP-5 is essential for T-cell proliferation (Zhang *et al*., 2009).

Nevertheless, in contrast to these studies, it was reported that MEFs and neonatal myocytes derived from MKP-3 KO mice exhibited greater proliferation rates during embryonic development and in the early postnatal period (Maillet *et al*., 2008). These studies and the data presented in this chapter indicate that deletion of some the MKPs lead to a decrease in cell growth whereas the loss of others example MKP-3, lead to hyperproliferation. This is interesting in a disease setting as some of these MKPs have already been implicated in the pathogenesis of cancer and this could provide a mechanistic approach in developing drug intervention strategies.

The decrease in proliferation in MKP-2 deficient MEFs correlated with a decrease in G_2 / M phase transition. This finding has not been replicated in any other DUSP KO models and is the first to denote a role for an MKP at this stage of the cycle (figure 3.21). However, analysis of some of the cell cycle regulatory proteins were not consistent with G_2 / M phase arrest, for example the expression patterns of cyclin B1 and p-cdc-2 were enhanced in MKP-$2^{-/-}$ MEFs when they might be expected to be reduced. Indeed, it was reported that siRNA mediated knock down of MKP-2 protein expression attenuated the proliferation of MKK-f cells *in vitro* and *in vivo*, which was correlated with the inhibition of cyclin B1 expression and cdc-2 phosphorylation (Hasegawa *et al*., 2008). The findings outlined in this chapter could possibly be due to the fact only a small proportion of cells were delayed in this phase of the cycle and that most of the cells progressed through the cycle normally or that the arrest is very late on and MKP-2 deletion is delaying mitosis. Further experiments would be required to investigate where within the nucleus MKP-

2 is located during mitotic segregation and to better understand the regulation of cyclin B1 expression and cdc-2 phosphorylation during G_2/M transition.

Alternatively the effect of MKP-2 deletion may be related to the function of p53. Early studies implicated p53 in the inhibition of G_2/M phase transition through decreasing cyclin B1 protein levels and reducing the activity of the cyclin B1 promoter (Innocente *et al*., 1999). Furthermore, it was demonstrated that p53 mediated the reduction of cyclin B1 promoter activity in both p21 wild type and KO cell lines. This group also observed that in wild type cells, p53 binds to Sp1 and the cyclin B1 promoter, indicating that transcriptional suppression of cyclin B1 via the Sp1 transcription factor is mediated by wild type p53 (Innocente *et al*., 2005). Utilizing syngenic MEFs, it has been reported that in response to ionizing radiation, cyclin B1 accumulation increases in mutant p53 cells relative to wild type p53 (Lanzini *et al*., 2006). Recently, a motif (CTGGCGCCAG) in the MKP-2 promoter was found to be a new binding site for p53 to stimulate the MKP-2 gene (Shen *et al*., 2006). This study demonstrated the p53-dependent induction of MKP-2 which is present in the cellular response to stress stimuli leading to cell death, however, the authors did not investigate this association in relation to G_2/M phase transition.

Similarly, MKP-1 has been identified as a transcriptional target of p53. It was reported that p53 bound to a consensus p53 binding site located in the second intron of the MKP-1 gene and transactivated MKP-1 in reporter gene assays (Li *et al*., 2003). MKP-1 mRNA and protein levels were elevated in response to p53 activation in many p53 controlled cell lines. However, attenuation of MKP-1 activity inhibited p53-mediated G1 cell cycle arrest not G_2/M transition as implicated for MKP-2. It has also been shown that endogenous p53 protein binds directly to the promoter region of the DUSP5 gene, suggesting a p53 dependent transcriptional activity (Ueda *et al*., 2003). However, the involvement of DUSP5 in the control of G_2/M transition, via

cyclin B1 and cdc-2 kinase, has not been demonstrated. Although a trend is emerging that some DUSPs are transcriptional targets of p53, it appears that each one of them has a different function in the regulation of specific phases of the cell cycle. Since it has been shown that the phosphorylation of p21 in G_2/M transition enhances cyclin B1-cdc2 kinase activity (Dash and Wafik, 2005), assessing p21 phosphorylation could give an indirect measurement of p53 activity and should be investigated in the MKP-2 KO model.

The gain of function studies established that over-expression of Adv. MKP-2 completely reversed the proliferative deficit observed in MKP-2 deficient fibroblasts (figure 3.20). This is the first study that demonstrated over-expression of Adv. MKP-2 could reverse a decrease in proliferation in fibroblasts and this suggested that MKP-2 is indeed an important regulator in cell growth. In contrast, a previous study has reported that MKP-2 protein is increased in senescent fibroblasts due to the increased stability of MKP-2 against proteolytic degradation (Torres *et al*., 2003), and more recent work implicates a direct role in the senescence process, that is ectopic MKP-2 expression results in early senescence. However, on the contrary, knock-down of MKP-2 expression via transduction of MKP-2 sequence-specific shRNA, or expression of the phosphatase resistant ERK2 (D319N) mutant, reverses the effects of increased endogenous MKP-2 levels and senescence was delayed. (Tresini *et al*., 2007). The gain of function experiments revealed something interesting in the sense that the MKP-2 deficient fibroblasts showed high rates of proliferation when MKP-2 was over-expressed in these cells, suggesting that MKP-2 might be directly involved in regulating growth.

The rate of cell proliferation within any population of cells is determined by three parameters, namely the rate of cell division, the fraction of cells within the population undergoing cell division (growth fraction), and the rate of cell loss from the population due to terminal differentiation or apoptosis (Hoekstra, 1997). So it is plausible that the observed inhibition of cell

proliferation in MKP-2 deficient MEFs could be due to increased susceptibilty to apoptosis. Many studies have implicated JNK and p38 MAPK in regulating apoptosis in response to stress agents (Hamdi *et al*., 2005). This present study observed enhanced JNK and p38 MAPK signalling in MKP-2$^{-/-}$ MEFs in response to anisomycin. These data are in line with a recent study in our laboratory denoting enhanced JNK signalling in MKP-2$^{-/-}$ macrophages (Al-Mutairi *et al*., 2010). JNK signalling has been shown to be linked to increased caspase-3 activity and γH2AX phosphorylation. Caspase-3 is an effector caspase within the caspase cascade, it cleaves proteins involved in nuclear envelope integrity (e.g. lamin B) and chromatin condensation (e.g. acinus), but spares other potential substrates (such as the major erythroid transcription factor GATA-1) (Galluzzi et al., 2008). It is well recognized to be regulated by JNK (Wang *et al*., 2008), whilst γH2AX is a variant of the histone H2A family and its function was understood to be related mainly with repair of DNA damage. Lu *et al*., (2006) showed that γH2AX was phosphorylated by UVA induced JNK activation which correlated with caspase-3 cleavage in both γH2AX KO and γH2AX wild type MEFs. This suggests that γH2AX is essential for the integrity of DNA and is associated with caspase-3 cleavage. In this present study it was found that Adv. MKP-2 over-expression reversed the enhanced anisomycin-induced cell death in MKP-2$^{-/-}$ fibroblasts including the increased caspase-3 degradation and phosphorylation of γH2AX (see figure 3.22), which correlated with JNK deactivation. These findings therefore link JNK signalling to regulation of apoptotic protein activity and apoptosis in the context of MKP-2 deletion.

The results in this present study are in line with the recent finding that MKP-1 deletion MEFs displayed enhanced cell death in response to anisomycin (Wu and Bennett, 2005). However, treatment with MAPK inhibitors revealed that enhanced p38 MAPK activity was responsible for increased cell death rather than JNK which is implicated in this present study. Also it has been reported that MKP-1 KO mice exhibited greater infarction injury as compared with

wild type littermates (Kaiser *et al*., 2004). It has been shown that ectopic MKP-1 expression inhibited DNA damage induced JNK activity and cell death (Hamdi *et al*., 2005), however, high levels of cellular MKP-1 may result in a lack of specificity. More recently, it has been demonstrated that MEFs derived from MKP-1$^{-/-}$ displayed enhanced sensitivity to UV-induced apoptosis compared with the wild type (Staples *et al*., 2010). Whilst other studies do demonstrate that MKP-1 can regulate JNK in certain cell types, it may not apply to fibroblasts. This current study plus previous work suggests that both MKP-2 and MKP-1 are essentially performing the same function in relation to cell survival but may do so by regulating different MAPKs. The quiescing conditions (48 h) used in the apoptosis assay experiments were based on the work of Wu and Bennett, 2005.

Finally there were a number of curious additional observations regarding the effect of MKP-2 deletion. In MKP-2$^{-/-}$ fibroblasts both caspase-3 and γH2AX phosphorylation was enhanced, two proteins found in different subcellular locations, caspase-3 being cytosolic prior to cleavage and γH2AX being nuclear. This suggests that MKP-2 can regulate both proteins via JNK signalling in different compartments despite being strictly nuclear located. To date no study has shown that MKP-2 is located in the cytosol, but MKP-1 has been found in the mitochondria (Rosini *et al*., 2004), so MKP-2 may have a function within the same compartment. Furthermore, in MKP-2$^{-/-}$ MEFs, Adv. MKP-2 was much more effective in reversing the increase in apoptosis than in wild type MEFs. The reason for this difference is unclear but may relate to different activities and binding strength of the human and mouse MKPs. This requires further investigation.

In conclusion, the findings in this study strongly suggest that MKP-2 is necessary for cell survival and may regulate vital anti-apoptotic signalling. It also demonstrates that MKP-2 is essential in cellular defense against DNA impairment. Given that apoptosis is relevant to heart disease, these findings

suggest that MKP-2 could play an important function in the heart. Also further studies would be required to establish if MKP-2 performs the same protection in cancer especially *in vivo*.

CHAPTER 4

CHARACTERIZATION OF MKP-2 INDUCTION AND MAPK KINASE SIGNALLING IN ADULT CARDIAC FIBROBLASTS AND CARDIAC PHENOTYPE AND FUNCTION IN MKP-2 DELETION MICE

Chapter 4: Characterization of MKP-2 induction and MAPK signalling in adult cardiac fibroblasts and cardiac phenotype and function in MKP-2 deletion mice

4.1: Introduction

4.2: RESULTS

The previous chapter fully described the kinetics of induction of MKP-2 in response to serum, PMA and PDGF and established the role of MKP-2 in regulating MAPK signalling in MEFs. It also demonstrated that MKP-2 was essential for MEF proliferation and survival. Numerous studies have recognized MAPK signalling pathways as key regulators of both cardiac function and dysfunction for example in developmental cardiac hypertrophy, and adult-onset hypertrophy in response to pathophysiological insult (Bueno *et al*., 2001). However, the role of MKPs in regulating MAPK signalling and the effects on cardiac function and cardiomyopathy has not been fully investigated. Previous studies have proved contradictory, the expression of MKP-2 was found to be down-regulated in the heart of rats following 5 months of pressure overload (Chaudhary *et al*., 2008) but conversely MKP-2 expression being up-regulated in adult human myocardium during myocardial failure (Communal *et al*., 2002).

In addition to direct effects on cardiac myocytes, the heart undergoes changes in both the cellular and extracellular composition during remodeling which involve changes in cardiac fibroblasts. CFs regulate the remodeling of ECM in the heart and hence its function. Changes in CFs include increased proliferation with increased and abnormal remodeling of ECM resulting in cardiac fibrosis which is associated with reduced contractility and disturbance of the electrical circuitry by ECM proteins, which eventually contributes to cardiac pathology (Kim *et al*., 2002; Porter and Turner, 2009).

The aims of this chapter were to examine whether MKP-2 contributes to cardiac phenotype and function by characterizing MKP-2 signalling in adult CF by; firstly examining MKP-2 induction in response to a variety of agonists, secondly, by establishing proliferation response of CF's isolated from MKP-2 $^{-/-}$ and MKP-2 $^{+/+}$ hearts and thirdly by assessing cardiac function in MKP-2$^{-/-}$ and MKP-2$^{+/+}$ mice using echocardiography *in vivo* and finally by examining MKP-2/MAPK protein expression in mouse model (MTAB) of cardiac hypertrophy.

4.3: Characterization of cardiac fibroblasts in culture by immunofluorescence

Initial experiments were conducted to characterise the phenotype of adult CF in culture using immunofluorecence staining (see section 2.7). It is well known that adult CF are capable of differentiating in culture into myofibroblasts, and the expression of smooth muscle α-actin is the key feature of this phenomenon (Leask, 2010). Smooth muscle α-actin is one of the few genes whose expression is reasonably limited to smooth muscle cells. As a positive control, smooth muscle cells (from guinea pig) were stained and found to express α-actin in the cytosol (figure 4.1, panel A). In contrast, no CF cultures (passage 1) showed any equivalent staining, panel B. This confirmed that CFs have not transformed to myofibroblasts. To avoid this event, all subsequent studies were performed on passage 1 cells.

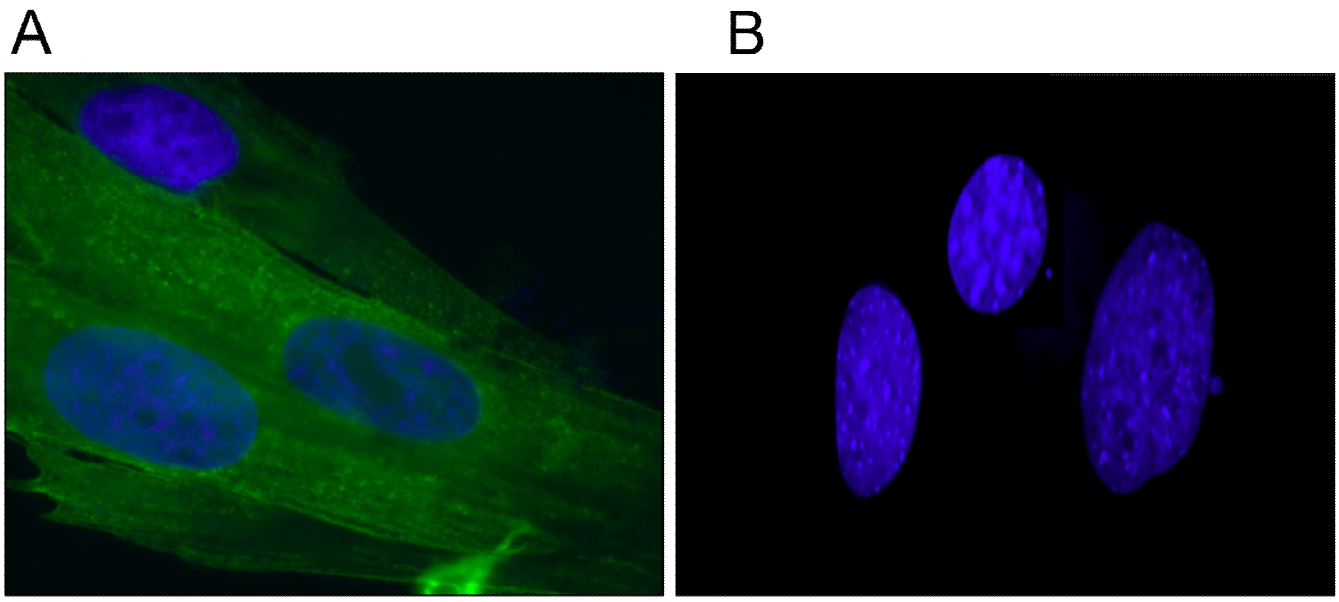

FIGURE 4.1: Immunofluorecence for expression of α-smooth muscle actin.

The immunofluorescence image (x400), of smooth muscle cells both stained with α-smooth muscle actin, in panel A the localization of α-smooth muscle actin (green) was shown in cultured smooth muscle cells, in panel B, CF nuclei stained with blue Dapi. The result is representative of three independent experiments.

4.4: Induction of MKP-2 in response to Serum, PDGF and Ang II in MKP-$2^{+/+}$ and MKP-$2^{-/-}$ CF

Having confirmed the identity of adult CFs, the kinetics of MKP-2 induction in response to FCS (10%), PDGF (10 ng/ml), and Ang II (100 nM) was examined over 120 min. Ang II was included because it is a well known agent that plays an important role in the heart both under normal physiological conditions and during hypertrophy and fibrosis and would help in identifying physiologically relevant agonist that would induce MKP-2 and stimulate MAPK phosphorylation in these cells (Mehta and Griendling, 2007). CFs were grown to confluency in 12-well plates and were serum starved for 24 h and incubated with above mentioned agonists. Whole cell lysates were analysed by Western blotting for MKP-2 expression (figure 4.2). As shown for MEFs, induction of MKP-2 was relatively slow with increased expression not apparent until 120 min after stimulation with FCS (FCS fold stim. at 120 min, MKP-$2^{+/+}$ = 1.64 ± 0.08, $p<0.01$ compared with control), panels A & B. Similarly, PDGF also stimulated the induction of MKP-2 protein after 120 min (PDGF 10 ng/ml fold stim. at 120 min, MKP-$2^{+/+}$ = 2.00 ± 0.95, $p<0.001$ compared with un-stimulated cells), panels A & C. However, in contrast, MKP-2 protein was not induced following stimulation with Ang II over the time course examined. On the other hand, no induction was observed in MKP-$2^{-/-}$ CFs in response to any of the agonists used (panels A & D). This confirmed the complete absence of MKP-2 protein in MKP-$2^{-/-}$ CFs. It also established that serum and PDGF activate endogenous MKP-2 expression in wild type CF but Ang II could not induce MKP-2 protein expression. Although these are adult cells, it also demonstrated that MKP-2 protein induction followed a similar pattern compared with MEFs.

Furthermore, the kinetics of MKP-2 induction in response to these agonists was examined over an extended time course (0-24 h) (figure 4.3). In MKP-$2^{+/+}$ CFs, MKP-2 protein expression was strongly induced in response to FCS after 2 h and reached maximal expression at 4 h at approximately 2.5 fold of basal

values (FCS fold stim. at 4 h, MKP-$2^{+/+}$ = 2.29 ± 0.19, $p<0.001$ compared with control). Expression then slowly declined and returned to basal values within 24 h (panels A & B). However, no induction was observed in CFs derived from MKP-$2^{-/-}$ mice. Similarly, PDGF simulated the induction of MKP-2 protein with the same efficacy and kinetics (PDGF 10 ng/ml fold stim. at 120 min, MKP-$2^{+/+}$ = 3.25 ± 0.21, $p<0.001$ compared with un-stimulated cells) (panels A & C). Again no induction was observed in CF derived from MKP-$2^{-/-}$ mice. However, in contrast, MKP-2 protein was not induced following stimulation with Ang II over the time course (panels A & D). This again confirmed the complete absence of MKP-2 protein in MKP-$2^{-/-}$ CF and also established that serum and PDGF activates endogenous MKP-2 expression in MKP-$2^{+/+}$ CF but 100 nM Ang II could not induce MKP-2 protein expression.

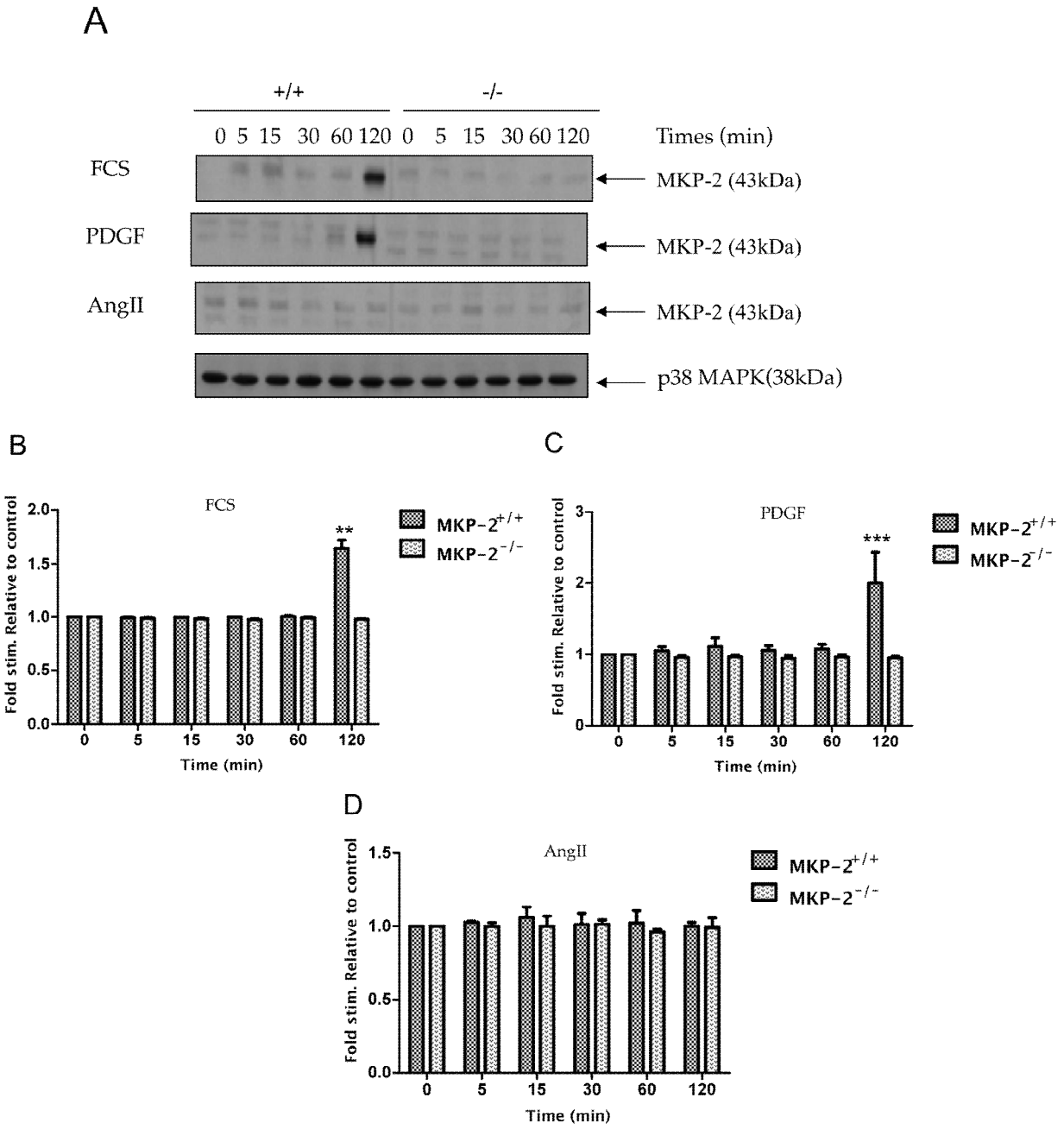

Figure 4.2: Induction of MKP-2 in response to FCS, PDGF and Ang II in MKP-2$^{+/+}$ and MKP-2$^{-/-}$ CF.

Confluent CFs were quiesced for 24 h in serum free media. The cells were incubated with 10% FCS, PDGF (10 ng/ml) and Ang II (100 nM) for 0-120 min. Whole cell extracts were resolved by SDS-PAGE and examined by Western blotting for induction of MKP-2 as outlined in section 2.16. Relative induction of MKP-2 is outlined in panel A while panels B-D illustrate quantification by densitometry, expressed as mean±s.e.m. Statistical analysis was by one-way ANOVA, post hoc test by Dunnett's test, **p<0.01, ***p<0.001 in comparison with control group. Each blot is representative of 3 individual experiments.

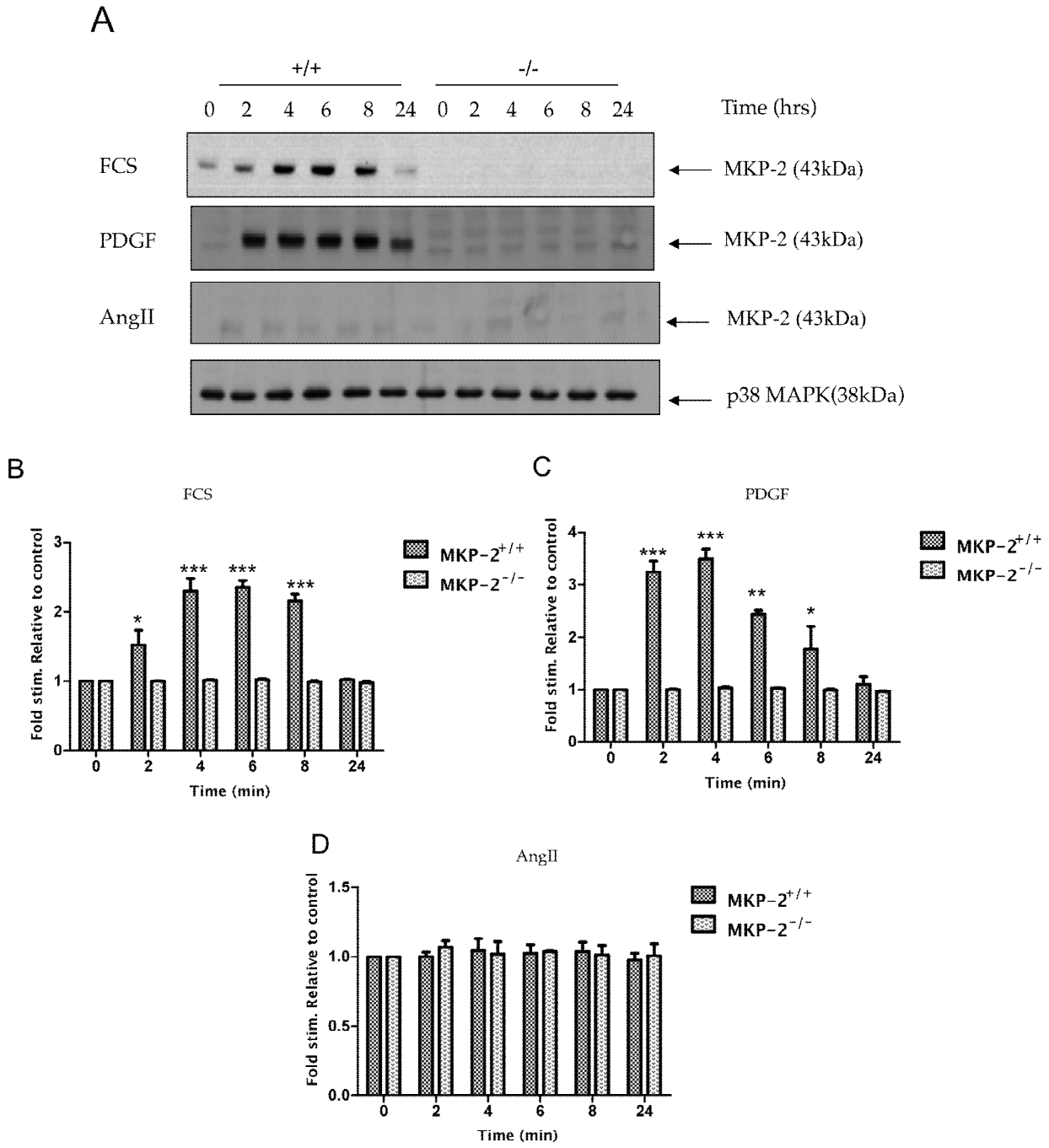

Figure 4.3: Induction of MKP-2 in response to FCS, PDGF and Ang II in MKP-2$^{+/+}$ and MKP-2$^{-/-}$ CF.

Confluent CFs were quiesced for 24 h in serum free media. The cells were incubated with 10% FCS, PDGF (10 ng/ml) and Ang II (100 nM) for 0-24 h. Whole cell extracts were resolved by SDS-PAGE and examined by Western blotting for induction of MKP-2 and total p38 MAPK as outlined in section 2.16. Relative induction of MKP-2 is outlined in panel A while panels B-D illustrate quantification by densitometry, expressed as the mean±s.e.m. Statistical analysis was by one-way ANOVA, post hoc test by Dunnett's test,*p<0.05, ***p<0.001 in comparison with control group. Each blot is representative of 3 individual experiments.

4.5: Effect of MKP-2 deletion on phosphorylation of MAPKs

4.5.1 Phosphorylation of ERK stimulated by FCS, PDGF and Ang II in MKP-$2^{+/+}$ and MKP-$2^{-/-}$ CFs

From previous experiments it was demonstrated that serum and PDGF stimulated MKP-2 protein expression, therefore in order to examine whether the deletion of MKP-2 altered the kinetics of MAPK phosphorylation these agonists, including Ang II, were used. Both ERK and JNK phosphorylation was examined over 0-120 min and 0-24 h in response to each agonist (figures 4.4 and 4.5). FCS caused a rapid increase in ERK phosphorylation which peaked at 5 min and was sustained up to 120 min. However, there was no significant difference between MKP-$2^{+/+}$ and MKP-$2^{-/-}$ CFs in either the magnitude or kinetics of phosphorylation (FCS fold stim. at 5 min., MKP-$2^{+/+}$ = 1.40 ± 0.02, MKP-$2^{-/-}$ = 1.28 ± 0.14) (panels A & B). Similarly, ERK phosphorylation was rapidly increased in response to PDGF which peaked at 5 min and was still detected after 120 min (PDGF 10 ng/ml fold stim. at 5 min., MKP-$2^{+/+}$ = 3.97 ± 0.43, MKP-$2^{-/-}$ = 3.55 ± 0.18). PDGF promoted a more sustained increase in ERK phosphorylation (panels A & C). Also Ang II stimulated a rapid phosphorylation of ERK which peaked within 5 min and declined thereafter (Ang II 100 nM fold stim. at 5 min., MKP-$2^{+/+}$ = 1.43 ± 0.03, MKP-$2^{-/-}$ = 1.05 ± 0.03), panel D, however, the magnitude of phosphorylation was less compared with FCS or PDGF. PDGF also promoted a more sustained increase in ERK phosphorylation (Figure 4.5) over the longer period, however, the loss of MKP-2 again did not alter the level of stimulation between the two cell types (PDGF 10 ng/ml stim., at 2 h: MKP-$2^{+/+}$ = 3.19 ± 0.25, MKP-$2^{-/-}$ = 3.58 ± 0.15). These results suggested that serum, PDGF and Ang II were capable of inducing similar phosphorylation of ERK in both MKP-$2^{+/+}$ and MKP-$2^{-/-}$ CFs.

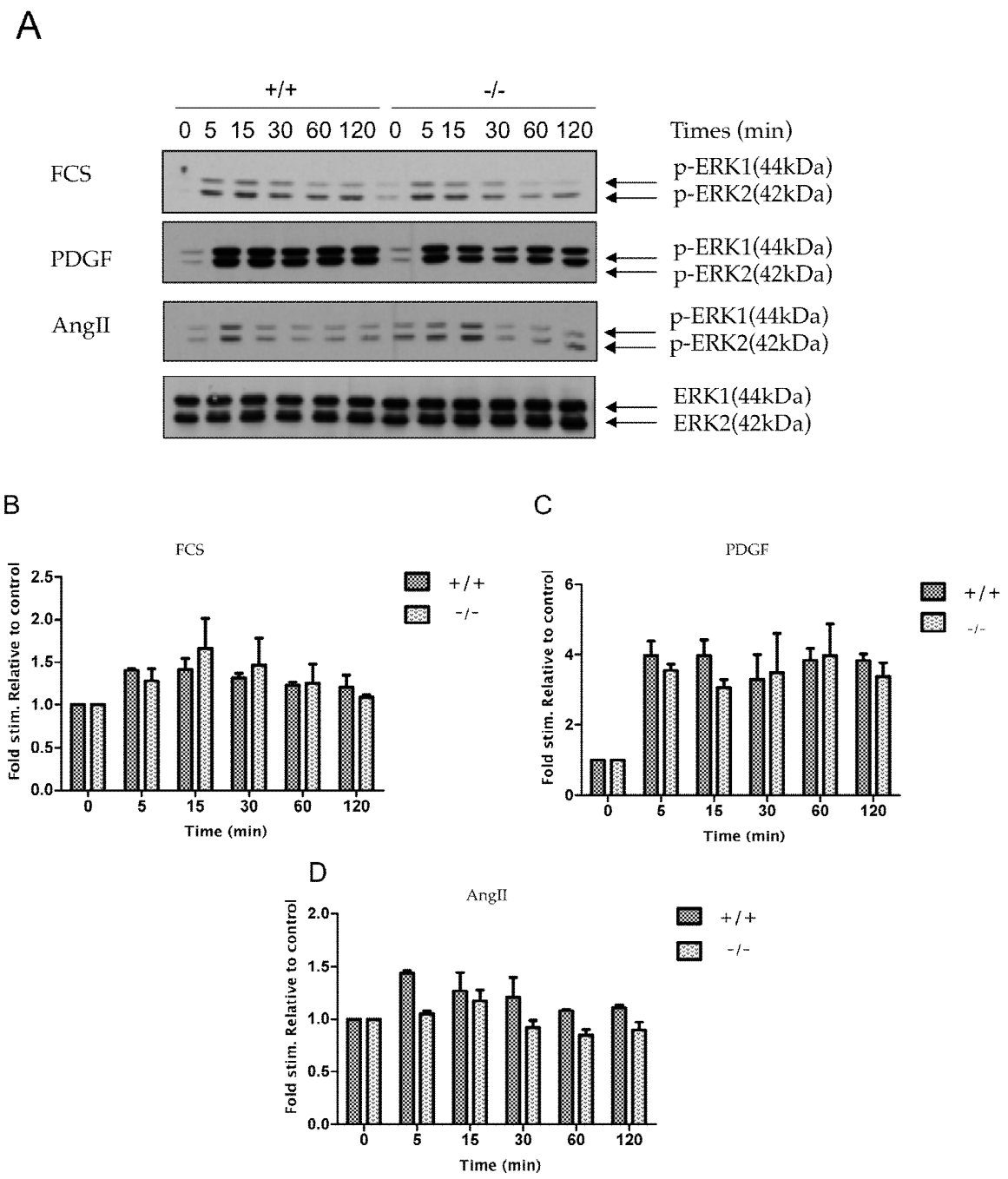

Figure 4.4: Phosphorylation of ERK by 10% FCS, PDGF and Ang II in MKP-2$^{+/+}$ and MKP-2$^{-/-}$ CFs.

CF were grown to confluency and quiesced for 24 h in serum free media. The cells were incubated with 10% FCS, PDGF (10 ng/ml) and Ang II (100 nM) for 0-120 min. Whole cell extracts were resolved by SDS-PAGE and examined by Western blotting for ERK phosphorylation as described in section 2.16. Relative phosphorylation of ERK is outlined in panel A while panels B, C & D illustrates quantification by densitometry. Data expressed as mean±s.e.m. Statistical analysis was by one-way ANOVA. Each blot is indicative of 3 separate experiments.

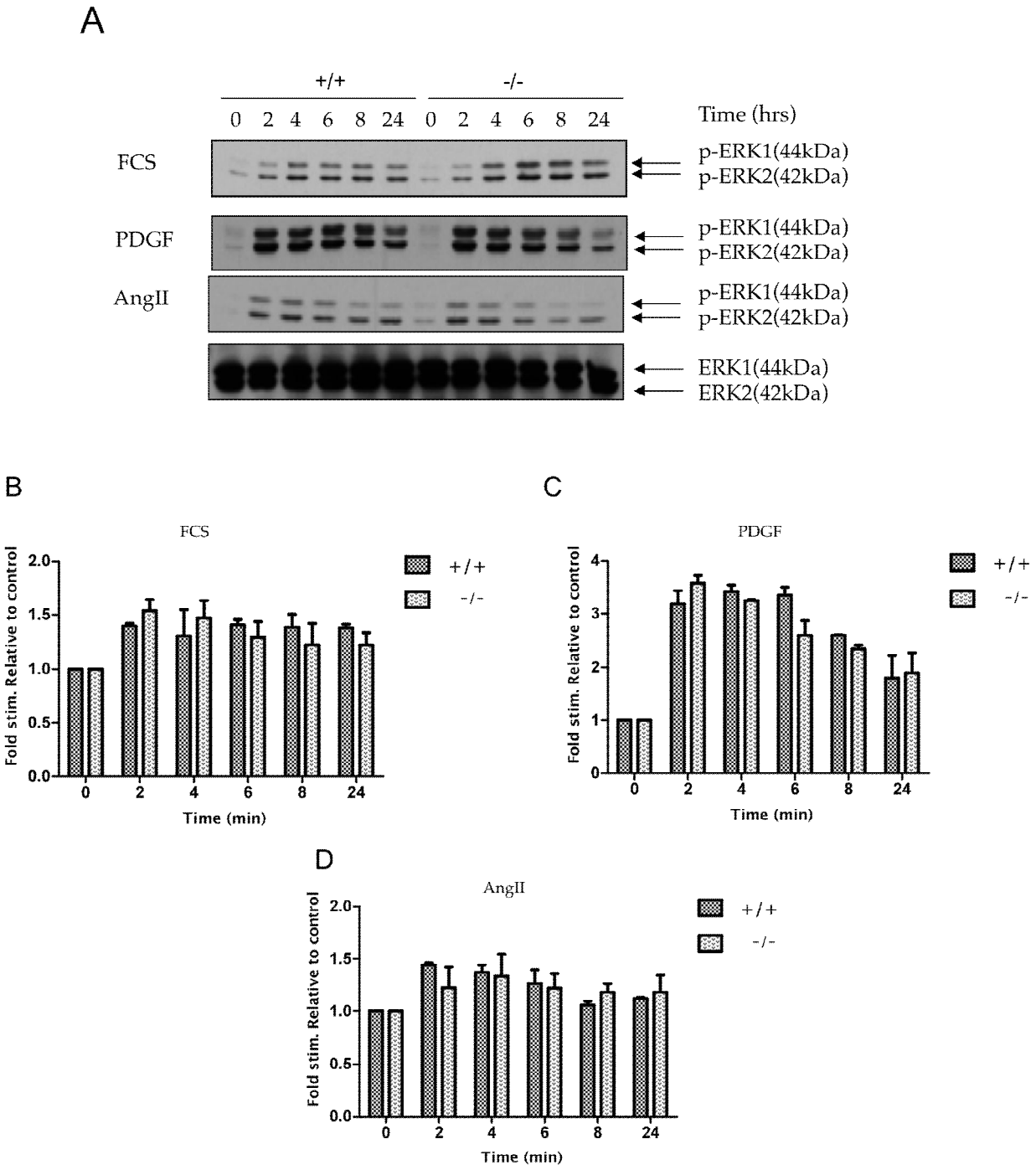

Figure 4.5: Phosphorylation of ERK by FCS, PDGF and Ang II in MKP-2$^{+/+}$ and MKP-2$^{-/-}$ CFs.

CF were grown to confluency and quiesced for 24 h in serum free media. The cells were incubated with 10% FCS, PDGF (10 ng/ml) and Ang II (100 nM) for 0-24 h. Whole cell extracts were resolved by SDS-PAGE and examined by Western blotting for ERK phosphorylation as described in section 2.16. Relative phosphorylation of ERK is outlined in panel A while panels B, C & D illustrates quantification by densitometry. Data expressed as mean±s.e.m. Statistical analysis was by one-way ANOVA. Each blot is indicative of 3 separate experiments.

4.5.2: Time course of FCS and Ang II stimulated JNK phosphorylation in MKP-$2^{+/+}$ and MKP-$2^{-/-}$ CFs.

The effect of MKP-2 deletion on JNK phosphorylation was also examined over both short and long time courses (figures 4.6 and 4.7). FCS caused a rapid phosphorylation of JNK within 5 min and reached maximum after 15 min and declined thereafter. However, over the long time course FCS caused a small and minor increase in JNK phosphorylation. In response to Ang II only a small and minor increase in JNK phosphorylation over both time spans which was not significantly different from non-stimulated cells was observed. Furthermore, there were no differences in the level of phosphorylation in MKP-$2^{-/-}$ CF relative to MKP-$2^{+/+}$ CFs.

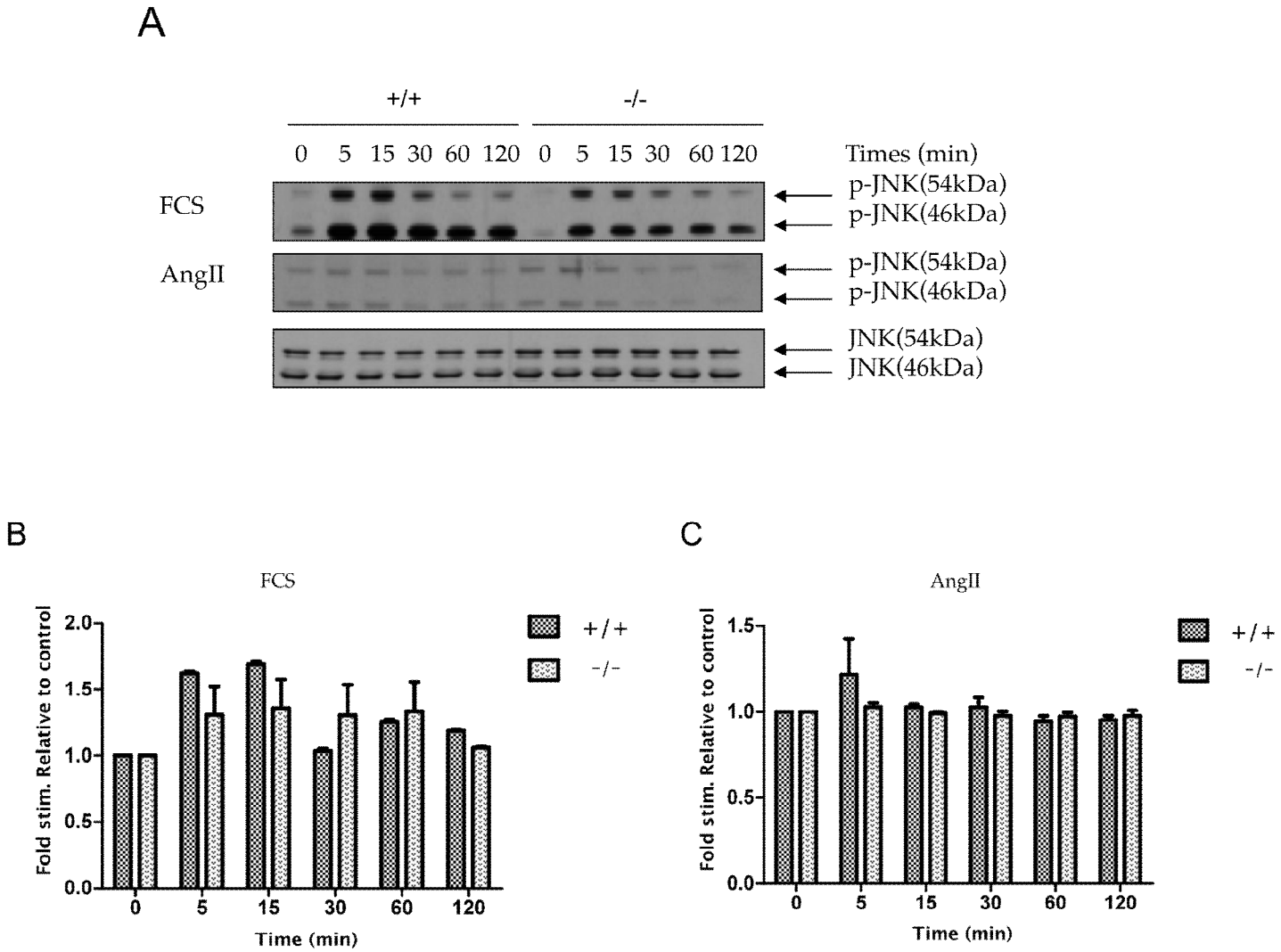

Figure 4.6: Time course of FCS and Ang II stimulated JNK phosphorylation in MKP-2$^{+/+}$ and MKP-2$^{-/-}$ CFs.

CFs were grown to confluency and quiesced for 24 h in serum free media. The cells were incubated with 10% FCS, PDGF (10 ng/ml) and Ang II (100 nM) for 120 min. Whole cell extracts were resolved by SDS-PAGE and examined by Western blotting for JNK phosphorylation as described in section 2.16. Relative phosphorylation of JNK is outlined in panel A while panels B & C illustrate quantification by densitometry, expressed as mean±s.e.m. Statistical analysis was by one-way ANOVA. Each blot is indicative of 3 separate experiments.

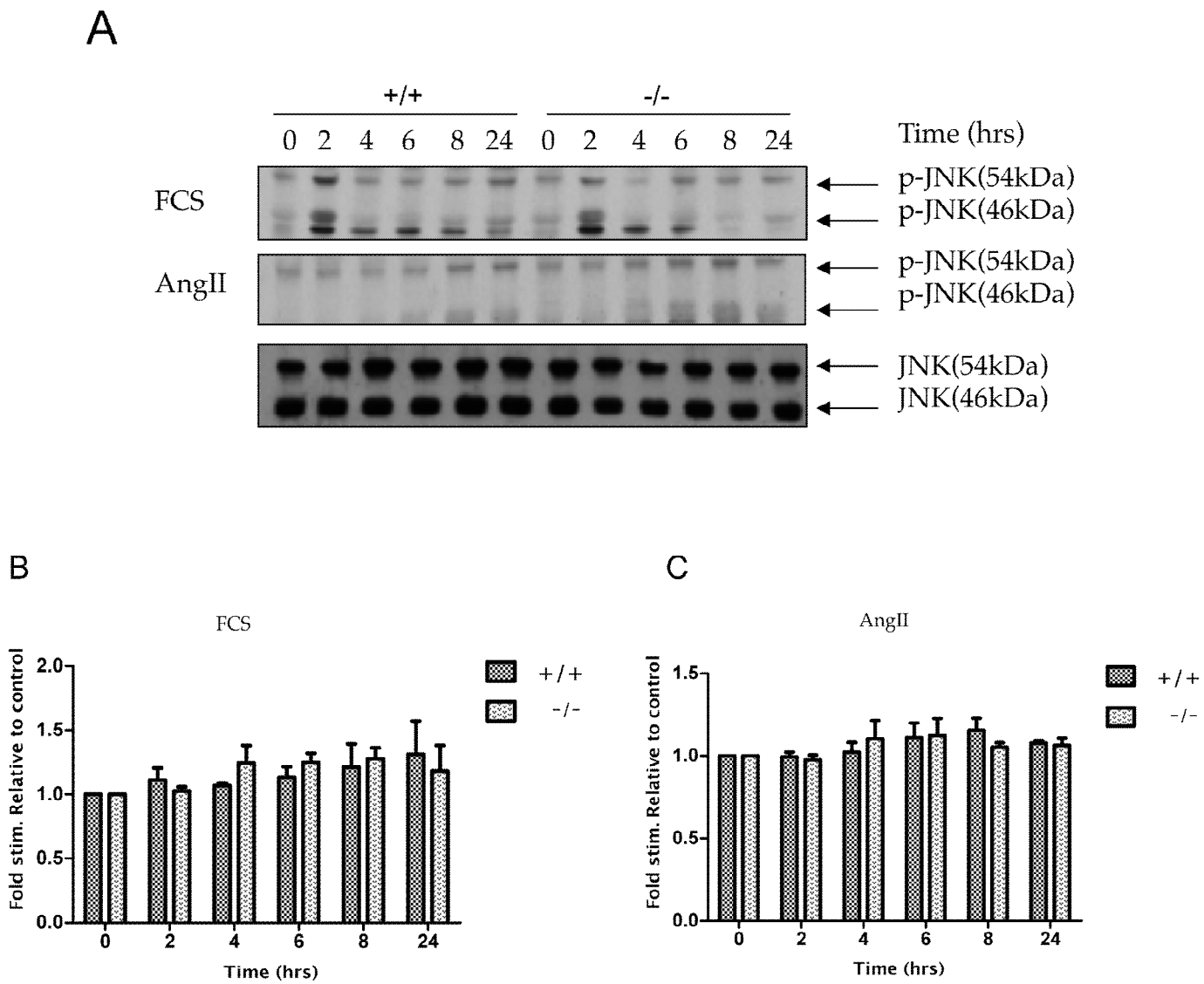

Figure 4.7: Time course of FCS and Ang II phsophoryaltion of JNK in MKP-2$^{+/+}$ and MKP-2$^{-/-}$ CFs.

CF were grown to confluency and quiesced for 24 h in serum free media. The cells were incubated with 10% FCS, PDGF (10 ng/ml) and Ang II (100 nM) for 0-24 h. Whole cell extracts were resolved by SDS-PAGE and examined by Western blotting for JNK phosphorylation as described in section 2.16. Relative phosphorylation of JNK is outlined in panel A while panels B & C illustrate quantification by densitometry, expressed as mean±s.e.m. Statistical analysis was by one-way ANOVA. Each blot is indicative of 3 separate experiments.

4.6: Loss of MKP-2 leads to alteration of CF proliferation

4.6.1: MKP-2 deletion leads to decrease in CF proliferation: [^{3}H]-thymidine incorporation assay

Having established the effect of MKP-2 deletion upon MAPK phosphorylation, this was correlated with the regulation of cellular proliferation. Initially, [^{3}H]-thymidine incorporation was examined to allow the estimation of DNA synthesis in CF (see section 2.8). The data presented in figure 4.8 demonstrated that in MKP-2$^{+/+}$ fibroblasts, serum gave a concentration-dependent increase in [^{3}H]-thymidine incorporation which was maximal between 5 and 10% FCS at approximately 6 fold of basal values. Similar to the results obtained with MEFs, in CFs lacking MKP-2, there was a significant reduction in DNA synthesis relative to wild type, particularly at the 10% FCS concentration, of approximately half (fold stim. DPM; MKP-2$^{+/+}$ = 804.31 ± 118.5, MKP-2$^{-/-}$ = 502.89 ± 121.2, $p<0.01$). This demonstrated that the deletion of MKP-2 protein has significantly inhibited proliferation in these cells establishing that MKP-2 is indeed involved in this process.

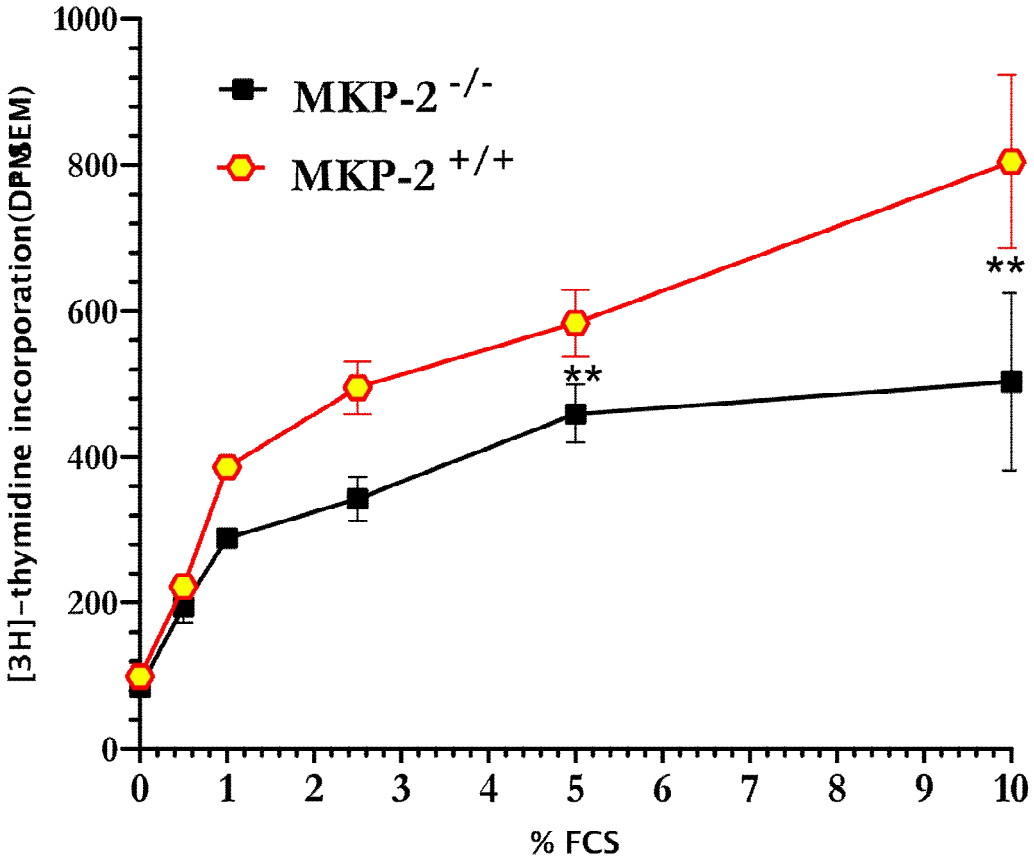

Figure 4.8: Loss of MKP-2 leads to alteration of CF proliferation.

Equal number of CF (5,000 cells / well) were plated on 24-well tissue culture plates and grown to approximately 60% confluency at 37° C and were serum starved for 24 h. The quiesced cells were stimulated with increasing FCS concentration for 24 h. DNA synthesis was measured using [^{3}H]-thymidine incorporation assay. Counts were measured in DPMs (disintegrations per minute) and cell proliferation was analysed using two way ANOVA. Post hoc test was by Bonferroni's multiple comparison tests, statistical significance is shown in relation to MKP-2$^{-/-}$, **P<0.01. Control values, DPM; MKP-2$^{-/-}$ = 84.50 ± 9.05, MKP-2$^{+/+}$ = 99.41 ± 0.81. Each point represents the mean±s.e.m. from 3 experiments performed in triplicate using 3 separate mouse cultures. (n=3).

4.6.2: MKP-2 deletion leads to decrease in CF proliferation: Cell counting by haematoxylin staining

The experiments assessing [^{3}H]-thymidine incorporation, are only an indirect measurement of proliferation and therefore cell counting using haematoxylin staining was used to directly measure cell number (see section 2.9). As expected in MKP-$2^{+/+}$ CF, over a 72 h period, serum caused an approximately 2-3 fold increase in cell number which was evident as early as 24 h (see figure 4.9). On the contrary, proliferation in MKP-$2^{-/-}$ CF was significantly impaired relative to wild type. No increase in cell number was observe in these cultures until at least 48 h, and by 72 h the difference in growth rate was approximately 50% (cell number per field; MKP-$2^{+/+}$ = 65.37 ± 2.6x10^5, MKP-$2^{-/-}$ = 33.13 ± 1.9x10^5, $P<0.01$). The proliferation assay by cell counting provided additional evidence that absence of MKP-2 has significantly reduced the growth of these cells. These results further established that MKP-2 is essential for CFs growth.

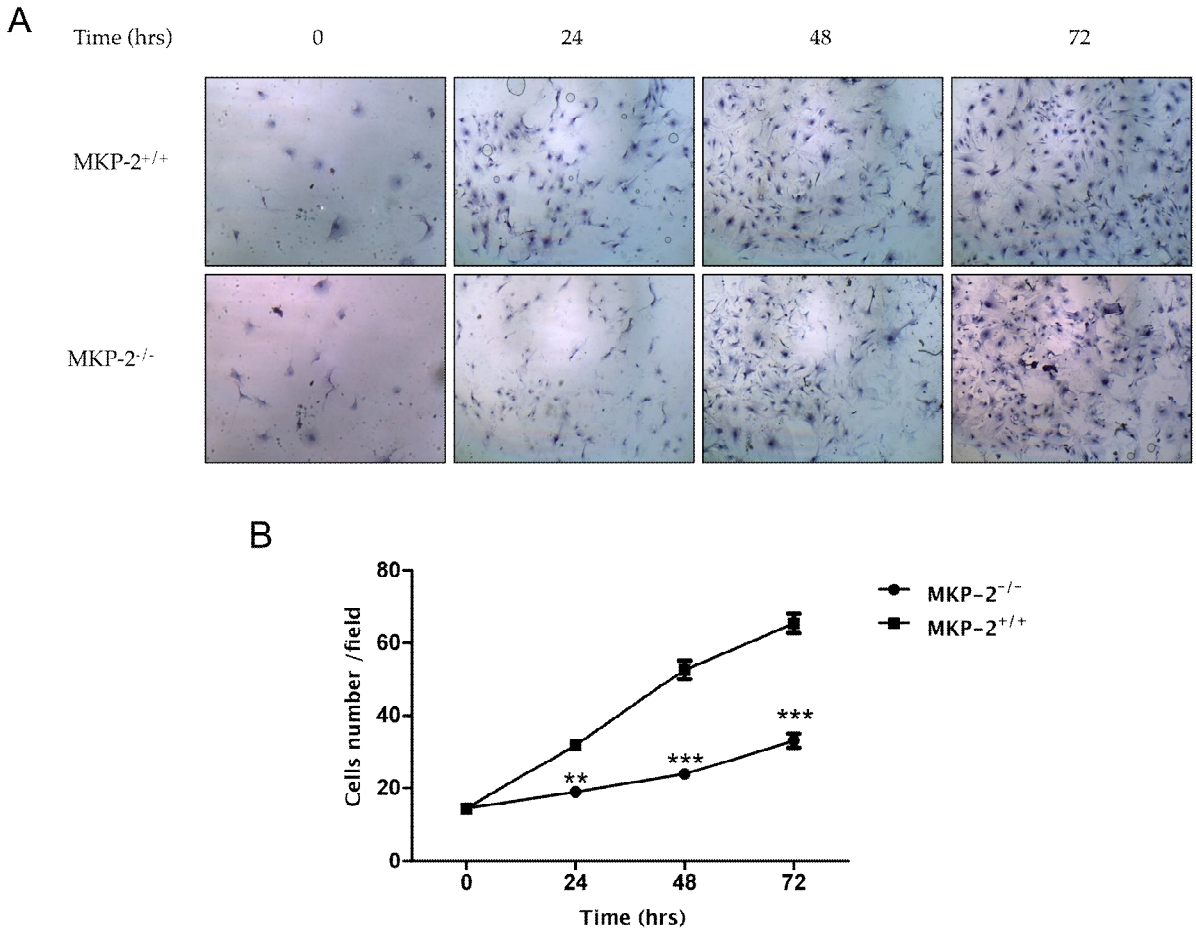

Figure 4.9: Loss of MKP-2 leads to decreased CFs proliferation

CF were serum starved for 24 h in serum free media and then stimulated for either 24, 48, 72 h with 10% FCS. Cultures were washed with PBS, and analysed using haematoxylin (panel A). The number of cells was determined from 10 random fields per each coverslip (panel B) (see section 2.9). Quantified data was analysed using two-way ANOVA. Post hoc test was by Bonferroni's multiple comparison tests, statistical significant is shown in relation to MKP-$2^{-/-}$, **p<0.01, ***P<0.001). Control values (0 h), cell number per field; MKP-$2^{+/+}$ = 14.53 ± 0.4x10^5, MKP-$2^{-/-}$ = 14.47 ± 0.5x10^5. Each value represents the mean±s.e.m. performed in triplicate from 3 separate experiments (n=3).

4.7 Characterization of MAPK Signalling using Cardiac Myocytes

Having established changes in CF an attempt to examine MAPK signalling in adult mouse cardiac myocytes was made. Isolation of myocytes using different protocols was employed in order to culture homogenous viable rod-shaped myocytes, however, this was not successful. Figure 4.10 demonstrated the picture of the acute morphological changes and loss of cardiac myocyte population that occurs in the adult cardiac myocyte preparations; top panel showed that the population of cells comprised of over 80% rod-shaped cardiac myocytes 8 minutes after isolation, middle panel indicated the loss of rod-shaped cardiac myocytes 1 hour after isolation, most of the cells became hypercontracted leading to their death, bottom panel shows that 5 hours after isolation very few cells were left and they were all hypercontracted. These results demonstrated that homogenous myocytes cultures could be not achieved in order to successfully use them for signalling studies.

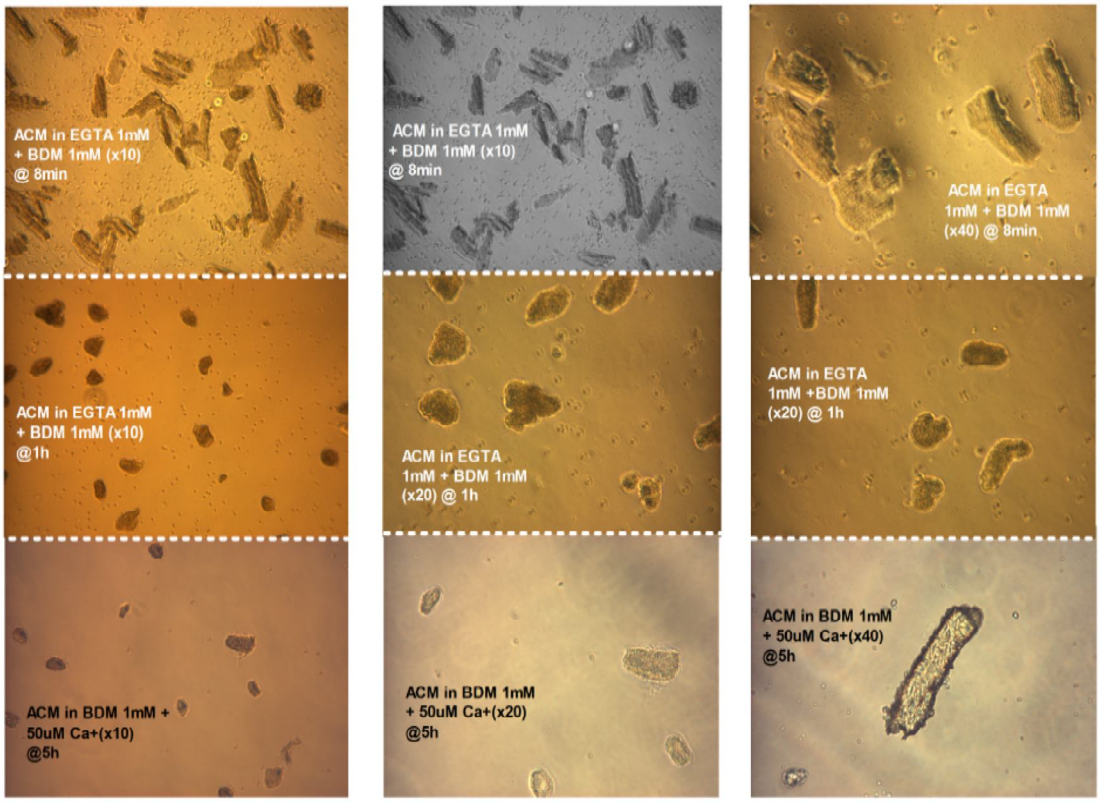

Figure 4.10: Acute changes in the Morphology of Freshly isolated Adult Mouse Cardiac Myocytes (ACM). Phase-microscopic appearance of cardiac myocytes after 8 min, 1 h and 5 h immediately after isolation (Nikon, Japan Magnification, x100 and x200) demonstrating the acute morphological changes and loss of myocyte population that occurs in the adult cardiac myocyte preparations, n=20.

4.8: Heart weight measurement in MKP-2$^{-/-}$ mice

Having established that cardiac fibroblasts, at least, showed deficits in proliferative characteristics, the potential effect of MKP-2 KO on cardiac function was examined. As mentioned in section 3.2.1 the MKP-2$^{-/-}$ mice demonstrated no apparent phenotypic defects, developmental or growth abnormalities in comparison with their wild type littermates. However, phenotypically, (see figure 4.11, panel A) the hearts derived from these mice appeared larger but analysis of the heart weight normalized to body weight (at 8-10 weeks of age) as shown in panels B & C demonstrated no significant difference when compared with MKP-2$^{+/+}$ hearts (HW/BW ratios; MKP-2$^{+/+}$ = 11.75 ± 0.24, MKP-2$^{-/-}$ = 12.34 ± 0.27, ns) (see table 4.1).

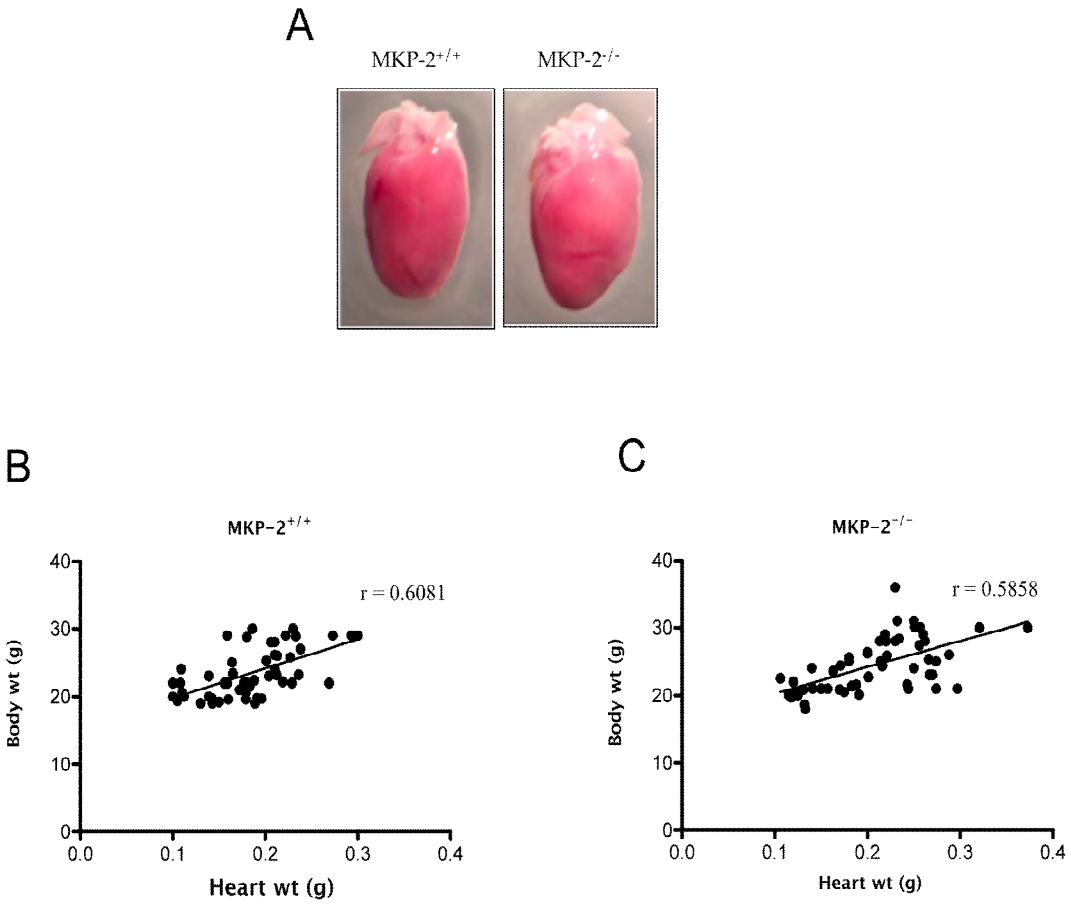

Figure 4.11: Comparison of hearts isolated from MKP-2$^{+/+}$ and MKP-2$^{-/-}$ mice. In panel A, representative photograph of 8-10 weeks old hearts from MKP-2$^{-/-}$ and MKP-2$^{+/+}$ mice while in panel B, scatter diagram showing the analysis of heart to body weight ratios (expressed in mg/g) in these mice, r is the pearson's correlation coefficient (n=53). No statistically significant difference in heart weight to body weight ratios.

4.9: Echocardiographic analysis of MKP-$2^{+/+}$ and MKP-$2^{-/-}$ mice at 8-10 weeks of age

Having examined the heart weight: body weight ratios of MKP-2 deletion mice, further baseline analysis were carried out on these mice by functionally assessing cardiac function using echocardiography *in vivo*. The data presented in figure 4.12 illustrates M-mode echocardiographic recording of a left parasternal transverse section showing the LV in short axis, with M-mode cursor line through its largest dimension (see section 2.12). Cardiac contractility was assessed during systole and diastole. The anterior and posterior walls of left ventricle, the papillary muscle including the interventricular septum were all conspicuous. Also the dimensions of end-systolic and end-diastolic diameters were clearly indicated by the arrows. These results demonstrated the locations of the various anatomical structures of the MKP-$2^{+/+}$ and MKP-$2^{-/-}$ hearts indicating normal heart structure.

4.10: Left ventricular chamber dimensions and Fractional shortening (FS) in 8-10 weeks old MKP-$2^{+/+}$ and MKP-$2^{-/-}$ mice

Having established the reproducibility of the method, a number of parameters were compared in both wild type and MKP-2 KO mice. Both LVEDD and LVESD dimensions were increased in MKP-2 deletion mice in comparison with wild type (LVEDD; MKP-$2^{+/+}$ = 0.32 ± 0.007, MKP-$2^{-/-}$ = 0.39 ± 0.007, $P<0.05$), (LVESD; MKP-$2^{+/+}$ = 0.21 ± 0.013, MKP-$2^{-/-}$ = 0.28 ± 0.010, $P<0.05$) (see figure 4.13, panel A). Associated with these anatomical changes, left ventricular function, as assessed by fractional shortening (FS), was decreased in MKP-$2^{-/-}$ compared with MKP-$2^{+/+}$ (FS, MKP-$2^{+/+}$ = 32.65 ± 1.40, MKP-$2^{-/-}$ = 22.41 ± 1.37, $P<0.05$) (see figure 4.13, panel B). The level of decrease was approximately 10% in comparison with wild type. However, no significant difference was observed in anterior and posterior wall dimensions. These data demonstrated that LVEDD and LVESD dimensions were each significantly larger in MKP-$2^{-/-}$ indicative of increased dilation, whilst

decreased FS signified compromised contractility. This suggests that MKP-2 deletion mice show evidence of altered cardiac contraction.

Parameters	**MKP-2$^{+/+}$**	**MKP-2$^{-/-}$**
LVEDD (mm)	0.32± 0.007	0.39± 0.007***
LVESD (mm)	0.21± 0.013	0.28± 0.010***
FS (%)	32.65± 1.40	22.41± 1.37**
PW (mm)	0.075± 0.005	0.072± 0.004
AW (mm)	0.088± 0.003	0.092± 0.005
BW (g)	23.40 ± 0.67	24.56 ± 0.80
HW (mg)	188.9 ± 10.40	205.0±11.26
HW/BW (mg/g)	11.75 ± 0.24	12.34± 0.27

Table 4.1: Functional cardiac parameters in MKP-2 KO mice.

Values are group mean±s.e.m. AW, anterior wall of left ventricle; LVEDD, left ventricular end-diastolic diameter; LVESD, left ventricular end-systolic diameter; PW, posterior wall of left ventricle; FS, fractional shortening; BW, body weight; HW, heart weight. The unpaired Student's t-test was used for comparison, **p<0.01, ***p<0.001. See figure 4.13.

A

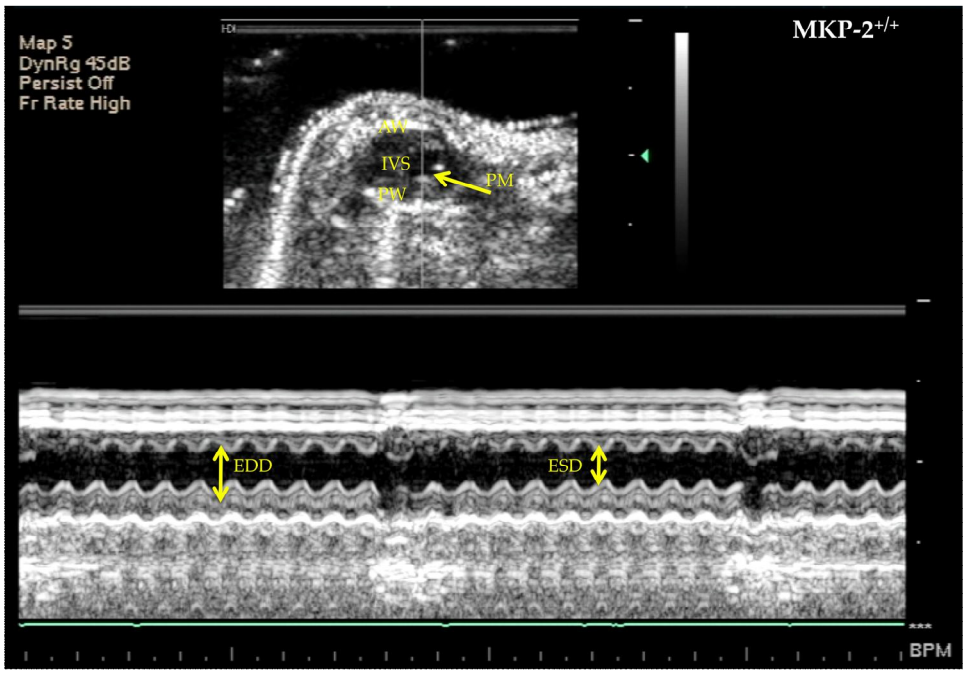

B

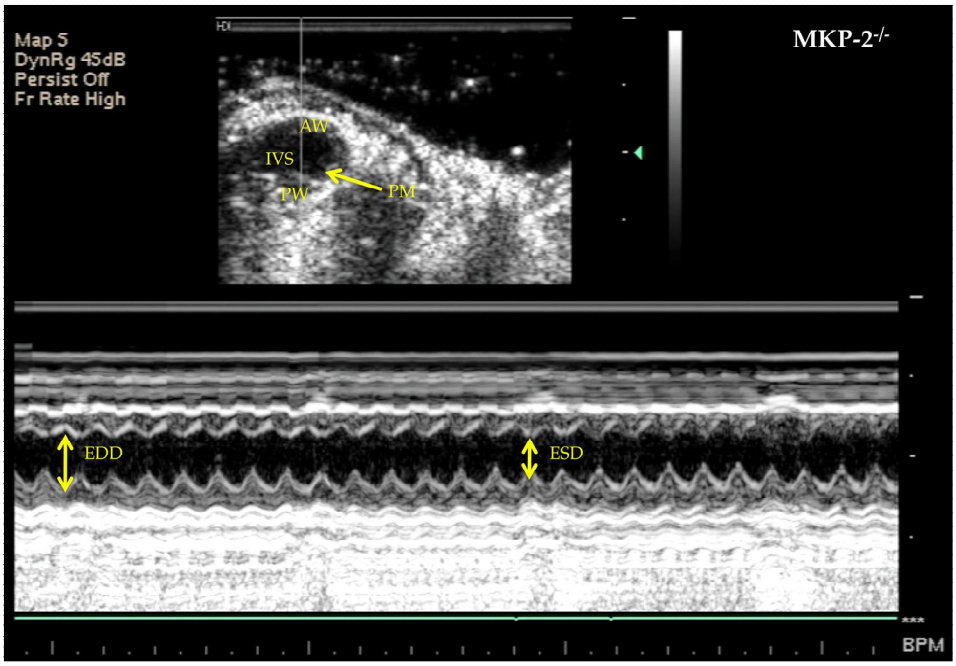

Figure: 4.12: Representative echocardiography of MKP-2$^{+/+}$ and MKP-2$^{-/-}$ mice at 8-10 weeks of age. Panel A, MKP-2$^{+/+}$ and panel B MKP-2$^{-/-}$; Headed arrows indicates PM, papillary muscle; AW, anterior wall of left ventricle; EDD, end-diastolic diameter; ESD, end-systolic diameter; IVS, inter-ventricular septum; PM, papillary muscle; PW, posterior wall of left ventricle. The parameters were measured on the M-mode tracings and averaged from three cardiac cycles.

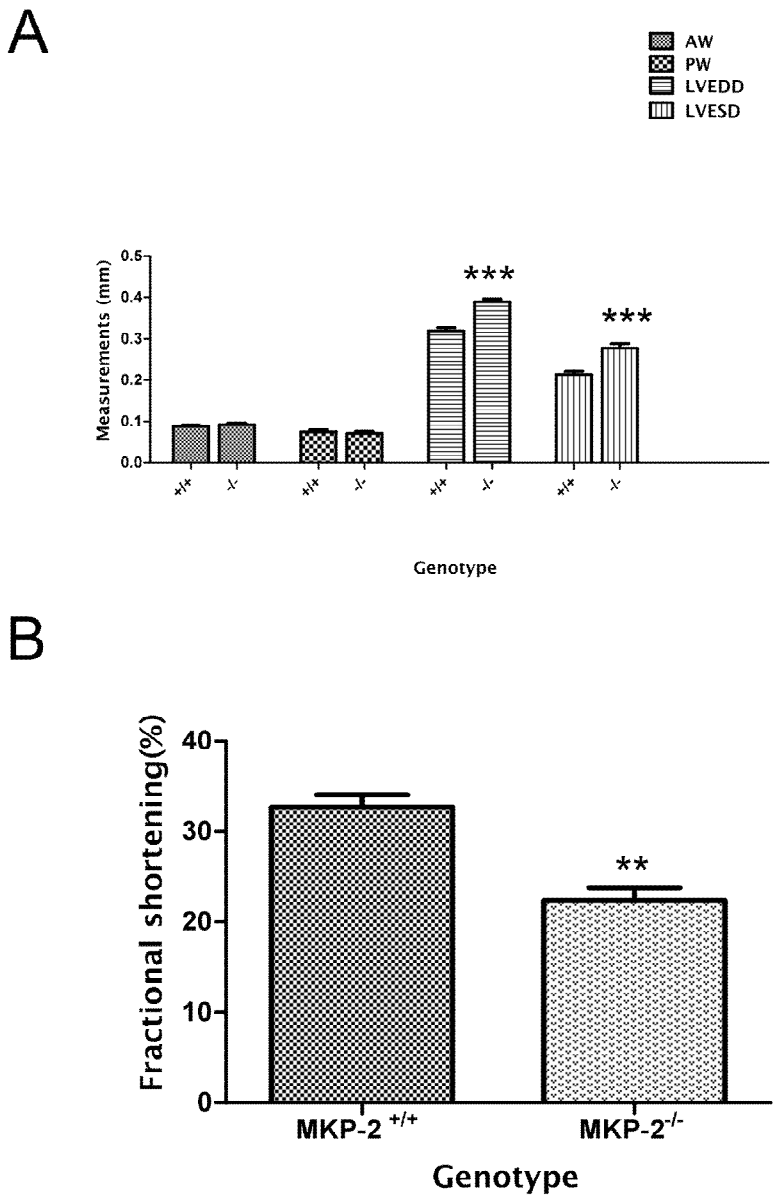

Figure 4.13: Cardiac anatomic and functional parameters, as assessed by echocardiography in MKP-2$^{+/+}$ and MKP-2$^{-/-}$ mice at 8-10 week old. In A, left ventricular dimensions in systole & diastole, in B FS. Quantified data was analysed using two-way ANOVA. Post hoc test was by Bonferroni's multiple comparison tests, statistical significant is shown in relation to MKP-2$^{-/-}$, **p<0.05, ***P<0.001). The unpaired Student's t-test was used for comparison of FS, FS = [(LVED - LVES) / LVED] x100 (%). (n=10). See table 4.1.

4.11: Enhanced proliferation in MTAB cardiac fibroblasts

Having established changes in fibroblast proliferation *in vitro* and basal cardiac function *in vivo* following MKP-2 deletion, experiments sought to establish a correlation in MTAB model. First of all proliferation was examined in CFs derived from hearts subjected to MTAB. For this purpose cell counting using haematoxylin staining was used to directly measure cell number (see section 2.9). The data presented in figure 4.14 demonstrated that in MTAB CF over a 72 h period, Ang II caused an approximately 1.6 fold increase in cell number which was evident after 72 h (see figure 4.14, panel A), in comparison to control (cell number per field; MKP-$2^{+/+}$ = 41.83 ± 2.3x10^5, MTAB = 63.93 ± 5.3x10^5 $p<0.01$). Initial proliferation assay in sham operated animals showed no significant difference in comparison to wild type (not shown). This data suggested that CF phenotype could be altered in MTAB hearts.

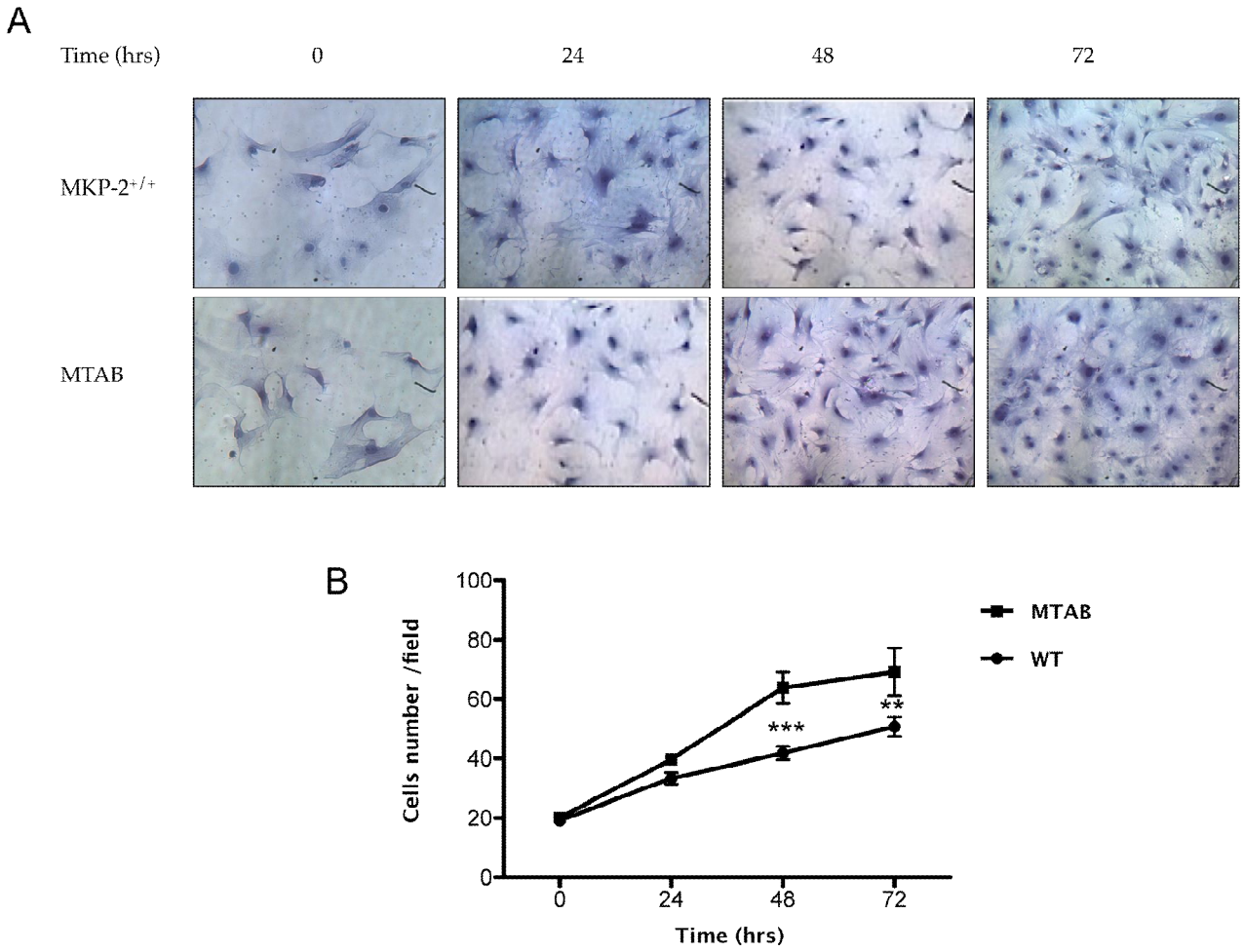

Figure 4.14: Increased CF proliferation in MTAB model

CF were serum starved for 24 h in serum free media and then stimulated for either 24, 48, 72 h with Ang II (1 μM). Cultures were washed with PBS, and analysed using haematoxylin (panel A). The number of cells was determined from 10 random fields per each coverslip (panel B) (see section 2.9). Quantified data was analysed using two-way ANOVA. Post hoc test was by Bonferroni's multiple comparison tests, statistical significant is shown in relation to MKP-$2^{-/-}$, **p<0.01, ***P<0.001). Control values (0 h): cell number per field; MKP-$2^{+/+}$ = 19.23± 0.5x10^5, MTAB= 20.20 ± 0.6x10^5. Each value represents the mean±s.e.m. performed in triplicate from 3 separate experiments (n=3).

4.12: MKP-2 protein and p-ERK expression from sham and MTAB preparations

Having examined cell growth in CF derived from MTAB models this was correlated with the expression of MKP-2 protein in the sham and 4-week (MTAB) left ventricular whole tissue homogenate preparations using quantitative western blotting. The expression of protein levels of MKP-2 and p-ERK were quantified in both sham/control and MTAB left ventricular whole tissue homogenate preparations using quantitative Western blotting. At first, total protein amount in each homogenate preparation was determined using Bradford protein assay as described in section 2.14. GAPDH was used as an internal standard to normalize quantified values and identified on the same gel as other proteins. All sham and MTAB left ventricular hypertrophy data for the proteins were then expressed as a ratio to GAPDH.

The data presented in figure 4.15, (panels A & B) showed a representative Western blot demonstrating that MKP-2 protein expression was significantly down-regulated in the 4-week MTAB compared with sham-operated animals (fold expression, MTAB = 0.32 ± 0.19, Sham = 1.20 ± 0.61, $P<0.05$). This data suggests that MKP-2 protein expression was decreased in MTAB.

Also the expression of ERK phosphorylation in the sham and 4-week (MTAB) left ventricular hypertrophy preparations were investigated using quantitative western blotting. Heart homogenates were prepared as described in section 2.13. The data presented in figure 4.15, panels A & C showed that ERK phosphorylation was increased in MTAB preparations in comparison with sham (fold expression, MTAB = 1.48 ± 0.85, Sham = 1.35 ± 0.25). However, this difference was not statistically significant. This result demonstrates that ERK activation was comparable in MTAB and sham heart homogenates.

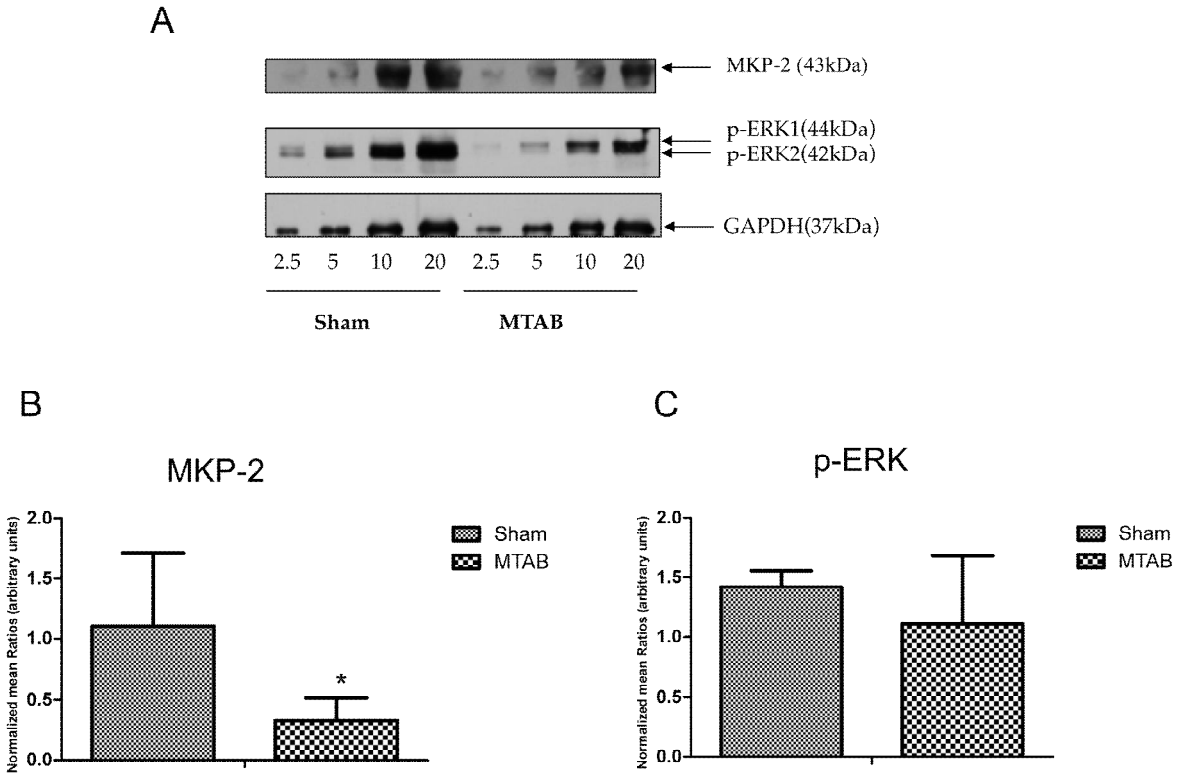

Figure 4.15: MKP-2 protein and p-ERK expression from sham and MTAB preparations.

Relative expression of MKP-2 and p-ERK, and GAPDH with similar protein loads for both sham-operated and MTAB preparations is outlined in panel A, and panel B & C illustrates quantification by densitometry and expressed as mean±s.e.m. Statistical analysis was by one-way ANOVA, post hoc test by Dunnett's test, *$p<0.05$ in comparison with sham group. All quantitative data have been normalized to GAPDH. (n=7).

4.13: DISCUSSION

As discussed in the previous chapter, the cellular function of this MKP family member is not well described especially in the heart. In this chapter a novel MAP kinase phosphatase-2 KO mouse was used to assess the consequences of deletion at the level of MAPK regulation, in relation to proliferation and also to cardiac phenotype and function *in vivo.* This chapter utilized a unique cell type, the adult cardiac fibroblast, that has recently emerged (Brown *et al*., 2005) to play an important role in cardiac development and contributes to cardiac structure and function, and during myocardial remodeling.

Similar to experiments conducted with MEFs (see chapter 3), in CFs the induction of MKP-2 was observed 2 h after serum and PDGF stimulation. However, Ang II could not induce MKP-2 protein expression (figures 4.2 & 4.3). This lack of effect of Ang II contrasts with one study which reported that MKP-1 protein was induced after 30 min in response to Ang II in rat neonatal cardiac myocytes (Liu *et al*., 2000). Similarly, another study demonstrated that in rat neonatal myocytes, MKP-1 gene expression was observed after 10 min in response to Ang II (10^{-6} M) while MKP-1 mRNA levels reached maximum after 30 min and decreased thereafter (Hiroi *et al*., 2001). Also it has been demonstrated that MKP-1 induction was observed 30-60 min in response to LPS in rat CF (Stawowy *et al*., 2003). These studies further highlight the fact that MKPs 1 and 2 have distinct mechanisms of induction which are partly agonist dependent. Results from chapter 3 indicated that MKP-2 induction was dependent upon prior ERK activation and it is notable that the magnitude of Ang II induced ERK phosphorylation in CFs was considerably lower than either PGDF or serum or in response to Ang II in other cell types. Since this the first study to assess the induction of MKP-2 in CFs it is unclear as to the mechanisms which may contribute to full expression. This data nevertheless helps to establish a potential role for MKP-2 in cardiac function.

In comparison to MKP-2, the role of MKP-1 in the regulation of cardiovascular disease has been examined more extensively. It was reported that ANP induced the expression of MKP-1 in cardiac myocytes and when MKP-1 was over-expressed in these cells it attenuated Ang II or ET-1 induced hypertrophic responses (Hayashi *et al*., 2004). This suggests that the hypertrophic growth of the myocardium is partly mediated by MKP-1 induction. Using immunostaining it has been shown that enhanced endothelial expression of MKP-1 inhibited proinflammatory activation at locations that were resistant to atherosclerosis (Zakkar *et al*., 2008). Dexamethasone administration following induction of ischaemia / reperfusion injury in rats was found to considerably improve post-ischaemic functional recovery and decreased infarct size in comparison to control and this was associated with increased MKP-1 protein expression (Fan *et al*., 2009). More recently it was reported that endothelial cells derived from MKP-1 KO mice were more prone to atherosclerotic lesions in compared with wild type (Choudhury *et al*., 2010). Similarly, it has been demonstrated that deficiency of MKP-1 protects ApoE KO mice against atherosclerosis (Shen *et al*., 2010). These studies have clearly established the protective role of MKP-1 in atherosclerosis. Studies about other MKPs are scanty, however, one study reported that in response to ischaemic post conditioning in leptin deficient obese mice, MKP-3 protein levels were decreased (Bouhidel *et al*., 2008).

These and other studies primarily focus on either cardiac myocytes or endothelial cells in relation to cardiac dysfunction. However, fibroblasts are now recognized to be directly involved in cardiac function. Proliferation is an important feature of CF activation and a key contributing aspect to the collective fibrotic potential of CFs. Again this chapter has established another novel finding that proliferation of CF derived from MKP-2 deletion mice was significantly inhibited relative to wild type, suggesting that MKP-2 is a crucial part of the intracellular homeostasis that regulates fibroblast growth (figures

4.8 & 4.9). Presumably this was due to an effect on G_2/M phase transition although lack of time did not allow this possibility to be examined.

Coupling of CFs and cardiac myocytes is essential for the progression of cardiac remodeling, therefore a decrease in the growth rate of CFs could have a profound effect on the function of cardiac myocytes and consequently on the whole heart. However, uninhibited CF proliferation is a characteristic of pathophysiological myocardial hypertrophy which could lead to excessive secretion of ECM and eventually to interstitial fibrosis (Brown *et al*., 2005). Similarly, it has been reported that treatment of CF with resveratrol inihibited their proliferation and differentiation and could decrease ECM secretion in the heart (Olson *et al*., 2005). More recently one study examined the temporal alterations in CF activity in response to increased cardiovascular load. More recently Stewart Jr. *et al*., 2010 demonstrated that rapid and active changes in CF phenotype contributed to the development of cardiac pathology. Cardiac hypertrophy which is initially beneficial, causes an increase in myocyte size and work output, which enhances cardiac output (Nadal-Ginard *et al*., 2003). In contrast when cardiac hypertrophy progresses in response to stress stimuli it is assosciated with myocyte loss, interstial fibrosis, and collagen deposition which leads to decreased compliance and increased risk of heart failure (Orr and Helmke, 2006). These findings could be linked to MKPs; silencing MKP-1 protein expression reversed the inhibitory effects of LPS on Ang II induced DNA synthesis and migration of rat CF (Stawowy *et al*., 2003), whilst proliferation of VSMC was inhibited by MKP-1 through inactivation of MAPKs (Li *et al*., 1999). Therefore the data from this current study suggests that MKP-2 could be beneficial to the overall myocardial remodeling process.

Considering that MKP-2 deletion impairs CFs proliferation and the importance of this cell type to overall heart function it would be interesting to see whether over-expression of Adv. MKP-2 in a gain of function study could reverse this growth deficit as demonstrated in MEFs. If this was the case it

could be an important milestone in elucidating the contribution of these cells in heart function. Modified CFs could be reintroduced into the failing heart in an attempt to restore function. However, further work needs to be conducted linking MKP-2 to other aspects of CF function. In particular, the expression and function of receptors such as gp 130/IL-6R which function to modulate not only cellular proliferation directly but also ECM turnover via decreased collagen synthesis and increased MMP expression (Fredj *et al*., 2005).

In this chapter, studies were conducted to assess the effect of MKP-2 deletion not only on CF function but also in cardiac myocytes. However, routine preparation of these cultures was not successful and this is a general limitation in this field. Studies often use neonatal cardiac myocytes from rat however, this model is not necessarily representative of adult function (Takeishi *et al*., 2001). Therefore it was decided to directly assess cardiac function *in vivo* and correlate this with the observations made in CFs.

Although there was a phenotypic difference observed in the heart between MKP-$2^{-/-}$ and wild type, analysis of heart weight normalized to body weight showed no significant difference between wild type and MKP-2 deletion mice. Whether this observation is pathological remained to be established, since the data from echocardiography revealed a significant difference in FS between these hearts. However, it has been reported that hearts derived from MKP-3 KO mice were significantly larger in comparison to wild type (Maillet *et al*., 2008).

Initial analysis of MKP-$2^{-/-}$ mice using echocardiography demonstrated that loss of MKP-2 significantly enhanced LVEDD and LVESD in comparison with the wild type. These results suggest that these mice exhibit some signs of cardiac abnormality and importantly, decreased FS which is a reflection of impaired ventricular contractility (Moreire *et al*., 2006) (figures 4.12 & 4.13). However, further work need to be carried out to establish whether it is

pathological or not. Assessment of some hypertrophic markers such as ANF, β-MHC, and SkM α-actin and cardiac myocyte cross-sectional area would be essential. Furthermore, assessment of cardiac function in these mice at different ages would give more in-depth analysis of these observations. Nevertheless, it is important to note that cardiac enlargement does not automatically mean disease, given that conditioned athletes can develop cardiac enlargement and enhanced myocardial mass and yet with no deleterious consequences (Dorn and Force, 2005, Lawan *et al*., 2006). Cardiac hypertrophy is initially a beneficial compensatory response that maintains cardiac output, however, sustained hypertrophy is associated with increased occurrence of cardiovascular disease. In fact recently it has been demonstrated that in a murine model of sepsis, ventricular dilation is associated with enhanced stroke volume and cardiac output which was linked with improved cardiovascular performance and survival (Cavazzoni *et al*., 2010).

Interestingly, Ang II had a significant effect on MTAB CF proliferation which is an indication of phenotype modification i.e. differentiation from fibroblast to myofibroblast in response to cardiac hypertrophy (figure 4.14). It has been reported that Ang II could induce proliferation of cardiac myofibroblast from sham hearts or the non-infarcted zone of myocardial infarction rat hearts, while myofibroblast obtained from the infarct zone exhibited a hypertrophic response (Staufenberger *et al*., 2001). These results demonstrate that Ang II acted as a mitogen in sham operated and non-infarct myofibroblasts and stimulated hypertrophy in infarct myofibroblasts. Further experiments which time did not allow would have been to establish whether increased proliferation of CFs following MTAB was a consistent phenomenon and importantly, whether it was associated with an increase in MKP-2 expression as this would be expected to enhance proliferation (see chapter 3)

Few studies have demonstrated the expression of MKPs in animal models of cardiac hypertrophy especially MTAB. However, some studies have demonstrated the expression of MKP-1 and MKP-2 in human tissues. In addition, studies examining the expression of MKP-1 and MKP-2 in cardiac hypertrophy or heart failure have been contradictory. Some authors reported increased MKP-1 and MKP-2 expression in failing human hearts (Communal *et al*., 2002), while others demonstrated decreased expression of MKP-1 (Dong *et al*., 2006). Furthermore, it was also found that cardiac MKP-1 and MKP-2 were not altered in response to aortic and pulmonary artery banding in fetal ovine heart whereas MKP-3 protein levels were significantly enhanced (Olson *et al*, 2006). Using whole heart homogenates prepared from mouse left ventricular tissue, the data in this present study demonstrated significant down-regulation of MKP-2 protein expression in the 4-week MTAB model which corresponds to the compensatory phase of cardiac remodeling during the development of myocardial hypertrophy. Whether this expression level would be the same or altered as the heart progressed to a decompensated state and into heart failure remains to be established. It would be interesting to investigate the effect of aortic banding on MKP-2 deletion mice. Similarly, studies examining the expression of MAPKs in cardiac hypertrophy have been conflicting. Some authors have demonstrated increased ERK expression (Communal *et al*., 2002; Dong *et al*, 2006), while others reported that ERK was not altered (Olson *et al*, 2006). The activity of ERK in left ventricular homogenates was decreased 24 h in response to aortic banding in rats but returned to normal after 2 weeks (Roussel *et al*., 2008). However, in this current study the protein level of ERK was similar in the 4-week MTAB models and sham-operated animals. It is possible that with more analysis of samples the difference could be significant, however because the homogenates consist primarily of myoctes it is difficult to establish if the increase in MKP-2 expression is related to CFs proliferation or an aspect of myocyte function during disease.

In conclusion this chapter has demonstrated for the first time the induction of MKP-2 in adult CF in reponse to serum and PDGF, decreased growth rate in CF derived from MKP-2 KO mice, decreased FS in MKP-2 deletion mice and decreased MKP-2 protein expression in MTAB model. In addtion it also showed that adult CF proliferation was enhanced in MTAB model. These novel data have demonstrated that MKP-2 contribute to cardiac phenotype and function and suggests that MKP-2 could play a protective role in response to heart injury.

CHAPTER 5
GENERAL DISCUSSION

In this thesis the characteristics of a novel DUSP-4 (MKP-2) knock out mouse were examined primarily at the level of the fibroblasts but also in respect to cardiac function. Novel data was generated in relation to changes in proliferation and cell cycle progression and preliminary observations were made in relation to basic cardiac function. However, a number of key questions remain to be answered and the implications of the findings of this thesis require to be put into context of the field as whole.

A key question relates to the function of MKP-2 *in vivo* in the context of kinase signalling. A number of studies suggest specificity of MKP-2 for JNK and ERK in particular the former (Cadalbert *et al*., 2005; Sloss *et al*., 2005). However, in this thesis MKP-2 deletion did not give rise to any consistent changes in kinase signalling. Whilst this might be unexpected it is recognized that MKPs have overlapping specificities and therefore redundancy may be a feature. One possibility to explain these results, not examined in this thesis, was the potential for deletion to affect the retention of phosphorylated MAP kinase within the nucleus which has been found to be a feature of the MKPs (Keyse, 2008). A second possibility is that MKP may have functions other than to dephosphorylate MAPKs. Kinney *et al*., 2009 has demonstrated recently that MKP-1 is able to dephosphorylate histone H3 although this was not a feature of MKP-2 in the cell type examined.

A related issue concerns compensation by other MKPs. Recently it has been demonstrated that MKP-1 induction was increased in MKP-$2^{-/-}$ bone marrow-derived macrophages in response to LPS and this results increased ERK signalling (Cornell *et al*., 2010). So further work would be needed to investigate the level of endogenous MKP-1 expression in MKP-$2^{-/-}$ fibroblasts in order to establish whether MKP-1 levels are increased in these cells to compensate for the loss of MKP-2 even though the compensation could be

cell, tissue or organ dependent, meaning that what was described above may not be the same in fibroblasts.

However, in respect of whether kinase signalling is not affected or if compensatory expression of MKP-1 is a feature it does not explain the striking phenotype at the level of fibroblast proliferation and this is the first study to link a deficit in cell cycle progression directly with MKP-2 loss using the KO model. It is well known that inhibition of cell growth is a feature of cellular senescence. Further study is required to establish the role of MKP-2 in cellular senescence in fibroblasts, since some studies have recently demonstrated this function as mentioned in section 3.2.14. The decrease in fibroblast proliferation observed in this current study was associated with enhanced G_2/M phase transition. To further investigate the role of MKP-2 in G_2/M phase transition possibly nocodazole, which is a mitotic inhibitor could be used to block the cells in mitosis and stain for MKP-2 or topotecan, which is a topoisomerase I inhibitor to induce G_2 arrest and assess the expression of cyclin B1 and cdc-2 kinase. Additional experiments could look at directly at mitosis itself since in some instances MKP deletion gave rise to binucleated cells (not shown).

Another area which requires further work relates to the promoter system involved in MKP-2 expression. Studies in this thesis indicate the presence of binding sites which could be regulated through the ERK MAPK pathway. However, for human MKP-2 the promoter region has not been well characterized and it is unclear as to what regulatory binding sites are present. Nevertheless, this may be important in cancer since a recent study showed that hypermethylation of the MKP-2 promoter was found to occur more frequently in diffuse or anaplastic astrocytomas and secondary glioblastomas relative to primary glioblastomas (Waha *et al*., 2010). The authors further demonstrated that promoter hypermethylation correlated with reduced expression of MKP-2 mRNA and protein. Related to this finding, a motif

(CTGGCGCCAG) in the MKP-2 promoter was found to be a new binding site for p53 to stimulate the MKP-2 gene (Shen *et al*., 2006). Furthermore, the transcription factor E2F-1 which mediates cell death and suppresses tumorgenesis, (sp) was also found to be physically associated with the MKP-2 promoter and to trans-activate the MKP-2 gene (Wang *et al*., 2007).

At present there is substantial amount of information about the biochemical structure of MKPs however, more work is needed to fully determine the specific MAPK substrates which individual members deactivate in order to exert their physiological functions *in vitro* and *in vivo.* For MKP-2 this is important since whilst it binds to JNK it might not require interaction with the KIM domain to do so. Indeed studies in the laboratory using peptide array show the potential of multiple sites within MKP-2 which facilitate binding to JNK (Cadalbert personal communication). Such information is crucial in the targeting of MKP-2 as a potential novel therapy in cancer treatment. Using a chemical screen in zebrafish, it has recently been demonstrated that (E)-2-benzydilene-3-(cyclohexilamino)-2,3-dihydro-1H-inden-1-one (BCI), an allosteric inhibitor of DUSP6 (MKP-3), prevents the catalytic activation of the phosphatase induced by substrate binding and regulates FGF mediated embryogenesis (Molina *et al*., 2009). Though the authors reported that BCI is not very specific, future work focused on the development of MKP inhibitors may be useful in a number of disease conditions. Specific inhibitors would also help in clarifying the physiological functions of each DUSP family member.

Considering the complex interaction between kinases and MKPs, which involve negative feedback regulation and crosstalk within the cascade and with other signalling pathways and coupled with the evidence that phosphatases have a more prominent effect than kinases on the rate and duration of signaling, whereas kinases mainly regulate signal amplitude (Heinrich *et al*., 2002), future work employing computational modelling of

these signalling pathways will go a long way in helping to interpret the data generated regarding their exact physiological role. Furthermore, using a combination of variety of model systems and techniques such as tissue specific knockouts, RNA interference, adenoviral infection (Al-Mutairi *et al*., 2010) or conditional over-expression will assist future investigations.

Considering the induction of MKP-2 and the kinetics of MAPK signaling, the magnitude of MKP-2 induction is slightly different considering all the agonists used in the two cell types. PMA and PDGF gave a stronger signal of MKP-2 induction in comparison to serum in MEFs. However, AngII could not induce MKP-2 in CFs (see section 3.2.2 & 4.4). The kinetics of ERK phosphorylation in response to serum, PMA and PDGF were similar over the time course considered in MEFs. However, serum gave a stronger JNK phosphorylation compared with PMA which gave a weak activation in MEFs Robinson *et al*., 2001, reported that the MAPK signalling is agonist and cell type dependent because different pattern of JNK phosphorylation kinetics was observed in EAhy926 endothelial cells. However, PDGF demonstrated an enhanced ERK signalling in the MKP-$2^{-/-}$ MEFs which was not observed in MKP-$2^{-/-}$ CFs. This could be due to the fact that MKP-2 induction was dependent on prior ERK activation in wild type MEFs. Another possibility is that other phosphatases could be involved in the dephosphorylation of these kinases (Wu *et al*., 2006). Although not much difference was observed in JNK signalling in both cell types with serum and PDGF, however, an enhanced JNK signalling in MKP-$2^{-/-}$ MEFs was observed compared with wild type when anisomycin was used. Similar, findings were observed in MEFs in derived from MKP-1 deletion mice (Wu and Bennett, 2005), although these authors did not examine CF in their studies. Also anisomycin is a stress agent which is expected to cause strong activation of the stress kinases compared to growth factors (Shin *et al*., 2006).

The response of the cells to serum induced proliferation was slightly different. The growth characteristics of the wild type cells in both MEFs and adult CFs was similar (see section 3.2.4 & 4.6). However, considering the deficit in growth in cells derived from the MKP-2 deletion mice, the MKP-2$^{-/-}$ adult CFs grow much better particularly over longer period of time (72 h) compared to the MKP-2$^{-/-}$ MEFs. It is possible that the amount of serum used (10%) could be partly responsible since serum derived from animal sources contain some endotoxin (Even *et al*., 2006) which could partly interfere with the growth of these cells in culture. 5% FCS could probably have produced slightly different pattern of proliferation in these cells and also the use of other agonists such as PDGF or FGF. It is also possible that the MKP-2$^{-/-}$ MEFs or CFs are more sensitive to this effect of serum compared to the wild type cells. It has been demonstrated that bone marrow derived dendritic cells behave differently with respect to survival, differentiation, activation and cytokine profile under different serum conditions (Sung and Betty, 2007). It has been shown that ammonia is toxic and inhibitory to mammalian cell cultures (Schneider *et al*., 1996), and the primary origin of ammonia in cell cultures is glutamine contained in the media. It is likely that the cells derived from MKP-2$^{-/-}$ mice are more susceptible to this effect of ammonia in comparison to the wild type which could be attributed to the lack of MKP-2 protein. Similarly, given that the deletion of MKP-2 inhibits the growth of these cells; the activity of MKP-2$^{-/-}$ MEFs or CFs could further be reduced in the presence of ammonia compared to the wild type cells, and also the adult CFs could be more resistant to this effect.

The idea that fibrosis and inflammation play a part in cardiac remodelling in response to pathological insult and the acknowledgement that CF regulate these processes is well established. So studies that involve CF detail understanding of their multiple function in cardiac physiology and disease is indispensable in increasing understanding of the central mechanisms of cells comprising the heart, and may lead to targeted and modified therapies for

diseases such as heart failure. Further work that will elucidate the signalling mechanisms that regulate CF phenotype in the normal and pathological myocardium *in vivo* would be valuable. For MKP-2 this would involve the generation of a CFs specific MKP-2 deletion mouse, similar models have been established for other key signalling proteins such as CF specific deletion (Takeda *et al*., 2010). The findings in this present study such as decreased FS in MKP-2 deletion mice signifies a hypertrophic phenotype and so decreased MKP-2 protein expression in MTAB model suggests that MKP-2 could play a protective function in response to cardiac hypertrophy. In this context future studies utilizing MTAB in MKP-2 KO mice models would immediately identify a role for MKP-2 in cardiac hypertrophy.

Interest in cell therapy as a means of regeneration or repair of the damaged heart is also currently under investigation, so future work that will emphasize the use of adult CF as opposed to neonatal cells should be encouraged. This will also help in gene therapy studies designed at targeting CF. Recently there has been interest in small non-coding microRNAs (miRNAs) with regard to their dysregulation in different disease conditions, including heart disease (Sayed *et al*., 2007). Some of these studies have demonstrated that miRNAs are expressed in CF and may signify future therapeutic targets for the management of cardiac hypertrophy and heart failure. It would be interesting to determine if such miRNAs can regulate the expression of MKP-2 in the heart.

CHAPTER 6
REFERENCES

Abu-Sitta S, Shalaby A, Abdel-Mottaleb A. (2003). Physiology in medical practice. *Lecture notes*. El Nagah, Helmyet El Zaitoun Sq. Cairo.

Adams RH, Porras A, Alonso G, Jones M, Vintersten K, Panelli S, Valladares A, Perez L, Klein R, Nebreda AR. (2000). Essential role of p38 [alpha] MAP kinase in placental but not embryonic cardiovascular development. *Mol. Cell*. **6**: 109–116.

Al-Mutairi M, Al-Harthi S, Cadalbert L, Plevin R. (2010). Over-expression of mitogen-activated protein kinase phosphatase-2 enhances adhesion molecule expression and protects against apoptosis in human endothelial cells. *Br J Pharmacol.* **161**: 782-98.

Alessi DR, Cuenda A, Cohen P, Dudley DT, Saltiel AR. (1995). PD 098059 Is a Specific Inhibitor of the Acivation of Mitogen-activated Protein Kinase Kinase *in vitro* and *in vivo. J Biol Chem*. **270**: 27489-27494.

Alessi DR, Smythe C, Keyse SM. (1993). The human CL100 gene encodes a tyr / thr-protein phosphatase which potently and specifically inactivates MAP kinase and suppresses its activation by oncogenic ras in xenopus oocyte extracts. *Oncogene.* **8**: 2015-20.

Alonso A, Sasin J, Bottini N, Friedberg I, Friedberg I, Osterman A, Godzik A, Hunter T, Dixon J, Mustelin T. (2004). Protein tyrosine phosphatases in the human genome. *Cell*. **117**: 699–711.

Andersen JN, Jansen PG, Echwald SM, Mortensen OH, Fukuda T, Del Vecchio R, Tonks NK, Moller NP. (2004). A genomic perspective on protein tyrosine phosphatases: gene structure, pseudogenes, and genetic disease linkage. *FASEB J.* **18**: 8–30.

Antonetti DA, Algenstaedt P, Kahn CR. (1996). Insulin receptor substrate 1 binds two novel splice variants of the regulatory subunit of phosphatidylinositol 3-kinase in muscle and brain. *Mol Cell Biol*. **16**: 2195–203.

Arnaout MA, Goodman SL, Xiong JP. (2007). Structure and mechanics of integrin-based cell adhesion. *Curr. Opin. Cell Biol.* 19: 495–507.

Baines CP, Molkentin JD. (2005). STRESS signaling pathways that modulate cardiac myocyte apoptosis. *J Mol Cell Cardiol*. **38**:47–62.

Bang YJ, Kwon JH, Kang SH, Kim JW, Yang YC. (1998). Increased MAPK activity and MKP-1 overexpression in human gastric adenocarcinoma. *Biochem Biophys Res Commun*. **250**: 43–47.

Banerjee I, Yekkala K, Borg TK, Baudino TA. (2006). Dynamic interactions between myocytes, fibroblasts, and extracellular matrix. Ann. NY. Acad. Sci. 1080: 76–84.

Barancik M, Htun P, Maeno Y, Zimmermann R, Shaper W. (1997). Differential regulation of distinct protein kinase cascades by ischemia and ischemia / reperfusion in porcine myocardium. *Circulation.* **96**: (abstr) I-252.

Barbosa ME, Alenina N, Bader M. (2005). Induction and analysis of cardiac hypertrophy in transgenic animal models. *Methods Mol Med.* **112**: 339-52.

Barr RK, Kendrick TS, Bogoyevitch MA. (2002). Identification of the critical features of a small peptide inhibitor of JNK activity. *J Biol Chem*. **277**: 10987–10997.

Baserga, R. (1985). The biology of cell reproduction. *Harvard University Press*: Cambridge, Mass., USA; London, England.

Baudino TA, Carver W, Giles W, Borg TK. (2006). Cardiac fibroblasts: friend or foe? *Am J Physiol Heart Circ Physiol*. **291**: H1015–H1026.

Beardmore VA, Hinton HJ, Eftychi C, Apostolaki M, Armaka M, Darragh J, McIlrath J, Carr JM, Armit LJ, Clacher C, Malone L, Kollias G, Arthur JSC. (2005). Generation and characterization of p38beta (MAPK11) gene-targeted mice. *Mol. Cell. Biol.* **25**: 10454–10464.

Behrens A, Sibilia M, Wagner EF. (1999). Amino-terminal phosphorylation of c-Jun regulates stress-induced apoptosis and cellular proliferation. *Nat Genet.* **21**: 326–329.

Bers DM, Guo T. (2005). Calcium Signaling in Cardiac Ventricular Myocytes. *Ann. N.Y. Acad. Sci.* **1047**: 86–98.

Bogoyevitch MA, Boehm I, Oakley A, Ketterman AJ, Barr RK. (2004). Targeting the JNK MAPK cascade for inhibition: basic science and therapeutic potential. *Biochim Biophys Acta.* 1**697**: 89–101.

Bogoyevitch MA, Court NW. (2004). Counting on mitogen-activated protein kinases– ERKs 3, 4, 5, 6, 7 and 8. *Cell Signal*. **16**: 1345–1354.

Bogoyevitch MA, Gillespie-Brown J, Ketterman AJ, Fuller SJ, Ben-Levy R, Ashworth A, Marshall CJ, Sugden PH. (1996). Stimulation of the stress-activated mitogen-activated protein kinase subfamilies in perfused heart. p38/RK mitogen-activated protein kinases and c-Jun N-terminal kinases are activated by ischemia/reperfusion. *Circ Res.* **79**: 162-73.

Bogoyevitch MA, Glennon PE, Andersson MB, Clerk A, Lazou A, Marshall CJ, Parker PJ, Sugden PH. (1994). Endothelin-I and fibroblast growth factors stimulate the mitogen-activated protein kinase signaling cascade in cardiac myocytes. The potential role of the cascade in the integration of two signaling pathways leading to myocyte hypertrophy. *J Biol Chem*. **269**: 1110-1119.

Bogoyevitch MA, Kobe B. (2006). Uses for JNK: the many and varied substrates of the c-Jun N-terminal kinases. *Microbiol Mol Biol Rev.* **70**:1061–1095.

Booz GW, Dostal DE, Singer HA, Baker KM. (1994). Involvement of protein kianse C and $Ca2^{+/+}$ in angiotensin II-induced mitogenesis of cardiac fibroblasts. *Am J Physio*. **1267**: C1308-C1318.

Booz GW, Taher MM, Baker KM, Singer HA. (1994). Angiotensin II induces phosphatidic acid formation in neonatal rat cardiac fibroblasts: evaluation of the roles of phospholipases C and D. *Mol Cell Biochem* **141**: 135-43.

Boron WF, Boulpaep EL. (2005). Chapter 21: The Heart As a Pump, *Medical Physiology*, updated Edition, 508-533.

Bost F, Aouadi M, Caron L, Even P, Belmonte N, Prot M, Dani C, Hofman P, Pages G, Pouyssegur J, Le Y, Binetruy MB. (2005). The extracellular signal-regulated kinase isoform ERK1 is specifically required for *in vitro* and *in vivo* adipogenesis. *Diabetes.* **54**: 402–411.

Boulton TG, Nye SH, Robbins DJ, Ip NY, Radziejewska E, Morgenbesser SD, DePinho RA, Panayotatos N, Cobb MH, Yanco-poulos GD. (1990). ERKs: a family of protein-serine/threonine kinases that are activated and tyrosine phosphorylated in response to insulin and NGF. *Cell*. **65**: 663– 675.

Boulton TG, Yancopoulos GD, Gregory JS, Slaughter C, Moomaw C, Hsu J, Cobb MH. (1991). An insulin-stimulated protein kinase similar to yeast kinases involved in cell cycle control. *Science*. **249**: 64–67.

Brancho D, Tanaka N, Jaeschke A, Ventura JJ, Kelkar N, Tanaka Y, Kyuuma M, Takeshita T, Flavell RA, and Davis RJ. (2003). Mechanism of p38 MAP kinase activation *in vivo*. *Genes Dev*. **17**: 1969–1978.

Braz JC, Bueno OF, Liang Q, Wilkins BJ, Dai YS, Parsons S, Braunwart J, Glascock BJ, Klevitsky R, Kimball TF, Hewett TE, Molkentin JD. (2003). Targeted inhibition of p38 MAPK promotes hypertrophic cardiomyopathy through upregulation of calcineurin-NFAT signaling. *J Clin invest.* **1**: 1475–1486.

Breathnach, R Chambon, P. (1981). Organisation and expression of eukaryotic split genes coding for proteins. *Annu Rev Biochem.* **50**: 349-386.

Brilla CG, Maisch B, Weber KT. (1992). Myocardial collagen matrix remodelling in arterial hypertension. *Eur Heart J.* **13**: 24–32.

Brondello J, Brunet A, Pouysse´gur J, McKenzie FR. (1977). The Dual Specificity Mitogen-activated Protein Kinase Phosphatase- 1 and -2 Are Induced by the p42/p44MAPK Cascade. *J Biol Chem.* **272**: 1368–1376.

Bronzwaer JG, Paulus WJ. (2005). Matrix, cytoskeleton, or myofilaments: which one to blame for diastolic left ventricular dysfunction? *Prog Cardiovasc Dis* **47**: 276 –284.

Brown RD, Ambler SK, Mitchell MD, Long CS. (2005). The cardiac fibroblast: therapeutic target in myocardial remodeling and failure. *Annu Rev Pharmacol Toxicol.* **45**: 657-87.

Bueno OF, De Windt LJ, Lim HW, Tymitz KM, Witt SA, Kimball TR, Molkentin JD. (2001). The dual-specificity phosphatase MKP-1 limits the cardiac hypertrophic response *in vitro* and *in vivo*. *Circ Res*. **19**: 88-96.

Bueno OF, De Windt LJ, Tymitz KM, Witt SA, Kimball TR, Klevitsky R. (2000). The MEK1-ERK1/2 signaling pathway promotes compensated cardiac hypertrophy in transgenic mice. *EMBO J.* **19**: 6341–50.

Bueno OF, Molkentin JD. (2002). Involement of extracellular signal-regulated kinases 1/2 in cardiac hypertrophy and cell death. *Circ Res.* **91**: 776–781.

Bursi F, Weston SA, Redfield MM, Jacobsen SJ, Pakhomov S, Nkomo VT, Meverden RA, Roger VL. (2006). Systolic and diastolic heart failure in the community. *JAMA. 296*: 2209–2216.

Cadalbert L, Sloss CM, Cameron P, Plevin R. (2005). Conditional expression of MAP kinase phosphatase-2 protects against genotoxic stress-induced apoptosis by binding and selective dephosphorylation of nuclear activated c-jun N-terminal kinase. *Cell Signal*. **17**: 1254–1264.

Cadalbert LC, Sloss CM, Cunningham MR, Al-Mutairi M, McIntire A, Shipley J, Plevin R. (2010). Differential regulation of MAP kinase activation by a novel splice variant of human MAP kinase phosphatase-2. *Cell Signal.* **3**: 357-65.

Camelliti P, Borg TK, Kohl P. (2005). Structural and functional characterization of cardiacfibroblasts. *Cardiovasc Res.* **65:** 40–51.

Camelliti P, Devlin GP, Matthews KG. (2004). Spatially and temporally distinct expression of fibroblast connexins after sheep ventricular infarction. *Cardiovasc Res.* **62**: 415–425.

Camelliti P, Green CR, Le Grice I. (2004). Fibroblast network in rabbit sinoatrial node: structural and functional identification of homogeneous and heterogeneous cell coupling. *Circ Res.* **94**: 828–835.

Camps M, Nicholas A, Gilleron C, Antonsson B, Muda M, Chabaert C, Bosschert U, Arkinstall S. (1998). Catalytic activation of the phosphatase MKP-3 by ERK2 mitogen-activated protein kinase. *Science.* **280**: 1262–1265.

Camps M, Nichols A, Arkinstall S. (2000). Dual specificity phosphatases: a gene family for control of MAP kinase function. *The FASEB Journal*. **14**: 6-16.

Canagarajah BJ, Khokhlatchev A, Cobb MH, Goldsmith EJ. (1997). Activation mechanism of the MAP kinase ERK2 by dual phosphorylation. *Cell*. **90**: 859–869.

Castelli M, Camps M, Gillieron C, Leroy D, Arkinstall S, Rommel C, Nichols A (2004). MAP kinase phosphatase 3 (MKP-3) interacts with and is phosphorylated by protein kinase CK2alpha. *J Biol Chem*. **279**: 44731–44739.

Cavazzoni SL, Guglielmi M, Parrillo JE, Walker T, Dellinger RP, Hollenberg SM. (2010). Ventricular dilation is associated with improved cardiovascular performance and survival in sepsis. *Chest.* **138**: 848-55.

Cefalu WT. (2006). Animal models of type 2 diabetes: Clinical presentation and pathophysiological relevance to the human condition. *ILAR J.* **47**: 186-198

Chang L, Karin M (2001): Mammalian MAP kinase signaling cascade. *Nature*. **410**: 37-40.

Charles CH, Abler AS, Lau LC. (1992). cDNA sequence of a growth factor-inducible immediate early gene and characterization of its encoded protein. *Oncogene.* **7**: 187-90.

Chaudhury H, Zakkar M, Boyle J, Cuhlmann S, van der Heiden K, Luong le A, Davis J, Platt A, Mason JC, Krams R, Haskard DO, Clark AR, Evans PC (2010). c-Jun N-terminal kinase primes endothelial cells at atheroprone sites for apoptosis. *Arterioscler Thromb Vasc Biol*. **30**: 546-53.

Chen C, Chang C, Liu H, Liao M, Chang C, Hsu J, Shih W. (2010). Apoptosis induction in befv-infected vero and mdbk cells through src-dependent jnk activation regulates caspase-3 and mitochondria pathways. *Vet Res*. **41**: 15.

Chen D, Mauvais-Jarvis F, Bluher M, Fisher SJ, Jozsi A, Goodyear LJ, Ueki K, Kahn. CR. (2004). p50alpha/p55alpha phosphoinositide 3-kinase knockout mice exhibit enhanced insulin sensitivity. *Mol Cell Biol.* **24**: 320–9.

Chen P, Hutter D, Yang X, Gorospe M, Davis RJ, Liu Y. (2001). Discordance between the binding affinity of mitogen-activated protein kinase subfamily members for MAP kinase phosphotase-2 and their ability to activate the phosphotase catalytically. *J Biol Chem.* **276**: 29440-29449.

Chen YR, Tan TH. (2000). The c-Jun N-terminal kinase pathway and apoptotic signaling. *Int J Oncol.* **16**: 651–662.

Cheng RL, Feng Z, Yong-yeon C, Faqing T, Tatyana Z, Wei-ya M, Ann MB.

Zigang D. (2006). Cell apoptosis: requirement of h2ax in DNA ladder formation but not for the activation of caspase-3. *Mol Cell*. **23**: 121–132.

Chi H, Barry SP, Roth RJ, Wu JJ, Jones EA, Bennett AM, Flavell RA. (2006). Dynamic regulation of pro- and anti-inflammatory cytokines by MAPK phosphatase 1 (MKP-1) in innate immune responses. *PNAS*. **103**: 2274–2279.

Chi H, Barry SP, Roth RJ, Wu JJ, Jones EA, Bennett AM, Flavell RA. (2006). Dynamic regulation of pro- and anti-inflammatory cytokines by MAPK phosphatase 1 (MKP-1) in innate immune responses. *PNAS.* **103**: 2274–2279.

Chiarugi P, Fiaschi T, Taddei ML, Talini D, Giannoni E, Raugei G, Ramponi G. (2001). Two vicinal cysteines confer a peculiar redox regulation to low molecular weight protein tyrosine phosphatase in response to platelet-derived growth factor receptor stimulation. *J Biol Chem.* 276: 33478-87.

Chiqueta M, Renedoa AS, Hubera F, Flu¨ckb M. (2003). How do fibroblasts translate mechanical signals into changes in extracellular matrix production? *Matrix Biology*. **22**: 73–80

Choi K-Y, Satterberg B, Lyons DM, Elion EA (1994). Ste5 tethers multiple protein kinases in the MAP kinase cascade required for mating in S. cerevisiae. *Cell*. **78**: 49 –512.

Choudhary R, Palm-Leis A, Scott RC 3rd, Guleria RS, Rachut E, Baker KM, Pan J. (2008). All-trans retinoic acid prevents development of cardiac remodeling in aortic banded rats by inhibiting the renin-angiotensin system. *Am J Physiol Heart Circ Physiol.* **294**: H633-44.

Christie GR, Williams DJ, MacIsaac F, Dickinson RJ, Rosewell I, Keyse SM. (2005). The Dual-Specificity Protein Phosphatase DUSP9/MKP-4 Is Essential for Placental Function but Is Not Required for Normal Embryonic

Development. *Molecular and Cellular Biology.* **25**: 8323-8333.

Chu WM, Ostertag D, Li ZW, et al. (1999). JNK2 and IKKβ are required for activating the innate response to viral infection. *Immunity.* **11**: 721-731.

Chu Y, Solski PA, Khosravi-Far R, Der CJ, Kelly K (1996). The mitogen-activated protein kinase phosphatases PAC1, MKP-1, and MKP-2 have unique substrate specificities and reduced activity in vivo toward the ERK2 sevenmaker mutation. *J Biol Chem.* **271:** 6497-6501.

Clerk A, Bogoyevitch MA, Anderson MB, Sugden PH (1994). Differential activation of protein kinase C isoforms by endothelin-I and phenylephrine and subsequent stimulation of p42 and p44 mitogen-activated protein kinases in ventricular myocytes cultured from neonatal rat hearts. *J Biol Chem*. **269**: 32848-32857.

Clerk A, Pham FH, Fuller SJ, Sahai E, Aktories K. (2001) Regulation of mitogen-activated protein kinases in cardiac myocytes through the small G protein, Rac1. *Mol Cell Biol.* **21**: 1173–1184.

Clerk A, Sugden PH. (2006). Inflame my heart (by p38-MAPK). *Circ Res.* **99**: 455-458.

Communal C, Colucci WS, Remondino A, Sawyer DB, Port JD, Wichman SE, Bristow MR, Singh K. (2002). Reciprocal modulation of mitogen-activated protein kinases and mitogen-activated protein kinase phosphatase 1 and 2 in failing human myocardium. *J Card Fail*. **8**: 86-92.

Constant SL, Dong C, Yang DD, Wysk M, Davis RJ, Flavell RA. (2000). JNK1 is required for T cell-mediated immunity against Leishmania major infection. *J Immunol.* **165**: 2671-2676.

Crabos M, Roth M, Hahn AW, Erne P. (1994). Characterization of angiotensin II receptors in cultured adult rat cardiac fibroblasts. Coupling to signalling systems and gene expression. *J Clin Invest.* **93**: 2372–2378.

Crackower MA, Oudit GY, Kozieradzki I, Sarao R, Sun H, Sasaki T, Hirsch E, Suzuki A, Shioi T, Irie-Sasaki J, Sah R, Cheng HY, Rybin VO, Lembo G, Fratta L, Oliveira-dos-Santos AJ, Benovic JL, Kahn CR, Izumo S, Steinberg SF, Wymann MP, Backx PH, Penninger JM. (2002). Regulation of myocardial contractility and cell size by distinct PI3K-PTEN signaling pathways. *Cell.* **110**: 737–49.

Cuenda A, Rousseau S. (2007). p38 MAP-kinases pathway regulation, function and role in human diseases. *Biochim Biophys Acta.* **1773**: 1358–1375.
Dadakhujaev S, Noh HS, Hah YS, Kim CJ, Kim DR. (2009). Interplay between autophagy and apoptosis in trka-induced cell death. *Autophagy.* **1**: 103-5.

Darren M, Mitchell RE, Laird R, Brown D, Long CS. (2007). IL-1beta stimulates rat cardiac fibroblast migration via MAP kinase pathways. *Am J Physiol Heart Circ Physiol.* **292**: H1139-H1147.

Dash BC, Wafik SE (2005). Phosphorylation of p21 in G2/M promotes cyclin b-Cdc2 kinase activity. *Molecular and Cellular Biology*. **25**: 3364–3387.

Dempsey EC, Newton AC, Mochly-Rosen D, Fields AP, Rey- land ME, Insel PA, Messing RO. (2000). Protein kinase C isozymes and the regulation of diverse cell responses. *Am J Physiol Lung Cell Mol Physiol.* **279**: L429–L438.

Denu JM, Dixon JE. (1995). A catalytic mechanism for dual-specificity phosphatases. *Proc. Natl. Acad. Sci. U.S.A.* **92**: 5910-4.

Denu JM, Dixon JE. (2007). Protein tyrosine phosphatases: mechanisms of catalysis and regulation. *Oncogene.* **26**: 3097-9.

Denu JM, Tanner KG. (1998). Specific and reversible inactivation of protein tyrosine phosphatases by hydrogen peroxide: evidence for a sulfenic acid intermediate and implications for redox regulation. *Biochemistry*. **37**: 5633-42.

Dhanasekaran DN, Johnson GL. (2007). MAPKs: function, regulation, role in cancer and therapeutic targeting. *J Biol Chem.* **271**: 29734-9.

Dickinson RJ, Keyse SM. (2006). Diverse physiological functions for dual-specificity MAP kinase phosphatases. *JCell Science.* **119**: 4607-4615.

Diez J, Lopez B, Gonzalez A, Querejeta R. 2001. Clinical aspects of hypertensive myocardial fibrosis. *Curr. Opin. Cardiol.* **16**: 328–35.

Diwan A, Dorn GW 2nd. (2007). Decompensation of cardiac hypertrophy: cellular mechanisms and novel therapeutic targets. *Physiology.* **22**: 56–64.

Dong C, Davis RJ, Flavell RA. (2001). Signaling by the JNK group of MAP kinases. c-jun N-terminal Kinase. *J Clin Immunol.* **21**: 253-257.

Dong C, Davis RJ, Flavell RA. (2002). MAP kinases in the immune response. *Annu Rev Immunol.* **20**: 55-72.

Dong C, Yang DD, Wysk M, Whitmarsh AJ, Davis RJ, Flavell RA. (1998). Defective T cell differentiation in the absence of Jnk1. *Science*. **282**: 2092–2095.

Dong YA, Daqing Gaob, Lei Chenb, Ruxian Lina, John V. Conteb, Chiming Weib. (2006). Increased ERK activation and decreased MKP-1 expression in

human myocardium with congestive heart failureJournal of *Cardiothoracic-Renal Research.* **1**: 123—130.

Dorfman K, Carrasco D, Gruda M, Ryan C, Lira SA, Bravo R. (1996). Disruption of the erp / mkp-1 gene does not affect mouse development: normal MAP kinase activity in ERP / MKP-1-deficient fibrolasts. *Oncogene.* **13**: 925-931.

Dorn GW 2nd, Robbins J, Ball N, Walsh RA. (1994). Myosin heavy chain regulation and myocyte contractile depression after LV hypertrophy in aortic-banded mice. *Am J Physiol.* **267**: H400–H405.

Dorn GW, Force T. (2005). Protein kinase cascades in the regulation of cardiac hypertrophy. *J Clin Invest.* **115**: 527–537.

Doubun Hayashia,b, Sumiyo Kudoha, Ichiro Shiojimaa, Yunzeng Zoud, Koichiro Haradaa, Masaki Shimoyamaa, Yasushi Imaia, Koshiro Monzena,b, Tsutomu Yamazakia,c,Yoshio Yazakie, Ryozo Nagaia, Issei Komurod (2004). Atrial natriuretic peptide inhibits cardiomyocyte hypertrophy through mitogen-activated protein kinase phosphatase-1. *Biochemical and Biophysical Research Communications.* **322**: 310–319.

Du J, Xu N, Song Y, Xu M, Lu Z, Han C, Zhang Y. (2005). AICAR stimulates IL-6 production via p38 MAPK in cardiac fibroblasts in adult mice: A possible role for AMPK. *Biochemical and Biophysical Research Communications.* **337**: 1139–1144.

Du W, Liao Y, Wang C, Zhang HY. (2005). Inhibitory effect of 14-3- 3 proteins on serum-induced proliferation of cardiac fibroblasts. *Eur. J. Cell Biol.* **84**: 843–852.

Élise Roussel, Martin Gaudreau1, Éric Plante, Marie-Claude Drolet, Catherine Breault, Jacques Couet, Marie Arsenault. (2008). Early responses of the left ventricle to pressure overload in Wistar rats. *Life Sciences*. **82**: 265–272.

Engel FB, Schebesta M, Duong MT, Lu G, Ren S, Madwed JB, Jiang H, Wang Y, Keating MT. (2005). p38 MAP kinase inhibition enables proliferation of adult mammalian cardiomyocytes. *Genes & Development.* **19**: 1175–1187.

Esposito G, Prasad SV, Rapacciuolo A, Mao L, Koch WJ, Rockman HA. (2001). Cardiac overexpression of a G(q) inhibitor blocks induction of extracellular signal-regulated kinase and c-Jun NH(2)-terminal kinase activity *in vivo* pressure overload. *Circulation.* **103**: 1453–1458.

Even, MS, Sandusky CB, Barnard ND. (2006). Serum-free hybridoma culture: ethical, scientific and safety considerations. *TRENDS in Biotechnology*. **24**; 3: 105-108.

Fan WJ, Genade S, Genis A, Huisamen B, Lochner A. (2009). Dexamethasone-induced cardioprotection: A role for the phosphatase MKP-1? *Life Sciences.* **84**: 838–846.

Farooq A, Chaturvedi G, Mujata S, Plotnikova O, Zeng L, Dhalluin C, Ashton R, Zhou MM. (2001). Solution structure of ERK2 binding domain of MAPK phosphatase MKP-3: structural insights into MKP-3 activation by ERK2. *Mol. Cell*. **7**: 387-399.

Farooq A, Zhou MM. (2004). Structure and regulation of MAPK phosphotases. *Cell Signal*. **16**: 769-779.

Ferrandi C, Ballerio R, Gaillard P, Giachetti C, Carboni S, Vitte PA et al. (2004). Inhibition of c-Jun N-terminal kinase decreases cardiomyocyte

apoptosis and infarct size after myocardial ischemia and reperfusion in anaesthetized rats. *Br J Pharmacol.* **142**: 953–960.

Fischer EH, Charbonneau H, Tonks NK. (1991). Protein tyrosine phosphatases: a diverse family of intracellular and transmembrane enzymes. *Science.* **253**: 401-406.

Flack EC, Lindsey ML, Squires CE, Kaplan BS, Stroud RE, Clark LL, Escobar PG, Yarbrough WM, Spinale FG. (2006). Alterations in cultured myocardial fibroblast function following the development of left ventricular failure. *J Mol Cell Cardiol.* **40**: 474–483.

Foster FM, Traer CJ, Abraham SM, Fry MJ. (2003). The phosphoinositide (PI) 3-kinase family. *J Cell Sci.* **116**: 3037–40.

Fox GC, Shafiq M, Briggs DC, Knowles PP, Collister M, Didmon MJ, Makrantoni V, Dickinson RJ, Hanrahan S, Totty N, Stark MJR, Keyse SM, McDonald NQ. (2007). Redox-mediated substrate recognition by Sdp1 defines a new group of tyrosine phosphatases. *Nature*. **447**: 487-492.

Fredj S, Bescond J, Louault C, Delwail A, Lecron JC, Potreau D. (2005). Role of interleukin-6 in cardiomyocyte/cardiac fibroblast interactions during myocyte hypertrophy and fibroblast proliferation. *J Cell Physiol*. **204**: 428−436.

Fredj S, Bescond J, Louault C, Potreau D. (2005). Interactions between cardiac cells enhance cardiomyocyte hypertrophy and increase fibroblast proliferation. *J. Cell. Physiol.* **202**: 891–899.

Freshney, RI. (1994). Culture of Animal Cells: A manual of basic technique. 3rd Ed. Wiley-Liss, Inc., 605 Third Avenue, New York, NY 10158-002.

Fryer RM, Hsu AK, Gross GJ. (1995). ERK and p38 MAP kinase activation are components of opioid-induced delayed cardioprotection. *Basic Res Cardiol.* **96**: 136–142.

Frey N, Katus HA, Olson EN, Hill JA. (2004). Hypertrophy of the heart: a new therapeutic target? *Circulation*. **109**: 1580–9.

Fu SL, Waha A, Vogt PK. (2000). Identification and characterization of genes upregulated in cells transformed by v-Jun. *Oncogene.* **19**: 3537-3545.

Fukunaga R, Hunter T. (1997). MNK1, a new MAP kinase-activated protein kinase, isolated by a novel expression screening method for identifying protein kinase substrates. *EMBO J.* **16**: 1921–1933.

Fuller SJ, Davies EL, Gillespie-brown J, Sun H, Tonks NK. (1997). Mitogen-activated protein kinase phosphatase 1 inhibits the stimulation of gene expression by hypertrophic agonists in cardiac myocytes. *Biochem j.* **323**: 313–319.

Furukawa T, Horii A. (2004). Molecular pathology of pancreatic cancer: in quest of tumor suppressor genes. *Pancreas*. **28**: 253–256.

Furukawa T, Sunamura M, Horii A (2006) Molecular mechanisms of pancreatic carcinogenesis. *Cancer Sci.* **97**: 1–7.

Galluzzi NJ, Tasdemir E, Maiuri MC, Hengartner M, Abrams JM, Tavernarakis N, Penninger J, Madeo F, Kroemer G. (2008). No death without life: Vital functions of apoptotic effectors. *Cell Death Differ*. **15**: 1113–1123.

Gaudesius G, Miragoli M, Thomas SP, Rohr S. (2003). Coupling of cardiac electrical activity over extended distances by fibroblasts of cardiac origin. *Circ*

Res. **93**: 421–428.

Giroux S, Tremblay M, Bernard D, Cardin-Girard JF, Aubry S, Larouche L et al. (1999). Embryonic death of Mek1- deficient mice reveals a role for this kinase in angiogenesis in the labyrinthine region of the placenta. *Curr Biol.* **9**: 369–372.

Goldberg LR. (2010). Heart failure. *Ann Intern Med.* **152**: ITC61-15.

Goldsmith EC, Hoffman A, Morales MO, Potts JD, Price RL, Mcfadden A, Rice M, Borg TK. (2004). Organization of fibroblasts in the heart. *Dev Dyn.* **230**: 787-94.

Green JA, Vistica DT, Young RC, Hamilton TC, Rogan AM. (1984). Potentiation of Melphalan cytotoxicity in Human Ovarian Cancer Cell lines by Glutathione Depletion. *Cancer Res.* **44**: 5427-5431.

Groen A, Lemeer S, van der Wijk T, Overvoorde J, Heck AJR, Ostman A, Barford D, Slijper M, den Hertog J. (2005). Differential Oxidation of Protein-tyrone Phosphatases. *J Biol Chem.* **280**: 10298-10304.

Groom LA, Sneddon AA, Alessi DR, Dowd S, Keyse SM. (1996) Differential regulation of the MAP, SAP and RK/p38 kinases by Pyst1, a novel cytosolic dual-specificity phosphatase. *EMBO J.* **15**: 3621–3632.

Grzyska PK, Kim Y, Jackson MD, Hengge AC, Denu JM. (2004). Probing the transition-state structure of dual-specificity protein phosphatases using a physiological substrate mimic *Biochemistry.* **43**: 8807-8814.

Guan KL, Butch E. (1995). Isolation and characterization of a novel dual specific phosphatase, HVH2, which selectively dephosphorylates the mitogen-activated protein kinase. *J Biol Chem.* **270**: 7197-7203.

Guo YL, Kang B, Williamson JR (1998). Inhibition of the expression of mitogen-activated protein phosphatase-1 potentiates apoptosis induced by tumor necrosis factor-alpha in rat mesangial cells. *J Biol Chem.* **273**: 10362–10366.

Gupta S, Campbell D, Derijard B, Davis RJ. (1995). Transcription factor ATF2 regulation by the JNK signal transduction pathway. *Science.* **267**: 389– 393.

Hamdi M, Kool J, Cornelissen-Steijger P, Carlotti F, Popeijus HE, van der Burgt C, Janssen JM, Yusai A, Hoeben RC, Terirth C, Mullenders LH, van Dam H. (2005). DNA damage in transcribed genes induces apoptosis via the JNK pathway and the JNK-phosphatase MKP-1. *Oncogene.* **24**: 7135–7144.

Hammer M, Mages J, Dietrich H, Servatius A, Howells N, Cato ACB, Lang R. (2006). Dual specificity phosphatase 1 (DUSP1) regulates a subset of LPS-induced genes and protects mice from lethal endotoxin shock. *J Exp Med*. **203**: 15–20.

Han J and Sun P (2007). The pathways to tumor suppression via route p38. *Trends Biochem Sci.* **32**: 364–371.

Han Z, Chang L, Yamanishi Y, Karin M, Firestein GS. (2002). Joint Damage and Inflammation in c-Jun N-Terminal Kinase 2 Knockout Mice With Passive Murine Collagen-Induced Arthritis. *Arthritis & Rheumatism*. **46**: 818–823.

Hanne V, Cynthia AS, Joshua JN, Birgit SK, William ET. (2009). DNA damage-induced cell death is enhanced by progression through mitosis. *Cell*

cycle. **8**: 2951-2963.

Haq S, Choukroun G, Lim H, Tymitz KM, del Monte F, Gwathmey J, Grazette L, Michael A, Hajjar R, Force T, Molkentin JD. (2001). Differential activation of signal transduction pathways in human hearts with hypertrophy versus advanced heart failure. *Circulation.* **103**: 670–677.

Harris IS, Zhang S, Treskov I, Kovacs A, Weinheimer C, Muslin AJ. (2004). Raf-1 kinase is required for cardiac hypertrophy and cardiomyocyte survival in response to pressure overload. *Circulation.* **110**: 718–23.

Harvey PR, Rosenthal N. (1991). Heart Development. Vol 1. New York: Academy.

Hasegawa T, Enomoto A, Kato T, Kawai K, Miyamoto R, Jijiwa M*, et al.* (2008). Roles of induced expression of MAPK phosphatase-2 in tumor development in RET-MEN2A transgenic mice. *Oncogene.* **27:** 5684-5695.

Hatano N, Mori Y, Oh-hora M, Kosugi A, Fujikawa T, Nakai N, Niwa H, Miyazaki J, Hamaoka T, Ogata M. (2003). Essential role for ERK2 mitogen-activated protein kinase in placental development. *Genes Cells.* **8**: 847–856.

Hayashi M, Kim SW, Imanaka-Yoshida K, Yoshida T, Abel ED, Eliceiri B, Yang Y, Ulevitch RJ, and Lee JD (2004a). Targeted deletion of BMK1/ERK5 in adult mice perturbs vascular integrity and leads to endothelial failure. *J Clin Invest.* **113**: 1138 –1148.

Hayashi M, Lee JD. (2004). Role of the BMK1/ERK5 signaling pathway: lessons from knockout mice. *J Mol Med.* **82**: 800–808.

Heineke J, Molkentin JD. (2006). Regulation of cardiac hypertrophy by intracellular sig-nalling pathways. *Nat Rev Mol Cell Biol*. **7**: 589–600.

Heinrich R, Neel BG, Rapoport TA. (2002). Mathematical Models of Protein Kinase Signal Transduction. *Molecular Cell.* **9**: 957–970.

Hilfiker-Kleiner D, Landmesser U, Drexler H. (2006). Molecular mechanisms in heart failure: focus on cardiac hypertrophy, inflammation, angiogenesis, and apoptosis. *J. Am. Coll. Cardiol.* **48**: 56-66.

Hindley A, Kolch W. (2002). Extracellular signal regulated kinase (ERK) / mitogen activated protein kinase (MAPK)-independent functions of Raf kinases. *J Cell Sci.* **115**: 1575–81.

Hinz B, Phan SH, Thannickal VJ, Galli A, Bochaton-Piallat ML, Gabbiani G. (2007). The myofibroblast: one function, multiple origins. *Am J Pathol.* **170**:1807–1816.

Hiroi Y, Hiroi J, Kudoh S, Yazaki Y, Nagai R, Komuro I, Li xu Bao S, Du J, Xu N, Song Y, Xu M, Lu Z, Han C, Zhang Y. (2005). AICAR stimulates IL-6 production via p38 MAPK in cardiac fibroblasts in adult mice: A possible role for AMPK. *Biochemical and Biophysical Research Communications.* **337**: 1139–1144.

Hiroi Y, Hiroi J, Kudoh S, Yazaki Y, Nagai R, Kumoru I. (2001). Two distinct mechanisms of angiotensin II-induced negative regulation of the mitogen-activated protein kinases in cultured cardiac myocytes. *Hypertens Res.* **24**: 385-94.

Hirosumi J, Tuncman G, Chang L, Gorgun CZ, Uysal KT, Maeda K, *et al.* (2002). A central role for JNK in obesity and insulin resistance. *Nature.* **420:** 333-336.

Hoekstra MF. (1997). Responses to DNA damage and regulation of cell cycle checkpoints by the ATM protein kinase family. *Curr Opin Genet Dev.* **7**: 170–175.

Hongo M, Ryoke T, and Ross Jr J.(1997). Animal models of heart failure: Recent developments and perspectives.*Trends Cardio Med*. **7**: 161-167.

Hu P, Zhang D, Sweson L, Chakrabarti G, Abel ED, Litwin SE. (2003). Minimally invasive aortic banding in mice: effects of altered cardiomyocyte insulin signaling during pressure overload. *Am J Physiol Heart Circ Physiol.* **285**: H1261-H1269.

Ieda M, Tsuchihashi T, Ivey KN, Ross RS, Hong TT, Shaw RM, Srivastava D. (2009). Cardiac fibroblasts regulate myocardial proliferation through beta1 integrin signaling. *Dev Cell.* **16**: 233–244.

Innocente SA, Abrahamson JLA, Cogswell JP, Lee JM. (1999). p53 regulates a G2 checkpoint through cyclin b1 (cell cycle cdc2 mitosis cancer) *Proc Natl Acad Sci USA* .**96**: 2147–2152.

Innocente SA, Lee JM. (2005). p53 is a NF-Y- and p21-independent, Sp1-dependent repressor of cyclin B1 transcription. *FEBS Letters.* **579**: 1001-1007.

Jaarsma T, Haaijer-Ruskamp FM, Sturm H, Van Veldhuisen DJ. (2005). Management of heart failure in The Netherlands. *Eur J Heart Fail.* **7**: 371-5.

Jacobs SS, Brandstatter M, Hafner K, Regitz-Zagrosek M, Ertl V, Schorb GW. (2001). Angiotensin II type 1 receptor regulation and differential trophic effects on rat cardiac myofibroblasts after acute myocardial infarction. *J Cell Physiol.* **187**: 326–335.

Jaeschke A, Rincon M, Doran B, Reilly J, Neuberg D, Greiner DL, Shultz LD, Rossini AA, Flavell RA, Davis RJ. (2005). Disruption of the jnk2 (Mapk9) gene reduces destructive insulitis and diabetes in a mouse model of type 1 diabetes. *Proc Natl Acad Sci USA.* **102**: 6931-5.

Jeffrey KL, Brummer T, Rolph MS, Liu SM, Callejas NA, Grumont RJ, Gillieron C, Mackay F, Grey S, Camps M. (2006). Positive regulation of immune cell function and inflammatory responses by phosphatase PAC-1. *Nat Immunol.* **7**: 274–283.

Jeong DG Jung S, Yoon T, Woo E, Kim JH, Park BC, Ryu SE, Kim SJ. (2009). Crystal structure of the catalytic domain of human MKP-2 reveals a 24-mer assembly. *Proteins.* 22423.

Jeong DG, Yoon TS, Kim JH, Shim MY, Jung SK, Son JH, Ryu SE, Kim SJ. (2006). Crystal structure of the catalytic domain of human MAP kinase phosphatase 5: structural insight into constitutively active phosphatase. *J Mol Biol.* **360**: 946–955.

Jianli Wang, Wen Hong Shen, Yan J. Jin, Paul W. Brandt-Rauf, and Yuxin YinA (2007). Molecular Link between E2F-1 and the MAPK Cascade. *J Biol Chem.* **282**: 18521–18531.

Jin Y, Calvert TJ, Chen B, Chicoine LG, Joshi M, Bauer JA, Liu Y, Nelin LD. (2010). Mice deficient in MKP-1 develop more severe pulmonary hypertension and greater lung protein levels of arginase in response to

chronic hypoxia. *Am J Physiol Heart Circ Physiol.* **298**: H1518–H1528, 2010.

Johnson GL, Dohlman HG, Graves LM. (2005). MAPK kinase kinases (MKKKs) as a target class for small-molecule inhibition to modulate signaling networks and gene expression. *Curr Opin Chem Biol*. **9**: 325–331.

Kamkin A, Kiseleva I, Isenberg G, Wagner KD, Gunther J, Theres H, Scholz H. (2003). Cardiac fibroblasts and the mechano-electric feedback mechanism in healthy and diseased hearts. *Prog Biophys Mol Biol.* **82**: 111–120.

Kaiser RA, Bueno OF, Lips DJ, Doevendans PA, Jones F, Kimball TF, Molkentin JD. (2004). Targeted inhibition of p38 mitogen-activated protein kinase antagonizes cardiac injury and cell death following ischemia-reperfusion *in vivo. J Biol Chem.* **279**: 15524–15530.

Kaiser RA, Lyons JM, Duffy JY, Wagner CJ, McLean KM, O'Neill TP, Pearl JM, Molkentin JD. (2005). Inhibition of p38 reduces myocardial infarction injury in the mouse but not pig after ischemia-reperfusion. *Am J Physiol Heart Circ Physiol.* **289**: H2747–H2751.

Kao S, Jaiswal RK, Kolch W, Landreth. (2001). Identification of the mechanisms regulating the differential activation of the mapk cascade by epidermal growth factor and nerve growth factor in PC12 cells. *J Biol Chem*. **276**: 18169-77.

Karin M, Gallagher E. (2005). From JNK to pay dirt: Jun kinases, their bio-chemistry, physiology and clinical importance. *IUBMB Life.* **57**: 283–295.

Karlsson M, Mathers J, Dickinson RJ, Mandl M, Keyse SM (2004). Both nuclear–cytoplasmic shuttling of the dual specificity phosphatase MKP-3 and its ability to anchor MAP kinase in the cytoplasm are mediated by a conserved nuclear export signal. *J Biol Chem*. **279**: 41882–41891.

Katagiri C, Masuda K, Urano T, Yamashita K, Araki Y, Kikuchi K, Shima H. (2005). Phosphorylation of Ser-446 Determines Stability of MKP-7. *J Biol Chem.* **280**: 14716-14722.

Kawamata N, Saitoh T, Sakajiri S, Koeffler PH. (2005). Identification of candidate tumor suppressor genes silenced epigenetically in mantle cell lymphoma. *Blood (ASH Ann Meet Abstr).* **106**: 300–301.

Kenchaiah S, Pfeffer MA. (2004). Cardiac remodeling in systemic hypertension. *Med. Clin. North Am.* **88**: 115–30.

Kerkela R, ForceT. (2006). p38 mitogen-activated protein kinase: a future target for heart failure therapy? J *Am Coll Cardiol.* **48**: 556–558.

Kerkela R, Force T. (2006). Recent insights into cardiac hypertrophy and left ventricular remodeling. *Curr Heart Fail Rep.* **1**: 14-8.

Kessler A, Uphues I, Ouwens DM, Till M, Eckel J. (2001). Diversification of cardiac insulin signaling involves the p85 alpha/beta subunits of phosphatidylinositol 3-kinase. *Am J Physiol Endocrinol Metab.* **280**: E65 74.

Keyse SM, Emslie EA. (1992). Oxidative stress and heat shock induce a human gene encoding a protein-tyrosine phosphatase. *Nature*. **359**: 644-64.

Keyse SM, Ginsburg M. (1993). Amino acid sequence similarity between CL100, a dual-specificity MAP kinase phosphotase and cdc25. *Trends Biochem Sci.* **18**: 377-378.

Keyse SM. (2000). Protein phosphatases and the regulation of mitogen-activated protein kinase signalling. *Curr Opin Cell Biol.* **12**: 186-92.

Keyse, SM. (1998). Protein phosphatases and the regulation of MAP kinase activity. *Cell Dev Biol.* **9**: 143–152.

Kim S, Bakre M, Yin H, Varner JA. (2002). Inhibition of endothelial cell survival and angiogenesis by protein kinase A. *J Clinical Investigation*. **110**: 933-941.

Kinney CM, Chandrasekharan UM, Yang L, Shen J, Kinter M, McDermott MS, DiCorleto PE. (2009). Histone H3 as a novel substrate for MAP kinase phosphatase-1. *Am J Physiol Cell Physiol.* **296**: C242-9.

Kizana E, Ginn SL, Smyth CM, Boyd A, Thomas SP, Allen DG, Ross DL & Alexander IE. (2006). Fibroblasts modulate cardiomyocyte excitability: implications for cardiac gene therapy. *Gene Ther*. **13**: 1611–1615.

Kjaer A. (2000). Neuroendocrine activation in heart failure I.Pathopysiology and pharmacological intervention. *Ugeskr Laeger.* **162**: 5905-9.

Knight RJ Buxton DB. (1996). Stimulation of c-Jun kinase and mitogen-activated protein kinase by ischemia and reperfusion in the perfused rat hearts. *Biochem Biophys Res Commun.* **218**: 83–88.

Kohl P, Kamkin AG, Kiseleva IS. (1994). Mechanosensitive fibroblasts in the sino-atrial node region of rat heart: interaction with cardiomyocytes and possible role. *Exp Physiol.* **79**: 943–956.

Kontaridis MI, Yang W, Bence KK, Cullen DMA, Wang B, Bodyak N, Ke Q, Hinek A, Kang PM, Liao R, Neel BG. (2008). Deletion of Ptpn11 (Shp2) in Cardiomyocytes Causes Dilated Cardiomyopathy via Effects on the Erk / MAPK and RhoA Signaling Pathways. *Circulation.* **117**: 1423–1435.

Krishnan AV, Moreno J, Nonn L, Malloy P, Swami S, Peng L, Peehl DM & Feldman D. (2007). Novel pathways that contribute to the anti-proliferative and chemopreventive activities of calcitriol in prostate cancer. *J Steroid Biochem Mol Biol.* **103**: 694–702.

Kucharska A, Linda KR, Christopher S, Nick AM, Keyse SM. (2009). Regulation of the inducible nuclear dual-specificity phosphatase DUSP5 by ERK MAPK. *Cellular Signalling*. **21**: 1794–1805.

Kuida K, Boucher DM. (2004). Functions of MAP kinases: insights from gene-targeting studies. *J Biochem.* **135**: 653–656.

Kuida K, Boucher DM. (2004). Functions of MAP kinases: insights from gene-targeting studies. *J. Biochem.* **135**: 653–656.

Kyoi S, Otani H, Matsuhisa S, Akita Y, Tatsumi K, Enoki C, Fujiwara H, Imamura H, Kamihata H, Iwasaka T. (2006). Opposing effect of p38 MAP kinase and JNK inhibitors on the development of heart failure in the cardiomyopathic hamster. *Cardiovasc Res.* **69**: 888 – 898.

Kyriakis JM, Avruch J (2001). Mammalian mitogen-activated protein kinase signal transduction pathways activated by stress and inflammation. *Physiol Rev.* **81**: 807-69.

LaFramboise WA, Scalise D, Stoodley P, Graner SR, Guthrie RD, Magovern JA, Becich MJ. (2007). Cardiac fibroblasts influence cardiomyocyte phenotype *in vitro. Am J Physiol Cell Physiol.* **292**: C1799 –C1808.

Lanzini F, Bertoldo A, Kosmacek EA, Phillips SL Mackey MA. (2006). Lack of p53 function promotes radiation-induced mitotic catastrophe in mouse

embryonic fibroblast cells. *Cancer Cell International*. **6**: 1-8.

Lau LF, Nathans D. (1985). Identification of a set of genes expressed during the G0/G1 transition of cul- tured mouse cells. *EMBO J.* **4**: 3145–3151.

Leask, A. (2010). Potential Therapeutic Targets for Cardiac Fibrosis: TGFβ, Angiotensin, Endothelin, CCN2, and PDGF, Partners in Fibroblast Activation. Circ Res. 106: 1675-80.

Lee JC, Laydon JT, McDonnell PC, Gallagher TF, Kumar S, Green D, Mc-Nulty D, Blumenthal MJ, Heys JR, Landvatter SW. (1994). A protein kinase involved in the regulation of inflammatory cytokine biosynthesis. *Nature.* **372**: 739-746.

Lewis TS, Shapiro PS, Ahn NG. (1998). Signal transduction through MAP kinase cascades. *Adv Cancer Res.* **74**: 49–139.

Lawan A, Ali MA, Dan-Bauchi SS. (2006). QT dispersion in dynamic and static group of athletes. *Niger J Physiol Sci.* **21**: 5-8.

Lazou A, Bogoyevitch MA, Clerk A, Fuller SJ, Marshall C, Sugden PH. (1994). Regulation of mitogen-activated protein kinase cascade in adult rat heart preparations in vitro. *Circ Res.* **75**: 932-941.

Li C, Scott DA, Hatch E, Tian X, Mansour SL. (2007). Dusp6 (MKP-3) is a negative feedback regulator of FGF-stimulated ERK signaling during mouse development. *Development.* **134**: 167–176.

Li C, Yanhua Hu, Manuel Mayr, and Qingbo Xu (1999). Cyclic Strain Stress-induced Mitogen-activated Protein Kinase (MAPK) Phosphatase 1 Expression

in Vascular Smooth Muscle Cells Is Regulated by Ras/Rac-MAPK Pathways. *J Biol Chem*. **274**: 25273–25280.

Li M, Jun-ying Z, Yubin G, Larry HM, Gen SW. (2003). The phosphatase MKP-1 is a transcriptional target of p53 involved in cell cycle regulation. *J Biol Chem*. **278**: 41059–41068.

Li Y, St John MA, Zhou X, Kim Y, Sinha U, Jordan RC, Eisele D, Abemayor E, Elashoff D, Park NH. (2004). Salivary transcriptome diagnostics for oral cancer detection. *Clin Cancer Res.* **10**: 8442–8450.

Li Z, Tran TT, Ma JY, O'Young G, Kapoun AM, Chakravarty S, Dugar S, Schreiner G, Protter AA. (2004). p38 Alpha mitogen-activated protein kinase inhibition improves cardiac function and reduces myocardial damage in isoproterenol-induced acute myocardial injury in rats. *J Cardiovasc Pharmacol.* **44**: 486-492.

Liang Q, Bueno OF, Wilkins BJ, Kuan CY, Xia Y, Molkentin JD. (2003). c-Jun N-terminal kinases (JNK) antagonize cardiac growth through cross-talk with calcineurin-NFAT signaling. *EMBO J.* **22**: 5079–5089.

Liang Q, Molkentin JD. (2003). Redefining the roles of p38 and JNK signaling in cardiac hypertrophy: Dichotomy between cultured myocytes and animal models. *J. Mol. Cell Cardiol.* **35**: 1385–1394.

Liao P, Georgakopoulos D, Kovacs A, Zheng M, Lerner D, Pu H, Saffitz J, Chien K, Xiao RP, Kass DA, Wang Y. (2001). The *in vivo* role of p38 MAP kinases in cardiac remodeling and restrictive cardiomyopathy. *Proc Natl Acad Sci USA* .**98**: 12283–12288.

Liao P, Wang SQ, Wang S, Zheng M, Zhang SJ, Cheng H, Wang Y, Xiao RP.

(2002). p38 Mitogen-activated protein kinase mediates a negative inotropic effect in cardiac myocytes. *Circ Res.* **90**: 190–196.

Lijnen PJ, Petrov VV. (2003). Role of intracardiac renin-angiotensin-aldosterone system in extracellular matrix remodeling. *Methods Find. Exp. Clin. Pharmacol.* **25**: 541–64.

Lin YW, Yang JL. (2006). Cooperation of ERK and SCFSkp2 for MKP-1 destruction provides a positive feedback regulation of proliferating signaling. *J Biol Chem*. **281**: 915–926.

Lipp PF, Chapman J, Pouyssegur RB. (2002). Knockout of ERK1 MAP kinase enhances synaptic plasticity in the striatum and facilitates striatal-mediated learning and memory. *Neuron* **34**: 807–820.

Little WC, Oh JK. (2009). Echocardiographic evaluation of diastolic function can be used to guide clinical care. *Circulation.* **120**: 802-809.

Liu C, Shi Y, Du Y, Ning X, Liu N, Huang D, Liang J, Xue Y, Fan D. (2005). Dual-specificity phosphatase DUSP1 protects overactivation of hypoxia-inducible factor 1 through inactivating ERK MAPK. *Exp Cell Res.* **309**: 410–418.

Liu PQ, Lu W, Wang TH, Pan JY. (2000). MKP-1 regulates the cardiomyocyte hypertrophic responses induced by angiotensin II. *Acta Physiologica Sinica.* **52**: 365-70.

Liu PQ, Lu W, Wang TH, Pan JY. (2000). MKP-1 regulates the cardiomyocyte hypertrophic responses induced by angiotensin II. *Sheng Li Xue Bao.* **52**: 365-70.

Liu S, Sun JP, Zhou B, Zhang ZY. (2006). Structural basis of docking interactions between ERK-2 and MAP kinase phosphatase 3. *Proc Natl Acad Sci USA.* **103**: 5326–5331.

Liu S, Sun JP, Zhou B, Zhang ZY. (2006). Structural basis of docking interactions between ERK-2 and MAP kinase phosphatase 3. *Proc Natl Acad Sci USA.* **103**: 5326–5331.

Lou YW, Chen YY, Hsu SF, Chen RK, Lee CL, Khoo KH, Tonks NK, Meng TC. (2008). Redox regulation of protein tyrosine phosphatase PTP1B in cancer cells. *FEBS J.* **275**: 69-88.

Lou YW, Chen YY1, Hsu1 SF, Chen RK, Lee CL, Khoo KH, Tonks NK, Meng TC. (2008). Redox regulation of the protein tyrosine phosphatase PTP1B in cancer cells. *FEBS J.* **275**: 69-88.

Lu C, Zhu F, Cho YY, Tang F, Zykova T, Ma W, Bode AM, Dong Z. (2006). Cell Apoptosis: Requirement of H2AX in DNA Ladder Formation but not for the Activation of Caspase-3. *Mol Cell.* **23**: 121–132.

Luttrell DK, Luttrell LM. (2003). Signaling in time and space: G protein-coupled receptors and mitogen-activated protein kinases. *Assay Drug Dev Technol.* **1**: 327–38.

Lyon MA, Ducruet AP Wipf P, Lazo JS. (2002). Dual-specificity phosphatases as targets for antineoplastic agents. *Nature Rev Drug Discov*. **1**: 961–976.

Ma XL, Kumar S, Gao F, Louden CS, Lopez BL, Christopher TA, Wang C, Lee JC, Feuerstein GZ, Yue TL. (1999). Inhibition of p38 mitogen-activated protein kinase decreases cardiomyocyte apoptosis and improves cardiac function after myocardial ischemia and reperfusion. *Circulation.* **99**: 1685–1691.

Mac Lennan DH, Kranias EG. (2003). Phospholamban: a crucial regulator of cardiac contractility. *Nat Rev Mol Cell Biol*. **4**: 566–577.

MacLennan DH, Asahi M, Tupling AR. (2003). The regulation of SERCA-type pumps by phospholamban and sarcolipin. *Ann NY Acad Sci.* **986**: 472–480.

Maillet M, Purcell NH, Sargent MA, York AJ, Bueno OF, Molkentin JD (2008). DUSP6 (MKP3) Null Mice Show Enhanced ERK1/2 Phosphorylation at Baseline and Increased Myocyte Proliferation in the Heart Affecting Disease Susceptibility. *J Biol Chem .* **283**: 31246–31255.

Manabe I, Shindo T, Nagai R. (2002). Gene expression in fibroblasts and fibrosis: involvement in cardiac hypertrophy. *Circ Res.* **91**: 1103–1113.

Mann DL, Bristow MR. (2005). Mechanisms and models in heart failure: the biomechanical model and beyond. *Circulation.* **111**: 2837–2849.

Marchetti S, Gimond C, Roux D, Gothie E, Pouyssegur J, Pages G. (2004). Inducible expression of a MAP kinase phosphatase-3-GFP chimera specifically blunts fibroblast growth and ras-dependent tumor formation in nude mice. *J Cell Physiol.* **199**: 441–450.

Marcus S, Polverino A, Barr M, Wigler M. (1994). Complexes between STE5 and components of the pheromone-responsive MAPK-module. *Proc Natl Acad Sci USA.* **91**: 7762–7766.

Maroney AC, Glicksman MA, Basma AN, Walton KM, Knight Jr E, Murphy CA, Barlett BA, Finn JP, Angeles T, Matsuda Y, Neff NT, Dionne CA. (1998). Motoneuron Apoptosis Is Blocked by CEP-1347 (KT 7515), a Novel Inhibitor of the JNK Signalling Pathway. *J Neuroscience.* **18**: 104-111.

Marshall AK, Barrett OPT, Cullingford TE, Shanmugasundram A, Sugden PH, Clerk A. (2010). ERK1/2 Signaling Dominates Over RhoA Signaling in Regulating Early Changes in RNA Expression Induced by Endothelin-1 in Neonatal Rat Cardiomyocytes. *PLoS one.* **5**:1-13.

Martial S, Giorgelli J, Renaudo A, Derijard B, Sorian O. (2008). SP600125 inhibits Kv channels through a JNK-independent pathway in cancer cells. *Biochemical and Biophysical Research Communications.* **366**: 944–950.

Martindale JJ, Wall JA, Martinez-Longoria DM, Aryal P, Rockman HA, Guo Y, Bolli R, Glembotski CC. (2005). Overexpression of mitogen-activated protein kinase kinase 6 in the heart improves functional recovery from ischemia in vitro and protects against myocardial infarction *in vivo. J Biol Chem.* **280**: 669 – 676.

Masuda K, Shima H, Kikuchi K, Watanabe Y, Matsuda Y. (2000). Expression and comparative chromosomal mapping of MKP-5 genes DUSP10 / Dusp10. *Cytogenet Cell Genet.* **90**: 71–74.

Masuda K, Shima H, Watanabe M, Kikuchi K. (2001). MKP-7, a novel mitogen-activated protein kinase phosphatase, functions as a shuttle protein. *J. Biol. Chem*. **276**: 39002–39011.

Matsuguchi T, Musikacharoen T, Johnson TR, Kraft AS, Yoshika Y. (2001). A novel mitogen-activated protein kinase phosphatase is an important negative regulator of lipopolysaccharide-mediated c-Jun N-terminal kinase activation in mouse macrophage cell lines. *Mol. Cell. Biol.* **21**: 6999-7009.

Matsushita T, Takamatsu T. (1997). Ischaemia-induced temporal expression of connexin43 in rat heart. *Virchows Arch.* **431**: 453-8.

Mayor F Jr, Jurado-Pueyo M, Campos PM, and Murga C. (2007). Interfering with MAP kinase docking interactions: implications and perspective for the p38 route. *Cell Cycle.* **6**: 528-33.

Mazzucchelli C, Vantaggiato C, Ciamel A, Fasano S, Krezel W, Weizi H, Wolfer DP, Pages G, Valverde O, Morowsky A, Porrazzo A, Orban PC, Maldonado R, Ehrengruber MU, Cestari V, Lipp HP, Chapman PF, Poussegur J, Brambilla R. 2002).Knockout of ERK1 MAP kinase enhances synaptic plasticity in the stratium and facilitates striatal-mediated leraning and memory. *Neuron.* **30**: 807-20.

McKay MM, Morrison DK. (2007). Integrating signals from RTKs to ERK / MAPK. *Oncogene.* **26**: 3113–3121.

McMullen JR, Shioi T, Zhang L, Tarnavski O, Sherwood MC, Kang PM, Izumo S. (2003). Phosphoinositide 3-kinase(p110alpha) plays a critical role for the induction of physiological, but not pathological, cardiac hypertrophy. *Proc Natl Acad Sci USA.* **100**: 12355–12360.

Mehta PK, Griendling KK. (2007). Angiotensin II cell signaling: physiological and pathological effects in the cardiovascular system. *Am J Physiol Cell Physiol*. **292**: C82–C97.

Meng TC, Fukada T, Tonks NK. (2002). Reversible oxidation and inactivation of protein tyrosine phosphatases *in vivo. Mol Cell.* **9**: 387-399.

Meszaros JG, Gonzalez AM, Endo-Mochizuki Y, Villegas S, Villarreal F, and Brunton LL. (2000). Identification of G protein-coupled signaling pathways in cardiac fibroblasts: cross-talk between G_q and G_s. *Am J Physiol Cell Physiol.* **278**: C154–C162.

Mikula M, Schreiber M, Husak Z, Kucerova L, Ruth J, Wieser R. (2001). Embryonic lethality and fetal liver apoptosis in mice lacking the c-raf-1 gene. *EMBO J.* **20**: 1952–62.

Misra-Press A, Rim CS, Yao H, Roberson MS, Stork PJ (1995). A novel mitogen-activated protein kinase phosphatase. Structure, expression, and regulation. *J Biol Chem.* **270:** 14587-14596.

Mitchell MD, Laird RE, Brown RD, Long CS. (2007). IL-1beta stimulates rat cardiac fibroblast migration via MAP kinase pathways. *Am J Physiol Heart Circ Physiol.* **292**: H1139-H1147.

Mitchell S, Ota A, Foster W, Zhang B, Fang Z, Patel S. (2006). Distinct gene expressionprofiles in adult mouse heart following targeted MAP kinase activation. *Physiol Genomics.* **25**: 50–9.

Mizukami Y, Yoshida K. (1997). Mitogen-activated protein kinase translocates to the nucleus during ischaemia and is activated during reperfusion. *Biochem J.* **323**: 785–90.

Mocanu M. M., Baxter G. F., Yue Y., Critz S. D., Yellon D. M. (2000). The p38 MAPK inhibitor, SB 203580, abrogates ischaemic preconditioning in rat heart but timing of administration is critical. *Basic Res Cardiol.* **95**: 472-478.

Molina G, Vogt A, Bakan A, Dai W, de Oliveira PQ, Znosko W, Smithgall TE, Bahar I, Lazo JS, Day BW, Tsang M. (2009). Zebrafish chemical screening reveals an inhibitor of Dusp6 that expands cardiac cell lineages. *Nat Chem Biol*. **5**: 680–687.

Molkentin JD, Dorn II GW. (2001). Cytoplasmic Signaling Pathways that Regulate Cardiac Hypertrophy. *Ann Rev Physiol.* **63**: 391-426.

Monnet E, Chachques JC. (2005). Animal models of heart failure: what is new? *Ann Thorac Surg.* **79**: 1445-53.

Montessuit C, Thorburn A. (1999). Transcriptional activation of the glucose transporter glut1 in ventricular cardiac myocytes by hypertrophic agonists. *J Biol Chem*. **274**: 9006–9012.

Moreira VO, de Castro AV, Yaegaschi MY, Cicogna AC, Okoshi MP, Pereira CA, Aragon FF, Bruno MB, Padovani CR, Okoshi K. (2006). Echocardiographic criteria for the definition of ventricular dysfunction severity in aortic banded rats. *Arq Bras Cardiol.* **86**: 432-8.

Muda M, Boschert U, Dickinson R, Martinou J, Martinou I, Camps M, Schlegel W, Arkinstall S. (1996). MKP-3, a Novel Cytosolic Protein-tyrosine Phosphatase That Exemplifies a New Class of Mitogen-activated Protein Kinase Phosphatase. *J Biol Chem.* **271**: 4319–4326,

Muda M, Theodosiou A, Gillieron C, Smith A, Chabert C, Camps M, Boschert U, Rodrigues U, Davies K, Ashworth A, Arkinstall S. (1998). The mitogen-activated protein kinase phosphatase-3 N-terminal noncatalytic region is responsible for tight substrate binding and enzymatic specificity. *J Biol Chem*. **273**: 9323-9329.

Mudgett JS, Ding J, Guh-Siesel L, Chartrain NA, Yang L, Gopal S, Shen MM. (2000). Essential role for p38alpha mitogen-activated protein kinase in placental angiogenesis. *Proc. Natl. Acad. Sci. USA.* **97**: 10454–10459.

Munzel F, Muhlhauser U, Zimmermann WH, Didie M, Schneiderbanger K, Schubert P. (2005). Endothelin-1 and isoprenaline co-stimulation causes contractile failure which is partially reversed by MEK inhibition. *Cardiovasc Res.* **68**: 464–74.

Muslin AJ. (2008). MAPK signalling in cardiovascular health and disease: molecular mechanisms and therapeutic targets. *Clin Sci (Lond).* **115**: 203–18.

Nadal-Ginard B, Kajstura J, Leri A, Anversa P. (2003). Myocyte death, growth and regeneration in cardiac hypertrophy and failure. *Circ Res.* **92**: 139–50.

Nakamura T, Colbert M, Krenz M, Molkentin JD, Hahn HS, Dorn 2nd GW. (2007). Mediating ERK 1/2 signaling rescues congenital heart defects in a mouse model of Noonan syndrome. *J Clin Invest.* **117**: 2123–32.

Nakano A, Baines CP, Kim SO, Pelech SL, Downey JM, Cohen MV. (2000). Ischemic preconditioning activates MAPKAPK2 in the isolated rabbit heart: evidence for involvement of p38 MAPK. *Circ Res.* **86**: 144–51.

Nishida K, Yamaguchi O, Hirotani S, Hikoso S, Higuchi Y, Watanabe T, Takeda T, Osuka S, Morita T, Kondoh G, Uno Y, Kashiwase K, Taniike M, Nakai A, Matsumura Y, Miyazaki J, Sudo T, Hongo K, Kusakari Y, Kurihara S, Chien KR, Takeda J, Hori M, Otsu K. (2004). p38alpha mitogen-activated protein kinase plays a critical role in cardiomyocyte survival but not in cardiac hypertrophic growth in response to pressure overload. *Mol Cell Biol.* **24**: 10611–10620.

Nishimoto S, Kusakabe M, Nishida E. (2005). Requirement of the MEK5–ERK5 pathway for neural differentiation in Xenopus embryonic development. *EMBO Rep.* **6**: 1064–1069.

Nishimoto S, Nishida E. (2006). MAPK signalling: ERK5 versus ERK1/2. *EMBO Rep.* **7**: 782–786.

Noguchi M, Tashiro H, Shirasaki R, Gotoh M, Kawasugi K, Shirafuji N. (2007). Dual-specificity phosphatase 10 is fused to MDS1/EVI1-like gene 1 in a case of acute myelogenous leukemia with der1t1;1(p36.3;q21). *Int J Hematol.* **85**: 175–176.

Noguchi T, Metz R, Chen L, Mattei M, Carrasco D, Bravo R. (1993). Structure, Mapping, and Expression of erp, a Growth Factor- Inducible Gene Encoding a Nontransmembrane Protein Tyrosine Phosphatase, and Effect of ERP on Cell Growth. *Mol Cell Biol.* **13**: 5195-5205.

Nonn L, Duong D, Peehl DM. (2007). Chemopreventive anti-inflammatory activities of curcumin and other phytochemicals mediated by MAP kinase phosphatase- 5 in prostate cells. *Carcinogenesis.* **28**: 1188–1196.

Nonn L, Peng L, Feldman D, Peehl DM. (2006). Inhibition of p38 by vitamin D reduces interleukin-6 production in normal prostate cells via mitogen-activated protein kinase phosphatase 5: implications for prostate cancer prevention by vitamin D. *Cancer Res.* **66**: 4516– 4524.

O'Toole CM, Povey S, Hepburn P, Franks LM. (1983). Identity of some human bladder cancer cell lines. *Nature.* **301**: 426-430.

Okin PM, Devereux RB, Jern S, Kjeldsen SE, Julius S, Nieminen MS, Snapinn S, Harris KE, Aurup P, Edelman JM, Wedel H, Lindholm LH, Dahlöf B. (2004). LIFE Study Investigators. Regression of electrocardiographic left ventricular hypertrophy during antihypertensive treatment and the prediction of major cardiovascular events. *JAMA.* **292**: 2343–2349.

Olson AK, Protheroe KN, Segar JL, Scholz TD. (2006). Mitogen-activated protein kinase activation and regulation in the pressure-loaded fetal ovine heart. *Am J Physiol Heart Circ Physiol.* **290**: H1587–H1595.

Olson ER, Naugle JE, Zhang X, Bomser JA, Meszaros JG. (2005). Inhibition of cardiac fibroblast proliferation and myofibroblast differentiation by resveratrol. *Am J Physiol Heart Circ Physio.l* **288**: H1131–H1138.

Orr AW, Helmke B P. (2006) Mechanisms of mechanotransduction. *Dev. Cell* **10**: 11–20.

Owan, TE, Hodge DO, Herges RM, Jacobsen SJ, Roger VL, Redfield MM. (2006). Trends in prevalence and outcome of heart failure with preserved ejection fraction. *N. Engl. J. Med.* 355: 251-259.

Owens DM, Keyse SM. (2007). Differential regulation of MAP kinase signalling by dual-specificity protein phosphatases. *Oncogene.* **26**: 3203–13

Oyamada M, Kimura H, Oyamada Y. (1994). The expression, phosphorylation, and localization of connexin 43 and gap-junctional intercellular communication during the establishment of a synchronized contraction of cultured neonatal rat cardiac myocytes. *Exp Cell Res.* **212**: 351–358.

Page` s G, Gue´rin S, Grall D, Bonino F, Smith A, Anjuere F, Auberger P, Pouysse´gur J. (1999). Defective thymocyte maturation in p44 MAP kinase (Erk 1) knockout mice. *Science.* **286**: 1374–1377.

Palm-Leis A, Singh US, Herbelin BS, Olsovsky GD, Baker KM, Pan J. (2004). Mitogen-activated Protein Kinases and Mitogen-activated Protein Kinase

Phosphatases Mediate the Inhibitory Effects of All-trans Retinoic Acid on the Hypertrophic Growth of Cardiomyocytes. *J Biol Chem*. **279**: 54905–54917.

Patrucco E, Notte A, Barberis L, Selvetella G, Maffei A, Brancaccio M, Marengo S, Russo G, Azzolino O, Rybalkin SD, Silengo L, Altruda F, Wetzker R, Wymann MP, Lembo G, Hirsch E. (2004). PI3Kgamma modulates the car diac response to chronic pressure overload by distinct kinase-dependent and -independent effects. *Cell*. **118**: 375–387.

Pawson T, Taylor L. (2009). Protein Phosphorylation Goes Negative. *Molecular cell.* **34**: 139-140.

Petrich BG, Eloff BC, Lerner DL, Kovacs A, Saffitz JE, Rosenbaum DS, Wang Y. (2004). Targeted activation of c-Jun N-terminal kinase in vivo induces restrictive cardiomyopathy and conduction defects. *J Biol chem.* **279**: 15330–15338.

Petrich BG, Wang Y. (2004). Stress-activated MAP kinases in cardiac remodeling and heart failure: new insights from transgenic studies. *Trends Cardiovasc Med.* **14**: 50–55.

Porter KE, Turner NA. (2009). Cardiac fibroblasts: At the heart of myocardial. *remodeling Pharmacology & Therapeutics.* **123**: 255–278.

Purcell NH, Wilkins BJ, York A, Saba-El-Leil MK, Meloche S, Robbins J. (2007). Genetic inhibition of cardiac ERK1/2 promotes stress-induced apoptosis and heart failure but has no effect on hypertrophy *in vivo. Proc Natl Acad Sci USA.* **104**: 14074–9.

Raingeaud J, Whitmarsh AJ, Barrett T, Derijard B, Davis RJ. (1996). MKK3- and MKK6-regulated gene expression is mediated by the p38 mitogen-activated protein kinase signal transduction pathway. *Mol Cell Biol.* **16**: 1247-55.

Raman M, Chen W, Cobb MH. (2007). Differential regulation and properties of MAPKs. *Oncogene.* **26**: 3100–3112.

Rapundalo ST. (1998). Cardiac protein phosphorylation: functional and pathophysiological correlates. *Cardiovascular Research.* **38**: 559-588.

Rauhala HE, Porkka KP, Tolonen TT, Martikainen PM, Tammela TL Visakorpi T. (2005). Dual-specificity phosphatase 1 and serum/glucocorticoid-regulated kinase are downregulated in prostate cancer. *Int J Cancer.* **117**: 738–745.

Ray IB, Sturgil TW. (1988). Insulin-stimulated microtubule-associated protein kinaseis phosphorylated on tyrosineand threonine *in vivo Proc. Natl. Acad. Sci. USA*. **85**: 3753-3757.

Regan CP, Diane WL, Boucher M, Spatz S, Su MS, Kuida K. (2002). Erk5 null mice display multiple extraembryonic vascular and embryonic cardiovascular defects. *PNAS*. **99**: 9248-9253.

Ren J, Zhang S, Kovacs A, Wang Y, Muslin AJ. (2005). Role of p38alpha MAPK in cardiac apoptosis and remodeling after myocardial infarction. *J Mol Cell Cardiol.* **38**: 617– 623.

Roberts PJ, Der CJ. (2007). Targeting the Raf-MEK-ERK mitogen-activated protein kinase cascade for the treatment of cancer. *Oncogene.* **26**: 3291–3310.

Robinson MJ, Cheng M, Khokhlatchev A, Ebert D, Ahn N, Guan K, Stein B, Goldsmith E, Cobb MH. (1996). Contribution of the MAP kinase backbone and phosphorylation lip to MEK specificity. *J Biol chem.* **271**: 29734 –29739.

Robinson MJ, Cheng M, Khokhlatchev A, Ebert D, Ahn N, Guan KL, Stein B, Goldsmith E, Cobb MH. (1998). Contributions of the mitogen-activated protein (MAP) kinase backbone and phosphorylation loop to MEK specificity. *Curr Opin Chem Biol.* **2**: 633-41.

Rockman HA, Wachhorst SP, Mao L, Ross J Jr. (1994). ANG II receptor blockade prevents ventricular hypertrophy and ANF gene expression with pressure overload in mice. *Am J Physiol.* **266**: H2468–H2475.

Rook MB, Jongsma HJ, de Jonge B. (1989). Single channel currents of homo- and heterologous gap junctions between cardiac fibroblasts and myocytes. *Pflügers Arch.* **414**: 95–98.

Rook MB, van Ginneken ACG, De Jonge B (1992). Differences in gap junction channels between cardiac myocytes, fibroblasts, and heterologous pairs. *Am J Physiol.* **263**: C959–C977.

Rosini P, De Chiara G, Bonini P, Lucibello M, Marcocci ME, Garaci E*, et al.* (2004). Nerve growth factor-dependent survival of CESS B cell line is mediated by increased expression and decreased degradation of MAPK phosphatase 1. *J Biol Chem.* **279:** 14016-14023.

Ross SH, Lindsay Y, Safrany ST, Lorenzo O, Villa F, Toth R, Clague MJ, Downes CP, Leslie NR. (2007). Differential redox regulation within the PTP super family. *Cellular Signalling.* **19**: 1521-1530.

Rousseau S, Houle F, Landry J, Huot J. (1997). p38 MAP kinase activation by vascular endothelial growth factor mediates actin reorganization and cell migration in human endothelial cells. *Oncogene.* **15**: 2169-2177.

Roussel E, Gaudreau M, Plante E, Drolet MC, Breault C, Couet J, Arsenault M. (2008). Early responses of the left ventricle to pressure overload in Wistar rats. **Life Sciences. 82**: 265–272.

Roth RJ, Le AM, Zhang L, Kahn M, Samuel VT, Shulman GI, Bennett AM. (2009). MAPK phosphatase-1 facilitates the loss of oxidative myofibers associated with obesity in mice. *J Clin Invest*. **119**: 3817–3829.

Roux PP, Blenis J. (2004). ERK and p38 MAPK-activated protein kinases: a family of protein kinases with diverse biological functions. *Microbiol Mol Biol Rev.* **68**: 320–344.

Sa´nchez-Perez I, Murgui JR, Perona R. (1998). Cisplatin induces a persistent activation of JNK that is related to cell death. *Oncogene.* **16**: 533–540.

Saba-El-Leil MK, Vella FD, Vernay B, Voisin L, Chen L, Labrecque N, Ang SL, Meloche S. (2003). An essential function of the mitogen- activated protein kinase Erk2 in mouse trophoblast development. *EMBO Rep*. **4**: 964–968.

Saba-El-Leil MK, Vella FDJ, Vernay B, Voisin L, Chen L, Labrecque N, Ang SL Meloche S. (2003) An essential function of the mitogen-activated protein kinase Erk2 in mouse trophoblast development. *EMBO J.* **4**: 964–968.

Sabapathy K, Kallunki T, David JP, Graef I, Karin M, Wagner EF. (2001). c-Jun NH2-terminal kinase (JNK)1 and JNK2 have similar and stage-dependent roles in regulating T cell apoptosis and proliferation. *J. Exp. Med.* **193**: 317–328.

Sabio G, Simon J, Arthur C, Kuma Y, Peggie M, Carr J, Murray-Tait V, Centeno F, Goedert M, Morrice NA, Cuenda A. (2005). p38 gamma regulates the localisation of SAP97 in the cytoskeleton by modulating its interaction with GKAP. *EMBO J.* **24**: 1134–1145.

Sabri A, Steinberg SF. (2003). Protein kinase C isoform-selective signals that lead to cardiac hypertrophy and the progression of heart failure. *Mol Cell Biochem.* **251**: 97–101.

Sadoshima J, Qiu Z, Morgan JP, Izumo S. (1995). Angiotensin II and other hypertrophic stimuli mediated by G protein-coupled receptors activate tyrosine kinase, mitogen-activated protein kinase, and 90-kD S6 kinase in cardiac myocytes. The critical role of Ca($^{2+}$)-dependent signaling. *Circ Res.* **76**: 1-15.

Sadoshima J, Qiu Z, Morgan JP, Izumo S. (1995). Angiotensin II and other hypertrophic stimuli mediated by G protein-coupled receptors activate tyrosine kinase, mitogen-activated protein kinase, and 90 kD S6 kinase in cardiac myocytes: The critical role of Ca2+-dependent signaling. *Circ Res.* **76**: 1–15.

Salojin KV, Owusu IB, Millerchip KA, Potter M, Platt KA, Oravecz T. (2006). Essential role of MAPK phosphatase-1 in the negative control of innate immune responses. *J Immunol.* **176**: 1899–1907.

Sanada S, Node K, Minamino T, Takashima S, Ogai A, Asanuma H. (2003). Long-acting Ca^{2+} blockers prevent myocardial remodeling induced by chronic NO inhibition in rats. *Hypertension.* **41**: 963–7.

Sayed D, Hong C, Chen IY, Lypowy J, Abdellatif M. (2007). MicroRNAs play an essential role in the development of cardiac hypertrophy. *Circ Res.* **100**: 416–424.

Schneider M, Marison IW, Stockar UV. (1996). The importance of ammonia in mammalian cell culture. *Journal of Biotechnology*, **46**: 161-185.

Schramek H. (2002). MAP Kinases: From Intracellular Signals to Physiology and Disease. *News. Physiol. Sci.* **17**: 62-67.

Selvetella G, Hirsch E, Notte A, Tarone G, Lembo G. (2004). Adaptive and maladaptive hypertrophic pathways: points of convergence and divergence. *Cardiovasc Res.* **63**: 373–380.

Seung-Keun Hong, Seunghee Yoon, Cas Moelling, Dumrongkiet Arthan, and Jong-In Park (2009). Noncatalytic Function of ERK1/2 Can Promote Raf/MEK/ERK-mediated Growth Arrest Signaling. *J Biol Chem.* 284: 33006–33018.

Shen J, Chandrasekharan UM, Ashraf MZ, Long E, Morton RE, Liu Y, Smith JD, DiCorleto PE. (2010). Lack of mitogen-activated protein kinase phosphatase-1 protects ApoE-null mice against atherosclerosis. *Circ Res.* **106**: 902-10.

Shen WH, Wang J, Wu J, Zhurkin VB, Yin Y (2006). Mitogen-activated protein kinase phosphatase 2: a novel transcription target of p53 in apoptosis. *Cancer Res* **66:** 6033-6039.

Shephard R, Semsarian C. (2009). Role of animal models in HCM research. *J Cardiovasc Transl Res.* 4: 471-82.

Shin SY, Lee JH, Min BW, Lee YH. (2006). The translation inhibitor anisomycin induces Elk-1-mediated transcriptional activation of egr-1 through multiple mitogen-activated protein kinase pathways. *Experimental and Molecular Medicine.* **38**: 677-685.

Skavdahl M, Steenbergen C, Clark J. (2005). Estrogen receptor-beta mediates male-female differences in the development of pressure overload hypertrophy. *Am J Physiol heart Circ Physiol.* **288**: H469-476.

Sloss CM, Cadalbert L, Finn SG, Fuller SJ, Plevin R (2005). Disruption of two putative nuclear localization sequences is required for cytosolic localization of mitogen-activated protein kinase phosphatase-2. *Cell Signal.* **17:** 709-716.

Smith JH, Green CR, Peters NS. (1991). Altered patterns of gap junction distribution in ischemic heart disease. An immunohistochemical study of human myocardium using laser scanning confocal microscopy. *Am J Pathol.* **139**: 801–821.

Smith TG, Karlsson M, Lunn JS, Eblaghie MC, Keenan ID, Farrell ER, Tickle C, Storey KG, Keyse SM. (2006). Negative feedback predominates over cross-regulation to control ERK MAPK activity in response to FGF signalling in embryos. *FEBS Letters.* **580**: 4242–4245.

Soule HD, Vazguez J, Long A, Albert S, Brennan SM. (1973). A human cell line from a pleural effusion derived from a breast carcinoma. *J Nat Cancer Inst.* **51**: 1408-1416.

Soulsby M, Bennett AM. (2009). Physiological Signaling Specificity by Protein Tyrosine Phosphatases. *Physiology.* **24**: 281–289.

Staufenberger S, Jacobs M, Brandstaè tter K, Hafner M, Regitz-zagrosek VG, Schorb W.(2001). Angiotensin II Type1 Receptor Regulation and Differential Trophic Effects on Rat Cardiac Myobroblasts After Acute Myocardial Infarction. *J Cell Physiology.* **187**: 326-35.

Stawowy P, Goetze S, Margeta C, Fleck E, Graf K. (2003). LPS regulate ERK1/2-dependent signaling in cardiac fibroblasts via PKC-mediated MKP-1 induction. *Biochem Biophys Res Commun..* **303**: 74–80.

Stephens BJ, Han H, Gokhale V, Von Hoff DD. (2005). PRL phosphatases as potential molecular tar- gets in cancer. *Mol Cancer Ther.* **4**: 1653–1661.

Stephens LR, Jackson TR, Hawkins PT. (1993). Agonist-stimulated synthesis of phosphatidylinositol(3,4,5)-trisphosphate: a new intracellular signalling system? *Biochim Biophys Acta.* **1179**: 27–75.

Steven AI, Jonathan ML. (2005). p53 is a nf-y- and p21-independent, sp1-dependent repressor of cyclin b1 transcription. *FEBS letters*. **579**: 1001–1007.

Stewart JA, Cashatt DO, Borck AC, Brown JE, Carver WE. (2006). 17 β-estradiol modulation of angiotensin II-stimulated response in cardiac fibroblasts. Journal of Molecular and Cellular Cardiology. **41**: 97–107.

Strohm C, Barancik M, Bruehl ML, Kilian SAR, Schaper W. (2000). Inhibition of the ER-Kinase by PD98059 and UO126 counteracts ischemic preconditioning in pig myocardium. *J Cardiovasc Pharmacol.* **36**: 218-229.

Sun H, Catherine HC, Lester FL, Tonks NK. (1993). MKP-1 (3ch134), an immediate early gene product, is a dual specificity phosphatase that dephosphorylates map kinase *in vivo*. *Cell*. **75**: 487-493.

Sung JK, Betty D. (2007). Generation and Maturation of Bone Marrow Derived DCs under serum-free conditions. *J Immunol Methods*. 323: 101–108.

Swynghedauw B. (1999). Molecular mechanisms of myocardial remodeling. *Physiol. Rev.* **79**: 215–62.

Tachibana H, Perrino C, Takaoka H, Davis RJ, Naga Prasad SV, Rockman HA. (2007). JNK1 is required to preserve cardiac function in the early response to pressure overload. *Biochem Biophys Res Commun.* **343**: 1060–1066.

Takeda N, Manabe I, Uchino Y, Eguchi K, Matsumoto S, Nishimura S, Shindo T, Sano M, Otsu K, Snider P, Conway SJ, Nagai R. (2010). Cardiac fibroblasts are essential for the adaptive response of the murine heart to pressure overload. *J Clin Invest.* **120**: 254–265.

Takeishi Y, Huang Q, Abe J, Glassman M, Che W. (2001). Src and multiple MAP kinase activation in cardiac hypertrophy and congestive heart failure under chronic pressure-overload: comparison with acute mechanical stretch. *J Mol Cell Cardiol.* **33**: 1637-48.

Talmor D, Applebaum A, Rudich A, Shapira Y, Tirosh A. (2000). Activation of mitogen-activated protein kinases in human heart during cardiopulmonary bypass. *Circ Res.* **86**: 1004–1007.

Tamemoto H, Kadowaki T, Tobe K, Kagi T, Sakura H, Hayakawa T. (1994). Insulin resistance and growth retardation in mice lacking insulin receptor

substrate-1. *Nature.* **372**: 182 – 186.

Tan Y, Rouse J, Zhang A, Cariati S, Cohen P, Comb MJ. (1996). FGF and stress regulate CREB and ATF-1 via a pathway involving p38 MAP kinase and MAPKAP kinase-2. *EMBO J.* **15**: 4629-4642.

Tanoue T, Adachi M, Moriguchi E, Nishida A. (2000). A conserved docking motif in MAP kinases common to substrates, activators and regulators. *Nat Cell Biol.* **2**: 110-116.

Tanoue T, Maeda R, Adachi M, Nishida E. (2001). Identification of a docking groove on ERK and p38 MAP kinases that regulates the specificity of docking interactions. *EMBO J.* **20**: 466-479.

Tanoue T, Moriguchi T, Nishida E. (1999). Molecular cloning and characterization of a novel dual specificity phosphatase, MKP-5. *J Biol Chem.* **274**: 19949–19956.

Tanoue T, Yamamoto T, Maeda R, Nishida E. (2001). A Novel MAPK Phosphatase MKP-7 Acts Preferentially on JNK/SAPK and p38α and β MAPKs. *J Biol Chem.* **276**: 26629–26639.

Tanoue T, Yamamoto T, Nishida E. (2002). Modular structure of a docking surface on MAPK phosphotases. *J. Biol. Chem.* **277**: 22942-22949.

Tao X, Tong L. (2007). Crystal structure of the MAP kinase binding domain and the catalytic domain of human MKP5. *Protein Sci*. **16**: 880–886.

Tarrega C, Rios P, Cejudo-Marin R, Blanco-Aparicio C, van den Berk L, Schepens J, Hendriks W, Tabernero L, Pulido R. (2005). ERK-2 shows a

restrictive and locally selective mechanism of recognition by its tyrosine phosphatase inactivators not shared by its activator MEK1. *J. Biol. Chem.* **280**: 37885–37894.

Teng C, Huang W, Meng T. (2007). Several dual specificity phosphatases coordinate to control the magnitude and duration of JNK activation in signaling response to oxidative stress. *J Biol Chem*. **282**: 28395–28407.

Theodosiou A, Ashworth A. (2002). MAP kinase phosphatases. *Genome Biol.* **26**: 3-7.

Theodosiou A, Ashworth A. (2002). MAP kinase phosphatases. Genome Biol.3.

Tigalis T, Bennett AM. (2007). Protein tyrosine phophatase function: the substrate perspective. *Biochem J.* **402**: 1-15.

Timothy T. Cornell, Paul Rodenhouse, Qing Cai, Lei Sun, and Thomas P. Shanley. (2010). Mitogen-Activated Protein Kinase Phosphatase 2 Regulates the Inflammatory Response in Sepsis. *Infection and immunity.* **287**: 2868–2876.

Tolias KF, Cantley LC. (1999). Pathways for phosphoinositide synthesis. *Chem Phys Lipid*. **98**: 69–77.

Tonks NK, Neel BG. (1996). From form to function: signaling by protein tyrosine phosphatases. *Cell.* **87**: 365–368.

Tonks NK, Neel BG. (2001). Combinatorial control of the specificity of protein tyrosine phosphatases. *Curr Opin Cell Biol.* **13**: 182–195.

Tonks NK. (2005). Redox redux: revisiting PTPs and the control of cell signalling. *Cell*. **121**: 667-670.

Torres C, Francis MK, Lorenzini A, Tresini M, Cristofalo VJ. (2003). Metabolic stabilization of MAP kinase phosphatase-2 in senescence of human fibroblasts. *Exp Cell Res.* **290**: 195–206.

Torii S, Nakayama K, Yamamoto T, Nishida E. (2004). Regulatory mechanisms and function of ERK MAP kinases. *J Biochem*. **136**: 557–561.

Tournier C, Hess P, Yang DD, Xu J, Turner TK, Nimnual A. (2000). Requirement of JNK for stress-induced activation of the cytochrome c-mediated death pathway. *Science.* **288**: 870–874.

Towbin H, Staehelin T, Gordon J. (1992). Electrophoretic transfer of proteins from polyacrylamide gels to nitrocellulose sheets: procedure and some applications. *Biotechnology.* **24**: 145-9.

Tresini M, Lorenzini A, Torres C, and Cristofalo VJ. (2007). Modulation of replicative senescence of diploid human cells by nuclear ERK signaling. *J Biol Chem*. **282**: 4136–4151.

Tsang M, Maegawa S, Kiang A, Habas R, Weinberg E, Dawid IB. (2004). A role for MKP-3 in axial patterning of the zebrafish embryo. *Development.* **131**: 2769–2779.

Tsuiki H, Tnani M, Okamoto I, Kenyon LC, Emlet DR, Holgado-Madruga M, Lanham IS, Joynes CJ, Vo KT, Wong AJ. (2003). Constitutively Active Forms of c-Jun NH2-terminal Kinase Are Expressed in Primary Glial Tumors. *Cancer Res.* **63**: 250-5.

Tsujita E, Taketomi A, Gion T, Kuroda Y, Endo K, Watanabe A, Nakashima H, Aishima S, Kohnoe S, Maehara Y. (2005). Suppressed MKP-1 is an indepen-

dent predictor of outcome in patients with hepatocellular carcinoma. *Oncology.* **69**: 342–347.

Turjanski AG, Vaque´ JP, Gutkind JS. (2007). MAP kinases and the control of nuclear events. *Oncogene.* **26**: 3240–3253.

Ueda K, Arakawa H, Nakamura Y. (2003). Dual-specificity phosphatase 5 (dusp5) as a direct transcriptional target of tumor suppressor p53. *Oncogene* **22**: 5586–5591.

Uehara T, Bennett B, Sakata ST, Satoh Y, Bilter GK, Westwick JK. (2005). JNK mediates hepatic ischemia reperfusion injury. *J Hepatol*. **242**: 850–859.

Vahebi S, Ota A, Li M, Warren CM, de Tombe PP, Wang Y, Solaro RJ. (2007). p38-MAPK induced dephosphorylation of alpha-tropomyosin is associated with depression of myocardial sarcomeric tension and ATPase activity. *Circ Res.* **100**: 408-415.

Vander A, Sherman J, Luciano D. (2004). Chapter 12: Cardiovascular physiology, Section B: The heart, *Human Physiology, The Mechanisms of Body Function.* 9th Edition, 375-399.

Vanhaesebroeck B, Leevers SJ, Ahmadi K, Timms J, Katso R, Driscoll PC, Woscholski R, Parker PJ, Waterfield MD. (2001). Synthesis and function of 3-phosphorylated inositol lipids. *Annu Rev Biochem.* **70**: 535–602.

Vicent S, Garayoa M, Lopez-Picazo JM, Lozano MD, Toledo G, Thunnissen FB, Manzano RG, Montuenga LM. (2004). Mitogen-activated protein kinase phosphatase-1 is overexpressed in non-small cell lung cancer and is an independent predictor of outcome in patients. *Clin Cancer Res.* **10**: 3639–3649.

Vieira C, Martinez S. (2005). Experimental study of MAP kinase phosphatase-3 (MKP-3) expression in the chick neural tube in relation to Fgf8 activity. *Brain Res Brain Res Rev.* **49**: 158–166.

Villarreal FJ, Kim NN, Ungab GD, Printz MP, Dillmann WH. (1993). Identification of functional angiotensin II receptors on rat cardiac fibroblasts. *Circulation.* **88**: 2849–2861.

Waetzig V, Herdegen T. (2005). Context-specific inhibition of JNKs: overcoming the dilemma of protection and damage. *Trends Pharmacol Sci.* **26**: 455–461.

Wang H, Chen A, Seth A, McCulloch CA. (2003). Mechanical force regulation of myofibroblast differentiation in cardiac fibroblasts. *Am J Physiol Heart Circ Physiol.* **285**: H1871–H1881.

Wang HY, Cheng Z, Malbon CC. (2003). Overexpression of mitogen activated protein kinase phosphatases MKP-1, MKP-2 in human breast cancer. *Cancer Letter.* **191**: 229–237.

Wang X, Tournier C. (2006). Regulation of cellular functions by the ERK5 signalling pathway. *Cell Signal.* **18**: 753–760.

Wang Y, Huang S, Sah VP, Ross J Jr. Brown JH, Han J, Chien KR. (1998). Cardiac muscle cell hypertrophy and apoptosis induced by distinct members of the p38 mitogen-activated protein kinase family. *J Biol Chem.* **273**: 2161–2168.

Wang Y. (2007). Mitogen-activated protein kinases in heart development and diseases. *Circulation.* **116**: 1413–23.

Wang Z, Cao N, Nantajit D, Fan M, Liu Y, Li JJ. (2008). Mitogen-activated Protein Kinase Phosphatase-1 Represses c-Jun NH2-terminal Kinase-mediated Apoptosis via NF-KB Regulation. *J Biol Chem.* **283**: 21011–21023.

Wanga Y, Peic D, Jia H, Xing S. (2008). Protective effect of a standardized ginkgo extract (ginaton) on renal ischemia/reperfusion injury via suppressing the activation of jnk signal pathway. *Phytomedicine*. **15**: 923–931.

Waskiewicz AJ, Flynn A, Proud CG, Cooper JA. (1997). Mitogen activated protein kinases activate the serine-threonine kinase Mnk1 and Mnk2. *EMBO J*. **16**: 1909 –1920.

Weber KT, Brilla CG, Campbell SE, Zhou G, Matsubara L, Guarda E. (1992). Pathologic hypertrophy with fibrosis: the structural basis for myocardial failure. *Blood Press.* **1**: 75– 85.

Weber KT, Brilla CG, Janicki JS, Reddy HK, Campbell SE. (1991). Myocardial fibrosis: role of ventricular systolic pressure, arterial hypertension, and circulating hormones. *Basic Res Cardiol.* **86**: 25–31.

Weber KT, Brilla CG. (1992). Myocardial fibrosis and the renin-angiotensin-aldosterone system. *J Cardiovasc Pharmacol.* **20**: S48 –S54.

Weber KT, Jalil JE, Janicki JS, Pick R. (1989). Myocardial collagen remodeling in pressure overload hypertrophy. A case for interstitial heart disease. *Am J Hypertens.* **2**: 931–940.

Weibrecht I, Böhmer SA, Dagnell M, Kappert K, Östman A, Böhmer FD, (2007). Oxidation sensitivity of the catalytic cysteine of the protein-tyrosine phosphatase SHP-1 and SHP-2. *Free Radic. Biol. Med.* **43**: 100-110.

Withers DJ, Gutierrez JS, Towery H, Burks DJ, Ren JM, Previs S. (1998). Disruption of IRS-2 causes type 2 diabetes in mice. *Nature.* **391**: 900 – 904.

Wu JJ, Roth RJ, Anderson EJ, Hong EG, Lee MK, Choi CS, Neufer PD, Shulman GI, Kim JK, Bennett AM. (2006). Mice lacking MAP kinase phosphatase-1 have enhanced MAP kinase activity and resistance to diet-induced obesity. *Cell Metab.* **4**: 61–73.

Wu JJ, Zhang L, Bennet AM. (2005). The noncatalytic amino terminus of mitogen-activated protein kinase phosphatase 1 directs nuclear targeting and serum response element transcriptional regulation. *Mol. Cell. Biol.* **25**: 4792-4803.

Wu JJ, Bennett AM. (2005). Essential Role for Mitogen-activated Protein (MAP) Kinase Phosphatase-1 in Stress-responsive MAP Kinase and Cell Survival Signaling. *J. Biol. Chem.* **280**: 16461–16466.

Wymann MP, Zvelebil M, Laffargue M. (2003). Phosphoinositide 3-kinase signalling—which way to target? *Trend Pharmacol Sci.* **24**: 366–76.

Yafeng D, Daqing G, Lei C, Ruxian L, John VC, Chiming W. (2006). Increased ERK activation and decreased MKP-1 expression in human myocardium with congestive heart failure. *Journal of Cardiothoracic-Renal Research.* **1**: 123-130.

Yamaguchi O, Watanabe T, Nishida K, Kashiwase K, Higuchi Y, Takeda T. (2004). Cardiac-specific disruption of the c-raf-1 gene induces cardiac dysfunction and apoptosis. *J Clin Invest.* **114**: 937–43.

Yan L, Carr J, Ashby PR, Murry-Tait V, Thompson C, Arthur JS. (2003). Knockout of ERK5 causes multiple defects in placental and embryonic development. *BMC Dev Biol.* **3**:11.

Yang DD, Conze D, Whitmarsh AJ, Barrett T, Davis RJ, Rincon M, Flavell RA. (1998). Differentiation of CD4(+) T cells to Th1 cells requires MAP kinase JNK2. *Immunity*. **9**: 575– 585.

Yang DD, Kuan CY, Whitmarsh AJ ,Rinco´n M, Zheng TS, Davis RJ et al. (1997). Absence of excitotoxicity-induced apoptosis in the hippocampus of mice lacking the Jnk3 gene. *Nature.* **389**: 865–870.

Yasuda J, Whitmarsh AJ, Cavanagh J, Sharma M, Davis RJ. (1999). The Jip group of MAP kinase scaffold proteins. *Mol Cell Biol.* **19**: 7245-7766.

Yip-Schneider MT, Lin A, Marshall MS (2001). Pancreatic tumor cells with mutant K-ras suppress ERK activity by MEK-dependent induction of MAP kinase phosphatase-2. *Biochem Biophys Res Commun.* **280:** 992-997.

Yokoyama A, Karasaki H, Urushibara N, Nomoto K, Imai Y, Nakamura K, Mizuno Y, Ogawa K, Kikuchi K. (1997). The characteristic gene expressions of MAPK phosphatases 1 and 2 in hepatocarcinogenesis, rat ascites hepatoma cells, and regenerating rat liver. *Biochem Biophys Res Commun.* **239**: 746-751.

Yong LZ, Joseph MR, Seon HC, Natalia M, Yeonseok C, Roza IN, Chen D. (2009). MKP-1 is necessary for t-cell activation and functions. *J Biol Chem*. **284**: 30815–30824.

Yong LZ, Joseph NB, Norman JK, Julie D, Thang N, Ying W, Roger JD, Philip DG, Richard AF. (2004). Regulation of innate and adaptive immune responses by MAP kinase phosphatase 5. *Nature*. 430.

Yoshida K, Yoshiyama M, Omura T, Nakamura Y, Kim S, Takeuchi K, Iwao H, Yoshikawa J. (2001). Activation of mitogen-activated protein kinasesin the non-ischemic myocardium of an acute myocardial infarction in rats. *Jpn Circ J.*

65: 808–814.

Yue T, Gu J, Wang C, Reith AD, Lee JC Mirabile RC, Kreutz R, Wang R, Maleeff B, Parsons AA, Ohlstein EH. (2000). Extracellular Signal-regulated Kinase Plays an Essential Role in Hypertrophic Agonists, Endothelin-1 and Phenylephrine-induced Cardiomyocyte Hypertrophy. *J Biol Chem*. **275**: 37895–37901.

Yue TL, Wang C, Gu JL, Ma XL, Kumar S, Lee JC. (2000). Inhibition of extracellular signal-regulated kinase enhances ischemia/reoxygenation-induced apoptosis in cultured cardiac myocytes and exaggerates reperfusion injury in isolated perfused heart. *Circ Res.* **86**: 692–9.

Zakkar M, Chaudhury H, Sandvik G, Enesa K, Luong LA, Cuhlmann S, Mason JC, Krams R, Clark AR, Haskard DO, Evans PC. (2008). Increased Endothelial Mitogen-Activated Protein Kinase Phosphatase-1 Expression Suppresses Proinflammatory Activation at Sites That Are Resistant to Atherosclerosis. *Circ. Res.* **103**: 726-732.

Zeliadta NA, Maurob LJ, Wattenberga EV. (2008). Reciprocal Regulation of Extracellular Signal Regulated Kinase 1/2 and Mitogen Activated Protein Kinase Phosphatase-3. *Toxicol Appl Pharmacol.* **232**: 408–417.

Zhang J, Zhou B, Zheng CF, Zhang ZY. (2003). A bipartite mechanism for ERK-2 recognition by its cog- nate regulators and substrates. *J Biol Chem.* **278**: 29901–29912.

Zhang S, Weinheimer C, Courtois M, Kovacs A, Zhang CE, Cheng AM, Wang Y, Muslin AJ. (2003). The role of the Grb2-p38 MAPK signaling pathway in cardiac hypertrophy and fibrosis. *J Clin Invest.* **111**: 833–841.

Zhang T, Choy M, Jo M, Roberson MS. (2001). Structural organization of the rat mitogen-activated protein kinase phosphatase 2 gene. *Gene.* **273**: 71-79.

Zhang Y, Reynolds JM, Chang SH, Martin-Orozco N, Chung Y, Nurieva RI, Dong C. (2009). MKP-1 Is Necessary for T Cell Activation and Function. *J Biol Chem.* **284**: 30815-30824.

Zhang ZY, Wang Y, Dixon JE. (1994). Dissecting the catalytic mechanism of protein-tyrosine phophatases. *Proc Natl Acad Sci U.S.A.* **91**: 1624-1627.

Zhao Q, Wang X, Nelin LD, Yao Y, Matta R, Manson ME, Baliga RS, Meng X, Smith CV, Bauer JA, Chang CH, Liu Y. (2006). MAP kinase phosphatase 1 controls innate immune responses and suppresses endotoxic shock. *J Exp Med.* **203**: 131–140.

Zheng CF, Guan K. (1993). Cloning and characterization of two distinct human extracellular signal-regulated kinase activator kinases, MEK1 and MEK2. *J Biol Chem.* **268**: 11435–11439

Zheng M, Dilly K, Dos Santos Cruz J, Li M, Gu Y, Ursitti JA. (2004). Sarcoplasmic reticulum calcium defect in Ras-induced hypertrophic cardiomyopathy heart. *Am J Physiol Heart Circ Physiol.* **286**: H424–33.

Zhou B, Wu L, Shen K, Zhang J, Lawrence DS, Zhang ZY. (2001). Multiple regions of MAP kinase phosphatase 3 are involved in its recognition and activation by ERK-2. *J Biol Chem.* **276**: 506–6515.

Zhou JY, Liu Y, Wu GS (2006). The role of mitogen-activated protein kinase phosphatase-1 in oxidative damage-induced cell death. *Cancer Res.* **66**: 4888–4894.

Zhu X, Rottkamp CA, Hartzler A, Sun Z, Takeda A, Boux H, Shimohama S, Perry G, Smith MA. (2001). Activation of MKK6, an upstream activator of p38, in Alzheimer's disease. *J Neurochemistry*. **79**: 311-318.

Zu, Q (2006). A handbook of mouse models of cardiovascular disease. John Wiley & Sons Ltd, The atrium, Southern Gate, Chichester, West Sussex PO 19 8 SQ, England.

PUBLICATIONS

Journal Publications

Ahmed Lawan, Sameer Al-Harthi, Laurence Cadalbert, Anthony McCluskey, Anne Grant, Marie Boyd, Susan Currie and Robin Plevin. (2010). Genetic deletion of the DUSP-4 gene reveals an essential non-redundant role for MKP-2 in cell survival. (submitted revised version to JBC, JBC/2010/181370).

Poster Presentation

Ahmed Lawan, Gianluca Grassia, Laurence Cadalbert, Susan Currie, Robin Plevin. (2009). MAP Kinase Phosphatase-2 deficiency leads to alteration of cardiac fibroblast growth. Europhosphatases 2009, Second EMBO Conference Series, Egmond aan Zee, The Netherlands.

G. Grassia, A. Lawan, S. Currie and R.J. Plevin. (2009). Characterization of cardiac phenotype and MAPK signalling in adult cardiac fibroblast isolated from MKP-2 knock-out mice. Scottish Cardiovascular Forum, Inverness, Scotland, UK.

Tamara Martin, Ahmed Lawan, Robin Plevin, Andrew Paul and Susan Currie. (2010). Altered cardiac fibroblast proliferation during cardiac hypertrophy is modulated by calcium/calmodulin dependent protein kinase II δ. (Submitted to Biophysical Society Meeting, March, 2011, U.S.A.